ON THE DESIGN OF LOW SENSITIVITY ACTIVE RC FILTERS BY SIMULATION OF LC FILTERS

by

BHAJAN SINGH

A Thesis submitted in fulfilment of the requirements for the Degree of Doctor of Philosophy of the University of London, and Diploma of membership of the Imperial College.

February 1983.

Department of Electrical Engineering,
Imperial College of Science and Technology,
University of London,
Exhibition Road, London SW7 2BT.

To my Mother and Father

A B S T R A C T

Filters are extensively used in all types of electronic equipment and are an essential part of any communication network. In the past most high precision filters were classical LC networks realised using discrete components. However, the advent of high quality Hybrid technology has made it possible to use active RC filters, which offer advantages such as reduced size and weight, and increased reliability.

Apart from trying to reduce the DC power consumption, which is done by reducing the number of operational amplifiers (OP-AMPs) used in the circuit, a primary objective in the design of active RC filters is to produce circuits whose responses are relatively insensitive to changes in component values. One way of achieving this objective is to design the active RC network to "simulate" a suitably designed LC network in such a way that the inherently low sensitivity property of the LC network is retained. In this thesis, two such methods of designing active RC filters are considered. In the first method, which is referred to as the signal flow graph simulation, the mathematical relationships between the voltages and currents in the LC network are simulated. In the second method, which is referred to as the simulation of the elements and the structure, impedances of certain branches of the LC prototype are simulated.

In the signal flow graph simulation method, single amplifier biquadratic (SAB) circuits are used as the basic building blocks. In order to design practical circuits the effect of the finite amplifier gain-bandwidth product (f_T) must be taken into account. In this context, it is shown that the available predistortion technique, while giving improved results, is not very satisfactory, and a method of fully compensating SAB circuits, by adding an extra resistor, is

developed. Also a method of minimising the sensitivity of high order filters, realised using SAB circuits, is described.

In the case of the element and the structure simulation method, a novel approach is presented in which the negative impedance converter (NIC) is used as the basic active unit. It is shown that, contrary to the common belief, filter circuits which use NICs can be designed to have low sensitivity. A method of reducing the effect of finite f_T in this type of circuit is also described. A detailed discussion of the stability properties of NIC circuits is presented and it is shown that the majority of the circuits derived by the new method are perfectly stable. However, for the unstable circuits a method of achieving stability by the introduction of few additional components is developed.

A C K N O W L E D G E M E N T S

The work reported in this dissertation was carried-out under the supervision of the late Dr. W. Saraga. I am deeply grateful to Dr. Saraga for his guidance and constant encouragement and especially for many discussions during the course of this work. It was indeed a pleasure and a privilege for having had the opportunity to work with such an enthusiastic and unique person.

Throughout the period of this research Dr. D.G. Haigh has made valuable comments and suggestions and his advice and encouragement made the preparation of this thesis an easier task. For all his help I would like to express my deep gratitude to Dr. Haigh with whom I have also had the privilege of working for the past three years.

An acknowledgement is made to M. Zyoute, R.W. Turpin, W.T. Ramsey and M.A. Kunes for many useful technical discussions.

My thanks are also due to Dr. R. Spence and Dr. R.A. King for the interest they have shown in this work.

In addition to the above, thanks are also due to the many fellow research students that I have had the pleasure of meeting during my stay at Imperial College. In particular, the warm friendship and general discussions with K.S. Tahim, R.S. Soin, G.S. Virk, A.M. Ali, N.P. Clarke and B.S. Tan are gratefully acknowledged.

Finally, I would like to thank M. Zyoute and H. Cantanhede for their help in preparing the diagrams.

TABLE OF CONTENTS

LIST OF TABLES AND FIGURES

CHAPTER 1

INTRODUCTION

1.1 General

This thesis is concerned with the design of active RC filters which are derived by simulation of resistively terminated inductor-capacitor filters (usually referred to as LC filters). The main reason for the interest in active RC filters stems from the fact that these can be realised microelectronically, which is advantageous for many reasons such as reduced size and weight, and increased reliability; whereas, on the other hand, the microminiaturization of LC filters has not been achieved because attempts to microelectronically realise inductors have been unsuccessful.

Active RC filters consist of active devices (usually operational amplifiers), resistors and capacitors. The engineering aim in this field is the development of low cost, high quality, high precision microelectronic filters. However, the integrated circuit technology used to fabricate the active devices cannot produce resistors and capacitors with the high stability required for high precision filters; hence, the resistors and the capacitors are fabricated using an alternative technology; the complete circuits being known as "Hybrid" circuits. There are two basic methods of fabricating high precision resistors, namely, thin-film [1] and thick-film [2]. Thin-film and thick-film techniques of producing resistors are similar in one respect that they can both produce resistors which can be adjusted to their required values very accurately by laser trimming. In general, thick-film resistors are preferred because they are cheaper, however some applications may require the use of thin-film resistors as these have lower temperature coefficient (TC). For example, typical values for the TCs of thick and thin-film resistors are 30 ppm/^{o}C and 5 ppm/^{o}C, respectively.

It is possible to fabricate capacitors with the thin-film technology whereas the thick-film technology cannot produce capacitors at all, and hence when using thick-film resistors it is necessary to add separate capacitors, which are usually of miniature NPO ceramic chip type [2]. Thin-film capacitors have certain practical disadvantages which make their use unfeasible in practice. For example, silicon-dioxide capacitors have low capacitance per unit area and tantalum capacitors suffer from low Q-values which are rather temperature dependant. The ceramic chip capacitors have very high Q-values ($Q > 2000$), their TC is very low (e.g. TC within $\pm$ 10 ppm/^{o}C for $-20^{o}C < T < +70^{o}C$), and their capacitance per unit volume is very high (typically 0.5 nF/mm^{3}). The main disadvantage of ceramic chip capacitors is that they are cheaply available only if their nominal values are restricted to manufacturers' preferred values and if they have wide manufacturing tolerances (e.g. $\pm$ 10 %). Since ceramic chip capacitors do not have individual markings to denote their values, the circuit manufacture is considerably simplified if <u>all</u> the capacitors in the circuit have the same nominal preferred value.

From the above discussion it follows that, in order to reduce the manufacturing costs of active RC circuits, it is desirable to adopt active RC circuits in which the capacitors can have preferred and equal nominal values (by appropriate design), and also it must be possible to adjust the circuit to obtain the desired response when using capacitors with wide manufacturing tolerances of $\pm$ 10 % (this is done by the application of suitably developed resistor-adjustment methods). The active RC circuits to be derived in this thesis will satisfy these desirable requirements.

Numerous methods of synthesising active RC networks have been proposed (e.g. see [3,4]) and many of these have been shown to be feasible in practice in that microelectronic models have been constructed successfully [5,6,7]. Historically, the first active RC synthesis method was proposed in 1954 by Linvill [8], who showed that any transfer function T(s) (where s is the complex frequency variable) can be realised by a passive RC circuit with the addition of one negative impedance converter (NIC) — which can be realised by a single operational amplifier (OP-AMP) and two resistors. Two other active RC synthesis methods, which also require one NIC each, have been proposed by Yanagisawa and Saraga [9,10]. However, the main problem with these synthesis methods, requiring only a single active device, is the high sensitivity of the loss-frequency response to changes in the values of the components of the circuit. Due partially to the unacceptably high sensitivities and partially to the practical difficulties encountered (e.g. circuit stability), this synthesis technique never became a serious contender as a basis for the design of active RC filter circuits. On the contrary, these factors have played a vital role in creating a myth in that all circuits which use NICs, regardless of their origin or derivation, are automatically labelled as high sensitivity circuits (one result of the work to be described in this thesis is to seriously challenge this myth).

There are various other different approaches to the design of active RC filters, all of which have sensitivities much lower than the Linvill approach, and these are usually classified as follows:

1. cascading of biquadratic circuits [11]
2. multiple feedback circuits [12,13,14]
3. simulation of the elements and the structure of low sensitivity resistively terminated LC ladder filters [15] or impedance scaled LC ladder filters [16]
4. linearly transformed active filters [17]

In the cascade design method we factorise the required voltage transfer ratio into second order factors and the product of the factors is then realised by cascading (without interaction) the second order active RC sections. Note that if the order of the filter is odd there will be one first order factor in the realisation — this can be realised by a passive RC network.

The multiple feedback approach can be considered as comprising a "cascade" connection of second order active RC sections (and one first order section in the case of odd order filters) which have feedback interconnections. The required voltage transfer ratio can be realised by various feedback topologies; however, one particular feedback structure (known as the leap-frog feedback), which was first suggested by Girling and Good [18,19], is equivalent to simulating the signal flow graph of (low sensitivity) LC filter; thus some of the active RC circuits in this category reproduce the low sensitivity properties of LC networks [20,21].

In the third method of active RC design listed in the above classification, active RC circuits are used to simulate the impedances of certain branches (e.g. the inductive branches) of a resistively terminated LC ladder filter. Now, the sensitivity of the loss-frequency response of an LC filter to changes in the values of

the elements can be very small [22,23], and hence by designing the active RC network to simulate an LC filter it is possible to retain the low sensitivity properties of the LC filter in its active RC counterpart.

Another approach to the design of active RC filters, which is also based on simulation of LC filters, is the so called linearly transformed active filter approach [17]. The basic principle of this approach is to linearly transform the variables of the LC prototype filter (i.e. the voltages and the currents) into new variables, the relationships between which are then realised using active RC circuits. Yet another method of simulating LC filters is the "wave active" filter [24], in which the relationship between the incedent and the reflected waves of the LC filter are simulated. This method has been interpretted as being a special case of the linearly transformed active filter approach [17].

In this thesis we shall consider two different methods of simulating LC filters; viz, the signal flow graph simulation method and the simulation of the elements and the structure of LC filters. After a discussion of LC filters in general we shall review the state of the art in these two methods and then give an outline of the thesis.

1.2 Introduction to LC filters

1.2.1 LC filter structures and types

There are two basic types of LC filter structures, namely the lattice and the ladder. The ladder type of structures are superior to

lattice type of structures in the sense that the sensitivity of their loss-frequency response to changes in element values is much lower than for the lattice structures. Because of the low sensitivity properties of LC ladder filters, they are ideal as prototypes for the design of active RC filters (a discussion on the sensitivity of LC filters is presented later on in this section).

The general form of a ladder type filter is shown in Fig 1.1(a), where R_s and R_L are the source and the load resistors, respectively. In the ladder structure of Fig 1.1(a) the series and the shunt arms of the ladder comprise inductors and capacitors only. Thus the elements of the ladder (e.g. $Z_1, Y_1, \ldots . Z_n, Y_n$) are purely reactive and for this reason, these type of structures are often referred to as lossless LC ladders with resistive terminations. A schematic representation of a resistively terminated LC ladder filter is shown in Fig 1.1(b).

It has been stated above that the series and the shunt arms of the ladder in Fig 1.1(a) are composed of inductors and capacitors; however, the actual composition of the ladder arms is dictated by the type of "loss*-frequency" characteristic for which the LC filter is designed. There are four basic types of filter function response (namely: lowpass, highpass, bandpass and bandstop) and for each of these types of reponse, there are four common types of approximating functions. For a lowpass filter, which is the one having a passband

---

* In this thesis we shall define the loss of a filter as,

$$\text{LOSS} = -20 \ \text{LOG}_{10} \left| V_o / V_i \right|$$

where V_o and V_i are the output and the input voltages, respectively, of the filter (see Fig 1.1(a)).

extending from zero frequency to a finite cut-off frequency, f_c, and an increasing loss above this frequency, the four types of approximating curve are shown in Fig 1.2. The Butterworth characteristic in Fig 1.2(a) provides a maximally flat passband (around zero frequency) and has monotonically increasing loss in the passband and the stopband. The Chebyshev characteristic in Fig 1.2(b) provides an equi-ripple passband and a monotonically increasing loss in the stopband. For a given order filter having equal amount of passband distortion, the Chebyshev characteristic achieves greater loss in the stopband than the Butterworth characteristic. The type of LC ladder structures suitable for the realisation of Butterworth or Chebyshev characteristic are often referred to as all-pole structures, because in these filters the transmission zeros (i.e. the points of infinite loss) do not occur at finite frequencies (in the case of lowpass all-pole filters, they occur only at infinite frequency).

The loss-frequency characteristic shown in Fig 1.2(c) is called the inverted Chebyshev characteristic for which the loss increases monotonically in the passband but oscillates between A_s and infinity in the stopband; the inverted Chebyshev function can be derived by transformation of the Chebyshev function [25]. The loss-frequency curve shown in Fig 1.2(d) is called the elliptic approximation function since it is based on elliptic function theory. From Fig 1.2(d) we note that for this type of characteristic the loss oscillates between zero and A_p in the passband, and between A_s and infinity in the stopband. Of the four loss-frequency characteristics shown in Fig 1.2, the elliptic is the most efficient in the sense that if a filter is to be designed to meet some specification with a maximum loss A_p in the passband and a minimum loss A_s in the stopband,

then the elliptic approximation will yield a filter with a lower order. Elliptic type filters are sometimes also referred to as Cauer filters.

Highpass filters, and certain bandpass and bandstop filters can be obtained from lowpass filters by frequency transformations [26]. These frequency transformations serve two main purposes. Firstly, for a given lowpass filter transfer function they enable us to derive the corresponding transfer function of the highpass, the bandpass or the bandstop filter. Secondly, for a given lowpass filter structure they enable us to derive the corresponding structures for the highpass, the bandpass and the bandstop filters. Let us illustrate this point by considering some examples.

A frequency transformation for obtaining a highpass filter characteristic from a lowpass filter characteristic is,

$$w \longrightarrow -w_o^2/w$$

where w is the frequency in radians per second and w_o is a reference frequency at which the lowpass and the highpass filters have identical loss (usually w_o is chosen equal to the cut-off frequency of the lowpass filter). The loss-frequency responses of a lowpass and a highpass filter derived from it, by applying the above transformation, are shown plotted, on a logarithmic scale, in Fig 1.3(a) and (b), respectively. Now, the effect of applying this transformation to a lowpass filter structure (to obtain the structure of the highpass filter) would be to replace each inductor, of value L, in the lowpass filter by a capacitor, of value $1/(w_o^2 L)$, and to replace each capacitor, of value C, in the lowpass filter by an inductor, of value $1/(w_o^2 C)$.

The above lowpass to highpass transformation may infact be applied to any type of LC filter and it has the effect of pivoting the loss-frequency response (on a logarithmic scale) about the frequency w_o.

In contrast, a frequency transformation for obtaining a bandpass filter characteristic from a lowpass filter characteristic is,

$$w \longrightarrow w - w_o^2/w$$

The loss-frequency response of the bandpass filter obtained by this transformation has a geometrical symmetry about the frequency w_o. The lowpass and the bandpass filter characteristics have the same bandwidth for any given loss value, as indicated in Figs 1.3(a) and (c). In particular, the passband width of the bandpass characteristic is equal to the cut-off frequency of the lowpass characteristic. The method of obtaining the bandpass filter structure, by applying the above transformation to a lowpass filter, is to replace each inductor, of value L, in the lowpass filter by a series combination of an inductor and a capacitor, of values L and $1/(w_o^2 L)$, respectively; whereas each capacitor, of value C, in the lowpass filter is replaced by a parallel combination of a capacitor and an inductor, of values C and $1/(w_o^2 C)$, respectively.

A bandstop characteristic can be obtained by applying the above lowpass to bandpass transformation to a highpass filter (e.g. see Fig 1.3(d)).

In the case of bandpass filters having very small relative bandwidth*, which have been obtained from lowpass filters by lowpass to bandpass transformation, a large spread in the component values is obtained. In order to reduce this large spread in the component values, use is made of some impedance transformations due to Norton. These transformations [27,28,29] affect the values of the elements without affecting the basic shape of the filter response.

Fig 1.4(a) shows the general left-hand "L" to right-hand "L" transformation, where ϕ is a constant transformation parameter. Since ϕ is a constant it follows that Z_A and Z_B must be same type of impedances. As indicated in Fig 1.4(a), the transformer may be removed if all the impedances to the right of it are multiplied by ϕ^2. As a direct consequence of the transformation, the values of the node voltages and branch currents are changed hence, although the basic shape of loss characteristic remains unaltered, the value of the passband loss may be shifted by a constant amount.

The right-hand "L" to left-hand "L" transformation may easily be obtained by reversing the left-to-right "L" transformation and it is shown in Fig 1.4(b).

1.2.2 Synthesis and design of LC filters

The first step in the design process is to determine the mathematical functions which, on the one hand, satisfy the required response specifications and, on the other hand, can be exactly

---

* The relative bandwidth of a bandpass filter is defined as the ratio of the filter passband-width to its centre frequency.

realised by a circuit structure. This latter requirement restricts the mathematical properties of these functions and gives rise to approximation theory. The design of circuits to realise an approximating function is known as synthesis. The approximation and the synthesis processes are highly specialised subjects in themselves and as such are outside the scope of this thesis. However it is seldom necessary to start the design process of the most commonly specified filter characteristics (discussed in the previous subsection) from first principles as catalogues of design tables already exist for these filter types.

Thus the first step in the design of LC filters begins with consultation of the published tables to find the element values of the LC network. The published tables [30,31] list the element and / or the values of the poles and zeros of the transfer function for lowpass filters only; the frequency transformation, presented in the previous subsection, are used to derive highpass, bandpass and bandstop filter structures.

If characteristic different from those tabulated are required it is necessary to obtain a suitable loss-frequency function from first principles or by use of a suitable computer program [32]. For example, loss-frequency functions with equal ripple in the passband and meeting an arbitrary specification in the stopband can be obtained by a partly graphical procedure using templates [25]. Filters with such characteristics are referred to as general parameter filters.

1.2.3 LC filter sensitivity

It has been stated previously in Sec. 1.2.1 that LC filter networks are usually inserted between a resistive source and a resistive load, as shown in Fig 1.1(b). In this subsection we shall discuss the sensitivity properties of a certain class of resistively terminated LC filters. Before we proceed any further, let us define what we mean by "sensitivity".

As filter designers we are mainly interested in realising a network which has a certain loss-frequency characteristics; hence the parameter of primary importance is the modulus of the voltage transfer ratio, $T(s)$ $(= V_o/V_i$, where V_o and V_i are the output and the input voltages, respectively). In particular, the sensitivity $S_{x_i}^{|T(s)|}$ of $T(s)$ to any component, x_i, of the network is defined as

$$S_{x_i}^{|T(s)|} = \frac{\partial |T(s)| / |T(s)|}{\partial x_i / x_i} \tag{1.1}$$

We shall now show, following the argument first put forward by Orchard [22], that a certain type of LC filters with resistive tersminations can be designed to have a very low sensitivity.

Consider the resistively terminated LC filter shown in Fig 1.1(b). Let us express the input impedance of the LC network terminated in R_L as $Z_{11} = R_{11} + jX_{11}$. Then, it can easily be shown that the real power, P_{IN}, flowing into the input port of the LC network is

$$P_{IN} = \frac{|V_i|^2 \cdot R_{11}}{(R_s + R_{11})^2 + X_{11}^2} \tag{1.2}$$

Now, the LC network is lossless; therefore, all the power delivered into the LC network must be dissipated in the load resistor R_L. Hence, if P_L is the power dissipated in R_L, then

$$P_L = \frac{|V_o|^2}{R_L} = P_{IN} = \frac{|V_i|^2 \; R_{11}}{(R_s + R_{11})^2 + X_{11}^2} \tag{1.3}$$

$$\therefore |T(s)|^2 = \left| \frac{V_o}{V_i} \right|^2 = \frac{|V_o|^2}{|V_i|^2} = \frac{R_{11} \; R_L}{(R_s + R_{11})^2 + X_{11}^2} \tag{1.4}$$

Let x be a reactive element of the LC network; then, the differential sensitivity of $|T(s)|$ with respect to element x can be written as

$$S_x^{|T(s)|} = \frac{x}{|T(s)|} \cdot \frac{\partial |T(s)|}{\partial x} \tag{1.5}$$

using the chain rule for differentiation, we have

$$\frac{\partial |T(s)|}{\partial x} = \frac{\partial |T(s)|}{\partial R_{11}} \cdot \frac{\partial R_{11}}{\partial x} + \frac{\partial |T(s)|}{\partial X_{11}} \cdot \frac{\partial X_{11}}{\partial x} \tag{1.6}$$

Using equation (1.4), we obtain

$$\frac{\partial |T(s)|}{\partial R_{11}} = \frac{1}{2 \, |T(s)|} \cdot \frac{R_s^2 - R_{11}^2 + X_{11}^2}{[(R_s + R_{11})^2 + X_{11}^2]} \tag{1.7}$$

$$\text{and} \quad \frac{\partial |T(s)|}{\partial X_{11}} = \frac{1}{2\,|T(s)|} \cdot \frac{-2\,R_{11}\,X_{11}}{[(R_s + R_{11})^2 + X_{11}^2]} \tag{1.8}$$

Now suppose $R_{11} = R_s$ and $X_{11} = 0$, then, from equations (1.3), (1.7) and (1.8), we have

$$P_L = P_{IN} = \frac{|V_i|^2}{4\,R_s} \tag{1.9}$$

$$\text{and} \quad \frac{\partial |T(s)|}{\partial R_{11}} = \frac{\partial |T(s)|}{\partial X_{11}} = 0 \tag{1.10}$$

Combining equations (1.10), (1.6), and (1.5) gives

$$S_x^{|T(s)|} = 0 \tag{1.11}$$

Note that equation (1.9) represents the power delivered to the load, R_L, and is equal to the maximum power that the source can supply. Therefore if we can design the LC network to transfer maximum power from the source into the load then the above assumed conditions (i.e. $R_{11} = R_s$ and $X_{11} = 0$) would be satisfied and the first order differential sensitivity of the modulus of the transfer function to any reactive component of the network would be zero, as indicated in equation (1.11). Now let us consider an intuitive interpretation of the above result.

Suppose the loss-frequency response of the network is equiripple in the passband and that maximum power is delivered to the network at frequencies w_1, w_2 and w_3, as illustrated in Fig 1.5(a). Since the LC part of the network is lossless, all the power entering the network at

these frequencies must be transmitted to the load R_L. Thus the power P_L delivered to the load is $P_L = |V_o|^2 / R_L$. Since maximum power is being transmitted to the load then any change in the value of a component x of the reactive part of the network, wether it be an increase or a decrease, can only cause a decrease in the power being delivered to the load. Hence the characteristics of the filter loss function, at the frequencies of maximum power transfer, plotted against the change in the value of the component x is as shown in Fig 1.5(b), from which we conclude that $\partial|T(s)| / \partial x_i = 0$. The result given in equation (1.11) follows directly on substituting for $\partial|T(s)| / \partial x_i$ in equation (1.5).

Now since the loss characteristic is a continuous function of frequency it is reasonable to expect that the sensitivity at frequencies between the frequency points of maximum power transfer will remain small. Therefore an LC filter which can be designed to deliver maximum power to the load at some frequencies in the passband will have low sensitivity in the entire passband. This argument of low sensitivity does not apply in the stopband or the transition-band (i.e. the region between the passband and the stopband), but this is not very serious limitation because in most filter applications the passband is the most critical region from the point of view of sensitivity.

We have shown above that the sensitivity of the modulus of the voltage transfer function of an LC filter network to changes in reactive elements is small. Let us now examine the sensitivity of $|T(s)|$ to changes in the terminating resistors (i.e. R_s and R_L in Fig 1.1(b)), under the assumption that the LC network has been designed to give maximum power transfer at some frequency points in

the passband. It has been stated earlier that at points of maximum power transfer, $R_{11} = R_s$ and $X_{11} = 0$; therefore, from equation (1.4) we see that the modulus of the voltage transfer ratio, T(s), is given by

$$|T(s)| = \frac{1}{2}\sqrt{\frac{R_L}{R_s}} \tag{1.12}$$

Hence, using equations (1.1) and (1.12), we can derive the sensitivity expressions for the terminating resistors.

$$\text{i.e.} \quad S_{R_L}^{|T(s)|} = -S_{R_s}^{|T(s)|} = \frac{1}{2} \tag{1.13}$$

By the same argument as in the case of reactive components, the sensitivity expressions given in equation (1.13) are expected to be of similar magnitude at other frequencies in the passband between the frequency points of maximum power transfer [33].

Thus the sensitivities of the response of an LC filter network to changes in the values of the reactive elements and the terminating resistors are 0 and $\pm\frac{1}{2}$, respectively, at frequencies of maximum power transfer. The only question now remaining to be answered is whether LC ladder networks can be designed to deliver maximum power to the load. It is indeed quite possible to design LC filter networks with all types of response characteristics (e.g. Butterworth, Chebyshev, inverted Chebyshev and elliptic) which satisfy this important requirement; infact the LC ladder networks obtained from most filter Tables fall into this class of networks.

Above we have only considered the sensitivity to infinitesmal changes in the element values; however there is much empirical

evidence to show that LC filters are also relatively insensitive, in the passband, to finite changes in element values [11,34,35].

The above low sensitivity argument applies to the passband sensitivity of a general LC network. However, the stopband sensitivity of LC networks is dependent on the type of structure used. For example, in the stopband, where the loss of an LC network is high, the LC lattice structure acts like a bridge which is close to balance (it is exactly balanced at frequencies of infinite loss). Consequently the response in the stopband is very sensitive to changes in the values of the reactive elements. On the other hand in the case of LC ladder structure each element is responsible for only a part of the total loss and consequently the response in the stopband is relatively insensitive to element value changes.

1.2.4 The idea of simulation of LC filters

In the previous subsection it has been shown that certain types of resistively terminated LC filters exhibit extremely low sensitivity of filter response (both in the passband and the stopband) to variation of component values. This low sensitivity performance of LC ladder filters, together with the wealth of knowledge that has accumulated over the years in the area of passive LC ladder filter design, provides a strong motivation for designing active RC filters based on the simulation of passive LC ladder prototypes. As mentioned in Section 1.1, the two most commonly used methods of simulating LC ladder filters, by active RC networks, are the signal flow graph simulation and the element and structure simulation of LC filters. In the signal flow graph simulation approach the relationships between the network variables (e.g. the nodal voltages and the branch

currents) are expressed mathematically in terms of the branch impedances and from these a signal flow graph of the circuit is constructed which is subsequently realised using active RC sections and summers [36] (the active RC sections can be first or second order sections, e.g. integrators or biquadratic sections). On the other hand, in the element and structure simulation approach impedances of certain branches (e.g. the inductor branches) are replace by active RC circuits simulating the corresponding impedances.

One main disadvantage of the above simulation methods is that they require relatively large number of amplifiers compared with the cascade method. In the cascade realisation method the required voltage transfer ratio is represented as a product of second order transfer functions (and one first order transfer function in the case of odd order filters), which are then realised using single or multiple amplifier second order sections; thus by this method an N-th order filter can be realised by N/2 amplifiers (the first order section, in the case of odd N, is usually realised as a passive RC section). In contrast, for the signal flow graph simulation method the number of amplifiers is equal to the number of reactive components in the prototype filter if first order sections (i.e. integrators) are used; whereas the element and structure simulation method requires two amplifiers to simulate a grounded element and four amplifiers to simulate a floating element.

In order to reduce the number of amplifiers some "tricks" of the trade are at the designer's disposal. For example, in the case of signal flow graph simulation the number of amplifiers can be reduced by carrying-out simple manipulations on the signal flow graph of the filter such that it allows the use of second order active RC sections;

whereas, in the element and structure simulation method the number of amplifiers can be reduced considerably by choosing a "suitable" structure to be simulated.

In view of the availability of low cost integrated circuit operational amplifiers, the above concern about the number of amplifiers may not appear as a serious economic matter. However increase in the DC power requirement and the problem of heat dissipation are often two important reasons for reducing the number of amplifiers.

The signal flow graph simulation and the element and structure simulation methods have been extensively studied over the past 10-15 years and as a result of this activity a large amount of litrature is available on these approaches. In the remainder of this chapter a short literature review on these simulation methods is presented. The emphesis is laid on presenting the fundamental principles of each approach and examining it from the practical implementation point-of-view, rather than carrying-out a critical comparison between the work of various authors. Since there is a fundamental difference between the design procedures of the two simulation techniques each is discussed separately.

The signal flow graph simulation (which is also often referred to as the leap-frog type multiple feedback) will be discussed in the wider context of multiple feedback filters. This is justified, since some multiple feedback topologies (e.g. follow the leader feedback, minimum sensitivity topology [12], etc.) which although they cannot be classified as simulation of LC filters, exhibit low sensitivity

properties and hence are appropriate for inclusion in the present discussion on low sensitivity filters.

1.3 Simulation of the signal flow graph of LC filters

1.3.1 General

The method of designing low sensitivity active RC filters by the so called multiple feedback approach can be divided into two main groups. The first of these groups encompasses multiple feedback structures which are obtained by means of a signal flow graph from LC filter prototypes; we shall refer to these as "leap-frog" type multiple feedback filters. All other multiple feedback structures fall within the second group and we shall refer to these as "other" types of multiple feedback filters.

The leap-frog multiple feedback method of simulating LC filters was first discussed in detail by Girling and Good [19], who proposed the name "leap-frog" [18] for the resulting networks. This method of LC filter simulation is also referred to as "direct signal flow graph simulation" [36] or "operational simulation" [37] of LC filters. For this method, negative integrators together with inverting summers form the basic building blocks. One apparent drawback of this method is that for a given order filter a relatively large number of active devices (i.e. operational amplifiers) would be required compared with other realisation techniques (e.g. the cascade or the element and structurs simulation methods). However, by carrying-out simple manipulative operations, the signal flow graph of the LC prototype filter can be modified such that it is possible to use biquadratic sections (and one first order section in the case of odd order

filters) and thus obtain a reduction in the number of amplifiers. The possibility of using biquadratic sections in the simulation of low sensitivity LC filters, via the leap-frog multiple feedback method, has led over the past ten years to much research activity in the general field of multiple feedback filters, and as a result of these efforts other multiple feedback topologies (e.g. follow the leader) [12,13] have been derived which, in some cases, give low sensitivity active RC realisations.

The use of biquadratic sections as the basic building blocks, in multiple feedback structures, introduces considerable flexibility in the design of these filters and it also has numerous other advantages. For example, the cascade method has led to successful production of microelectronic filters [11,38], therefore the type of fabrication technology used for this method is readily adaptable for the multiple feedback filters which use the biquadratic section as the basic building block. The amount of knowledge and experience that has been gained over the years in the area of design and adjustment of second order biquadratic sections, provides a strong motivation to adopt the biquadratic section as the basic building block. Another advantage of using biquadratic sections is that there is a considerable reduction in the total number of OP-AMPs required, compared with the operational simulation method [37], since each biquadratic section can be realised using only a single OP-AMP.

In this thesis, we shall only consider multiple feedback structures which employ the biquadratic section as the basic building block; we shall further assume that this building block is realised by means of single amplifier biquadratic (SAB) circuits. The problem of designing multiple feedback filters thus involves the design of SAB

circuits. In subsection 1.3.3 we shall present some typical well known SAB circuits and discuss the points which should be taken into account when deciding which of the many available SAB circuits to use.

1.3.2 Leap-frog type multiple feedback filters

There are two ways of deriving filter structures employing leap-frog type multiple feedback. Firstly, if we are given a specific transfer function to synthesise then by assuming a general leap-frog type feedback structure we can derive design equations by equating coefficients of the given transfer function with those of the transfer function obtained by analysis of the multiple feedback structure. Secondly, in the case when an LC prototype filter is given the corresponding leap-frog multiple feedback structure can be obtained by deriving a signal flow graph or by carrying-out matrix operations on the state variable equations. In the former method, referred to as coefficient matching, the design equations obtained become non-linear for transfer functions of order greater than three [12], and hence these equations can only be solved numerically. An alternative approach to the transfer function synthesis method is presented in [14], where a "pseudo-ladder" network is formed by assigning biquad voltage transfer functions to the series impedances and the shunt admittances of the pseudo-ladder network; this enables one to synthesise the leap-frog ladder in a manner similar to passive ladders.

Since the central theme of this thesis is the simulation of LC filters, we shall now show how to derive leap-frog feedback structures using the second approach mentioned above.

Let us consider the fifth order all-pole lowpass LC prototype filter shown in Fig 1.6(a). The equations describing this circuit are :

$$\left.\begin{aligned} I_1 &= \frac{1}{R_s}(V_i - V_1) \\ V_1 &= \frac{1}{sC_1}(I_1 - I_2) \\ I_2 &= \frac{1}{sL_2}(V_1 - V_2) \\ V_2 &= \frac{1}{sC_3}(I_2 - I_3) \\ I_3 &= \frac{1}{sL_4}(V_2 - V_o) \\ V_o &= \frac{R_L}{sC_5 + 1} I_3 \end{aligned}\right\} \qquad (1.14)$$

The above network equations can be represented by the signal flow graph block diagram shown in Fig 1.6(b), from which we observe that the structure is realisable using first order blocks (i.e. integrators); also note that the variables at the output of these blocks are either the node voltages of the prototype filter, or the currents of the series branches of the prototype filter. Since our intention is to use biquadratic sections (with one first order section in the case of odd order filters), we need to carry-out some manipulative steps on the signal flow graph of the filter in order to obtain the signal flow graph in the desired form. For this purpose, equations (1.14) are represented in a more familiar signal flow graph form which is shown in Fig 1.6(c).

There are many ways in which a given signal flow graph can be manipulated in order to yield the same end result; intermediate steps of one such manipulative procedure are shown in Fig 1.6(c) —— (h). Note that the realisation of the signal flow graph in Fig 1.6(h)

requires two biquadratic sections and one first order section (a positive integrator); furthermore, since the sections are coupled by negative feedback loops, at the inputs of sections one and two we require to produce the difference of two signals and usually extra OP-AMPs would be needed to perform this task. However, the coupling feedback loops in Fig 1.6(h) can be made positive if the central section is negated (i.e. if it is made a negative integrator), in which case the summers at the input of the first and second sections can be incorporated into the appropriate section without requiring any extra OP-AMPs [13,39].

Therefore, the fifth order lowpass filter of Fig 1.6(a) can be realised by the block diagram of Fig 1.6(i), in which the second order sections are represented by their usual intermediate parameters, i.e. the resonance frequency (w_o), the Q-factor (Q_o) and the gain factor (A). The relationship between the sectional parameters and the components of the ladder prototype of Fig 1.6(a) are given in Table 1.1. Note that the restriction of feedback coefficients to a value of unity in Fig 1.6(i) can be removed by scaling the structure accordingly, e.g. in Fig 1.6(i) the feedback factor from output of the second section to the input of the first section can be made F_{12} (>0) if we simultaneously divide and multiply the transfer functions of the second and the third sections by F_{12}, respectively. This technique of scaling can infact be used to optimise the dynamic range of such filter structures [37]. The above scaling method ensures that the loop gains are not altered; thus as long as we keep the loop gains constant, the forward gain factors of the sections

(i.e. A_1, A_2 and A_3) can be scaled to achieve any desired overall gain.

It has been shown above that the signal flow graph of a filter can be reduced such that the resulting structure can be realised with biquadratic sections (and one first order section in the case of odd order filters) which are connected in a so-called leap-frog configuration. It has been stated previously that there is not a unique way of obtaining a suitable signal flow graph, and furthermore the end result in itself is not unique. For example, there are three possible realisation schemes for the fifth order filter discussed above. The first scheme is the one shown in Fig 1.6(i) in which the outer two sections are biquadratic in form (with finite Q-factors) and the central section is of first order. In the second scheme we can have sections one and two as biquadratic and the third section as a lossy-integrator. Altenatively, in the third scheme we can have the first section as a lossy-integrator and sections two and three as biquadratic sections. It can be easily shown that if the signal flow graph is manipulated such that we obtain a biquadratic section in the middle (e.g. schemes two and three discussed above) then its Q-factor will be infinite. Due to high sensitivity and the practical difficulties associated with very high-Q circuits, the use of infinite Q-factor biquadratic sections is undesireable and for this reason the signal flow graph manipulation in Fig 1.6 is aimed towards producing the structure shown in Fig 1.6(i).

Let us now make some observations regarding the sensitivity of the leap-frog multiple feedback structure derived above. In Fig 1.6(a), a change in any of the feed-forward blocks can be directly related to an equivalent change in one of the components of the LC

ladder prototype. As a consequence of this fact, it is sometimes stated in the litrature that there is one-to-one relationship between the elements of the prototype filter of Fig 1.6(a) and the elements of the active realisation of Fig 1.6(b). It can be shown that a change in any of the feedback factor in Fig 1.6(b) can be translated as representing a simultaneous changes in one or more components of the prototype filter (this is done by scaling the structure in Fig 1.6(b) such that all feedback loops have a value of minus one). Thus the structure of Fig 1.6(b) is said to retain the low sensitivity properties of its LC counterpart.

In the case of the leap-frog structure of Fig 1.6(i), any change in the parameters of the sections cannot be considered as being representative of an equivalent change in one of the elements of the prototype ladder; therefore, we do not have a direct one-to-one correspondence between the components of the ladder prototype and the parameters of the sections in Fig 1.6(i). However, suppose a component in the active RC circuit realising the first section in Fig 1.6(i) changes such that the resonance frequency, the Q-factor and the gain-factor of the circuit are changed. These changes in w_{o1}, Q_1 and A_1 can be interpreted , through Table 1.1, as some equivalent changes in terms of the ladder elements (e.g. C_1, L_2, R_L, etc.). The changes in the feedback factors, in Fig 1.6(i), can also be interpreted in terms of some equivalent changes in the gain-factors of the feed-forward sections. Thus, the leap-frog structure of Fig 1.6(i) is said to "duplicate" the low sensitivity properties of its LC prototype; this fact has also been confirmed by pratical observations [21].

As a second illustrative example of deriving leap-frog filter structures, which use biquadratic sections as the basic building blocks, we shall discuss an all-pole bandpass filter which has been obtained from a lowpass filter by application of the lowpass to bandpass transformation.

Consider the third order lowpass LC filter and its signal flow graph block diagram shown in Figs 1.7(a) and (b), respectively. Now, we can obtain a sixth order all-pole bandpass LC filter structure (see Fig 1.8(a)) by applying the lowpass to bandpass transformation to the structure of Fig 1.7(a). If we apply the mathematical equivalent of the lowpass to bandpass transformation (i.e. $s \longrightarrow s + w_o^2/s$) to the signal flow graph block diagram of Fig 1.7(a), then the signal flow graph block diagram of the corresponding bandpass filter is obtained [40] (see Fig 1.8(b)). Note that all the blocks in Fig 1.8(b) will have biquadratic transfer functions of the bandpass form, i.e.

$$T_i'(s) = \frac{A_i' \ (s/w_{oi})}{(s/w_{oi})^2 + Q_i^{-1} \ (s/w_{oi}) + 1} \qquad (1.15)$$

where i= 1, 2, 3 and w_{oi}, Q_i and A_i' are the resonance frequency, the Q-factor and the gain-factor, respectively, of the biquadratic section.

The relationships between the sectional parameters (i.e. w_{oi}, Q_i and A_i') and the components of the LC bandpass filter are given in Table 1.2. Note that in Fig 1.8(b) all the sections have the same

resonance frequency, w_o, where w_o is also the midband frequency of the LC bandpass filter; furthermore, the first and the third sections have finite Q-factors whereas the second section has an infinite Q-factor.

From Table 1.2 we note that any changes in the parameters of the sections in Fig 1.8(b) can be directly interpreted in terms of some equivalent changes in the elements of the prototype LC filter of Fig 1.8(a). For example, for the first section in Fig 1.8(b), changes in w_{o1}, Q_1 and A_1' can be interpreted as some equivalent changes in R_s, C_1 and L_1 of the prototype filter. As explained earlier for the lowpass filter, any changes in the feedback factors can be translated into equivalent changes in the gain-factors of the forward sections. Therefore the leap-frog feedback structure of Fig 1.8(b) retains the low sensitivity properties of its LC counterpart in Fig 1.8(a). It is relevant to point-out here that in single amplifier biquadratic circuits, the realisation of infinite Q-factor transfer functions is usually achieved by cancellation of terms; consequently, if this cancellation is not exact the Q-factor of the circuit becomes finite and if such a circuit is used for the realisation of the middle section in Fig 1.8(b) then this would be equivalent to an appearance of a resistor in series with L_2 and C_2 in Fig 1.8(a).

It has previously been mentioned that the restriction of feedback factors to values of minus one can be removed as long as the loop gains of the structure remain unaltered. In order to show how this can be implemented let us consider the leap-frog feedback structure of Fig 1.8(b). The form of the transfer function of each section in Fig 1.8(b) is given by equation (1.15), whereas the relationships between the sectional parameters (i.e. w_{oi}, Q_i and A_i') and the

components of the LC prototype filter are given in Table 1.2. Now let us assume that F_{12} and F_{23} are to be the feedback factors coupling the various sections of the multiple feedback topology, as shown in Fig 1.9. The transfer functions of the second order sections in Fig 1.9 have the form

$$T_i(s) = \frac{A_i \, (s/w_{oi})}{(s/w_{oi})^2 + Q_i^{-1} \, (s/w_{oi}) + 1} \qquad (1.16)$$

where $i = 1, 2, 3$ and w_{oi} and Q_i are given in Table 1.2.

Now, by equating the loop gains of the multiple feedback structures of Figs 1.8(b) and 1.9(a), we obtain

$$-1 \cdot T_1'(s) \cdot T_2'(s) = -F_{12} \cdot T_1(s) \cdot T_2(s) \qquad (1.17a)$$

and $$-1 \cdot T_2'(s) \cdot T_3'(s) = -F_{23} \cdot T_2(s) \cdot T_3(s) \qquad (1.17b)$$

Substituting in the above equations from equations (1.15) and (1.16) and making use of Table 1.2, we obtain

$$F_{12} = [\, w_{o1} \;\; w_{o2} \;\; C_1 \;\; L_2 \;\; A_1 \;\; A_2 \,]^{-1} \qquad (1.18a)$$

and $$F_{23} = [\, w_{o2} \;\; w_{o3} \;\; C_3 \;\; L_2 \;\; A_2 \;\; A_3 \,]^{-1} \qquad (1.18b)$$

Hence, the restriction of the feedback factors, in Fig 1.8(b), to unity can be removed if the relationships expressed in equation (1.18) are observed.

As explained previously, negative feedback factors are undesireable because they give rise to the requirement of extra OP-AMPs to perform the difference at the inputs of sections one and two, in Figs 1.8(b) and 1.9(a). However, if the feedback factors are positive then the summation at the input of a section can be performed by a resistive summation junction using the technique of [39]. In the multiple feedback structure of Fig 1.9(a) the feedback factors F_{12} and F_{23} can be made positive if the signs of $T_1(s)$ and $T_3(s)$ are negated, as shown in Fig 1.9(b).

The overall transfer function, T(s), of the feedback structure in Fig 1.9(b) is given by

$$T(s) = \frac{T_1(s)\ T_2(s)\ T_3(s)}{1 + F_{12}\ T_1(s)\ T_2(s) + F_{23}\ T_2(s)\ T_3(s)} \qquad (1.19)$$

It can be shown that the gain, G_o, at the midband frequency, w_o, is given by

$$G_o = T(jw)_{w=w_o} = \left[\frac{F_{12}}{A_3\ Q_3} + \frac{F_{23}}{A_1\ Q_1} \right]^{-1} \qquad (1.20)$$

In equations (1.18) and (1.20) we have six unknowns (i.e. F_{12}, F_{23}, A_1, A_2, A_3 and G_o), and thus by selecting any three, the values of the remaining unknowns can be calculated by solving these design equations. Hence we have the means of choosing the midband gain of the filter to be any desired value; this can be considered as an advantage of active RC filters, since in LC filters it is generally not possible to achieve this result.

We have shown above how leap-frog type multiple feedback structures are derived from LC prototype filters and have briefly examined the mechanism through which the low sensitivity of the prototype filters is retained in the active RC realisation. Only all-pole filters have been considered, but the leap-frog structures for elliptic filters can be derived in a similar way by starting with an appropriate prototype. Alternatively, the transmission zeros at finite frequencies can also be formed by the "feed-forward" techniques described in [12].

Another type of multiple feedback structure which is also derivable from LC prototypes is the so called "modified" leap-frog feedback topology. In the conventional leap-frog feedback structures the synthesis procedure is based on LC filters which are resistively terminated and as a consequence of this the two sections at either end of the feedback structure have finite Q-factors while all other sections have infinite Q-factors. In contrast, the synthesis of modified leap-frog structures is based on LC filter prototypes in which resistors appear through-out the ladder structure in such a way that all the sections in the feedback structure have finite Q-factors. Hence the modified leap-frog feedback structures do not have minimum passband sensitivity; however the extra degrees of freedom available in the modified leap-frog structures can be used to improve the transition-band and the stopband sensitivities [12,41].

Let us now briefly consider another two multiple feedback topologies which are not of the leap-frog type, but whose low sensitivity behaviour has been substantiated both by computational and practical results. These are the so called follow-the-leader feedback and the minimum sensitivity feedback topologies, which are shown

schematically in Fig 1.10, for a sixth order filter (the transfer function of each block in Fig 1.10 is of second order). The synthesis of these type of feedback networks proceed directly from the required transfer function [12,13].

The follow-the-leader feedback is a general feedback topology which encompasses the primary-resonator-block [42] and the shifted-companion-form [43] as special cases. Furthermore, the minimum sensitivity feedback topology [44] is the most general multiple feedback topology in that all other feedback structures can be considered as special cases of the minimum sensitivity topology. An attractive feature of the minimum sensitivity feedback topology is that it gives lower sensitivity, both in the passband and the stopband, than that is obtainable from the leap-frog or the follow-the-leader feedback topologies [12]. The synthesis procedures for the follow-the-leader and the minimum sensitivity topologies are very complex; since these types of feedback structures are not to be considered in this work the treatment of their synthesis procedures are out side the scope of this thesis. A very good review of all the multiple feedback topologies and a discussion of their basic design philosophies is given in [12].

1.3.3 Single amplifier biquadratic circuits for use in leap-frog multiple feedback filters

In the design of multiple feedback active RC filters biquadratic sections are used as basic building blocks for two main reasons. Firstly, use of single amplifier biquadratic (SAB) circuits allows high order filters to be realised with considerable reduction in the total number of amplifiers required. Secondly, a lot of work has been

done on the design and methods of adjusting second order sections (which have been successfully used in manufacturing active RC circuits designed by the cascade tcchnique) and hence this knowledge can be directly utilised for the realisation of multiple feedback filters.

The general form of the transfer function of a biquadratic section is

$$T(s) = \frac{N(s)}{(s/w_r)^2 + Q^{-1}(s/w_r) + 1} \qquad (1.21)$$

where w_r and Q are the resonance frequency and the Q-factor, respectively, of the section and N(s) determines the type of section, e.g.

$N(s) = a$		Lowpass
$N(s) = b.(s/w_r)$		Bandpass
$N(s) = c.(s/w_r)^2$		Highpass
$N(s) = d.[(s/e)^2 + 1]$	$e = w_r$	Bandstop
	$e > w_r$	Lowpass Notch
	$e < w_r$	Highpass Notch

where a, b, c, d and e are constants.

There are many active RC circuits available for implementing equation (1.21) and the number of OP-AMPs required by these circuits range from a minimum of one to a maximum of four. For high order

filters the use of multi-amplifier biquadratic circuits is unattractive since a large number of amplifiers would be necessary and this would result in increased cost and heat dissipation would be a serious problem. On the other hand, we can over-come these limitations by using single amplifier biquadratic circuits.

A search through the active RC filter literature shows that many different single amplifier topologies have been proposed [45,46,47] for realising the basic biquadratic transfer function of equation (1.21). No systematic procedure is available for selecting tha SAB circuits for a given application. Each SAB circuit has its advantages and disadvantages; hence a direct comparison to determine which SAB circuit is "best" is unfeasible, because the criteria for comparison would be different in different applications. In this subsection we shall present a brief discussion of the points which should be born in mind when considering which SAB circuit to use. We shall also present a few SAB circuits which are frequently used in practice; infact some of these SAB circuits will be referred to in Chapters 2 and 3.

Although, as stated above, there is no general criterion for comparing the different SAB circuits the two most important parameters to be taken into account are cost and performance. In the area of cost, attributes such as the ease of realising the different biquadratic transfer functions, the number of passive components (i.e. resistors and capacitors) required, the resulting spread in element values and the convenience of tuning the SAB circuit, to compensate for initial component tolerances, are considered; whereas the sensitivity of the transfer function, due to changes in passive and

active components, is considered in evaluating the circuit performance.

One SAB circuit, which has the advantage of versatility (i.e. lowpass, highpass, bandpass and bandstop functions are available by using different input terminals) and acceptability of preferred value wide tolerance capacitors, has been proposed by Lim [46]. It basically consists of a unity-gain amplifier with a balanced twin-T feedback network. The bandpass version of this SAB circuit is shown in Fig 1.11(a) from which we note that the circuit is non-cannonic since it requires three capacitors to realise a second order transfer function. In order to obtain the required transfer function a pole-zero cancellation has to take place; also the Q-factor of the circuit is proportional to a ratio of two resistors but the gain factor of the circuit is inversely proportional to the Q-factor. This implies that this circuit is not suitable for realising the infinite Q-factor sections in the leap-frog feedback structures because the spread in the component values would be very unrealistic for practical purposes. For this reason and also due to the effect of the parasitic input capacitance of the OP-AMP, the operation of this circuit is restricted to below 10 kHz and the Q-factor of the circuit is usually restricted to be less than 50. The adjustment procedure for the Lim type SAB circuit is discussed in [11].

Another SAB topology which can be used to realise any of the biquadratic transfer functions and which can also accept preferred value wide tolerance capacitors, has been proposed by Friend [47]. This topology is based on a bandpass design first published by Delyannis [48]. The flexibility and the general usefulness of the Friend SAB topology is stated in [49] and this has resulted in the

development of the STAR (standard tantalum active resonator) circuits in a thin-film hybrid integrated form. The bandpass version of the Friend SAB topology is shown in Fig 1.11(b) and its transfer function (assuming the OP-AMP to be ideal) is given in equation (1.22)

$$T_F(s) = \frac{-A\,(s/w_o)}{(s/w_o)^2 + Q^{-1}\,(s/w_o) + 1} \qquad (1.22)$$

where $$w_o = [C_1C_2R_1R_2]^{-1/2} \qquad (1.22a)$$

$$Q = [(C_1R_1/C_2R_2)^{1/2} + (C_2R_1/C_1R_2)^{1/2} - (R_b/R_a)\,(C_1R_2/C_2R_1)^{1/2}\,]^{-1} \qquad (1.22b)$$

and $$A = (C_1R_2/C_2R_1)^{1/2}\,(1 + R_b/R_a) \qquad (1.22c)$$

From equations (1.22a) and (1.22b) we note that the resonance frequency (w_o) and the Q-factor (Q) of the SAB bandpass circuit can be adjusted independently, e.g. w_o by means of R_2 and Q by means of R_b. Furthermore, the gain factor A of the circuit can be reduced from the value given by equation (1.22c) by splitting resistor R_1 into a voltage divider, as shown in Fig 1.11(b). This principle can be used to form a summation junction at the input of a section [39] as required in multiple feedback structures. Since the Q-factor of the circuit is defined by the difference of terms (see equation (1.22b)), it is possible to realise transfer functions with very high Q-values

(even infinite Q-values, if desired), without having a large spread in component values.

Another family of SAB circuits which is frequently used in practice was first proposed by Sallen and Key [45]. The bandpass version of the Sallen and Key SAB circuit is shown in Fig 1.11(c) and its transfer function (assuming the OP-AMP is ideal) is given by

$$T_{SK}(s) = \frac{A\,(s/w_o)}{(s/w_o)^2 + Q^{-1}\,(s/w_o) + 1} \tag{1.23}$$

where $$w_o = [(C_1C_2R_1R_2)/(1 + R_1/R_3)\,]^{-1/2} \tag{1.23a}$$

$$Q = (1 + R_1/R_3)^{1/2}\,[(C_1R_1/C_2R_2)^{1/2} + (C_2R_1/C_1R_2)^{1/2} + (C_2R_2/C_1R_1)^{1/2} - (R_1R_a/R_3R_b)\,(C_2R_2/C_1R_1)^{1/2}\,]^{-1} \tag{1.23b}$$

and $$A = (1 + R_a/R_b)\,[\,C_2R_2/(C_1R_1(1 + R_1/R_3))\,]^{1/2} \tag{1.23c}$$

This SAB bandpass circuit offers the same sort of flexibility as the Friend SAB circuit; e.g. preferred value wide tolerance capacitors can be used, the resonance frequency and the Q-factor of the circuit can be adjusted independently (see equations (1.23a) and (1.23b)), and transfer functions with very high (including infinite) Q-factors can be realised. Also the gain factor A of the circuit can be reduced from the value given by equation (1.23c) by splitting resistor R_1 into a voltage divider, as explained above.

From equations (1.22) and (1.23) we note that the transfer function of the Friend SAB bandpass circuit has a negative sign, whereas the transfer function of the Sallen and Key SAB bandpass circuit has a positive sign. In leap-frog multiple feedback filters we need SAB sections with positive and negative sign transfer functions (e.g. see Fig 1.9(b)). In the realisation of a sixth order leap-frog feedback bandpass filter to be considered in the next Chapter we shall adopt the Friend and the Sallen and Key SAB circuits discussed above. The Lim circuit (Fig 1.11(a)) is not adopted because it is not canonic.

It is seen from above that under the assumption of ideal OP-AMPs the design equations of the Friend and the Sallen and Key SAB bandpass circuits are simple. However, a very complex set of design equations results if the OP-AMP imperfections are taken into account. Neglecting the imperfections of the OP-AMPs would confine the operation of the circuits to very low frequencies and it would not be possible to design practical circuits. Of all the OP-AMP imperfections the one which limits the frequency range, and hence is most serious, is the finite gain-bandwidth product, f_T, of the OP-AMP. In Chapter 2 we shall examine more closely the effect of finite f_T on the Friend and the Sallen and Key SAB bandpass circuits. It will be shown there that while the technique of predistorting the design allows practical design of SAB circuits in the presence of finite f_T OP-AMPs, the overall response of the structure in which these SAB circuits are used may not be satisfactory; hence, it may be necessary to resort to other ways of counter-acting the effect of the finite f_T (one such possibility will be presented in Chapter 2).

1.4 Simulation of the elements and the structure of LC filters

1.4.1 General

It has been shown in Section 1.2.3 that resistively terminated LC ladder filters, which are designed for maximum power transfer, have very low sensitivity of their response to changes in component values in both the passband and the stopband. The necessity to simulate LC filter structures using active RC networks stems from the fact that we wish to retain the low sensitivity properties of the LC networks in active RC realisations. The basic philosophy of the element and structure simulation method is to some-how "eliminate" the inductors (which cannot be realised microelectronically) by using active RC circuits. There are two main approaches for accomplishing this task

1. inductors in the prototype filter are replaced by active RC circuits,
2. the prototype LC filter is impedance scaled by a factor (w_{ref}/s) which has the effect of transforming the resistors, inductors and capacitors of the prototype LC filter into capacitors, resistors and super-capacitors (i.e. impedance proportional to s^{-2}), respectively, and the objective in this case is to replace these super-capacitors by active RC circuits.

The above two simulation approaches have been extensively studied in the past and as a consequence of this a large amount of literature is available on the subject. In this section we shall discuss the basic principles of the above two simulation approaches, which can be viewed as impedance simulation methods. The design of structure simulation methods is usually based on some sort of conceptual units, such as impedance converters and impedance inverters, which are

realised by means of active RC circuits. Gyrators and positive impedance converters (PICs) form two such conceptual units and these have been extensively used in the element and structure simulation method. Hence it is appropriate to start our discussion by reviewing the definitions and some properties of these building blocks.

A gyrator, the symbolic representation of which is shown in Fig 1.12(a), is a 2-port network having the transmission matrix

$$\begin{bmatrix} V_1 \\ I_1 \end{bmatrix} = \begin{bmatrix} A & B \\ C & D \end{bmatrix} \begin{bmatrix} V_2 \\ I_2 \end{bmatrix} = \begin{bmatrix} 0 & R_o \\ R_o^{-1} & 0 \end{bmatrix} \begin{bmatrix} V_2 \\ I_2 \end{bmatrix} \qquad (1.24)$$

where R_o is called the gyration resistance.

Now if port 2 in Fig 1.12(a) is terminated by impedance Z then the impedance presented at port 1 is R_o^2/Z. Hence if Z represents a grounded capacitor then a grounded inductor is realised at port 1, as shown in Fig 1.12(b) [50]. This concept has been extended to realise a floating inductor as shown in Fig 1.12(c) [51]. Thus we have the means of simulating any inductor network and hence any LC filter. In the 3-terminal circuits realising gyrators, the zeros in the transmission matrix (see equation (1.24)) are produced by cancellation of terms and as a consequence of this extra sensitivities are introduced into the active circuit, which have no counterpart in the LC network, when the conditions for the cancellation are not satisfied. This problem does not rise in 4-terminal gyrator circuits [52]; however 4-terminal gyrator circuits cannot be used to realise floating inductors because they require floating power supplies, which is undesireable for practical reasons.

The positive impedance converter (PIC) is a 2-port network which when terminated at one port in an impedance Z, represents an impedance k.Z at the other port (k is a dimensionless quantity and is called the PIC scaling factor) [53]. The transmission matrix definition of a commonly used "current" converting type PIC is

$$\begin{bmatrix} V_1 \\ I_1 \end{bmatrix} = \begin{bmatrix} A & B \\ C & D \end{bmatrix} \begin{bmatrix} V_2 \\ I_2 \end{bmatrix} = \begin{bmatrix} 1 & 0 \\ 0 & k \end{bmatrix} \begin{bmatrix} V_2 \\ I_2 \end{bmatrix} \qquad (1.25)$$

The symbolic representation of a PIC together with the directions of the port voltages and currents are shown in Fig 1.13(a). Suppose we load the PIC in Fig 1.13(a) with impedance Z at port 2, then the impedance presented at port 1 is $Z_{in_1} = k^{-1} Z$, whereas if Z is connected across port 1, then the impedance presented at port 2 is $Z_{in_2} = k Z$; hence the PIC has impedance transforming properties.

The PIC scaling factor, k, can have either of two forms corresponding to two types of PICs; these are the s-type PIC, for which k is proportional to $s^{\pm 1}$, and the s^2-type PIC, for which k is proportional to $s^{\pm 2}$. The above current converting type PIC is usually realised as shown in Fig 1.13(b). This circuit was first proposed by Antoniou [52] and is sometimes referred to as a generalised impedance converter (GIC). The value of the PIC scaling factor k is related to the impedances in Fig 1.13(b) by the following expression

$$k = \frac{Z_2 Z_4}{Z_1 Z_3} \qquad (1.26)$$

From equation (1.26), we note that the realisation of the s-type PIC would require one of the four impedances to be a capacitor, whereas

the s^2-type PIC would require two of the four impedances to be capacitors.

Simulation of a grounded inductor can be achieved by terminating a s-type PIC by a resistor, as illustrated in Fig 1.13(c). Floating inductors can be simulated by using two s-type PICs and a resistor, as shown in Fig 1.13(d). Furthermore, simulation of super-capacitors (i.e. impedance proportional to s^{-2}) and super-inductors (i.e. impedance proportional to s^2 can be obtained by using s^2-type PICs terminated by resistors. Hence we can simulate any inductor or super-capacitor network and hence effectively have the means of simulating any LC filter.

Unlike some gyrator circuits, the zeros in the transmission matrix (see equation (1.25)) are not produced by cancellation of terms and hence any changes in the impedances of the circuit in Fig 1.13(b) can be interpreted as only affecting the PIC scaling factor (see equation (1.26)). Thus no extra sensitivities are introduced by the passive components forming the PIC circuit. The effect of the finite gain-bandwidth products (f_T's) of the OP-AMPs in the circuit has been studied in detail and various methods of designing the PICs "optimally", to minimise the active sensitivity, have been proposed [54,55,56,57]. The functional adjustment of PIC circuits has been studied [29] which allows the use of preferred value wide tolerance capacitors and also full compensation for the finite f_T effects can be achived, at a single frequency, by laser trimming of resistors. These efforts have culminated in the development of low cost, high quality, high precision microelectronic filters, in the frequency range from about 10 Hz to about 110 kHz, which are now in

production [5,7] and are based on a design philosophy [6] which uses the PIC as the basic building block.

Several impedance converter / inverter circuits which use only a single OP-AMP have been proposed for simulating grounded inductors [58,59,60] and grounded super-capacitors [35,61]. These circuits derive their impedance expressions by cancellation and matching of terms and hence they generally have higher sensitivities than the circuits using the PIC. Another major disadvantage of these single amplifier circuits is that it is not possible for all the capacitors in the simulated filter to have preferred values or wide tolerances. However by using these single amplifier circuits a considerable reduction in the total number of OP-AMPs used for the overall filter can be achieved than if the same filter is realised with PICs.

In the next subsection we shall discuss the various methods which have been described in the literature over the past fifteen years for simulating the elements and the structure of LC filters.

1.4.2 Method of simulation

The very first methods proposed for simulating resistively terminated LC ladder filters by active RC networks may be classified as inductor simulating methods [22,50,62,63]. The basic principle of the inductor simulation methods is that each inductor in the LC prototype network is replaced by an active RC circuit while the resistors and capacitors of the prototype network remain unchanged. The inductors are realised either by capacitively terminated gyrators or by resistively terminated PICs; one gyrator or one PIC is required

for a grounded inductor while two gyrators or two PICs are required for a floating inductor. The major drawback of this approach of simulating each inductor separately is that large number of OP-AMPs would be required. However, the inductor simulation method using PICs has been generalised by Gorski-Popiel [15] which results, in most cases, in a significant reduction in the number of PICs that are required to realise a given filter network. The basic principle of Gorski-Popiel's method is illustrated in Fig 1.14, where we start with an LC network from which we "pull-out" all inductors to create an L subnetwork and an RC subnetwork, while maintaining all the links between the two subnetworks. The L subnetwork is now replaced by a topologically equivalent R subnetwork and PICs (with scaling factor proportional to s^{-1}) are inserted in the links between the R subnetwork and the RC subnetwork*.

In the above method of simulation only the inductive part of the prototype network is simulated and the resistive and the capacitive parts of the prototype network appear unaltered in the active realisation. Now in LC networks the capacitors in general have non-preferred values and require narrow tolerances hence it follows that the active RC networks derived by the above method will also require non-preferred value narrow tolerance capacitors, which leads to increase in production costs as mentioned in Section 1.1. Note that the capacitors occuring within the PIC circuits can have wide tolerances since we can adjust the scaling factors of the PICs by means of resistors within the PIC circuit.

---

* A similar generalisation has been proposed for the gyrator approach in which case the L subnetwork is replaced by a network of capacitors viewed via a multi-gyrator [64].

As an illustrative example of the above simulation method, let us consider the LC network shown in Fig 1.15(a). The active RC realisation of this network is shown in Fig 1.15(b) for the case when each inductor is simulated individually (note that in order to save one PIC, we have interchanged the positions of L_6 and C_5 to make L_6 grounded). The active RC realisation of the LC network in Fig 1.15(a), using the Gorski-Popiel's method is shown in Fig 1.15(c). The fewer number of PICs required by the Gorski-Popiel's method is quite obvious from Figs 1.15(b) and (c).

Another approach to the simulation of LC ladder filters, which is usually referred to as the impedance scaling method, was originally proposed by Bruton [16]. The basic principle of this approach is that the voltage (or the current) transfer ratio of a filter being a dimensionless quantity is not affected if the impedances of all the branches of the ladder filter are multiplied (i.e. are scaled) by the same factor. Thus by appropriatly choosing the scaling factor, we can eliminate the inductors in the prototype network. For example, consider the lowpass filter shown in Fig 1.6(a); if all the impedances in Fig 1.6(a) are multiplied by w_{ref}/s (where s is the complex frequency variable and w_{ref} is a reference frequency) then the inductors become resistors, the resistors become capacitors and the capacitors become components with an impedance proportional to s^{-2}, which Bruton termed "frequency dependent negative resistors" (fdnr's) because their impedances become proportional to $-1/w^2$ at real frequencies (i.e. s=jw) [65]. The impedance scaled version of the circuit in Fig 1.16(a) is shown in Fig 1.16(b) together with the symbol for the fdnr elements, which we shall refer to as super-capacitors in order to distinguish these components from those

with impedances proportional to s^2, which are another type of fdnr's and we shall refer to these as super-inductors. The super-capacitors in Fig 1.16(b) can be realised using s-type PICs (with scaling factor proportional to s^{+1}) terminated by a capacitor [16], as shown in Fig 1.16(c), or by s^2-type PICs (with scaling factor proportional to s^{+2}) terminated by resistors [7]. In Fig 1.16(c) all capacitors, with the exception of C_s and C_L, may have preferred values with wide tolerances, since the resistors within each PIC circuit can be adjusted to compensate for any variations in the capacitor values; however, the manufacturing tolerance for C_s and C_L is restricted to be that of R_s and R_L in the prototype filter (this tolerance is typically $\pm$ 2 % to $\pm$ 5 % [5]).

In the above example, we have only encountered grounded super-capacitors whereas for bandpass and bandstop filters both grounded and floating super-capacitors would be obtained. In order to minimise the number of PICs required for such circuits, use can be made of Gorski-Popiel's idea of splitting the impedance scaled version of the prototype network into one subnetwork containing resistors and capacitors and another subnetwork containing super-capacitors; the super-capacitor subnetwork is then realised either by a topologically equivalent capacitor subnetwork, or by a topologically equivalent resistor subnetwork which is connected to the RC subnetwork via PICs having the appropriate scaling factors.

The Gorski-Popiel's and Bruton's methods of simulating LC filters have been interpreted in a slightly different way [6,7,29], and are referred to as partial, and modified partial, impedance scaling methods, respectively. The term "partial" arises from the fact that in the Gorski-Popiel's method only part of the prototype network

(i.e. only the inductive part) is impedance scaled. Bruton's method of simulating lowpass filter structures (in which all capacitors are grounded) can be viewed as modification of the Gorski-Popiel's method. For example, in Fig 1.16(a) if we had used the Gorski-Popiel's partial impedance scaling method, then the active RC realisation would have been as shown in Fig 1.16(c) with two s-type PICs inserted at positions marked "X" and capacitors C_s and C_L replaced by resistors R_s and R_L, respectively. Hence the circuit in Fig 1.16(c) can be considered as being obtainable by "modifying" the partial impedance scaling approach of Gorski-Popiel.

In the "full" impedance scaling approach mentioned in [6,7,29], the LC network is partitioned into an inductor and a capacitor subnetworks with the terminating resistors being associated with the inductor subnetwork. The subnetwork containing inductors and the terminating resistors is impedance scaled by a factor k_L/s , where k_L is a constant; this has the effect of transforming the inductors and the resistors into resistors and capacitors, respectively. The capacitor subnetwork of the LC filter is also impedance scaled but using a scaling factor s/k_C , where k_C is a constant, which transforms the capacitor subnetwork into a resistor subnetwork. The effect of impedance scaling the subnetworks is compensated by inserting PICs, having a scaling factor $s^2/(k_L\ k_C)$, in the links between the two subnetworks. The principle of the full impedance scaling method is illustrated in Fig 1.17. In the full impedance scaling method of simulating LC filters, all capacitors, except the two corresponding to the terminating resistors, occur inside the PIC circuits and thus they can have any preferred values by design, with wide manufacturing tolerances.

Let us now look at the sensitivity aspects of the active RC networks derived by the above simulation methods. The passive components in the active RC realisations can be classified into two groups; those within the subnetworks and those within the PICs. By the virtue of the fact that the impedance of each element in the subnetworks is proportional to the impedance of an element in the corresponding prototype network it follows that the sensitivity of the amplitude response of the active network to changes in the values of the subnetwork elements is low [22]. It can be shown that the sensitivity of the amplitude response of the active RC network to the passive elements within the PICs is low provided the network satisfies the "PIC embedding constraint" given in [6,7,29]. The main contribution to the active sensitivity of the simulated network arises from the finite gain-bandwidth products of the OP-AMPs used in the realisation of the PIC circuits. Methods of compensating for the finite f_T's by adjusting the resistors inside the PIC circuits and techniques for designing the PIC circuit to minimise the effect of finite f_T's have been proposed in the litrature [6,29,54,56]. Thus the simulated active RC networks can be designed to retain the low sensitivity properties of their passive LC prototype counterparts.

1.5 Purpose of present thesis

The purpose of this thesis is to study in detail two methods suitable for designing high-precision low sensitivity active RC filters. The design methods to be studied are the "signal flow graph" simulation of LC filters and the simulation of the "elements and the structure" of LC filters. In both of these methods low sensitivity resistively terminated LC filters are used as prototypes. The

attractiveness of these methods lies in the fact that the active RC circuits obtained, retain the low sensitivity properties of their LC prototype counterparts.

The signal flow graph simulation method gives rise to leap-frog type multiple feedback structures in which integrators and / or biquadratic sections are used as the basic building blocks. Thus the design problem of this approach involves the design of first and / or second order sections. In Chapter 2, we consider the design of an all-pole sixth order bandpass filter which can be realised using three second order bandpass sections interconnected with leap-frog type feedback. This filter is realised using three single amplifier biquadratic (SAB) circuits (in order to minimise cost, power consumption and heat dissipation) and it is shown that in order to design practical circuits the effect of the finite f_T of the OP-AMPs must be taken into account at the design stage; it is further shown that the conventional techniques of predistorting the design of SAB circuits leads to unsatisfactory results. A compensation technique, which involves the modification of the SAB circuit topology, is proposed and it is shown that by means of this it is possible to fully compensate for any value of the f_T and hence to obtain ideal nominal response characteristics inspite of non-ideal OP-AMPs.

In Chapter 3, the sensitivity aspects of the sixth order leap-frog type bandpass filter considered in Chapter 2 are examined with the view of minimising the sensitivity of the filter due to post-adjustment variations in the components (both passive and active) of the SAB circuits. A criteria is developed for minimising the sensitivity of multiple feedback filters. This criterion is then applied to obtain the optimum design of the sixth order leap-frog

feedback bandpass filter. The active sensitivities of the optimised and the unoptimised designs of the multiple feedback filter are compared in order to show the validity of the sensitivity minimisation criterion. Some practical measurements carried out on the discrete component model of the filter are given together with a brief description of the adjustment method used for the discrete component model.

In Chapter 4, a novel approach to the simulation of the elements and the structure of LC filters is presented. In contrast to the conventional approach of element/structure simulation which uses the positive impedance converter (PIC) as the basic active unit, the new method uses negative impedance converter (NIC) as the basic active unit. Active RC subcircuits are developed for simulating grounded and floating inductors and super-capacitors which are then used in the LC structure (or an impedance scaled version of it) in a novel way such that the number of amplifiers required is in many cases less than the number required by the conventional approaches. Great emphasis is placed on the ability of the resulting active RC circuits to accept preferred value wide tolerance capacitors, which is desirable in order to minimise production costs. The basic principles of the new approach are illustrated by considering all types of filter design examples (e.g. all-pole and elliptic lowpass, highpass and bandpass filters). The sensitivity of the active RC structures is examined by considering a lowpass filter example and it is shown that the active RC circuit retains the low sensitivity properties of its LC prototype.

In Chapter 5, a study of the effect of the finite amplifier gain-bandwidth product (f_T) in NIC circuits is presented. A criterion

for reducing the effect of finite f_T is developed and its effectiveness is illustrated by means of a computed example. Also in Chapter 5, the problem of stability associated with circuits using NICs is considered at some length and it is shown that the stability of most of the NIC circuits can be predicted simply by looking at the amounts of positive and negative feedbacks being applied at zero and infinite frequency to the non-inverting and the inverting terminals, respectively, of the OP-AMP used to realise the NIC.

1.6 Statement of originality

The following main items presented in this thesis are, as far as the author is aware, original:

Chapter 2 ——— The method of fully compensating for the effect of finite f_T's for the Friend SAB bandpass and the Sallen and Key SAB bandpass circuits.

Chapter 3 ——— The sensitivity minimisation criterion developed and used in this chapter.

Chapter 4 ——— The systematic development of the essential subcircuits for simulating grounded and floating inductors and supercapacitors. The derivation of a multitude of simulated inductor and super-capacitor circuits. The novel way (out-lined in Section 4.5) in which these essential subcircuits are used to design filters. The interpretation of the sensitivity of the simulated active RC structures in terms of the sensitivity of an "equivalent" LC filter.

Chapter 5 ——— The method of reducing the effect of finite f_T's in NIC circuits (developed in Section 5.2) and the simple method of determining the stability of, and / or stabilisation of "potentially" unstable, NIC circuits (reported in Section 5.4).

Some of the results of the present work have been published [84].

C H A P T E R 2

A METHOD OF COMPENSATING FOR THE EFFECT OF FINITE AMPLIFIER GAIN BANDWIDTH PRODUCT IN MULTIPLE FEEDBACK FILTERS

2.1 Introduction

The interest in designing multiple feedback active RC networks arises from the fact that these networks possess low sensitivity and, as described in Chapter 1, their design can be based on biquadratic sections which is desireable for two reasons. Firstly, a considerable reduction in the total number of amplifiers required, in order to realise a given order filter, can be obtained by using single amplifier biquadratic (SAB) sections; secondly, the past experience of designing and adjusting such biquadratic sections can be directly utilised. Once the synthesis procedure has been carried-out to obtain the transfer functions of the various blocks in the multiple feedback structure, the design problem reduces to that of designing the second order biquadratic sections.

In the realisation of the biquadratic sections operational amplifiers (OP-AMPs) are usually employed as the basic active elements. Basically an OP-AMP consists of high gain differential amplifiers which are DC coupled. An ideal OP-AMP has infinite input impedance, zero output impedance, infinite common mode rejection ratio (CMRR) and infinite gain at all frequencies. However, a practical OP-AMP has finite input impedance, non-zero output impedance, finite CMRR and finite gain which is dependent on frequency. Assuming the OP-AMP is internally compensated by a dominant pole, which is the usual case, then for all practical purposes the open loop gain, A(s), of the OP-AMP is characterised by

$$A(s) = \frac{A_o \, w_c}{s + w_c} = \frac{w_T}{s + w_c} \qquad (2.1)$$

where A_o and w_c are the DC gain and the 3 dB frequency of the OP-AMP, respectively, s is the complex frequency variable and w_T (= $2\pi f_T$) is the gain bandwidth product of the OP-AMP. The finite values of the CMRR encountered in pratice, for commercially available OP-AMPs, are such that it is not a limiting factor. Furthermore the effect of the typical values of the finite input impedance and the non-zero output impedance of the OP-AMPs can usually be made negligible by appropriately choosing the impedance level of the RC circuit in which the OP-AMP is embedded. However, the effect of the frequency dependent nature of the OP-AMP gain given by equation (2.1) cannot be neglected unless the operation of the circuit is confined to very low frequencies (e.g. a few kilohertz or even less if common OP-AMPs such as the type 741 are being used). Therefore in order to design useful circuits at higher frequencies it is necessary to take account of the effect of finite f_T of the OP-AMP at the design stage.

In this Chapter we shall examine in some detail the effect of finite gain bandwidth product in <u>single</u> amplifier biquadratic (SAB) circuits. The basic concepts of two distinct methods, namely predistortion and compensation, which can be used to take account of the effect of the finite f_T will be discussed in Section 2.2. The scheme proposed in Section 2.2.2 for fully compensating for the f_T of the OP-AMP in SAB circuits will be applied to the Friend and the Sallen and Key SAB bandpass circuits in Sections 2.3 and 2.4, respectively. The application of the predistortion or the compensation technique results in a set of non-linear equations. Derivation of the design equations for the two SAB bandpass circuits and a numerical procedure, based on a simple computer program, for solving these non-linear equations will be described in Section 2.5.

In Section 2.6 we shall carry-out a comparison of the computed responses for the predistorted and the compensated designs of the SAB circuits. We shall also examine the response of a sixth order all-pole leap-frog feedback bandpass filter realised using these predistorted and compensated SAB circuits. The derivation of the leap-frog feedback bandpass filter structure, which is to be used as an example, was given in Section 1.3.2. This filter can be realised as shown in Fig 1.9(b) with three second order sections. The relationship between the parameters of the second order sections and the elements of the prototype filter of Fig 1.8(a) are shown in Table 1.2. Now, if this filter is designed for a centre frequency of 15 kHz, bandwidth of 500 Hz, passband ripple of 0.5 dB and for feedback factors and midband gain of unity, then the values of the parameters of the second order sections are as shown in Table 2.1. We shall use the above specification for the leap-frog feedback bandpass filter to be considered here as an example.

2.2 The concepts of predistortion and compensation

2.2.1 Predistortion

The design of circuits is often carried-out assuming the components of the circuit are free from any parasitic effects as this leads to simpler design equations. Consequently if the circuit is analysed by taking into account the parasitic effects of the components then the actual characteristic of the circuit may depart considerably, from those for which the circuit was designed, such that the circuit no longer remains useful. For example, suppose we design the Friend and the Sallen and Key SAB bandpass circuits in Figs 1.11(b) and (c) to have a resonance frequency of 15 kHz and

Q-factors of value 47.8875 and infinity, respectively. Assuming the OP-AMPs to be ideal, the component values of the Friend circuit can be obtained by solving equations (1.22a) and (1.22b); similarly, the component values for the Sallen and Key circuit can be obtained by solving equations (1.23a) and (1.23b). Now, if both SAB circuits are analysed assuming the OP-AMPs to be ideal and assuming the OP-AMPs to be characterised by equation (2.1) with f_T = 1 MHz, then the amplitude-frequency characteristics obtained for the two circuits are as shown in Figs 2.1(a) and (b). From Fig 2.1 we note that both SAB circuits realise the desired characteristics if the OP-AMPs are ideal; however, significant errors in the responses occur when the OP-AMPs have a finite f_T's (= 1 MHz). In Fig 2.1 the effect of the finite f_T's can be interpretted as causing changes in the values of the resonance frequencies and the Q-factors of the circuits.

The above example clearly shows that in order to design practical circuits (i.e. which use OP-AMPs of finite f_T), we must take into account the effect of the finite f_T at the design stage; this can be achieved using a design step that is usually referred to as predistortion . In essence the predistortion technique involves the prediction of the changes in the circuit parameters (e.g. the resonance frequency and the Q-factor in the case of the above SAB circuits) that would result when the components of the circuit become non-ideal; in accordance with these changes, the initial values of the circuit parameters are modified (i.e. are "predistorted") in the opposite direction by the appropriate amounts and the design of the circuit is carried-out using these parameter values in the ideal circuit design equations; thus when the circuit is analysed taking into account the parasitics of the components, the circuit parameters

attain their desired nominal values. Obviously the limitation of the predistortion technique is governed by how accurately we can predict the changes in the circuit parameters.

One method of predistorting the design of biquadratic sections is presented in [66], where analytical expressions are derived to predict the change in the resonance frequency, $-\Delta w_o$, and the change in the Q-value, $-\Delta Q$, of the sections. These values of Δw_o and ΔQ are then used as corrective factors. For example, if the biquadratic section is designed for a resonance frequency of $(w_o + \Delta w_o)$ and a Q-factor of value $(Q + \Delta Q)$, assuming the OP-AMP(s) to be ideal, then in the presence of non-ideal OP-AMP(s) the resonance frequency and the Q-factor of the circuit would be w_o and Q, respectively. In [66], the expressions for Δw_o and ΔQ are obtained by considering the rate of change of the complex pole-pair locations with respect to the gain bandwidth product at the nominal pole positions and hence are only valid if these changes are small; this imposes an upper limit on the frequency at which this predistortion technique can be applied.

In the following we shall present two methods of predistorting the design of biquadratic sections which are better than the method of [66] in the sense that they can cope with higher operating frequencies. The basic principle of these methods can be applied to predistort the design of multi-amplifier biquadratic circuits; however in order to keep the analysis simple we shall only consider SAB circuits here. The basic philosophy of these methods can be better understood if we first examine the effect of the amplifier finite f_T on the transfer functions of SAB circuits.

It can be shown that the general form of the voltage transfer ratio of a SAB circuit can be put into the following form :

$$T(s) = \frac{N(s)}{P(s)} = \frac{N(s)}{D_1(s) + \frac{K_1}{A(s)} D_2(s)} \qquad (2.2)$$

where $N(s) = G_1 \left[(s/w_z)^2 + Q_z^{-1} (s/w_z) + 1\right]$

$$D_1(s) = (s/w_p)^2 + Q_p^{-1} (s/w_p) + 1$$

$$D_2(s) = (s/w_p)^2 + \{ Q_p^{-1} + K_2\} (s/w_p) + 1$$

where w_z, w_p, Q_z, Q_p, G_1, K_1 and K_2 are constants and A(s) is the gain of the amplifier. In the case of bandpass filters, equation (2.2) reduces to the form

$$T_{BP}(s) = \frac{G_1 (s/w_o)}{s/w_o)^2 + Q_o^{-1} (s/w_o) + 1 + K_1 A^{-1}(s) \left[(s/w_o)^2 + (Q_o^{-1} + K_2) (s/w_o) + 1\right]} \qquad (2.3)$$

where w_o and Q_o are the resonance frequency and the Q-factor of the circuit when the OP-AMP is ideal. From equation (2.3) we can deduce that in the case of an ideal OP-AMP the transfer function of a bandpass filter becomes

$$T_{BP}(s)\Big|_{A(s)\longrightarrow\infty} = \frac{G_1\,(s/w_o)}{(s/w_o)^2 + Q_o^{-1}\,(s/w_o) + 1} \qquad (2.4)$$

If we substitute for A(s) from equation (2.1) into equation (2.3), then $T_{BP}(s)$ can be written as

$$T_{BP}(s) = \frac{G_2\,s}{a_3s^3 + a_2s^2 + a_1s + 1} \qquad (2.5)$$

where G_2, a_3, a_2 and a_1 are constants. From equation (2.5) we note that the effect of the non-ideal OP-AMP is to convert the <u>biquadratic transfer function</u>, of the ideal OP-AMP case, into a <u>third order transfer function</u>. This effect can alternatively be interpreted as producing a <u>shift</u> in the position of the dominant complex pole pair and introducing an <u>unwanted</u> pole on the negative real axis of the complex s-plane.

The dominant complex pole pair can be shifted back to its nominal position in the s-plane by predistorting the design. There are two ways in which predistortion can be implemented in the case of equation (2.5). Firstly, we can factorise the denominator of equation (2.5) into a first order term and a biquadratic term, viz:

$$T_{BP}(s) = \frac{G_2\,s}{(b_3s + 1)\,(b_2s^2 + b_1s + 1)} \qquad (2.6)$$

where b_3, b_2 and b_1 can be related to a_3, a_2 and a_1 by equating the coefficients in the denominator polynomials of equations (2.5) and (2.6). Equation (2.6) can be rewritten in the following form

$$T_{BP}(s) = \frac{G_3\ (s/w_r)}{(b_3 s + 1)\ [(s/w_r)^2 + Q_r^{-1}\ (s/w_r) + 1]} \tag{2.7}$$

where $w_r = [b_2]^{-1/2}$ (2.7a)

$Q_r = [b_2]^{1/2}/b_1$ (2.7b)

and $G_3 = G_2\ [b_2]^{1/2}$ (2.7c)

Now if the frequency of interest is such that $b_3 w << 1$, then the first order term in denominator of equation (2.7) can be approximated to unity, and hence we can treat $T_{BP}(s)$ as being the transfer function of a biquadratic section with a resonance frequency w_r and a Q-factor Q_r. Working through equations (2.7), (2.6), (2.5) and (2.3), it is possible to obtain expressions relating w_o, Q_o and G_1 in terms of w_r, Q_r, G_3 and the gain of the OP-AMP; however, these expressions are non-linear (this will be shown in Section 2.5) and hence they cannot be solved analytically, but this problem can be overcome by obtaining a numerical solution using the method of successive substitution (one such method will be described in Section 2.5).

The second method of predistortion can be illustrated as follows. Suppose we substitute $s = jw$ in equations (2.5) and (2.4), respectively, then

$$T_{BP}(jw) = \frac{G_3\ j(w/w_r)}{1 - (w/w_r)^2 + j(w/w_r)\ Q_r^{-1}(w)} \tag{2.8}$$

where $w_r = [a_2]^{-1/2}$ (2.8a)

$Q_r(w) = [a_2]^{1/2}\ [a_1 - a_3 w^2]^{-1}$ (2.8b)

$G_3 = [a_2]^{1/2}\ G_2$ (2.8c)

$$\text{and} \quad T_{BP}(jw)\Big|_{A(jw) \longrightarrow \infty} = \frac{G_1 \, j(w/w_o)}{1 - (w/w_o)^2 + j(w/w_o)\, Q_o^{-1}} \qquad (2.9)$$

Now, the bandpass transfer function in equation (2.9) has a resonance frequency w_o and a Q-factor Q_o. Therefore by comparing equations (2.8) and (2.9), it can be argued that equation (2.8) represents a biquadratic bandpass transfer function with a resonance frequency w_r and a Q-factor $Q_r(w)$. Note that whereas the Q-factor of a biquadratic circuit is normally a constant, $Q_r(w)$ in equation (2.8b) is dependent on frequency. The variation of $Q_r(w)$ with frequency are expected to be small because in practice the value of a_1 will be very much greater than the value of a_3w^2 in the frequency range of interest. Clearly the frequency dependent Q-factor, $Q_r(w)$, can be made identical with the required Q-factor, Q_o, at any chosen finite frequency. Expressions for w_o, Q_o and G_1 can be derived in terms of w_r, $Q_r(w)$, G_3 and the gain of the OP-AMP, but again a set of non-linear equations is obtained which can only be solved numerically.

We have presented two methods for predistorting the design of SAB bandpass circuits but the general idea is also applicable to other type of circuits (e.g. lowpass, highpass, etc.), both single amplifier and multi-amplifier. However, it is relevant to point-out that the predistortion technique makes the transfer function of the circuit only "approximately" ideal; this is apparent from the fact that even after predistortion we still have a third order transfer function instead of the required second order. Note that in the first method of predistortion described above we assume the effect of the first order term to be negligible and hence the actual amplitude and phase of the circuit suffer small deviations from their respective

nominal values over the entire frequency range. In contrast to this, in the second method of predistortion the response is exact at the frequency where $Q_r(w) = Q_o$ but suffers deviations at all other frequencies. Hence the performance of the circuits designed by the second predistortion method will be slightly superior to those designed by the first predistortion method.

The amplitude and the phase of the circuit predistorted by the second method can exhibit its nominal values at any one frequency, whereas the amplitude and the phase of the circuit predistorted by the first method can only attain their nominal values, simultaneously, at zero frequency. This is equivalent to saying that in the second predistortion method we can take into account the effect of the unwanted real pole at a single finite frequency, whereas this is not possible in the case of the first method.

It is also interesting to note that the amplitude characteristics of the cascade and the multiple feedback filters, which use the biquadratic section as the basic building block, are affected differently by the errors in the amplitude and the phase of the biquadratic transfer functions. For example, the amplitude characteristics of cascade filters depends only on the <u>amplitude</u> characteristics of the biquadratic sections, whereas in the case of multiple feedback filters, the amplitude characteristics of the overall structure is dependent on both the <u>amplitude</u> and the <u>phase</u> of <u>each</u> biquadratic section.

2.2.2 Compensation

It has been shown in the previous subsection that finite amplifier f_T causes two effects in SAB circuits. Firstly, the dominant complex pole pair is displaced from its nominal location; secondly, an additional pole is introduced into the transfer function due to the singularity of the OP-AMP. Predistortion techniques can be used to shift the dominant complex pole pair to its nominal location; however, due to the presence of the additional unwanted real pole, the resulting transfer function suffers from small deviations in both amplitude and phase. This short-coming of the predistortion technique can be avoided by adopting a completely different approach, which we shall refer to as compensation .

The fundamental difference between the predistortion and the compensation techniques is that the latter requires modification to the circuit topology in the sense that extra components (passive and/or active) are added to the existing circuit, whereas no alteration is made to the circuit topology in the former. For biquadratic circuits, various schemes have been proposed in the literature for compensating both single and multi amplifier circuits. In the following we shall consider the basic principles of these compensation schemes and also comment on the advantages and disadvantages of these schemes from the practical implementation point of view.

In principle a circuit can be either compensated actively or passively. In the methods of active compensation [67,68] extra OP-AMPs (together with passive components, if necessary) are added to the existing circuit in such a way that some OP-AMPs of the circuit

provide compensation for other OP-AMPs of the same circuit. The "mechanism" by which this compensation method works is that the addition of the extra OP-AMPs introduces additional zeros and poles into the transfer function of the circuit and due to the location of these zeros and poles in the s-plane it is possible to a first order approximation to achieve cancellation of the excess phase produced by the OP-AMPs. This compensation technique works well if the characteristics of the OP-AMPs are matched closely — a condition easily satisfied in practice for OP-AMPs fabricated on the same chip. The main advantage of active compensation is that since the characteristics of the OP-AMPs track each other with changes in ambient temperature and supply voltage, the circuit performance is not affected by changes in the environmental conditions. The main disadvantages of the active compensation are that it is not possible to "fully" compensate the circuit to achieve ideal amplitude and phase characteristics and also this compensation method cannot be applied in circumstances where DC power consumption and the problem of heat dissipation are major considerations, i.e. in SAB circuits.

In contrast to active compensation, passive compensation is achieved by modifying the topology of the passive RC part of the circuit by adding extra passive component(s). The basic principle of this approach is to add the compensating component(s) in such a way so as to create a zero in the transfer function of the circuit. The phase lead resulting from this zero is used to cancel the excess phase lag arising from the unwanted poles introduced by the OP-AMPs of the circuit. By adding a single compensating component to multi-amplifier biquadratic circuits [69,70] it is possible to achieve compensation only over a limited frequency band; however, for

SAB circuits in which the numerator of the transfer function is at least one degree lower than the denominator, full compensation for amplitude and phase can be achieved at the expense of adding a single passive component to the circuit [71], over the entire frequency range in which the OP-AMP gain can be adequately described by the first order roll-off model depicted in equation (2.1). We shall now examine more closely the means by which this full compensation is implemented.

Let us again consider the SAB bandpass transfer function discussed in the previous subsection. Suppose we can modify the circuit topology so as to introduce a zero into the transfer function. Then the transfer function of the circuit, assuming the OP-AMP to be characterised by equation (2.1), can be written as

$$T_{BP}(s) = \frac{G_2 s\ (b_1 s + 1)}{a_3 s^3 + a_2 s^2 + a_1 s + 1} \qquad (2.10)$$

where G_2, b_1, a_3, a_2 and a_1 are constants expressible in terms of the circuit components and the open loop gain of the OP-AMP. Factorising the denominator of equation (2.10) into a first order term and a biquadratic term gives

$$T_{BP}(s) = \frac{G_2 s\ (b_1 s + 1)}{(a_4 s + 1)\ (a_5 s^2 + a_6 s + 1)} \qquad (2.11)$$

where a_4, a_5 and a_6 can be determined in terms of the circuit components by equating coefficients in equations (2.10) and (2.11). In equation (2.11) a pole-zero cancellation takes place if $b_1 = a_4$,

and we are then left with a biquadratic bandpass transfer function, i.e.

$$T_{BP}(s) = \frac{G_3 \, (s/w_r)}{(s/w_r)^2 + Q_r^{-1} \, (s/w_r) + 1} \tag{2.12}$$

where $w_r = [a_5]^{-1/2}$ (2.12a)

$$Q_r = [a_5/a_6^2]^{1/2} \tag{2.12b}$$

and $G_3 = G_2 \, [a_5]^{-1/2}$ (2.12c)

Thus full compensation has been achieved and the resulting transfer function has the required form over the frequency range in which the gain of the OP-AMP can be characterised by equation (2.1).

The main advantages of passive compensation are that it can be easily implemented; the amount of additional circuitry required is small (e.g. usually one passive component); in the case of single amplifier circuits, if the degree of the transfer function numerator is lower than the degree of the denominator, both amplitude and phase characteristics of the circuit can be fully compensated. The main disadvantage of the passive compensation is that the compensating element has to adjusted for a given OP-AMP at a specific ambient conditions of temperature and power supply voltage; hence under changing ambient conditions, the compensation will not be exact. With respect to the last remark it is important to realise that although the change in the ambient conditions causes the poles and zeros of the transfer function to be displaced from their nominal positions, the

fact that the compensating zero still lies in the vicinity of the OP-AMP created pole will result in less deviations in the amplitude and phase than if no compensation is used.

The active or passive compensation methods lead to circuits requiring more components than the minimum necessary. Therefore extra sensitivities introduced by these additional elements have to be taken into account. In Chapter 3 we shall discuss sensitivity minimisation of a multiple feedback bandpass filter which uses passively compensated SAB bandpass circuits, and it will be shown there that the sensitivity introduced by the compensating elements is relatively small compared with the sensitivities of the other elements of the SAB circuits.

2.3 Compensation of the Friend bandpass section

Consider the basic Friend SAB bandpass circuit shown in Fig 2.2(a). By straight forward analysis, the transfer function of this circuit can be shown to be given by

$$T(s) = \frac{-sC_2R_2\,(1 + R_b/R_a)}{[s^2C_1C_2R_1R_2 + s(C_1R_1 + C_2R_1 - C_2R_2R_b/R_a) + 1] + \dfrac{(1 + R_b/R_a)}{A(s)}\,[s^2C_1C_2R_1R_2 + s(C_1R_1 + C_2R_1 + C_2R_2) + 1]} \qquad (2.13)$$

where A(s) is the open loop gain of the amplifier, given by equation (2.1). In order to be able to compensate for the non-ideal OP-AMP we need to modify the passive part of the circuit such that a

zero is introduced into the transfer function of the circuit. Let us examine how this can be achieved.

Suppose a capacitor C_3 is connected in parallel with the resistor R_1 in the circuit of Fig 2.2(a). The transfer function of the resulting circuit, given in equation (2.14), can be obtained by making the following substitution in equation (2.13)

$$R_1 \longrightarrow \frac{R_1}{sC_3R_1 + 1}$$

$$T(s) = \frac{-sC_2R_2\ (1+R_b/R_a)\ (sC_3R_1+1)}{[s^2C_2R_2(C_1R_1-C_3R_1R_b/R_a)+s(C_1R_1+C_2R_1-C_2R_2R_b/R_a+C_3R_1)+1]} \qquad (2.14)$$
$$+\frac{(1+R_b/R_a)}{A(s)}\ [s^2C_2R_2(C_1R_1+C_3R_1)+s(C_1R_1+C_2R_1+C_2R_2+C_3R_1)+1]$$

Alternatively, suppose a resistor is connected in series with the capacitor C_1 in the circuit of Fig 2.2(a). The transfer function of the resulting circuit is given in equation (2.15) and it can be obtained from equation (2.13) by making the following substitution:

$$sC_1 \longrightarrow \frac{sC_1}{sC_1R_3 + 1}$$

$$T(s) = \frac{-sC_2R_2\ (1+R_b/R_a)\ (sC_1R_3+1)}{[s^2C_1C_2R_1R_2(1+R_3/R_2-R_3R_b/R_1R_a)+s(C_1R_1+C_2R_1+C_1R_3-C_2R_2R_b/R_a)+1]} \qquad (2.15)$$
$$+\frac{(1+R_b/R_a)}{A(s)}\ [s^2C_1C_2R_1R_2(1+R_3/R_2+R_3/R_1)+s(C_1R_1+C_2R_1+C_1R_3+C_2R_2)+1]$$

Therefore, we effectively have two ways of compensating the circuit,

but the capacitive compensation method is undesirable for four reasons, viz:

1. number of capacitors used will not be minimum (note that we are realising a second order transfer function and hence only two capacitors are required)

2. all the capacitors in the circuit cannot have equal values without having unpractical spread in resistor values

3. capacitors are often added as discrete components and hence their values cannot be trimmed

4. the resistor R_1 in the circuit of Fig 2.2(a) can be split-up to provide a summation point and to obtain a required gain constant, but this possibility is precluded if a compensating capacitor is connected in parallel with R_1.

On the other hand, the method of adding a resistor in order to compensate for the finite amplifier f_T does not have any of the above difficulties and hence is a practical proposition; we shall make use of this resistive compensation method.

The circuit diagram of the compensated Friend SAB bandpass circuit is given in Fig 2.2(b) and its transfer function is given by equation (2.15). The derivation of the relevant design equations is given in Section 2.5.

2.4 Compensation of the Sallen and Key bandpass section

Let us consider the Sallen and Key SAB bandpass circuit shown in Fig 2.3(a). By straight forward analysis, the transfer function of

this circuit can be shown to be

$$T(s) = \frac{sC_2R_2\ (1 + R_a/R_b)}{[s^2C_1C_2R_1R_2+s(C_1R_1+C_2R_1+C_2R_2 - C_2R_2R_1R_a/R_3R_b)+1+R_1/R_3]} \quad (2.16)$$
$$+ \frac{(1 + R_a/R_b)}{A(s)}\ [s^2C_1C_2R_1R_2+s(C_1R_1+C_2R_1+C_2R_2+C_2R_2R_1/R_3)+1+R_1/R_3]$$

where A(s) specifies the open loop gain of the amplifier. In order to compensate for the non-ideal OP-AMP, we need to modify the passive part of the circuit in Fig 2.3(a) such that a zero is introduced into the transfer function of the circuit. Let us examine the possible ways of achieving this.

Suppose a capacitor C_3 is connected in parallel with the resistor R_1 in the circuit of Fig 2.3(a). The transfer function of the resulting circuit is given in equation (2.17) and it can be obtained from equation (2.16) by making the following substitution:

$$R_1 \longrightarrow \frac{R_1}{sC_1R_1 + 1}$$

$$T(s) = \frac{sC_2R_2\ (1+R_a/R_b)\ (sC_3R_1+1)}{[s^2C_2R_2(C_1R_1+C_3R_1)+s(C_1R_1+C_2R_1+C_2R_2+C_3R_1-C_2R_2R_1R_a/R_3R_b)} \quad (2.17)$$
$$+ 1+R_1/R_3] + \frac{(1+R_a/R_b)}{A(s)}\ [s^2C_2R_2(C_1R_1+C_3R_1)$$
$$+ s(C_1R_1+C_2R_1+C_2R_2+C_3R_1+C_2R_2R_1/R_3)+1+R_1/R_3]$$

Now suppose that in addition to capacitor C_3 being connected in

parallel with resistor R_1, another capacitor C_4 is connected in parallel with resistor R_3. The transfer function of the circuit thus modified is given in equation (2.18) which can be obtained by making the following substitution in equation (2.17):

$$R_3 \longrightarrow \frac{R_3}{sC_4R_3 + 1}$$

$$T(s) = \frac{sC_2R_2\ (1+R_a/R_b)\ (sC_3R_1+1)}{[s^2C_2R_2(C_1R_1+C_3R_1-C_4R_1R_a/R_b)+s(C_1R_1+C_2R_1+C_2R_2+C_3R_1+C_4R_1} \quad (2.18)$$

$$-C_2R_2R_1R_a/R_3R_b)\ +1+R_1/R_3] + \frac{(1+R_a/R_b)}{A(s)}\ [s^2C_2R_2(C_1R_1+C_3R_1+C_4R_1)$$

$$+s(C_1R_1+C_2R_1+C_2R_2+C_3R_1+C_4R_1+C_2R_2R_1/R_3)+1+R_1/R_3]$$

Alternatively, suppose a resistor R_4 is connected in series with the capacitor C_1 in the circuit of Fig 2.3(a). The transfer function of the resulting circuit is given in equation (2.19) which can be obtained from equation (2.16) by making the following substitution:

$$sC_1 \longrightarrow \frac{sC_1}{sC_1R_4 + 1}$$

$$T(s) = \frac{sC_2R_2\ (1+R_a/R_b)\ (sC_1R_4+1)}{[s^2C_1C_2R_1R_2(1+R_4/R_1+R_4/R_2-R_4R_a/R_3R_b)+s(C_1R_1+C_2R_1} \quad (2.19)$$

$$+C_2R_2+C_1R_4+C_1R_4R_1/R_3-C_2R_2R_1R_a/R_3R_b)\ +1+R_1/R_3]$$

$$+\ \frac{(1+R_a/R_b)}{A(s)}[s^2C_1C_2R_1R_2(1+R_4/R_1+R_4/R_2+R_4/R_3)$$

$$+s(C_1R_1+C_2R_1+C_2R_2+C_1R_4+C_1R_4R_1/R_3+C_2R_2R_1/R_3)+1+R_1/R_3]$$

Hence there are three possible schemes for compensating the circuit of Fig 2.3(a); two of these schemes require one or two additional capacitors whereas the third requires an additional resistor. Reasons for not using additional capacitors, in order to compensate for finite f_T , were given in Section 2.3. For these reasons, we shall use the method which requires an additional resistor in order to compensate for the finite amplifier gain bandwidth product.

Hence the circuit diagram of the compensated Sallen and Key SAB bandpass circuit is as shown in Fig 2.3(b) and its transfer function is given by equation (2.19). The derivation of the relevant design equations for this circuit are considered in the next section.

2.5 Derivation and solution of the design equations for the compensated SAB bandpass circuits

In this section we shall derive the design equations for the Friend and the Sallen and Key SAB bandpass circuits which have been compensated for the finite gain bandwidth product of the amplifier. It will be shown that the design equations obtained cannot be solved analytically because they are non-linear. A numerical procedure used for solving these non-linear equations, which is based on a simple computer program, will also be described.

2.5.1 Compensated Friend bandpass circuit

The compensated form of the Friend SAB bandpass circuit is shown in Fig 2.2(b) and its transfer function is given by equation (2.15). For the purpose of convenience, equation (2.15) can be expressed in

terms of new variables as shown below:

$$T(s)= \frac{-(s/w_o)\ K'K_R K_C\ [(s/w_o)(K_1-1)+1]}{[(s/w_o)^2\{K_1-(K_1-1)(K'-1)\ K_R^2\}+(s/w_o)\{1/Q_o+(K_1-1)\ K_R/K_C\}+1]} \quad (2.20)$$

$$+ \frac{K'}{A(s)}\ [(s/w_o)^2\{K_1+(K_1-1)\ K_R^2\}+(s/w_o)\{1/Q_o+K'K_RK_C+(K_1-1)\ K_R/K_C\}+1]$$

where
$$K_R = [R_2/R_1]^{1/2} \quad (2.20a)$$
$$K_C = [C_2/C_1]^{1/2} \quad (2.20b)$$
$$K' = 1 + R_b/R_a \quad (2.20c)$$
$$K_1 = 1 + R_3/R_2 \quad (2.20d)$$
$$w_o = [C_1C_2R_1R_2]^{-1/2} \quad (2.20e)$$
$$Q_o = [1/K_RK_C + K_C/K_R - (K'-1)\ K_R\ K_C] \quad (2.20f)$$

Note that in equation (2.20), if A(s) is infinite (i.e. ideal OP-AMP) and $K_1 = 1$ (i.e. $R_3 = 0$), then T(s) reduces to a biquadratic transfer function for which the resonance frequency is w_o and the Q-factor is Q_o. Rewriting A(s) in equation (2.1) as

$$A(s) = \frac{w_T/w_o}{(s/w_o) + (w_c/w_o)} = \frac{w_{Tn}}{(s/w_o) + w_{cn}} \quad (2.21)$$

and substituting for A(s) in equation (2.20) gives

$$T(s)= \frac{-(s/w_o)\ K_2K'K_CK_R\ [(s/w_o)(K_1-1)\ K_R/K_C+1]}{(s/w_o)^3(K'K_2/w_{Tn})\{K_1+(K_1-1)\ K_R^2\}+(s/w_o)^2K_2\{K_1-(K_1-1)(K'-1)\ K_R^2} \quad (2.22)$$

$$+(k'/w_{Tn})\ [K_1w_{cn}+(K_1-1)\ K_R^2w_{cn}+1/Q_o+K'K_RK_C+(K_1-1)\ K_R/K_C]\}$$

$$+(s/w_o)K_2\{1/Q_o+(K_1-1)\ K_R/K_C+(K'/w_{Tn})$$

$$[1+w_{cn}/Q_o+w_{cn}K'K_RK_C+(K_1-1)\ K_Rw_{cn}/K_C]\}+1$$

where $K_2 = [K'w_{cn}/w_{Tn} + 1]^{-1}$ (2.22a)

We may now factorise the denominator of equation (2.22) into a first order term (which will subsequently be cancelled by the first order term in the numerator) and a biquadratic term. Suppose the resonance frequency and the Q-factor of the resulting transfer function are w_r and Q_r, respectively. Then

$$T(s)= \frac{-(s/w_r)\ (w_r/w_o)\ K_2K'K_CK_R\ [(s/w_o)(K_1-1)\ K_R/K_C+1]}{[(s/w_o)(w_r/w_o)^2(K'K_2/w_{Tn})\{K_1+(K_1-1)\ K_R^2\}+1]\ [(s/w_r)^2+Q_r^{-1}(s/w_r)+1]} \quad (2.23)$$

where $w_r = w_o\ [K_1K_2-(K_1-1)(K'-1)K_R^2K_2+(K'K_2/w_{Tn})\{K_1w_{cn}+(K_1-1)K_R^2w_{cn}+Q_o^{-1}$

$$+K'K_RK_C+(K_1-1)\ K_R/K_C-Q_r^{-1}(w_r/w_o)(K_1+(K_1-1)\ K_R^2)\}]^{-1/2} \quad (2.23a)$$

and $Q_r = (w_o/w_r)\ [K_2/Q_o+(K_1-1)\ K_RK_2/K_C+(K'K_2/w_{Tn})\{1+w_{cn}/Q_o$

$$+w_{cn}K'K_RK_C+(K_1-1)K_Rw_{cn}/K_C-(w_r/w_o)^2(K_1+(K_1-1)K_R^2\}]^{-1} \quad (2.23b)$$

also, in order to have a cancellation of the real pole and the real zero in equation (2.23), we must have

$$(k_1 - 1)\, K_R/K_C = (w_r/w_o)^2\, (K'K_2/w_{Tn})\, \{K_1 + (K_1 - 1)\, K_R^2\} \qquad (2.23c)$$

when the pole-zero cancellation takes place, the transfer function of the circuit becomes

$$T(s) = \frac{-(s/w_r)\, G}{(s/w_r)^2 + Q_r^{-1}\, (s/w_r) + 1} \qquad (2.24)$$

where G = gain-factor $= (w_r/w_o)\, K_2K'K_CK_R$ (2.24a)

Let us now consider how we can calculate the component values. In the circuit of Fig 2.2(b) we have seven passive components and hence seven degrees of freedom. In order to realise the required transfer function, we need to set four parameters; namely, the resonance frequency, the Q-factor, the condition for the pole-zero cancellation and the gain factor of the circuit. Thus the values of four components of the circuit are determined by the required transfer function and hence by arbitrarily choosing the values of the three components of the circuit, we can solve the design equations to determine the values of the remaining components. It is desirable to select the two capacitors of the circuit in Fig 2.2(b) as the two arbitrarily chosen components because the capacitors cannot be trimmed. For the sake of argument, let the third arbitrarily chosen component be the resistor R_a. Then, in order to calculate the values of the remaining components of the circuit, we first need to determine the values of the intermediate variables w_o, Q_o, K_1, K_R and K'. This

can be done using the following equations, which are obtained by rearranging equations (2.23a), (2.23b), . (2.23c), (2.24a) and (2.20f), respectively.

$$w_o = w_r [K_1K_2-(K_1-1)(K'-1) K_R^2K_2+(K'K_2/w_{Tn}) \{K_1w_{cn}+(K_1-1) K_R^2w_{cn}+Q_o^{-1} + K'K_RK_C+(K_1-1) K_R/K_C-Q_r^{-1} (w_r/w_o)(K_1+(K_1-1) K_R^2)\}]^{1/2} \quad (2.25)$$

$$Q_o = [(Q_rK_2)^{-1}(w_o/w_r)-(K_1-1) K_R/K_C-(K'/w_{Tn})\{1+w_{cn}/Q_o+w_{cn}K'K_RK_C + (K_1-1) K_Rw_{cn}/K_C-(W_r/w_o)^2(K_1+(K_1-1) K_R^2)\}] \quad (2.26)$$

$$K_1 = 1 + (w_r/w_o)^2 (K'K_CK_2/w_{Tn}K_R) \{K_1 + (K_1 - 1) K_R^2\} \quad (2.27)$$

$$K_R = Gw_o/(w_rK'K_CK_2) \quad (2.28)$$

$$K' = 1 + (K_RK_C)^{-1} \{(K_RK_C)^{-1} + K_C/K_R - Q_o^{-1}\} \quad (2.29)$$

The non-linear nature of the above equations is quite apparent, hence an analytical solution is not feasible; therefore we have to resort to solving these equations numerically. A flow chart of a simple computer program for performing this task is shown in Fig 2.4, which uses the method of successive substitution in order to obtain the solution. That is, we make an initial guess of the values of w_o, Q_o, K_1, K_R and K'; substitute these into equations (2.25) ⟶ (2.29) to obtain the updated values which are then resubstituted into the equations. This procedure is repeated until the values of the variables change less than some specified amount (assumed 10^{-10} in the actual program) with subsequent iterations. The number of iterations required to reach the final solution is highly dependent on the values

used for the initial guesses. A method of assigning these initial values, which has been found to be successful in practice, is to assume $w_o = w_r$, $Q_o = Q_r$, $K_1 = 1$, arbitrarily choose K' and then evaluate K_R from equation (2.20f) taking the positive solution.

Once the final values of w_o, Q_o, K_1, K_R and K' have been obtained, the following equations, which are obtained by rearranging equations (2.20e), (2.20a), (2.20d) and (2.20c), respectively, are used to evaluate R_1, R_2, R_3 and R_b.

$$R_1 = [w_o K_R K_C C_1]^{-1} \tag{2.30}$$

$$R_2 = K_R^2 R_1 \tag{2.31}$$

$$R_3 = (K_1 - 1) R_2 \tag{2.32}$$

$$R_b = (K' - 1) R_a \tag{2.33}$$

Note that the computer program based on the flow chart given in Fig 2.4 can also be used for predistorting the design of the Friend SAB bandpass circuit in accordance with the first predistortion method discussed in Section 2.2. This is done by forcing K_1 to be equal to unity. Furthermore, the same program can also be used for designing circuits assuming the OP-AMP to be ideal; this is achieved by forcing K_1 to be equal to unity and by assigning A_o and w_c to be large numbers (e.g. 10^{99}).

2.5.2 Compensated Sallen and Key bandpass circuit

The compensated form of the Sallen and Key SAB bandpass circuit is shown in Fig 2.3(b) and its transfer function is given by equation (2.19). For the sake of convenience, equation (2.19) can be expressed in terms of new variables as shown below.

$$T(s)= \frac{(s/w_o)\ (K_R K_C K'/K_1)\ [(s/w_o)(k_2-1)\ K_R K_1/K_C+1]}{[(s/w_o)^2\{K_2+(K_2-1)K_R^2-(K'-1)(K_2-1)(K_1^2-1)K_R^2\}} \quad (2.34)$$
$$+(s/w_o)\{Q_o^{-1}+(K_2-1)K_R K_1/K_C\}+1]+\frac{K'}{A(s)}\ [(s/w_o)^2\{K_2+(K_2-1)K_R^2K_1^2\}$$
$$+(s/w_o)\{Q_o^{-1}+(K_1^2-1)K_R K_C K'/K_1+(K_2-1)K_R K_1/K_C\}+1]$$

where
$$K_R = [R_2/R_1]^{1/2} \quad (2.34a)$$
$$K_C = [C_2/C_1]^{1/2} \quad (2.34b)$$
$$K' = 1 + R_a/R_b \quad (2.34c)$$
$$K_1 = [1 + R_1/R_3]^{1/2} \quad (2.34d)$$
$$K_2 = 1 + R_4/R_2 \quad (2.34e)$$
$$w_o = [(1 + R_3/R_2)/(C_1C_2R_1R_2)]^{1/2} \quad (2.34f)$$
$$Q_o = [(K_R K_C K_1)^{-1} + K_C/K_R K_1 + K_R K_C/K_1$$
$$- (K' - 1)(K_1^2 - 1)K_R K_C/K_1]^{-1} \quad (2.34g)$$

Note that if A(s) is infinite (i.e. ideal OP-AMP) and if $K_2 = 1$ (i.e. $R_4 = 0$), then equation (2.34) reduces to a biquadratic transfer function for which the resonance frequency is w_o and the Q-factor is Q_o. Substituting for A(s) from equation (2.21) into equation (2.34) gives

$$T(s)= \frac{(s/w_o)\ (K_R K_C K' K_3/K_1)\ [(s/w_o)(K_2 - 1)\ K_R K_1/K_C + 1]}{(s/w_o)^3(K' K_3/w_{Tn})\{K_2+(K_2-1)K_R^2K_1^2\}+(s/w_o)^2 K_3\{K_2-(K_2-1)K_R^2 - (K'-1)(K_1^2-1)\ K_R^2 +(K'/w_{Tn})\ [K_2 w_{cn}+(K_2-1)K_R^2K_1^2 w_{cn}+Q_o^{-1} +(K_1^2-1)K_R K_C K'/K_1+(K_2-1)K_R K_1/K_C]\} +(s/w_o)\ K_3\{Q_o^{-1}+(K_2-1)\ K_R K_1/K_C+(K'/w_{Tn})[1+w_{cn}/Q_o +(K_1^2-1)K_R K_C K' w_{cn}/K_1+(K_2-1)\ K_R K_1 w_{cn}/K_C]\}+1} \quad (2.35)$$

where $K_3 = [K' w_{cn}/w_{Tn} + 1]^{-1}$ (2.35a)

We now want to factorise the denominator of equation (2.35) into a first order term and a biquadratic term so that the first order term can be cancelled with the zero in the numerator. Suppose the resonance frequency and the Q-factor of the resulting transfer function are w_r and Q_r, respectively. Then

$$T(s)= \frac{(s/w_r)\ (w_r/w_o)(K_R K_C K' K_3/K_1)\ [(s/w_o)(K_2-1)\ K_R K_1/K_C + 1]}{[(s/w_o)(w_r/w_o)^2(K' K_3/w_{Tn})\{K_2+(K_2-1)K_R^2K_1^2\}+1][(s/w_r)^2+Q_r^{-1}(s/w_r)+1]} \quad (2.36)$$

where $w_r = w_o[K_2K_3-(K_2-1)K_R^2K_3-(K'-1)(K_2-1)(K_1^2-1)K_R^2K_3+(K'K_3/w_{Tn})\{K_2 w_{cn} +(K_2-1)K_R^2K_1^2 w_{cn}+Q_o^{-1}+(K_1^2-1)K_R K_C K'/K_1+(K_2-1)K_R K_1/K_C -Q_r^{-1}(w_r/w_o)(K_2+(K_2-1)K_R^2K_1^2)\}]$ (2.36a)

$$\text{and} \quad Q_r = (w_o/w_r)\,[K_3 Q_o^{-1} + (K_2-1)(K_R K_1 K_3/K_C) + (K' K_3/w_{Tn})\{1 + w_{cn} Q_o^{-1} + (K_1^2-1)(K_R K_C K' w_{cn}/K_1) + (K_2-1)(K_R K_1 w_{cn}/K_C) - (w_r/w_o)^2 (K_2 + (K_2-1) K_R^2 K_1^2)\}]^{-1} \tag{2.36b}$$

also, in order to have a pole-zero cancellation, we must have

$$(K_2-1)\,(K_R K_1/K_C) = (w_r/w_o)^2\,(K' K_3/w_{Tn})\,\{K_2 + (K_2-1)\,K_R^2 K_1^2\} \tag{2.36c}$$

When the pole-zero cancellation takes place the transfer function of the circuit becomes

$$T(s) = \frac{(s/w_r)\,G}{(s/w_r)^2 + Q_r^{-1}\,(s/w_r) + 1} \tag{2.37}$$

where G = gain-factor $= (w_r K_R K_C K' K_3/w_o K_1)$ (2.37a)

In the circuit of Fig 2.3(b) we have eight passive components, thus giving eight degrees of freedom. We require one degree of freedom each to adjust for the resonance frequency, the Q-factor, the pole-zero cancellation and the gain factor. Thus by arbitrarily choosing the values of four components of the circuit we can determine the values of the remaining components by solving the appropriate design equations. For the same reasons as mentioned previously, two of the arbitrarily chosen components were the two circuit capacitors. For the remaining two degrees of freedom we can either arbitrarily choose the values of two resistors or, alternatively, arbitrarily choose the value of one resistor and a resistor ratio (i.e. K', K_1, etc.) as the other degree of freedom. It was decided to use the latter scheme and thus the remaining

arbitrarily chosen variables were the resistor R_b and the resistor ratio K_1 (see equation (2.34d)).

In order to calculate the values of the remaining components we first need to determine the values of the intermediate variables w_o, Q_o, K_2, K_R and K'; this can be done by solving the following equations, which are obtained by rearranging equations (2.36a), (2.36b), (2.36c), (2.37a) and (2.34g), respectively.

$$w_o = w_r \left[K_2K_3-(K_2-1)\, K_R^2K_3-(K'-1)(K_2-1)\, K_R^2K_3+(K'K_3/w_{Tn}) \cdot \{K_2w_{cn}+(K_2-1)(K_R^2K_1^2w_{cn} +Q_o^{-1}+(K_1^2-1)\, K_RK_CK'/K_1+(K_2-1)\, K_RK_C/K_1 -Q_r^{-1}(w_r/w_o)(K_2+(K_2-1)\, K_R^2K_1^2)\}\right]^{1/2} \quad (2.38)$$

$$Q_o = [(w_o/w_rQ_rK_3)-(K_2-1)\, K_RK_1/K_C-(K'/w_{Tn}) \cdot \{1+w_{cn}/Q_o+(K_1^2-1)\, K_RK_CK'w_{cn}/K_1 +(K_2-1)\, K_RK_1w_{cn}/K_C -(w_r/w_o)^2(K_2+(K_2-1)\, K_R^2K_1^2)\}] \quad (2.39)$$

$$K_2 = 1+(K'K_3K_C/K_RK_1w_{Tn})\, (w_r/w_o)^2\, \{K_2+(K_2-1)\, K_R^2\, K_1^2\} \quad (2.40)$$

$$K_R = (w_o/w_r)\, (G\, K_1/K_RK_CK') \quad (2.41)$$

$$K' = 1+K_1/(K_RK_C(K_1^2-1))\, \{(K_RK_CK_1)^{-1}+K_C/K_RK_1+K_RK_C/K_1-Q_o^{-1}\} \quad (2.42)$$

Again, the non-linear nature of the above equations is quite apparent; hence we have to resort to solving these equations numerically using the same technique as for the Friend circuit. The flow chart of a computer program for solving these equations is given in Fig 2.5. The initial guess values of w_o, Q_o, K_2, K' and K_R are chosen as follows: $w_o = w_r$, $Q_o = Q_r$, $K_2 = 1$, arbitrarily choose K' and evaluate K_R from

equation (2.34g), taking the positive solution, i.e.

$$K_{R_i} = \frac{[(K_1/Q_{o_i})^2 + 4(1+K_C^2)\{(K_i'-1)(K_1^2-1)-1\}]^{1/2} - K_1/Q_{o_i}}{2K_C[(K_i'-1)(K_1^2-1)-1]} \qquad (2.43)$$

where suffix i denotes "initial value".

Once w_o, Q_o, K_2, K_R and K' have been determined, the values of resistors R_1, R_2, R_3, R_4 and R_a can be evaluated from the following equations, which have been obtained by rearranging equations (2.34f), (2.34a), (2.34d), (2.34e) and (2.34c), respectively.

$$R_1 = [w_o K_R K_C C_1/K_1]^{-1} \qquad (2.44)$$

$$R_2 = K_R^2 R_1 \qquad (2.45)$$

$$R_3 = R_1 [K_1^2 - 1]^{-1} \qquad (2.46)$$

$$R_4 = (K_2 - 1) R_2 \qquad (2.47)$$

$$R_a = R_b (K' - 1) \qquad (2.48)$$

The computer program based on the flow chart diagram of Fig 2.5 can also be used for predistorting the design (in accordance with the method one presented in Section 2.2.1) as well as designing the Sallen and Key SAB bandpass circuit in the case of an ideal OP-AMP. The predistorted design is obtained by forcing K_2 to be equal to unity, whereas the ideal design is obtained by forcing K_2 to be equal to unity and by setting A_o and w_c to be very large.

In the preceeding discussion we have derived design equations for the compensated Friend and the Sallen and Key SAB bandpass circuits; also a numerical procedure has been proposed for solving these equations. The design equations are solved using an iterative

procedure and obviously the number of iterations taken to reach the final solution is highly dependent on the initial values used to start the iteration process; for poor initial values the process may not even converge. One way of choosing the initial guess values, which will always guarantee a solution, is as follows.

We begin by assuming f_T of the OP-AMP to be infinite (i.e. ideal OP-AMP), in which case the initial values are identical to the nominal values (e.g. $w_o = w_r$, $Q_o = Q_r$, etc.). Now the idea is to reduce the value of f_T from infinity to its actual finite value by decreasing it in steps. At each step the iteration procedure is repeated to determine the values of the intermediate variables; these values are then used as the initial guess values for the next decrement step of f_T. The size of the step is adjusted, if necessary, such that the iteration process always converges. Therefore if the ideal design of the circuit exists, then the above procedure guarantees a compensated design of the circuit for any value of f_T (>0).

It was found that the circuits of Figs 2.2(b) and 2.3(b) could be designed quite satisfactorarily by reducing the value of f_T from infinity to its actual value of 1 MHz in just one step.

2.6 Comparison of the computed results of the compensated and predistorted designs with the nominal design

In this section we shall compare the amplitude and phase characteristics of the SAB bandpass circuits considered above for three different designs of each circuit; in addition, the amplitude and phase characteristics of the three sixth order leap-frog multiple feedback bandpass filter circuits corresponding to these three designs

of the SAB circuits will also be compared. Each SAB bandpass circuit is designed as follows:

1. the OP-AMP is assumed to be ideal

2. assuming an OP-AMP gain bandwidth product of 1 MHz and predistortion of the design of the SAB circuits according to method one discussed in Section 2.2.1, with A(s) characterised by $A(s) = w_T/s$

3. assuming an OP-AMP gain bandwidth product of 1 MHz and compensation of the design of the SAB circuits by using an extra resistor.

The method of designing the Friend and the Sallen and Key SAB bandpass circuits was discussed in Section 2.5 and the three sets of component values, corresponding to the above three designs, for each SAB circuit are shown in Table 2.2 and Table 2.3,respectively.

The three sets of component values shown in Tables 2.2 and 2.3 were used in a network analysis program, assuming an appropriate model for the OP-AMP, and the results obtained are shown plotted in Figs 2.6 and 2.7. From Figs 2.6 and 2.7, we observe that whereas the response curves of the compensated design are in good agreement with the nominal curves, the response curves of the predistorted designs show small deviations as predicted in Section 2.2.

The circuit of Fig 2.8 is obtained by connecting two Friend SAB bandpass circuits and one Sallen and Key SAB bandpass circuit to realise the feedback topology shown in Fig 1.9(b). The summers at the input of the first and the second sections in Fig 1.9(b) and the

correct gain factors for the sections are realised by splitting-up the input resistor (i.e. R_1) of each SAB circuit as mentioned in Section 1.3.2. The three sets of component values for the circuit of Fig 2.8 are given in Table 2.4.

The computed response curves for the three designs of the multiple feedback filter are given in Fig 2.9, from which we note that while the characteristics of the compensated circuit are exactly coincedent with the nominal, the characteristics of the predistorted design shows the expected deviation. The difference between the predistorted and the nominal characteristics is a direct result of neglecting the effect of the real pole, created by the OP-AMP, in the predistortion method used to design the SAB circuits.

2.7 Conclusions

In this Chapter the effect of the amplifier finite gain bandwidth product of SAB circuits was discussed in the context of multiple feedback filters. It has been shown that the effect of frequency dependent nature of the amplifier gain is to perturb the poles of the transfer function from their nominal locations and to give rise to additional unwanted poles. For single amplifier biquadratic (SAB) circuits, two methods of predistorting the design, in order to counter act the effect of finite f_T, were discussed. Using predistortion techniques it is possible to move the dominant complex pole pair of the transfer function back to its nominal position; however, the effect of the OP-AMP created poles cannot be eliminated, and at best can only be taken fully into account at a single frequency.

The basic principles of actively and passively compensating for the effect of the OP-AMP created poles were also discussed. While active or passive compensation of multi-amplifier circuits is only approximate, it has been shown that in the case of SAB circuits which realise a lowpass or a bandpass type of transfer function, it is possible to fully compensate for the effect of the finite f_T. Passive compensation method was used to design the Friend and the Sallen and Key SAB circuits which were subsequently used to realise a sixth order multiple feedback bandpass filter. The computed amplitude and phase responses showed an excellent agreement between the nominal and the compensated designs, whereas the expected deviations between the predistorted and the nominal designs were confirmed.

C H A P T E R 3

MINIMISATION OF THE SENSITIVITY OF MULTIPLE FEEDBACK FILTERS

3.1 Introduction

In Chapter 2 we discussed a method of compensating for the effect of finite amplifier gain bandwidth product, f_T, in multiple feedback filters. It was shown there that the multiple feedback filter can be designed to have nominal response characteristics even in the presence of non-ideal operational amplifiers (OP-AMPs). The purpose of this chapter is to examine how the filter response is affected when the components of the second order sections vary from their nominal design values, and also to present a method of designing the single amplifier biquadratic (SAB) circuits, which are used as the basic building blocks in high order filters, in such a way that variations in the overall filter response, due to variations in the values of the components, are minimised.

In practice there are two types of component variations; values of components may differ from their respective nominal values due to manufacturing tolerances or due to changes in ambient conditions such as temperature, supply voltage, etc.. The manufacturing tolerances of the components can be accounted for by tuning the circuit [49], deterministically or functionally [72], and hence the circuit can be adjusted to obtain the desired characteristics at the time of manufacture. In this case the main factor contributing towards the sensitivity of the filter is that due to the post-adjustment variations of the components.

The main cause of post-adjustment variation is due to changes in the temperature. A typical value of the temperature coefficient of passive components (e.g. thick film resistors and ceramic chip capacitors) is of the order of 28 ppm/^{o}C, whereas the temperature

coefficient for the f_T of the amplifier is of the order of - 2500 ppm/^oC. Thus, a temperature variation of $\pm$ 40 ^oC around the ambient would produce $\pm$ 0.112 % change in passive components and $\pm$ 10 % change in the gain bandwidth product of the OP-AMP. Note that the temperature coefficient of thick film resistors may be positive for both an increase or a decrease of the ambient temperature [2].

There are two basic approaches for minimising the sensitivity of multiple feedback filters. The first of these, which is explained in more detail in [12], is concerned with choosing the parameters of the sections in the multiple feedback structure in such a way that the sensitivity of the structure to changes in the sectional parameters is minimised. In the case of leap-frog type multiple feedback structures, with which we are concerned in this thesis, the parameters which we utilise to minimise the sensitivity of the structure are the Q-factors and the gain factors of the sections, and also the feedback factors [12].

In contrast to the above approach to sensitivity minimisation, in the second approach we are concerned with minimising the effect on the filter response of changes in the values of the components (i.e. R, C or f_T) of the second order sections. In this case, the sectional parameters are regarded as constant and the optimisation exploits the degrees of freedom available in the design of the individual sections. This is more relevant to what we are interested in, but it is also more difficult to achieve in that it requires greater computational effort. Our aim in this chapter is the implementation of this latter approach for minimising the sensitivity of the multiple feedback filter response to changes in the element values of the second order sections.

In order to illustrate the basic principles of the sensitivity minimisation method, and to provide continuity, we shall consider the compensated leap-frog feedback bandpass filter discussed in Chapter 2. We shall refer to the multiple feedback filter circuit developed in Chapter 2 as the compensated but "un-optimised" circuit, and later we shall compare its sensitivity performance with the "optimised" version which is to be developed in this chapter.

3.2 General method and optimisation criterion

In this section we shall present a general method, and also develop a criterion, for minimising the sensitivity of multiple feedback filters. The basic principle of the sensitivity minimisation criterion can be more effectively explained by considering a particular example. For this end, we shall formulate the problem to minimise the sensitivity of the sixth order leap-frog feedback bandpass filter circuit discussed in Chapter 2. However, before we begin a detailed discussion of the actual method, a few general remarks, which are relevant to the problem under consideration, are in order.

Firstly, for the schematic diagram of Fig 1.9(b), we note that the transfer function of the multiple feedback structure is given by

$$T(s) = \frac{T_1(s)\, T_2(s)\, T_3(s)}{1 + F_{12}\, T_1(s)\, T_2(s) + F_{23}\, T_2(s)\, T_3(s)} \qquad (3.1)$$

$$\text{where} \quad T_i(s) = \frac{(-1)^i \, (s/w_{r_i}) \, G_i}{(s/w_{r_i})^2 + Q_{r_i}^{-1} \, (s/w_{r_i}) + 1} \qquad (3.1a)$$

and i = 1, 2, 3

Now, in Chapter 2 the multiple feedback filter of Fig 1.9(b) was designed for the case $F_{12} = F_{23} = 1$. Therefore, from equation (3.1) we note that for this condition we can interchange $T_1(s)$ and $T_3(s)$ without affecting the overall transfer function, T(s). Moreover, this coupled with the fact that the parameters (i.e. the resonance frequency, the Q-factor and the gain factor) of $T_1(s)$ and $T_3(s)$ are identical (see Table 2.1) suggests that the sensitivity of T(s) to variations in the components of the circuits realising $T_1(s)$ and $T_3(s)$ is also identical. Thus in the multiple feedback filter of Fig 1.9(b) we have only to minimise the sensitivity of T(s) to variations in the components of $T_1(s)$ and $T_2(s)$; the design of $T_3(s)$ is then made identical to the design of $T_1(s)$.

Secondly, we note that in the design of the Friend and the Sallen and Key SAB bandpass circuits the frequency dependent nature of the gain of the OP-AMPs is fully compensated by achieving a pole-zero cancellation. Therefore when the components of the circuit change from their respective nominal values the pole-zero cancellation no longer takes place and the transfer function of the SAB circuit under these conditions becomes of the form

$$\overline{T_i(s)} = \frac{(-1)^i \, G'_i \, (s/w'_{r_i}) \, (a_i s + 1)}{(b_i s + 1) \, [(s/w'_{r_i})^2 + Q'^{-1}_{r_i} \, (s/w'_{r_i}) + 1]} \qquad (3.2)$$

where $i = 1, 2, 3$

Equation (3.2) shows that in addition to the pole-zero cancellation not taking place, the values of the resonance frequency, the Q-factor and the gain factor of the circuit also deviate from their respective nominal values. In equation (3.2), due to the magnitude of the changes that we shall be considering and also because of the locations, in the s-plane, of the real pole and the zero relative to the position of the dominant complex pole-pair, the effect on the transfer function of the SAB circuit of the non-cancellation of the pole-zero is negligible compared with the effects caused by the changes in the "dominant variables" (i.e. the resonance frequency, the Q-factor and the gain factor of the circuit). Thus for all practical purposes we can regard the pole-zero cancellation as taking place and then we have only to consider the effect of changes in the dominant variables.

Thirdly, we note that in practical situations variations in the environmental conditions would produce correlated changes in the like components of the circuit and thus the resonance frequency of the SAB circuit would be affected more severely than its gain factor or the Q-factor, because the latter two variables are functions of component value ratios, whereas the former is dependent on the product of component values. Hence, if we assume the component variations to be correlated then the sensitivity of the filter transfer function to

only the resonance frequency of each biquadratic section needs to be minimised; however, for uncorrelated component changes, we need to consider the sensitivity of the filter transfer function to three parameters of each biquadratic section, i.e. the resonance frequency, the Q-factor and the gain factor. In the case of uncorrelated changes, the problem of selecting the direction of the component variations can be avoided by choosing the sets of variations which produce worst case change in the resonance frequency, the Q-factor or the gain factor. For the remainder of this chapter we shall assume that although the magnitude of the post-adjustment variations in the components of the circuit are equal (i.e. $\pm$ 0.112 % for the passive components and $\pm$ 10 % for the f_T's of the OP-AMPs), the direction of the variations are independent of each other.

Fourthly, one way of minimising the sensitivity of the multiple feedback filter would be to formulate the objective function to minimise the sensitivity of each biquadratic section individually in isolation. This type of objective function has been used by Fleischer [73] to minimise the sensitivity of the resonance frequency and the Q-factor of the Friend SAB circuit to variations in its component values. However, since we are interested in minimising the sensitivity of the multiple feedback filter structure this may be done more effectively if the objective function is based on the transfer function of the overall filter; indeed, we shall adopt this approach for the problem under consideration.

The sensitivity of the filter response to changes in the values of the components (i.e. R's, C's and f_T's) can be considered in two steps. In the first step we consider the sensitivity of the sectional parameters to changes in the values of the components of the SAB

circuits; and as a second step, we consider the sensitivity of filter transfer function to changes in the sectional parameters.

Let us now consider the development of the sensitivity minimisation criterion in detail. In Chapter 2, in the course of designing the compensated Friend and the Sallen and Key SAB bandpass circuits we utilised four component parameters to achieve the following:

1. a pole-zero cancellation
2. a specific value for the resonance frequency
3. a specific value for the Q-factor
4. a specific value for the gain factor of the circuit

While it is necessary to satisfy conditions 1, 2 and 3, the condition 4 is optional since we can design the SAB circuits to have maximum gain and then achieve gain reduction by splitting resistor R_1, in Figs 2.2(b) and 2.3(b), into a voltage divider as mentioned in Section 1.3.2. Thus, another degree of freedom results which may be used to minimise the sensitivity of the SAB circuits to post-adjustment variations in the values of the components of the circuits. We shall designate this optimisable parameter as the "closed loop gain" (CLG) and define it as

$$\text{CLG} \triangleq \frac{K'}{K' - 1} \tag{3.3}$$

where K' for the circuits of Figs 2.2(b) and 2.3(b) is given by equations (2.20c) and (2.34c), respectively.

Now, we are interested in acquiring a figure of merit (i.e. an objective function) which relates the sensitivity of the multiple feedback filter transfer function to the variations in the components of the SAB sections. For this purpose the objective function to be formulated here is concerned with minimising two parameters of the multiple feedback filter; namely, "reduction in useful bandwidth" and "variation of loss in useful bandwidth". The definition of the above terms and the basic principle of the sensitivity minimisation criterion can be more effectively made by considering an example.

Suppose we want to minimise the sensitivity of the transfer function of the multiple feedback filter circuit of Fig 1.9(b) to variations in the components of the compensated Friend SAB bandpass circuit of Fig 2.2(b) which realises $T_1(s)$ in Fig 1.9(b). Then we design the Friend SAB circuit for various values of the closed loop gain using the computer program described in Section 2.5.1. Note that the equations used in this program are rearranged such that the closed loop gain (see equations (3.3) and (2.20c)) is a free parameter. For each value of the closed loop gain, the f_T of the OP-AMP is varied by $\pm$ 10 % and then each passive component is varied, individually, by $\pm$ 0.112 % and the resulting changes produced in the values of the resonance frequency, the Q-factor and the gain factor are plotted as functions of the closed loop gain. From these curves the signs of the variations of the components required to produce the worst case changes in the resonance frequency, the Q-factor and the gain factor are established. Starting at some value of the closed loop gain, we simultaneously change all the components of the SAB circuit in the appropriate directions to produce the worst case change in the resonance frequency, and then calculate

the actual value of the resonance frequency and the corresponding values of the Q-factor and the gain factor. These parameters which define $T_1(s)$ are then substituted into equation (3.1) (assuming the parameters of $T_2(s)$ and $T_3(s)$ to have their respective nominal values) to evaluate the frequency response of the overall filter transfer function. Note that one set of component variations gives worst case positive change in the resonance frequency, whereas the complementary set of component variations gives worst case negative change (this argument also applies for the Q-factor and the gain factor); in order to evaluate equation (3.1) we use the larger of these two changes.

From the loss-frequency response of the filter computed assuming the parameters of $T_1(s)$ vary as stated above, we need to determine the two objective function parameters, i.e. the reduction in the useful bandwidth and the variation of loss in the useful bandwidth. In order to define these terms more precisely, we shall now consider some examples of loss-frequency responses. Fig 3.1 shows some typical response curves (shown in dashed line) which result when all components of one of the section in the multiple feedback structure are changed simultaneously to produce worst case change in the resonance frequency (the nominal response curves are shown in continuous line). From Fig 3.1, we note that when the sectional parameters of one of the section in the multiple feedback structure change from their respective nominal values, the loss-frequency response of the resulting filter has four observable differences compared with the nominal response. Firstly, the response is shifted in frequency; secondly, the passband loss is no longer equi-ripple; thirdly, the variation of loss in the passband is different from the passband loss variation of the nominal response, which is equal to the

ripple value; fourthly, the response has a level shift, i.e. the minimum loss points of the two responses are not at the same level. It is not very important that the loss-frequency response should be equi-ripple or have the same level as the nominal response; however, in order to minimise the sensitivity, it is necessary to ensure that the frequency shift and the variation of loss in the passband are as small as possible in the frequency band of interest.

In Fig 3.1(a), the bandwidth B_w and the variation of loss in the passband V_L for the nominal response are given by $B_w = f_2 - f_1$ and $V_L = d_2 - d_1$, respectively; whereas, when the components of one of the SAB section are changed the bandwidth and the variation of the loss in the passband of the filter become $B'_w = f'_2 - f'_1$ and $V'_L = d'_2 - d'_1$, respectively. We can now define the useful bandwidth, B_u, as the portion of B'_w which lies inside B_w; whereas the variation of loss in the useful bandwidth, V_u, is simply given by the difference between the maximum and the minimum losses occuring in the useful bandwidth. Thus, in Fig 3.1(a), $B_u = f'_2 - f_1$ and $V_u = d'_2 - d'_1$. Now the bandwidth for which the filter was designed is B_w and the useful bandwidth obtained is B_u; therefore the reduction in the useful bandwidth is given by $B_r = B_w - B_u$. The determination of the useful bandwidth (and hence the reduction in the useful bandwidth) and the variation of loss in the useful bandwidth for another typical response curve is shown marked in Fig 3.1.

We have shown above how to determine the two objective function parameters (i.e. the reduction in useful bandwidth and the variation of loss in the useful bandwidth) when the SAB bandpass circuit realising $T_1(s)$ in Fig 1.9(b) is designed for a specific value of the closed loop gain and when all the components of the SAB circuit are

changed to produce the worst case change in the resonance frequency. By designing the SAB circuit for other values of the closed loop gain, we can plot the reduction in the useful bandwidth and the variation of loss in the useful bandwidth as functions of the closed loop gain. Furthermore, if we repeat the above procedure for the cases when the component changes are selected to produce worst case changes in the Q-factor and the gain factor, then we can obtain another two pairs of graphs which are also plotted as functions of the closed loop gain. From these six curves obtained in this way (three for reduction in the useful bandwidth and three for the variation of loss in the useful bandwidth), we will have to choose a single "compromised" value of the closed loop gain which minimises the sensitivity of the overall transfer function to the component variations of the SAB circuit under consideration. The name compromised value of the closed loop gain is appropriate because the minima of the six curves may not occur at the same value of the closed loop gain. One way of overcoming this difficulty would be to combine these six curves, using appropriate weighting factors, to yield just a single curve; we shall not consider this approach here because the weighting factors can only be based upon a given specification that the filter is designed to meet and we have no such specification for the filter under consideration. In evaluating the compromised closed loop gain we shall use two curves only which correspond to the largest reduction in the useful bandwidth and the largest variation of the loss in the useful bandwidth. When we consider the sensitivity minimisation of the compensated Friend and the Sallen and Key SAB bandpass circuits, in the next section, it will be seen that as long as the closed loop gain value lies within a certain range the increase in the sensitivity of the overall response

is quite small. Thus the above criterion of determining the compromised value of the closed loop gain is quite justified.

We have described above a method of designing one of biquadratic sections in the multiple feedback structure such that the sensitivity of the overall filter response to post-adjustment variations in the values of the components in the biquadratic section is minimised. By repeating the procedure outlined above, we can design the remaining biquadratic sections in the same way to yield an optimum design of the multiple feedback filter.

Note that the objective function described above minimises the variations in the bandwidth and the passband loss of the filter. Frequently it may be necessary to minimise the response variations of the transition-band or the stopband; this can be achieved by formulating a different objective function. Indeed, it would be quite possible to obtain a "weighted" objective function which takes into account the response variations in the passband, the transition-band and the stopband. However, we shall only use the objective function based on the passband variations since the purpose of the exercise is to present a general method of minimising the sensitivity rather than to formulate the "best" objective function; anyway, the latter can only be done if we have some specification to meet, but as stated previously this is not the case for the example under consideration.

3.3 Example of sensitivity minimisation of a leap-frog feedback bandpass filter

3.3.1 General

In the previous section a method of minimising the sensitivity of multiple feedback filters to the post-adjustment variation in the values of the components of the biquadratic sections, which are used to realise multiple feedback structures, was presented. In this section we shall apply this method to minimise the sensitivity of the sixth order leap-frog feedback bandpass filter discussed in Chapter 2. This multiple feedback filter consists of three second order sections, two of which are realised with the compensated Friend SAB bandpass circuit of Fig 2.2(b), while a compensated Sallen and Key SAB bandpass circuit of Fig 2.3(b) is used for realising the other section. As explained in Section 3.2, since the first and the third sections in the multiple feedback realisation, in Fig 2.8, are identical we need only minimise the sensitivity of the multiple feedback filter with respect to sections one and two. In Section 3.3.2, we shall consider the sensitivity minimisation of the multiple feedback filter to variations in the component values of the compensated Friend SAB bandpass circuit; whereas, the problem of minimising the sensitivity to variations in the component values of the compensated Sallen and Key SAB bandpass circuit is to be discussed in Section 3.3.3.

After the minimum sensitivity designs of the compensated Friend and the Sallen and Key SAB bandpass circuits have been obtained we shall compute the sensitivity of the optimised leap-frog feedback filter and compare the results with a corresponding analysis of the un-optimised design obtained in Chapter 2.

3.3.2 Sensitivity minimisation of the Friend SAB bandpass circuit

In this subsection we shall consider the sensitivity minimisation of the compensated Friend SAB bandpass circuit of Fig 2.2(b), which realises the first biquadratic section in the multiple feedback filter of Fig 2.8. In order to carry-out the sensitivity minimisation procedure we need to establish the sets of component variations required to produce the worst case change in the resonance frequency, the Q-factor and the gain factor. To achieve this we proceed as follows.

By arbitrarily choosing the value of the closed loop gain (i.e. the optimising parameter), we design the SAB circuit for some nominal f_T value, which we shall assume to be 1 MHz, using the computer program based on the flow chart of Fig 2.4. We now select a particular component of the SAB circuit and change its value by a certain specified amount (for the f_T this variation is $\pm$ 10 %, whereas for the passive components it is $\pm$ 0.112 %) and calculate the magnitude and the sign of the changes in the resonance frequency, the Q-factor and the gain factor of the circuit. The selected component is now varied in the opposite direction by the same amount and the corresponding magnitude and sign of the changes in the resonance frequency, the Q-factor and the gain factor are noted. By repeating this procedure for other values of the closed loop gain we can plot a pair of graphs each for the changes in the resonance frequency, the Q-factor and the gain factor as functions of the closed loop gain. Similarly, the whole procedure is repeated by varying each component of the circuit in turn. Some typical results obtained for the circuit of Fig 2.2(b), which is designed for a resonance frequency

of 15 kHz and a Q-factor of 47.8875 (for nominal f_T of 1 MHz), will be discussed presently.

The graphs in Fig 3.2 show the changes in the resonance frequency, the Q-factor and the gain factor of the circuit of Fig 2.2(b) when the gain bandwidth product of the OP-AMP is changed by $\pm$ 10 % from its nominal value. The corresponding curves are shown in Fig 3.3 for the case when the value of resistor R_1, in the circuit of Fig 2.2(b), is changed by $\pm$ 0.112 % from its nominal value. The changes which occur when all the passive components are varied individually by $\pm$ 0.112 %, from their respective nominal values, are shown in Fig 3.4. From the graphs in Fig 3.4, the relative effects of the passive components on the resonance frequency, the Q-factor and the gain factor of the circuit can be seen at a glance. It is interesting to note that the sensitivities of the compensating resistor, R_3, in the circuit of Fig 2.2(b) are either less than or comparable with the sensitivities of the other components of the circuit.

In Table 3.1, the sign of component variations required to produce a positive and a negative change in the resonance frequency, the Q-factor and the gain factor of the circuit are tabulated. The worst case change in the resonance frequency (or the Q-factor or the gain factor) is obtained by changing all the components of the circuit simultaneously according to the appropriate set of signs given in Table 3.1. The results for the worst case variations are shown in Fig 3.5. From Table 3.1, we note that in order to produce worst case changes in the Q-factor and the gain factor, the set of component variations required is the same. Hence we need only consider the worst case changes in the resonance frequency and the Q-factor.

Having done the preliminary work we now proceed to evaluate the objective function parameters.

We design the SAB circuit for some value of the closed loop gain and vary all components of the circuit to produce worst case negative change in the resonance frequency. The resulting actual changes in the resonance frequency, the Q-factor and the gain factor of the circuit are determined. The sectional parameters of $T_1(s)$ are changed by the corresponding percentage amounts and the loss-frequency response of the multiple feedback filter structure is computed by evaluating equation (3.1), assuming $T_2(s)$ and $T_3(s)$ to have their respective nominal sectional parameters. The components of the circuit are now varied so as to produce the worst case negative change in the Q-factor and the actual values of the sectional parameters are determined and the equivalent percentage changes are introduced in the parameters of $T_1(s)$ when evaluating equation (3.1). Some typical graphs obtained for the worst case changes in the resonance frequency and the Q-factor are shown in Fig 3.6; from these curves we measure the useful bandwidth and the variation of loss in the useful bandwidth in accordance with the procedure described in Section 3.2. The above procedure is repeated for other values of the closed loop gain and from the results obtained in this way we plot the reduction in the useful bandwidth and the variation of loss in the useful bandwidth as functions of the closed loop gain, as shown in Fig 3.7.

From the graphs of Fig 3.7 it is seen at a glance that the optimum value of the closed loop gain lies between about four and ten; this region of Fig 3.7 is shown on an expanded scale in Fig 3.8. In order to obtain the optimum value of the closed loop gain, we have to consider the curve corresponding to the worst case Q-factor change in

Fig 3.8(a) and the curve corresponding to the worst case resonance frequency change in Fig 3.8(b). It was decided to select seven as being the compromised value of the closed loop gain. We note from Fig 3.8 that very small changes in the reduction of the useful bandwidth and the variation of loss in the useful bandwidth result if the closed loop gain value varies from the chosen optimum of seven; therefore, the optimum value is not very critical as long as it lies in a certain range. This range is from about four to ten in Fig 3.8.

3.3.3 Sensitivity minimisation of the Sallen and Key SAB bandpass circuit

The sensitivity minimisation of the compensated Sallen and Key SAB bandpass circuit of Fig 2.3(b), which is used to realise the central section in the multiple feedback filter of Fig 2.8, is carried-out with an identical procedure to that described in Section 3.3.2 for the compensated Friend SAB bandpass circuit. However, with regard to the sensitivity minimisation of the Sallen and Key SAB bandpass circuit, there are two additional factors which must be taken into account.

Firstly, compared with the Friend SAB circuit, the Sallen and Key SAB circuit has one more component; hence whereas in the case of the Friend circuit we just had one parameter to optimise the circuit for the Sallen and Key circuit we effectively have two parameters. Secondly, the central section of the multiple feedback filter of Fig 2.8 is designed for a resonance frequency of 15 kHz and a Q-factor of value infinity; hence in the case of such a section it would be meaningless to talk about "changes" in the Q-factor.

The difficulties arising in the terminology, with respect to the latter of above two points, can be overcome by replacing the phrase "worst case change in the Q-factor", used in conjunction with the Friend SAB circuit, with the phrase "worst case Q-factor" for the present circuit. However, the dilemma of having two free parameters for minimising the sensitivity is of more complex nature. An ideal solution to this problem would be to choose one of these parameters as the optimising parameter and then carry-out the sensitivity minimisation procedure with the constraint that the value of the other free parameter is chosen optimally for each value of the optimising parameter. Obviously the implementation of this scheme would require a large amount of computing effort and may not be practically feasible. Instead, it was decided to adopt an alternative strategy which is out-lined in the following.

We assume one of the free parameter as our optimising variable while the value of the other parameter is chosen arbitrarily. The sensitivity minimisation procedure is now carried-out as before with different values of the optimising parameter; if the results obtained are considered satisfactory then the current circuit is taken as the optimum circuit; otherwise the optimisation procedure is repeated by choosing a different value for the second free parameter.

In the case of the compensated Sallen and Key SAB bandpass circuit of Fig 2.3(b), the two free parameters are the closed loop gain, K', and the resistor ratio K_1. In the first instant the value of K_1 was chosen as $K_1 = \{301\}^{1/2}$ and the sensitivity minimisation was carried-out with respect to the closed loop gain. However, it was found that the spread in the circuit component values corresponding to the optimum closed loop gain was unpractical. When the sensitivity

minimisation procedure was repeated for $K_1 = \{31\}^{1/2}$, the circuit component spread was satisfactory. Furthermore, it was observed that very little changes result in the values of the reduction in useful bandwidth and the variation of the loss in the useful bandwidth corresponding to the two values of K_1. It was also noticed that the variations in the sectional parameters which are produced when the value of compensating resistor is changed from its nominal value are generally very much less than the corresponding variations resulting as a consequence of a similar change in the value of any other component of the circuit.

Table 3.2 shows the set of component variations required to produce the worst case change in the resonance frequency, the worst case Q-factor and the worst case change in the gain factor. We note from Table 3.2 that the same set of component variations are required for the worst case Q-factors and the worst case changes in the gain factors; hence we need only consider the effect of worst case change in the resonance frequency and the worst case Q-factor when evaluating the objective function parameters.

The plot of the objective function parameters against the closed loop gain is shown in Fig 3.9. Note that in order to obtain the optimum value of the closed loop gain we have to consider the curves corresponding to the worst case change in the resonance frequency in Fig 3.9(a) and the worst case Q-factor in Fig 3.9(b). From these curves of Fig 3.9 it is seen that in order to have a smaller reduction in the useful bandwidth we need to choose our compromised optimum value of the closed loop gain between 1.4 and 1.56; whereas in order to have a smaller value of the variation of loss in the useful bandwidth the value of the closed loop gain should be

chosen to lie between 1.06 and 1.12. In this sort of a situation, we would require more information about the specification the filter is required to meet, so that we can decide as to wether the reduction in the useful bandwidth or the variation of loss in the useful bandwidth is a more critical factor. In the present filter under discussion, it was decided to take the reduction in the useful bandwidth as being the critical factor and the compromised value of the optimum closed loop gain was chosen to be equal to 1.4021.

3.3.4 Computed and practical results

In Subsections 3.3.2 and 3.3.3 we discussed the sensitivity minimisation of the compensated Friend and the compensated Sallen and Key SAB bandpass circuits, respectively. The sensitivity minimisation was carried-out in the context of a sixth order leap-frog feedback bandpass filter assuming a reasonable variations in the passive component values and in the f_T's of the amplifiers. The optimum circuit obtained by such a procedure should ideally be tested by means of a Monte-Carlo analysis in which all the circuit components are allowed to vary by their respective tolerances in a statistical manner. However, such a sophisticated program was not available to test the optimum design; therefore, it was decided to carry-out some limited computer simulation tests and to construct a discrete component model of the optimum design. The results of these efforts are presented in the following.

The circuit diagram of the multiple feedback filter is shown in Fig 3.10 and the component values of the optimised circuit are listed in Table 3.3 for the case when the multiple feedback filter is designed to have feedback factors, F_{12} and F_{23}, equal to unity and the

midband frequency gain also equal to unity. The loss-frequency response of this circuit is to be compared with the loss-frequency response of the un-optimised circuit whose component values are listed in Table 2.4.

The loss-frequency responses of the un-optimised and the optimised circuits were computed using a circuit analysis program for the case of nominal component values (with f_T's of the OP-AMPs equal to 1 MHz) and when the gain bandwidth product of each OP-AMP is varied by $\pm$ 10 %, individually, and also when the gain bandwidth products of all the OP-AMP are varied simutaneously by $\pm$ 10 % in the same direction. The results are shown in Figs 3.11 and 3.12, respectively.

On comparing the computed results of the un-optimised circuit, shown in Fig 3.11, with those of the optimised circuit, shown in Fig 3.12, we observe that the performance of the latter is very much better than the performance of the former, although for the nominal values of the gain bandwidth products both circuits have ideal response curves. In particular, comparing the responses in Figs 3.11(d) and 3.12(d), we note that as well as there being a smaller reduction in the useful bandwidth, the optimised circuit also has a smaller increase in the variation of loss in the useful bandwidth. For example, with a - 10 % change in the gain bandwidth products of all three OP-AMPs, the reduction in the useful bandwidth and the variation of loss in the useful bandwidth for the un-optimised circuit are 180.69 Hz and 1.14 dB, respectively; whereas the corresponding figures for the optimised circuit are 58.0 Hz and 0.53 dB, respectively; note that the nominal response is designed for a passband ripple value of 0.5 dB. This

limited sensitivity test indicates that the objectives of the sensitivity minimisation has been achieved as far as variations in the amplifier gain bandwidth product are concerned.

It was decided to construct a discrete component model of the optimised leap-frog feedback filter for two main reasons:

1. to show that the circuit under investigation is practically viable, i.e. to show that it does not suffer from instability, large DC offsets, etc.

2. to show that the sensitivity of the optimised circuit is sufficiently low to enable excellent response curve to be obtained quite easily in practice.

For the practical model, it was considered that the values of resistors R'_{2a} and R'_{2b} in Table 3.3 are too high and thus the stray capacitances associated with these resistor values may have a significant effect. In order to overcome this problem, the impedance level of the multiple feedback circuit was decreased by a factor of ten, and also the circuit was redesigned to have a midband frequency gain of 0.5; the resulting component values of the filter are listed in the second column of Table 3.4. It should be appreciated that the above modifications would <u>not</u> have any effect what-so-ever on the optimisation procedure, and hence the resulting circuit is still optimum.

The capacitors for the discrete component model were taken from a batch of 10 nF polystyrene capacitors having a nominal tolerance of $\pm$ 2.5 %. All resistors, except two, in each SAB section were taken from a batch of the nearest standard available value, having a

nominal tolerance of $\pm$ 5 %. The amplifiers used in the practical circuit were of the type 741, which have a nominal f_T of 1MHz. The remaining two resistors in each section were made variable in order to functionally adjust for the resonance frequency and the Q-factor of each SAB section.

Note that the funtional adjustment of the first and the third sections, which have finite Q-factors, is quite straight forward. For the adjustment of the second section, which has an infinite Q-factor, it was found necessary to apply, for the purpose of adjustment, a negative feedback path around the section in order to make its Q-factor of finite value. Thus the second section was adjusted for a finite Q-factor, but since the negative feedback loop around the second section does not exist in the multiple feedback circuit, its Q-factor enhances to an infinite value when it is used in the multiple feedback circuit. In the adjustment of the sections, it was found that an iterative procedure was not necessary, and hence only two adjustments per section were made. The element values of the adjusted circuit were measured and are listed in column three of Table 3.4. The measured response of the discrete component model is shown in Fig 3.13.

3.4 Conclusions

A method of minimising the sensitivity of multiple feedback filters has been presented. In the sensitivity minimisation, post-adjustment variations of both the passive and the active components are taken into account. The basic principle of the sensitivity minimisation criterion is that each biquadratic section in the multiple feedback filter structure is designed such that the

variations in its component values has a minimum effect on the overall filter transfer function. In order to achieve this, an objective function which characterises some desirable features of the overall filter response was introduced.

The basic idea of the sensitivity minimisation was applied to the bandpass filter discussed in Chapter 2 and a computer sensitivity analysis due to changes in the f_T's of the amplifiers showed a marked improvement in the performance of the optimised circuit, compared with that of the un-optimised circuit which was developed in Chapter 2.

A discrete component model of one version of the optimised filter circuit has been built. Each second order section was adjusted for resonance frequency and Q-factor using two adjustments per section. The measured response characteristics are found to be satisfactory.

C H A P T E R 4

A NOVEL APPROACH TO THE SIMULATION OF LC FILTERS USING NEGATIVE IMPEDANCE CONVERTERS

4.1 Introduction

In this chapter we shall describe a novel approach to the active RC simulation of low sensitivity LC ladder filter structures. In the conventional methods of simulating LC filter structures, positive impedance converters (PICs) or positive impedance inverters (e.g. gyrators) are used as the basic active units. In contrast, in the new approach to be presented here, negative impedance converters (NICs) are used as the basic active units.

As mentioned in Section 1.1, Linvill [8] proposed a synthesis technique in 1954 for realising any transfer impedance by a passive RC network together with one NIC; subsequently, two other techniques [9,10] which also required only one NIC were also proposed. The active RC filter circuits derived by these methods had unacceptably high sensitivities of the transfer function to variation in the values of the components of the circuit. This fact together with the practical difficulties encountered in building stable NIC circuits has led to general mistrust of all circuits which use NICs. A search through the active RC filter litrature shows a consensus of opinion which automatically labels all circuits which use NICs, regardless of their origin or method of derivation, as high sensitivity circuits. Therefore, it must be stressed here that the basic philosophy of the new approach to be described here is completely different from the above mentioned single NIC methods. It will be shown in Section 4.8 that the sensitivities of the active RC circuits to be derived here is indeed low. Furthermore, in Chapter 5, it is shown that the stability or the instability of these circuits can be predicted very simply and that it is possible to design guaranteed stable circuits.

The definition of the NIC and some of its properties which are relevant to the present discussion are presented in Section 4.2. In Section 4.3, a simple procedure is presented for obtaining, in a "visual" way, novel active RC subcircuits which simulate grounded and floating inductors and grounded and floating frequency dependent negative resistors (fdnr's) of the supercapacitor type (i.e. elements with impedance proportional to s^{-2}, where s is the complex frequency variable). For ease of reference, we shall refer to these grounded and floating simulated inductors and supercapacitors as the "essential subcircuits". The essential subcircuits derived in Section 4.3 are 2-port networks, and it is shown in Section 4.4 that by "viewing" these circuits in various ways, we can obtain a multitude of other simulated 2-port inductor and supercapacitor circuits. The novel essential subcircuits developed in Sections 4.3 and 4.4 can be interpreted as consisting of grounded and floating positive and negative resistors and capacitors ($\pm$ R, $\pm$ C). These $\pm$ R, $\pm$ C subcircuits can be realised by means of +R and +C circuits and NICs; however the resulting circuits are not very attractive because they require rather large numbers of components (both passive and active). The second most important step of the novel approach is the way in which these $\pm$R, $\pm$C essential subcircuits are used in the realisation of high order filters; this principle is discussed more fully in Section 4.5. In the essential subcircuits derived in Sections 4.3 and 4.4, all components except one are of the same type (i.e. either resistor or capacitor) and are of equal value which can be chosen arbitrarily. In Section 4.6 it is shown by considering some design examples that by appropriately choosing the values of these components, it is possible to obtain active RC filter circuits which are competitive from the total number of components and the

ease of circuit adjustment points of view, with other LC filter simulation techniques.

The advantages and disadvantages of the active RC filter circuits developed in Section 4.6 are discussed in the context of comparisons with the active RC circuits which are designed by the conventional partial or full impedance scaling methods [5,6,7].

In order to show that the active RC circuits obtained by the new method are practically feasible, some computed and measured results (for discrete component models) are presented in Section 4.7. The sensitivity aspects of the active RC circuits developed in Section 4.6 are considered in Section 4.8.

The novel approach to active RC filter design presented in this chapter has been published by the author [84] together with some design examples and measured results. It is of interest to note that in a recent publication [79], this novel method has been interpreted as being derivable by an application of a new type of linear transformation.

The novel approach to be described here makes frequent use of the star-delta equivalences; hence, for the sake of convenience, we reproduce these equivalences here (see Fig 4.1):

Star ⟶ Delta

$$Z_1 = Z_A + Z_C + Z_A Z_C / Z_B$$

$$Z_2 = Z_A + Z_B + Z_A Z_B / Z_C$$

$$Z_3 = Z_B + Z_C + Z_B Z_C / Z_A$$

Delta ⟶ Star

$$Z_A = Z_1Z_2/(Z_1 + Z_2 + Z_3)$$

$$Z_B = Z_2Z_3/(Z_1 + Z_2 + Z_3)$$

$$Z_C = Z_1Z_3/(Z_1 + Z_2 + Z_3)$$

4.2 Negative impedance converter —— definition and some properties

A negative impedance converter (NIC) is a 2-port network which is defined by the following transmission matrix:

$$\begin{bmatrix} V_1 \\ I_1 \end{bmatrix} = \begin{bmatrix} A & B \\ C & D \end{bmatrix} \begin{bmatrix} V_2 \\ I_2 \end{bmatrix} = \begin{bmatrix} 1 & 0 \\ 0 & -k \end{bmatrix} \begin{bmatrix} V_2 \\ I_2 \end{bmatrix} \qquad (4.1)$$

The 2-port representation of a NIC together with the conventions for the signs of the voltages and currents are shown in Fig 4.2(a). Equation (4.1) defines what is commonly referred to as the "current converting" type of NIC. The parameter k in equation (4.1) is referred to as the NIC "conversion factor" and it is a dimensionless quantity. In general k may be a function of frequency but for all the NICs to be used in this thesis we require k to be independent of frequency.

The current converting type of NIC, in which k is independent of frequency, can be realised using a single operational amplifier (OP-AMP) and two resistors, as shown in Fig 4.2(b). The circuit symbol which is to be used in this thesis for the 3-terminal NIC of Fig 4.2(b) is shown in Fig 4.2(c). The conversion factor, k, of the NIC is also stated in Fig 4.2(c) and we shall assume that terminal 1 of the NIC is always marked by a "•"; in this case the

electrical properties of the NIC are described by equation (4.1). Now, if the 3-terminal NIC of Fig 4.2(c) is terminated at port 2 by an impedance Z_2, as shown in Fig 4.2(d), then it can be shown that the input impedance presented at port 1 is given by

$$Z_{i1} = - Z_2 \, k^{-1} \tag{4.2}$$

Similarly, if as shown in Fig 4.2(e) the NIC is terminated at port 1 by an impedance Z_1 then the input impedance presented at port 2 is given by

$$Z_{i2} = - k \, Z_1 \tag{4.3}$$

The configurations in Figs 4.2(d) and (e) show how to realise negative grounded impedances. In order to realise a floating negative impedance, say Z, we require two NICs connected as shown in Fig 4.2(f). The use of NICs for the realisation of the $\pm$R, $\pm$C circuits to be developed in the next section becomes really attractive when a number of identical NICs (termed as a multi-NIC) are terminated in a network N_1, as shown in Fig 4.3(a). In this case, the impedance matrix of the equivalent network N_2 is related to the impedance matrix of network N_1 by

$$[Z_2] = - k^{-1} \, [Z_1] \tag{4.4}$$

where it is assumed all the NICs are identical and the value of the conversion factor is k. Thus the network N_2 may be simulated by using a multi-NIC which is terminated by network N_1, the impedance matrix of which is given by

$$[Z_1] = - k [Z_2] \tag{4.5}$$

It is convenient to let the network N_1 have the same topology as that of network N_2; then the impedance of each element in N_1 is simply the impedance of the corresponding element in N_2 multiplied by k^{-1}. Furthermore a change in the impedance of any element in the network N_1 is equivalent to the same change in the impedance of the corresponding element in the network N_2. A general network topology will contain both positive and negative impedances and it can be realised with positive impedances and a multi-NIC in the following manner.

We divide the network into two subnetworks, viz: a subnetwork containing all the positive impedances and a subnetwork containing all the negative impedances. The subnetwork comprising negative impedances is now replaced by a topologically similar subnetwork comprising positive impedances and this subnetwork is then connected to the other positive subnetwork via the multi-NIC, as shown in Fig 4.3(b).

Note that, as stated previously, equation (4.1) represents a current converting type NIC whereas a voltage converting type NIC would be obtained if in equation (4.1) we have $A = - k$, $B = C = 0$ and $D = 1$; but such NICs are not suitable for the present discussion and hence these are not considered here. The effect of the finite gain bandwidth product, f_T, of the OP-AMP for the current converting type NIC will be examined in Chapter 5 where a discussion of the stability of NIC circuits will also be presented.

4.3 Realisation of essential subcircuits

4.3.1 Grounded inductors

Let us consider the grounded inductor 2-port shown in Fig 4.4(a), which consists of a shunt arm inductor. This inductor can be equivalently represented —— using "redundant" elements —— by the 2-port in Fig 4.4(b), where at this stage R can have any convenient positive value. The encircled part of Fig 4.4(b) can then be equivalently replaced (using the star ⟶ delta transformation) by the encircled part of the circuit in Fig 4.4(c). Thus we have obtained a $\pm$R, $\pm$C circuit which simulates a grounded inductor. The basic principle illustrated in Fig 4.3(b) can be used to realise this $\pm$R, $\pm$C circuit by means of +R, +C circuit and three NICs, as shown in Fig 4.4(d). Note the the circuit in Fig 4.4(d), as it stands, is not very attractive since it require a large number of components (both passive and active). This problem will be overcome in Section 4.5.

4.3.2 Floating inductors

Let us consider the floating inductor 2-port shown in Fig 4.5(a), which is equivalently represented in Fig 4.5(b) by connecting some redundant $\pm$R's. In Fig 4.5(b), transforming the encircled delta network into its star equivalent gives the $\pm$R, $\pm$C network shown in Fig 4.5(c), which can be realised using NICs as shown in Fig 4.5(d). Again, the circuit in Fig 4.5(d) is not very suitable for use in filter design because it requires a large number of components.

The floating inductor simulation circuit of Fig 4.5(d) has also been proposed in [74] and more recently in [75]. The application of

the simulated inductor circuits of [74,75] to filter design differs from the approach to be outlined in Section 4.5. It has been pointed-out to the author that the circuit of Fig 4.5(d) can also be derived from a TYPE 1 circulator [76], which has been proposed in [77]. The author is grateful to D.J. Perry for this information.

4.3.3 Grounded supercapacitor

Fig 4.6(a) shows the 2-port representation of a grounded supercapacitor of value D (i.e. its impedance is given by $Z = D^{-1}s^{-2}$). Its $\pm R$, $\pm C$ equivalent circuit can be obtained by connecting positive and negative redundant series-arm capacitors to the circuit in Fig 4.6(a) and then transforming the resulting star subcircuit into its equivalent delta to yield the circuit of Fig 4.6(b). Alternatively, if we appreciate the fact that an R⟷C interchange transforms the impedance of an active RC simulated inductor into an impedance of an active RC simulated supercapacitor*, then we can obtain the $\pm R$, $\pm C$ circuit of Fig 4.6(b) by simply carrying-out R⟷C interchange in the circuit of Fig 4.4(c). The realisation of the circuit in Fig 4.6(b) using NICs is shown in Fig 4.6(c).

---

* Note that an impedance Z_s of a simulated inductor is given by an expression of the type, $Z_s = Z_1Z_2/Z_3$, in which we make Z_1 and Z_2 as resistors and Z_3 as a capacitor. Now, if we were to choose Z_1 and Z_2 as capacitors and Z_3 as a resistor, then Z_s becomes $Z_s = 1/(s^2C_1C_2R_3)$ which is an impedance of a simulated supercapacitor.

4.3.4 Floating supercapacitor

Let us consider the floating supercapacitor shown in Fig 4.7(a). Following the argument presented in the preceeding subsection, we obtain the $\pm$R, $\pm$C representation of the supercapacitor in Fig 4.7(a) by carrying-out R$\longleftrightarrow$C interchange in the circuit of Fig 4.5(c); the resulting circuit is shown in Fig 4.7(b). The circuit in Fig 4.7(b) can be realised using NICs as shown in Fig 4.7(c).

4.4 Derivation of a multitude of simulated inductor and supercapacitor circuits

In the preceeding section we developed $\pm$R, $\pm$C circuits for simulating grounded and floating inductors and supercapacitors. In this section we shall show that by "viewing" these $\pm$R, $\pm$C circuits in different ways, many more $\pm$R, $\pm$C circuits can be obtained for simulating grounded and floating inductors and supercapacitors.

Let us consider the 2-port grounded inductor shown in Fig 4.4(a) and its $\pm$R, $\pm$C equivalent circuit of Fig 4.4(c). In Figs 4.4(a) and (c), suppose we create a "new" terminal 2 which is directly connected to the "old" terminal 1, as shown in Fig 4.8(a). Thus we have obtained another $\pm$R, $\pm$C circuit for simulating a grounded inductor 2-port. In a similar manner we can create a new terminal 1 in Figs 4.4(a) and (b) to give yet another $\pm$R, $\pm$C circuit for simulating a grounded inductor 2-port; this is shown in Fig 4.8(b). Alternatively, if we create two new terminals, i.e. terminals 1 and 2 as shown in Fig 4.8(c), then one more simulated grounded inductor circuit is obtained.

The floating inductor 2-port in Fig 4.5(a) can be interpretted as a grounded inductor 2-port either by shorting terminal 2 to terminal 2′ and then creating a new terminal 2 which is directly connected to terminal 1, or by shorting terminal 1 to terminal 1′ and then creating a new terminal 1 which is directly connected to terminal 2. Now if these terminal modifications are also performed on the $\pm$R, $\pm$C circuit of the floating inductor of Fig 4.5(c) then another two circuits for simulating grounded inductors are obtained, as shown in Figs 4.8(d) and (e).

Therefore, altogether we have six different $\pm$R, $\pm$C circuits for simulating 2-port grounded inductors; i.e. five in Fig 4.8 and one in Fig 4.4(c). These $\pm$R, $\pm$C circuits have been obtained from the $\pm$R, $\pm$C circuits of Figs 4.4 and 4.5 by terminal modification; alternatively, we could have obtained these $\pm$R, $\pm$C circuits by starting with a grounded inductor and then connecting the redundant $\pm$R′s to it in various ways so as to form delta (star) networks, comprising +R, -R and the inductor, which are then transformed into star (delta) networks in order to eliminate the inductor. However, it is thought that the above approach of terminal modification is much more elegant and systematic, and hence is preferrable to the latter. It is interesting to note that the $\pm$R, $\pm$C circuits in Figs 4.8(a), (b), (d) and (e) can be interpretted as negative impedance inverters [3] terminated in negative capacitors.

Each grounded inductor 2-port in Fig 4.8 can be considered as a floating inductor 2-port, with respect to another arbitrary ground reference, for which terminals 1 and 2′ (or 1′ and 2) comprise the floating terminals of the inductor. Therefore, we effectively have six different $\pm$R, $\pm$C circuits for simulating 2-port floating

inductors; i.e. five corresponding to Fig 4.8 with the above mentioned terminal modification, and one in Fig 4.5(c). For ease of reference, all the six $\pm$R, $\pm$C circuits derived so far for the grounded and floating inductors are given in Figs 4.9 and 4.10, respectively. These $\pm$R, $\pm$C circuit can be realised with positive value resistors and capacitors by inserting NICs at positions marked "X" in Figs 4.9 and 4.10.

It is possible to obtain yet more $\pm$R, $\pm$C circuits for simulating grounded and floating inductors. In order to derive these additional circuits we make use of the port symmetry properties of grounded and floating inductors. For example, in the case of the grounded inductor 2-port of Fig 4.4(a), we can interchange the position of port 1 (formed by terminal pair 1 and 1′) with the position of port 2 (formed by the terminal pair 2 and 2′) without affecting the electrical properties of the inductor with respect to either port. Since the $\pm$R, $\pm$C circuit of Fig 4.4(c) simulates a grounded inductor we can also carry-out the above port interchange on this structure without affecting its electrical port symmetry. However, we note that the port interchange in the circuit of Fig 4.4(c) would result in a structurally different $\pm$R, $\pm$C circuit for simulating a grounded inductor. Again, referring to the grounded inductor 2-port of Fig 4.4(a) we note that the electrical properties of the inductor are not changed if we refer the ground reference to terminals 1 and 2 and then use terminals 1′ and 2′ as the floating terminals of the inductor. Now, if this terminal interchange is implemented in the $\pm$R, $\pm$C circuits of Fig 4.9, then another five structurally different $\pm$R, $\pm$C circuits for simulating a grounded inductor would be obtained. Finally, another structurally

different $\pm$R, $\pm$C circuit for simulating a grounded inductor is obtained if we simultaneously carry-out terminal and port interchanges on the $\pm$R, $\pm$C circuit of Fig 4.9(a). Thus, in addition to the six $\pm$R, $\pm$C circuits shown in Fig 4.9, another seven $\pm$R, $\pm$C circuits are available for simulating grounded inductors.

It can be shown that if the above concepts of terminal and port interchange are applied to the $\pm$R, $\pm$C circuits of a simulated floating inductor, then in addition to the six circuits shown in Fig 4.10, it is possible to obtain another seven $\pm$R, $\pm$C circuits for simulating floating inductors.

In order to derive a multitude of $\pm$R, $\pm$C circuits for simulating grounded and floating supercapacitors we can simply make an R ⟷ C interchange in the corresponding $\pm$R, $\pm$C circuits of the grounded and floating inductors, in accordance with the argument presented in Section 4.3.3. A set of six $\pm$R, $\pm$C circuits each for simulating grounded and floating supercapacitors are shown in Figs 4.11 and 4.12, respectively.

It has been shown above that the $\pm$R, $\pm$C circuits of Figs 4.4 ⟷ 4.7 can be viewed in many different ways to generate other $\pm$R, $\pm$C circuits which simulate grounded and floating inductors and supercapacitors. Due to the requirement of a large number of components (both passive and active) most of these circuits are only of theoretical interst. However, by using the novel design technique discussed in the next section, it will become apparent that some of these $\pm$R, $\pm$C circuits are well suited for simulating LC ladder type filters.

4.5 The basic principle of the novel approach

In the previous two sections a systematic method of deriving $\pm$R, $\pm$C circuits for simulating grounded and floating inductors and supercapacitors was described. At first sight the application of these simulated circuits to filter design does not appear very attractive because the active RC realisation of these simulating circuits require a rather large number of components. In this section we shall discuss the basic principle of the novel approach which allows us to make an efficient use of these $\pm$R, $\pm$C circuits in the design of high order filters. The word "efficient" is used in this context to mean that the final active RC network obtained is competitive with other simulation methods in the sense that it retains the low sensitivity properties of its prototype, the total number of components required is less than or equal to other simulation methods and that it is possible to use preferred and equal value capacitors which can have wide manufacturing tolerances.

The process of filter design by the new approach involves three steps, viz:

1. selection of suitable $\pm$R, $\pm$C circuits
2. selection of appropriate type of prototype filter
3. sensible selection of the free parameters in the $\pm$R, $\pm$C circuits

Let us now discuss the above three steps in greater detail.

There are two ways in which a given LC prototype filter can be simulated; i.e. we can either simulate the inductors in the prototype filter or impedance scale the prototype filter by a scaling factor $w_{ref}s^{-1}$ (where w_{ref} is a reference frequency and s is the complex frequency variable) and then simulate the supercapacitors in the resulting impedance scaled structure. Thus the selection of suitable $\pm R$, $\pm C$ circuits depends in the first instant on whether we decide to simulate the original prototype filter or an impedance scaled version of it. Only some of the $\pm R$, $\pm C$ circuits derived in the previous sections have been found useful for designing high order filters. For example, of all the inductor simulation circuits the circuits of Figs 4.9(a) and 4.10(a) have been found to be very useful, whereas the circuits of Figs 4.11(a) and 4.12(a) have been found to be very useful for simulating supercapacitors. As mentioned in the previous section, these $\pm R$, $\pm C$ circuits although electrically port symmetrical are structurally unsymmetrical; this gives two possible active RC realisations per simulated element. Thus for a prototype filter in which N elments are being simulated there are 2^N different active RC realisations possible.

Let us now consider the second step of the design procedure, i.e. the selection of an appropriate type of prototype structure. As far as the design of all-pole lowpass filters, all-pole highpass filters and all-pole bandpass filters derived from lowpass filters via the lowpass to bandpass transformation is concerned, the structure of the LC prototype filter is not very critical and we can usually design these filter types with minimum number of capacitors (i.e. the number of capacitors is equal to the order of the filter) and all these capacitors can have preferred values with wide manufacturing tolerances

(assuming that laser trimming of resistors is possible). In the case of lowpass and highpass elliptic filters, if the prototype filter leads to an active RC realisation in which the number of capacitors is not a minimum and if all capacitors cannot have equal and preferred values with wide tolerances, then basing the active RC design on the dual structure of the prototype will usually lead to a circuit in which the number of capacitors is minimum and all capcitors can have preferred values with wide manufacturing tolerances. In the case of elliptic and asymmetric all-pole bandpass filters, in addition to using the dual structure, it may be necessary to carry-out Norton transformations on the prototype structure in order to reduce the spread of component values. In general, if inductor simulation is to be used then it is desirable to have the minimum number of inductors in the prototype structure, whereas the prototype structure should have the minimum number of capacitors if supercapacitor simulation is to be used. Observing the above rule for all-pole filters would lead to active RC circuits with minimum number of OP-AMPs. However, as a general rule for elliptic filters, the simulation of inductors would lead to active RC circuits in which all the capacitors cannot have equal values or wide manufacturing tolerances; on the other hand, if the design is based on simulation of supercapacitors, then the active RC circuits obtained can be designed to have equal value capacitor and also the circuit can cope with wide tolerance capacitors.

Once we have selected an LC prototype to be simulated, the corresponding $^{+}_{-}R$, $^{+}_{-}C$ circuits (i.e. for the inductors or the supercapacitors) are substitutes in the prototype structure. Now the values of the "redundant" resistors (capacitors) can be chosen

arbitrarily and the objective of implementing step three is achieved by choosing these "free" parameters in such a way that we obtain cancellation between the positive and negative resistors (capacitors). This idea of cancelling impedances results in two main advantages. Firstly, the complexity of the overall filter structure is considerably reduced, which results in a simpler procedure for adjusting the circuits. Secondly, the number of negative elements in the overall filter structure are also considerably reduced, which implies that the active RC realisation requires fewer passive and active components.

The three design steps discussed above are very much inter-dependent and therefore the design process is an inter-active process. However as will become apparent in the next section the whole exercise of the design process is quite straight forward in the sense that after some familiarity with the approach described above, the selection of an appropriate prototype and the selection of the $\pm$R, $\pm$C circuits can be readily made.

4.6 Filter design using the essential subcircuits

4.6.1 Lowpass filters

4.6.1.1 All-pole structures

All-pole lowpass filters comprise inductors in the series arms and capacitors in the shunt arms of the LC ladder structures. Therefore, the active RC realisation of lowpass filters can be achieved either by simulating the floating inductors in the series arms of the prototype filter, or by simulating the shunt arm

supercapacitors in the impedance scaled version of the prototype filter. In the following, we shall consider the design of all-pole lowpass filters by both of these methods.

Let us consider the fifth order all-pole lowpass filter shown in Fig 4.13(a); we shall obtain the active RC realisation of this filter by simulating the floating inductors using the $\pm R$, $\pm C$ circuit of Fig 4.5(c). As stated in the previous section, it is one of the characteristic feature of the novel design approach that even using the same essential subcircuits we can, depending on the port orientation of the essential subcircuits, obtain 2^N different active RC realisations of a prototype in which N elements are being simulated. In order to illustrate this point, the four possible realisations, designated designs 1, 2, 3 and 4, of the filter in Fig 4.13(a) will now be derived.

Design 1

The circuit shown in Fig 4.13(b) is obtained by replacing each of the floating inductor in Fig 4.13(a) by its equivalent circuit in accordance with Fig 4.5(c). In Fig 4.13(b), the resistor values R_{L_2} and R_{L_4} can be chosen arbitrarily, but if we choose $R_{L_2} = R_{L_4} = R_{L_n} = R_{s_n}$, then we achieve cancellation of the positive and negative shunt resistors at nodes 3 and 4, giving the circuit in Fig 4.13(c). The negative elements in this circuit can be realised by means of NICs as shown in Fig 4.13(d); all NICs have unity conversion factor.

Note that in the prototype filter of Fig 4.13(a) we have assumed that the values of the terminating resistors (i.e. R_{s_n} and R_{L_n}) are

equal. This would be the case for odd order filters which are designed for maximum power transfer. However, this may not be the case for even order filters which have also been designed for maximum power transfer. As far as the new approach is concerned it can be applied equally as well for the design of odd or even order filters, but even order filters may require one more component than would be necessary if the terminating resistors are equal.

Note that the shunt resistor R_{s_n} at node 2 and the series source resistor R_{s_n} can be replaced by a single series resistor in accordance with Thevenin's theorem; the value of this single resistor would be equal to the parallel combination of the two resistors it is replacing. This modification would result in the transfer function of the active circuit being multiplied by a factor of two.

It is useful to interpret the circuit in Fig 4.13(d) as consisting of five RC sections which are coupled by four NICs; we shall refer to these RC sections as the "inverted L-sections". These inverted L-sections can be defined by their time constants (i.e. $\frac{1}{2}C_{1_n}R_{s_n}$, $C_{L_2}R_{s_n}$, $C_{3_n}R_{s_n}$, $C_{L_4}R_{s_n}$ and $C_{5_n}R_{s_n}$) and by their impedance levels. Whereas the time constants are fully specified by the required transfer function, the impedance levels may have arbitrary values if the NICs are used to provide appropriate impedance matching between the adjacent L-sections. This flexibility can be used to obtain nominally equal (and preferred) value capacitors throughout the filter since we can still obtain each required time constant by adjusting the appropriate time constant resistor and then adjust the conversion factor of each NIC to match the impedance levels of the adjacent inverted L-sections. Note that since the time constant resistors and the NIC resistors are adjustable then by the

above argument the capacitors can also have arbitrarily large manufacturing tolerances. Fig 4.13(e) shows an active RC realisation of the filter in Fig 4.13(a) in which all capacitors have equal value; the conversion factors of the NICs are also shown in Fig4.13(e). Note that the active RC circuit requires only five capacitors (i.e. the theoretical minimum) which are all grounded and four operational amplifiers.

Design 2

As mentioned earlier, the essential subcircuit of Fig 4.5(c) is electrically port symmetrical but it is structurally unsymmetrical. Thus, we can interchange the ports in Fig 4.13(b) of the subcircuit which simulates the inductor L_2 and the resulting circuit is then as shown in Fig 4.14(a). The circuit of Fig 4.14(b) is obtained if we choose $R_{L_2} = R_{L_4} = 2R_{s_n}$ in Fig 4.14(a). A very attractive feature of this circuit is that it can be realised with only three NICs as shown in Fig 4.14(c), whereas Design 1 required four NICs.

Note that the resistive potential divider at node 2 in Fig 4.14(b), formed by the resistors R_{s_n} and $-2R_{s_n}$, has been replaced by a single series resistor of value $+2R_{s_n}$ which is connected between nodes 1 and 2 in Fig 4.14(c). This has the effect of multiplying the transfer function of the active RC circuit of Fig 4.14(c) by a factor of half.

It can be shown that it is also possible to interpret the circuit of Fig 4.14(c) as consisting of five RC sections which in this case are coupled by three NICs. However, the interpretation is not as straight forward as in the case of Design 1. These RC sections can be

defined by their time constants and impedance levels. Therefore, by the same argument as for Design 1, it would be quite feasible to have nominally equal (and preferred) value capacitors throughout the filter circuit. For example, the circuit in Fig 4.14(d) shows the equal capacitor realisation of the circuit in Fig 4.14(c); the values of the components are determined by using the design equations derived in Appendix A.

In the case of the four NIC circuit (Design 1) it was stated that if we assume that the time constant forming resistors and the NIC resistors are trimmable then the capacitors of the circuit can have arbitrarily large manufacturing tolerances. In contrast, it is only possible to design the three NIC circuit with arbitrarily chosen capacitors provided the spread between some capacitors of the circuit is restricted to lie within a certain range. The derivation of the design equations for calculating the resistor values, when all the capacitor values are known, for the three NIC circuit are given in Appendix A where it is also shown that the circuit is well suited for deterministic adjustment only, whereas the four NIC circuit can be adjusted either deterministically or functionally. Hence, although the adjustment of the three NIC circuit is not very flexible it does provide a saving of one OP-AMP compared with the four NIC circuit.

Design 3

Another active RC realisation of the the fifth order lowpass filter is obtained by reversing the port orientations of the subcircuits simulating inductors L_2 and L_4 in Fig 4.13(b) and the resulting circuit is shown in Fig 4.15(a). The circuit of Fig 4.15(b) is obtained if we choose $R_{L_2} = R_{L_4} = 2R_{s_n}$ in the circuit of Fig 4.15(a).

The negative elements in this circuit can be realised by means of four NICs, as shown in Fig 4.15(c).

The resistive potential divider at node 2 in Fig 4.15(b), formed by resistors R_{s_n} and $-2R_{s_n}$, has been replaced by a single series resistor of value $+2R_{s_n}$ which is connected between nodes 1 and 2 in Fig 4.15(c). As a consequence of this modification the transfer function of the circuit in Fig 4.15(c) is multiplied by a factor of half compared with the transfer function of the prototype filter of Fig 4.13(a).

Like the circuit of Fig 4.13(d), it is also possible to interpret the circuit of Fig 4.15(c) as consisting of five RC sections which are coupled by four NICs. Again, these RC sections can be defined by their time constants and impedance levels and hence by the same argument as for Design 1, we can design the circuit such that nominally equal (and preferred) value capacitors are used throughout the circuit, as shown in Fig 4.15(d). Furthermore, following the same reasoning as in the case of Design 1, all capacitors can have arbitrarily large manufacturing tolerances and the circuit can be adjusted either deterministically or functionally.

Now let us supose that the impedance terminating the right hand side of the NIC which has a conversion factor k_4 in the circuit of Fig 4.15(d) is Z. Then the impedance represented at the left hand side of the NIC under consideration is $-k_4Z$. Now it has been shown [78] that an impedance $-k_4Z$ can be realised with an impedance $+Z$ and a voltage amplifier of gain $(1 + k_4)$, as shown in Fig 4.15(e). If the output voltage in Fig 4.15(d) is V_o, then when $-k_4Z$ is realised using an amplifier of gain $(1 + k_4)$, the voltage at the output of this

amplifier is $V_o(1 + k_4)$; thus the filter output can be taken from the output of the amplifier with the consequence that the transfer function of the filter has been multiplied by a constant factor $(1 + k_4)$. Therefore the circuit can be realised with three NICs and one voltage amplifier of gain $(1 + k_4)$, i.e. four OP-AMPs altogether. The main advantage of this four OP-AMP circuit, compared with the four OP-AMP circuit of Design 1, is that it provides a buffered output.

Design 4

The fourth active RC realisation of the prototype filter of Fig 4.13(a) is obtained by reversing the port orientation, in Fig 4.13(b), of the subnetwork which simulates the inductor L_4; the resulting circuit is shown in Fig 4.16(a). The circuit of Fig 4.16(b) is obtained if we choose $R_{L_2} = R_{L_4} = R_{s_n}$, which can be realised using five NICs, as shown in Fig 4.16(c). Note that the shunt resistor at node 2 in Fig 4.16(b) has been incorporated into the source resistor, as shown in Fig 4.16(c); this has the effect of multiplying the transfer function of the filter circuit by a factor of two.

Again, the circuit of Fig 4.16(c) can also be interpreted as consisting of five RC sections which are coupled by four NICs. Hence, by the same argument as for Design 1, we can design this circuit to obtain nominally equal (and preferred) value capacitors throughout the filter circuit. The equal capacitor realisation of the circuit in Fig 4.16(c) is shown in Fig 4.16(d). By virtue of the same reasoning as before, all the capacitors in the circuit can have arbitrarily large manufacturing tolerances and the circuit can also be adjusted deterministically or functionally.

As already explained for the circuit of Fig 4.15(d), it is quite apparent that the circuit of Fig 4.16(d) can be modified to have a buffered output. However the circuit of Fig 4.16(d) is not very attractive because it requires more passive and active components than the corresponding circuits of Figs 4.13(e), 4.14(d) and 4.15(d). As a consequence of requiring a larger number of components, the adjustment of the circuit in Fig 4.16(d) would involve more steps than the adjustment of any of the other three circuits; hence this circuit is not very attractive for practical applications.

Above we have generated all the four possible active RC designs of the fifth order lowpass filter of Fig 4.13(a) using the $\pm$R, $\pm$C circuit of Fig 4.5(c). It has been shown that in all the four designs the filter circuit can be designed to have nominally equal (and preferred) value capacitors which can also have wide manufacturing tolerances. Another approach to the active RC realisation of lowpass filters would be to impedance scale the prototype filter structure, using a scaling factor inversely proportional to the frequency variable s, and then to simulate the grounded supercapacitors in the impedance scaled prototype structure. We shall presently explore this possibility by designing a fifth order lowpass filter. In the first instance we need to select an "appropriate" prototype structure. Fig 4.17(a) shows the dual structure of the fifth order lowpass filter discussed above; this structure is more suitable because it has the minimum number of capacitors.

Let us consider the impedance scaled version, shown in Fig 4.17(b), of the prototype filter of Fig 4.17(a). The circuit

shown in Fig 4.17(c) is obtained by replacing each of the grounded supercapacitor in Fig 4.17(b) by its $\pm$R, $\pm$C equivalent circuit in accordance with Fig 4.6(b). In Fig 4.17(c) the capacitor values C_{D_2} and C_{D_4} can be chosen arbitrarily, but if we make $C_{D_2} = C_{D_4} = C_{s_n}$, then we achieve cancellation of the positive and negative capacitors in series with resistors R_{1_n} and R_{3_n} giving the circuit shown in Fig 4.17(d). The capacitive potential divider at the output of the filter circuit in Fig 4.17(d) can be replaced by a single shunt capacitor of value $\frac{1}{2}C_{s_n}$ and the resulting circuit can be realised with four NICs and equal value capacitors, as shown in Fig 4.17(e). As a consequence of replacing the capacitive potential divider by a single capacitor the transfer function of the filter is multiplied by a factor of two.

The circuit in Fig 4.17(e) can be interpretted as consisting of five RC inverted L-sections which are coupled by four NICs. Thus by a similar argument to one presented for the circuit of Fig 4.13(e), all the capacitors in the circuit of Fig 4.17(e) can also have arbitrarily large manufacturing tolerances.

Note that the active RC realisations shown in Figs 4.13(e) and 4.17(e) have identical structures, although for equal value capacitor designs the values of the NIC scaling factors are different in the two cases. It will be shown in Section 4.7 that the sensitivity behaviour of the two circuits is also quite different, inspite of the fact that structures of the two circuits are similar.

We have only obtained one realisation of the circuit in Fig 4.17(b), whereas another three different realisations are possible by interchanging the orientation of the ports of the $\pm$R, $\pm$C circuits

simulating the supercapacitors D_2 and D_4 in Fig 4.17(c). However, these other three realisations give rise to structures which are not cannonic with respect to the number of capacitors and/or which require a larger number of NICs. Hence, since these other realisations do not have any practical advantages over the one shown in Fig 4.17(e), they are not discussed here.

In order to compare the number of capacitors and OP-AMPs used in the above realisations of the fifth order all-pole lowpass filter, we shall now briefly consider the design of the same filter by conventional methods which use positive impedance converters (PICs) as the basic active unit (note that as mentioned in Section 1.4.1, two amplifiers together with four passive components are required for the realisation of a PIC). For the partial impedance scaling approach of Gorski-Popiel's method [15], the circuit of Fig 4.13(a) is most suitable as a prototype. The active RC realisation of this circuit would require three PICs (i.e. six OP-AMPs) and six capacitors. All the capacitors can have equal (and preferred) values with wide manufacturing tolerances. Using the modified partial impedance scaling approach [29] the filter of Fig 4.13(a) can be realised by three PICs and seven capacitors but by appropriately designing the circuit it is possible to obtain a buffered output. Again, all capacitors can have equal and preferred values with wide manufacturing tolerances.

The circuit of Fig 4.17(a) is suitable as a prototype for obtaining the active RC realisation by the modified or the full impedance scaling approach [16,29]. This approach is most likely to be used in actual practice because it requires only two PICs (i.e. four OP-AMPs). The number of capacitors required by this method

is six and four of these capacitors can have arbitrary values and tolerances, whereas the relative tolerance of the two capacitors corresponding to the terminating resistors in the prototype is restricted. Note that in order to obtain a buffered output, it would be necessary to use another OP-AMP.

4.6.1.2 Elliptic structures

The application of the new design approach to lowpass elliptic filters will be illustrated in this subsection by considering the design of a fifth order lowpass elliptic filter shown in Fig 4.18(a). In the all-pole lowpass filter of Fig 4.13(a) we note that if capacitors C_{2_n} and C_{4_n} are connected in parallel with inductors L_{2_n} and L_{4_n}, respectively, then we obtain the lowpass elliptic structure of Fig 4.18(a). Therefore the active RC realisation of the circuit in Fig 4.18(a) can be obtained by connecting, in any active RC realisation of the circuit in Fig 4.13(a), a capacitor C_{2_n} between nodes 2 and 3 and a capacitor C_{4_n} between nodes 3 and 4. For example, one active RC simulation circuit of the elliptic lowpass filter of Fig 4.18(a) is shown in Fig 4.18(b), which has been obtained by modifying the circuit in Fig 4.13(d). In the case of all-pole circuits it is possible to design the filter circuit to have equal (and preferred) value capacitors which can have wide manufacturing tolerances; however, for the circuit of Fig 4.18(b) all capacitors except C_{L_2} and C_{L_4}, are restricted to have non-preferred values with narrow manufacturing tolerances. The capacitors C_{L_2} and C_{L_4} can have any preferred values with wide manufacturing tolerances; this is achieved by changing the value of the time constant resistor associated with each capacitor to maintain the time constants of each

of these two RC sections at their nominal values and then using the NICs adjacent to these RC sections to match the impedance levels.

Another three active RC realisations of the circuit in Fig 4.18(a) can be obtained by connecting a capacitor C_{2_n} between nodes 1 and 3 and a capacitor C_{4_n} between nodes 3 and 4 in the circuits of Figs 4.14(c), 4.15(c) and 4.16(c), but the requirement of non-preferred narrow tolerance capacitors make all these circuits unattractive from the practical point of view.

Let us now consider the dual prototype filter circuit, shown in Fig 4.19(a), of the fifth order elliptic lowpass filter of Fig 4.18(a). The impedance scaled version of the circuit in Fig 4.19(a) is shown in Fig 4.19(b). The active RC realisation of this circuit can be achieved by simulating the supercapacitors D_2 and D_4. The circuit in Fig 4.19(c) is obtained by replacing each supercapacitor in Fig 4.19(b) by its equivalent $\pm R$, $\pm C$ circuit in accordance with Fig 4.6(b). The values of capacitors C_{L_2} and C_{L_4}, in Fig 4.19(c), can be chosen arbitrarily but if we choose $C_{L_2} = C_{L_4} = C_{s_n}$ then the simplified circuit of Fig 4.19(d) is obtained which can be realised with six NICs, as shown in Fig 4.19(e).

Note that the capacitive potential divider at the output of the circuit in Fig 4.19(d) has been replace by a single capacitor in Fig 4.19(e). This modification has the effect of multiplying the transfer function of the circuit by a factor of two.

The circuit in Fig 4.19(e) can be described by seven RC sections which are coupled by six NICs. The time constants of these RC sections are given by the specifications for which the filter is designed. Therefore using the same argument as in the case of

all-pole lowpass filters, it is feasible to use capacitors of arbitrary values and manufacturing tolerances in the circuit of Fig 4.19(e).

Note that the realisation of the circuit in Fig 4.19(e) requires five capacitors and six operational amplifiers.

For the purpose of comparison we note that the circuit in Fig 4.18(a) has the minimum number of inductors and hence it is a suitable prototype for realisation by the Gorski-Popiel's method [15]; whereas the circuit of in Fig 4.19(a) has the minimum number of capacitors and hence it is most suitable prototype for the Bruton's method [16] of impedance scaling. The active RC realisation of the circuit in Fig 4.18(a) by Gorski-Popiel's method would require three PICs (i.e. six OP-AMPs) and eight capacitors, most of which will have non-preferred values with narrow manufacturing tolerances. In contrast, the active RC realisation of the circuit in Fig 4.19(b) by Bruton's method would require two PICs (i.e. four OP-AMPs) and six capacitors, all of which can have equal and preferred values with wide manufacturing tolerances. Alternatively, if the circuits of Figs 4.18(a) and 4.19(a) are simulated using the full impedance scaling method [29], then three PICs and eight capacitors or two PICs and six capacitors, respectively, would be required; all capacitors can have equal and preferred values with wide manufacturing tolerances.

Therefore, in comparison, if preferred value capacitors with wide manufacturing tolerances are to be used, then the best active RC circuit that can be realised by the new approach requires two OP-AMPs more than the corresponding best circuit realised by the full

impedance scaling method; however, the new method requires one less capacitor.

4.6.2 Highpass filters

4.6.2.1 All-pole structures

All-pole highpass filter structures comprise inductors in the shunt arms and capacitors in the series arms of the LC prototype ladder. Thus active RC realisation of these structures can be achieved by either simulating the grounded inductors or by impedance scaling the prototype structure and then simulating the floating supercapacitors. In order to illustrate the design of highpass filters by the new method we shall make use of both of these approaches.

Let us consider the fifth order all-pole highpass filter shown in Fig 4.20(b), which is the impedance scaled version of the prototype filter shown in Fig 4.20(a). If the floating supercapacitors in Fig 4.20(b) are replaced by the $\pm R$, $\pm C$ circuit of Fig 4.7(b), then we obtain the circuit shown in Fig 4.20(c). The values of capacitors C_{D_2} and C_{D_4}, in Fig 4.20(c), can be chosen arbitrarily but the circuit of Fig 4.20(d) is obtained if we choose $C_{D_2} = C_{D_4} = C_{s_n}$; this circuit can be realised using four NICs, as shown in Fig 4.20(e).

The capacitive potential divider at the input of the filter circuit in Fig 4.20(d) has been replaced by a single capacitor of value $2C_{s_n}$ in Fig 4.20(e). As a consequence of this modification the transfer function of the circuit in Fig 4.20(e) has been multiplied by a factor of two.

The circuit in Fig4.20(e) can be thought as being composed of five RC inverted L-sections which are coupled by four NICs. Hence by the virtue of the discussion presented in Section 4.6.1.1 we conclude that it would be quite feasible to use equal and preferred value capacitors which can have wide manufacturing tolerances.

It is interesting to note that the circuit of Fig 4.20(d) could have been obtained by carrying-out R ⟷ C interchange in the circuit of Fig 4.13(c); the reason for this is as follows. In Fig 4.13 we are simulating floating inductors and the impedance of the simulated inductor is of the form $Z_L = Z_1 Z_2 / Z_3$, where we choose Z_1 and Z_2 to be resistors and Z_3 to be a capacitor. Now if we interchange resistors and capacitors in the expression for Z_L, then Z_L will become an impedance of a supercapacitor. Thus in the circuit of Fig 4.13(a) if we assume the floating inductors to be simulated by $\pm$R, $\pm$C circuits, then as a consequence of carrying-out an R ⟷ C interchange, the terminating resistors would become capacitors, the shunt capacitors would become shunt resistors and the floating inductors would become floating supercapacitors in the transformed circuit; i.e. we would obtain the circuit of Fig 4.20(b), which is an impedance scaled version of a highpass filter. Therefore, following the above argument we observe that if we carry-out R ⟷ C transformation in the $\pm$RC circuit realisation of a lowpass filter, which has been obtained by simulating inductors, then we obtain a $\pm$RC circuit realisation of an impedance scaled highpass filter whose prototype corresponds to the prototype of the lowpass filter. By a similar argument to the one presented above, it can be shown that if an R ⟷ C transformation is carried-out on an impedance scaled lowpass prototype filter in which the supercapacitors

are simulated by $\pm$R, $\pm$C circuits, then we would also obtain a highpass filter structure. This implies that if we carry-out an R $\longleftrightarrow$ C interchange on the $\pm$RC lowpass circuit of Fig 4.17(d), then we would obtain a $\pm$RC highpass filter circuit which could altenatively have been obtained by applying the lowpass to highpass transformation to the circuit of Fig 4.17(a) and then simulating the grounded inductors in the highpass filter structure.

From the above argument it is apparent that another three active RC realisations of Fig 4.20(b) can be obtained by simply carrying-out a R $\longleftrightarrow$ C transformation in the circuits of Figs 4.14(c), 4.15(c) and 4.16(c). The highpass circuits corresponding to the circuits of Figs 4.14(c) and 4.16(c) would each require seven capacitors whereas the highpass circuit corresponding to the circuit of Fig 4.15(c) would require only six capacitors. All of these circuits can be designed with equal (and preferred) value capacitors but only the highpass circuits corresponding to the circuits of Figs 4.15(c) and 4.16(c) can have capacitors with wide manufacturing tolerances. If we obtain the three NIC realisation of Fig 4.20(b) by carrying-out an R $\longleftrightarrow$ C transformation in the circuit of Fig 4.14(c) then, as stated above, a total of seven capacitors (all of which can have nominally equal values) would be required; however if we are prepared to accept a spread of two in the capacitor values then this circuit can be designed with only six capacitors as we shall show in the following.

The circuit of Fig 4.21(a) is obtained from the circuit in Fig 4.20(c) by interchanging the ports of the $\pm$R, $\pm$C circuit simulating the supercapacitor D_2 (see Fig 4.20(b)). The circuit in Fig 4.21(b) results if we choose $C_{D_2} = \frac{1}{2}C_{s_n}$ and $C_{D_4} = C_{s_n}$ in

Fig 4.21(a). The realisation of the circuit in Fig 4.21(b) using NICs is shown in Fig 4.21(c). Note that the shunt capacitor of value $-\frac{1}{2}C_{s_n}$, at node 2 in Fig 4.21(b) can be combined with the series capacitor between nodes 1 and 2 (as shown in Fig 4.21(c)) with the effect of dividing the filter transfer function by a factor of two.

The use of wide tolerance capacitors in the circuit of Fig 4.21(c) is not possible and hence from the practical implementation point of view it is not a very important circuit. However this circuit will be used in Chapter 5 as an example when we discuss a method of reducing the effect of finite amplifier gain bandwidth product of the OP-AMP in NIC filter circuits.

The dual form of the filter circuit of Fig 4.20(a) is shown in Fig 4.22(a). The circuit of Fig 4.22(b) is obtained by replacing inductors L_{2_n} and L_{4_n} in Fig 4.22(a) by their equivalent $\pm R$, $\pm C$ circuits in accordance with Fig 4.4(c). In Fig 4.22(b), choosing $R_{L_2} = R_{L_4} = R_{s_n}$ results in the circuit of Fig 4.22(c). The resistive potential divider at the output of the circuit in Fig 4.22(c) can be replaced by a single shunt resistor with the consequence of multiplying the transfer function of the circuit by a factor of two. The resulting circuit can be realised with four NICs and it is shown in Fig 4.22(d).

Again, the circuit of Fig 4.22(d) can be thought of as comprising five RC inverted L-sections which are coupled by four NICs. Hence it would be quite feasible to use preferred value capacitors in this circuit and these capacitors can also have wide manufacturing tolerances.

Note that as explained previously the circuit of Fig 4.22(c) could have been obtained by carrying-out an R ⟷ C transformation on the circuit of Fig 4.17(d).

For the purpose of comparison, we note that the circuit in Fig 4.20(a) can be realised either by partial or full impedance scaling methods and in each case three PICs would be required; but whereas the partial impedance scaling method leads to a requirement for non-preferred value narrow tolerance capacitors, the circuit designed by the full impedance scaling method can have preferred value capacitors which can have wide manufacturing tolerances. The highpass filter of Fig 4.22(a) can be designed by the partial impedance scaling method with only two PICs (i.e. four OP-AMPs), but this leads to the requirement of non-preferred value narrow tolerance capacitors. The full impedance scaling method of realising the filter of Fig 4.22(a) although permits the use of preferred value wide tolerance capacitors, requires four PICs (i.e. eight OP-AMPs) and hence it is pratically unattractive.

Therefore as far as the design of all-pole highpass filters is concerned the new approach seems to offer some practical advantages over the conventional method in the sense that if we want to use preferred value capacitors with wide manufacturing tolerances, then the circuits realised by the new approach require only four OP-AMPs whereas the corresponding circuit realised by the conventional approach requires at least six OP-AMPs.

4.6.2.2 Elliptic structures

The fifth order all-pole highpass filter of Fig 4.20(a) can be transformed into an elliptic structure by connecting inductors L_{2_n} and L_{4_n} in parallel with capacitors C_{2_n} and C_{4_n}, respectively, as shown in Fig 4.23(a). The impedance scaled version of this circuit is shown in Fig 4.23(b). The active RC realisation of the circuit in Fig 4.23(b) is shown in Fig 4.23(c) and it has been obtained from the circuit of Fig 4.20(e) by connecting resistors R_{2_n} and R_{4_n} between node pairs 2,3 and 3,4 respectively.

Note that the circuit of Fig 4.23(c) requires five capacitors (the theoretical minimum) and only four NICs. At first sight this circuit appears very promising; however a closer examination shows that the circuit cannot be designed to have equal value capacitors and furthermore the capacitors cannot be allowed to have wide manufacturing tolerances. At this point it may be appropriate to consider what conditions or limitations determine whether the type of NIC circuits that we have derived can be designed to have arbitrary capacitor values and tolerances.

If we observe the lowpass filter structures derived in the previous subsection, and also observe the the all-pole highpass filter structures derived above, then we note that for the structures in which the capacitors can have arbitrary values and wide tolerances, the capacitors inside the filter structure are always connected to other capacitors in the circuit via NICs. Thus a sufficient condition for obtaining structures which can have arbitrary value (and tolerance) capacitors is that the a capacitor in the filter structure should only be connected to other capacitors in the circuit via NICs.

In the case of Fig 4.23(c) the capacitors connecting to nodes 2, 3 and 4 have direct connecting paths via resistors R_{2_n} and R_{4_n}, and therefore the capacitors in this circuit cannot have arbitrary values and tolerances. One possible way of removing this constraint from the circuit of Fig 4.23(c) is to replace each of the NIC connected to nodes 2 and 3 by two NICs, as shown in Fig 4.23(d). Now the circuit of Fig 4.23(d) can be interpretted as consisting of five RC sections which are coupled by six NICs. Each of these RC sections can be defined by one or two time constant(s) and an impedance level. While the time constants are defined by the filter characteristics the impedance levels within each RC sections are arbitrary as long as appropriate impedance matching is maintained between the various RC sections using the NICs. Therefore, following the same argument as before, we conclude that the capacitor values in the circuit of Fig 4.23(d) can be chosen arbitrarily, and futhermore, by extension of the same argument, it is obvious that the capacitors can also have arbitrarily large manufacturing tolerances.

For the purpose of comparison, we note that if the fifth order highpass elliptic filter is to be realised with preferred value capacitors, which can have wide manufacturing tolerances, then the approach described in [5], which requires four PICs (i.e. eight OP-AMPs) would be most suitable. Therefore, as far as the number of amplifiers is concerned, the circuit of Fig 4.23(d) uses two amplifiers less than its PIC counterpart; also it is canonic with respect to the number of capacitors.

4.6.3 Bandpass filters

4.6.3.1 All-pole structures derived by lowpass to bandpass transformation

In the case of all-pole bandpass filters derived from all-pole lowpass filters via the lowpass to bandpass transformation, we encounter inductors and capacitors both in the series and the shunt arms of the ladder structure. The obvious consequence of this is the requirement for two different types of $\pm$R, $\pm$C circuits for simulating the grounded and floating inductors (or supercapacitors). The selection of the $\pm$R, $\pm$C circuits is made with the aim of achieving cancellation between the positive and negative elements of the simulated structure such that the resulting circuit does not require excessive number of components.

In the following if the bandpass filter is to be realised by simulating the inductors then the $\pm$R, $\pm$c circuits of Figs 4.4(c), 4.5(c) and 4.9(f) will be used; whereas if the supercapacitors in the impedance scaled version of the bandpass filter are to be simulated then the $\pm$R, $\pm$C circuits of Figs 4.6(b), 4.7(b) and 4.11(f) will be used. Let us now consider some examples of designing bandpass filters.

Consider the third order all-pole lowpass filter shown in Fig 4.24(a), which has been denormalised to have a cut-off frequency equal to the bandwidth of the bandpass filter. We obtain the all-pole bandpass filter shown in Fig 4.24(b) by applying the lowpass to bandpass transformation to the filter circuit in Fig 4.24(a). In Fig 4.24(b) if we replace the inductors L_{1_n} and L_{3_n} by the $\pm$R,

$\pm$C circuit of Fig 4.5(c) and replace the inductor L_{2_n} by its equivalent circuit of Fig 4.9(f) then we obtain the circuit shown in Fig 4.24(c). The values of resistors R_{L_1}, R_{L_2} and R_{L_3} in Fig 4.24(c) can be chosen arbitrarily, but the circuit of Fig 4.24(d) is obtained if we choose $R_{L_1} = R_{L_2} = R_{L_3} = R_{s_n}$. The realisation of the circuit in Fig 4.24(d) using NICs is shown in Fig 4.24(e) from which we note that the circuit requires six OP-AMPs and six capacitors.

The NICs in Fig 4.24(e) can be thought of as separating the network into seven isolated subnetworks, six of which comprise resistors and capacitors (RC subnetworks) while one contains a single resistor (R subnetwork). Each of the RC subnetworks is defined by an impedance level and one or more time constants, whereas the R subnetwork is defined just by an impedance level. The time constants of the RC subnetworks are specified by the filter characteristics whereas the impedance levels of all the subnetworks are arbitrary as long as the impedance levels of the adjacent sections are correctly matched. Therefore using the same argument as for the lowpass and highpass filter circuits we conclude that the capacitors in the circuit of Fig 4.24(e) can have arbitrary values and tolerances if we adjust the resistors in each RC subnetwork to achieve the correct time constants and then adjust the conversion factor of each NIC to match the impedance levels of the subnetworks on either side of the NIC under consideration.

The above approach of carrying-out a lowpass to bandpass transformation on a lowpass filter and then simulating the elements in the bandpass filter to obtain an active RC realisation works satisfactorarily for wide-band filters. However, if the relative

bandwidth (i.e. the ratio of the passband frequency to the centre frequency) is small (< 0.1), then the spread in element values of the bandpass filter becomes very large; e.g. if a filter has a bandwidth B_w, centre frequency w_o and the maximum values of an inductor and a capacitor in the normalised lowpass prototype filter are L_m and C_m, respectively, then it can be easily shown that the maximum spread in the inductor and the capacitor values of the bandpass filter is $[L_m C_m (w_o/B_w)^2]$. In order to reduce the element spread for bandpass filters with relatively small bandwidths, Norton transformations are used frequently; but this technique usually increases the number of elements to be simulated and leads also to the requirement for narrow tolerance capacitors (if we are simulating the inductors). Therefore, the conventional method of applying Norton transformations to reduce the spread in component values is not very well suited for the new approach being considered here. We shall now describe an alternative approach to the design of all-pole bandpass filters which does <u>not</u> result in large spread in the element values of the bandpass filter.

Let us consider the third order all-pole lowpass filter shown in Fig 4.25(a). The circuit of Fig 4.25(b) is obtained by replacing the inductor L_{2_n} in Fig 4.25(a) by its $\pm R$, $\pm C$ equivalent circuit of Fig 4.5(c). In Fig 4.25(b), if we choose $R_{L_2} = R_{s_n}$ then we achieve cancellation of the positive and negative resistances at node 3 and the series resistor R_{s_n} between nodes 1 and 2 and the shunt resistor at node 2 can be combined together as explained previously with the effect of multiplying the transfer function of the filter by a factor of two. The circuit in Fig 4.25(c) is obtained by applying the lowpass to bandpass transformation to the circuit of Fig 4.25(b). In

the circuit of Fig 4.25(c) we note that the spread in capacitor and inductor values would be same as the spread in the capacitor values of the active lowpass circuit of Fig 4.25(b). The circuit of Fig 4.25(d) has been obtained by replacing each shunt inductor in Fig 4.25(c) by its $\pm R$, $\pm C$ equivalent circuit of Fig 4.9(f). The realisation of the circuit in Fig 4.25(d) can be accomplished using six NICs, as shown in Fig 4.25(e).

As in the case of the circuit in Fig 4.24(e) it can be shown, by following a similar argument, that it would be quite feasible to use preferred value capacitors in the case of the circuit of Fig 4.25(e); also the capacitors can have wide manufacturing tolerances. Note that in Fig 4.25(e) we have a NIC at the output of the filter, which is terminated by a resistor R_{L_3}, and this can be used to provide a buffered output and to control the overall gain of the filter.

For the purpose of comparison, we note that in order to realise a sixth order all-pole bandpass filter, using the full impedance scaling method, at least three PICs (i.e. six OP-AMPs) and six capacitors would be required [21].

4.6.3.2 Elliptic structures derived by lowpass to bandpass transformation

Let us now consider the design of elliptic bandpass filters which are obtained from lowpass filters by the lowpass to bandpass transformation. The elliptic bandpass filter of Fig 4.26(b) is obtained from the third order elliptic lowpass filter of Fig 4.26(a) by the following two steps. Firstly, the lowpass to bandpass transformation is applied to the circuit of Fig 4.26(a) to obtain a

bandpass filter. In the second step, the tuned-circuit transformation [27] is applied to this bandpass filter in order to obtain the circuit shown in Fig 4.26(b).

The circuit in Fig 4.26(c) is obtained from the circuit of Fig 4.26(b) as follows. The inductor L_{1_n} is replaced by its $\pm$R, $\pm$C equivalent circuit of Fig 4.9(f); the inductors L_4 and L_5 are replaced by the $\pm$R, $\pm$C circuit of Fig 4.10(a); and inductor L_{3_n} is replaced by its $\pm$R, $\pm$C equivalent circuit of Fig 4.9(a). Note that the load resistor in Fig 4.26(b) has been replaced by two shunt resistors, each of value $2R_s$, in Fig 4.26(c); the reasons for doing this will become apparent shortly. The values of resistors R_{L_1}, R_{L_4}, R_{L_5} and R_{L_3}, in Fig 4.26(c), can be chosen arbitrarily, but if we chose $R_{L_1} = R_{L_4} = R_{L_5} = R_{L_3} = 2R_s$, then we achieve cancellation of the positive and negative shunt resistances at nodes 2, 2′ and 3′ such that the resulting circuit can be realised using ten NICs, having conversion factors of unity, as shown in Fig 4.26(d).

The circuit in Fig 4.26(d) can be thought of as comprising eight RC sections and one R section which are coupled by ten NICs. Therefore, following the same reasoning as before, we conclude that the circuit in Fig 4.26(d) can be designed for preferred value capacitors which may also have wide manufacturing tolerances.

As mentioned in the case of all-pole filters, the application of the lowpass to bandpass transformation would result in bandpass filter structures which have a large spread in component values if the relative bandwidth of the filter is very small. It was shown in the case of all-pole bandpass filters that the problem of component spread is avoided if we obtain an active RC simulation of the prototype

lowpass filter and then carry-out the lowpass to bandpass transformation on this active RC circuit. This technique can also be applied in the case of elliptic bandpass filters which are derived from lowpass prototypes.

Note that in the design examples of all-pole and elliptic bandpass filters we have not used the impedance scaling method because this would lead to structures which are not cannonic in the number of capacitors and consequently large number of NICs would be required if the capacitors are to have preferred values and wide manufacturing tolerances.

For the purpose of comparison, we note that if the sixth order elliptic bandpass filter of Fig 4.26(b) is realised using the full impedance scaling method then three PICs (i.e. six OP-AMPs) and eight capacitors would be required. Therefore, from the number of amplifiers the circuit of Fig 4.26(d) is not very attractive.

4.6.3.3 Other types of bandpass filter structures

In Subsections 4.6.3.1 and 4.6.3.2 we described the design of all-pole and elliptic bandpass filters which are derived from lowpass prototypes by the lowpass to bandpass transformation. In this subsection we shall consider the design of bandpass filters which are not derived from lowpass filter prototypes. In particular we shall consider the design of an eight order elliptic (zig-zag) bandpass filter which has been previously studied in [17,36]. The prototype of the filter used in [17,36] is shown in Fig 4.27(a) and its dual form is depicted in Fig 4.27(b). The active RC realisation of the desired filter can thus be obtained by either simulating the inductors

in the circuits of Figs 4.27(a) and (b) or by simulating the supercapacitors in the impedance scaled versions of the circuits in Figs 4.27(a) and (b). We shall use the latter method and for this the circuit of Fig 4.27(b) is most suitable as it contains the minimum number of capacitors. The modified form of the filter circuit in Fig 4.27(b) is shown in Fig 4.27(c), which has been obtained from the former using the Norton left-to-right L transformation to split-up the inductors L_3 and L_4 into an inductor-T (formed by L_{3_n}, L_{4_n} and L_{5_n} in Fig 4.27(c)). This operation is necessary in order to have equal value capacitors in the final circuit.

The impedance scaled version of the circuit in Fig 4.27(c) is shown in Fig 4.27(d) which has four supercapacitors. We shall use the $\pm$R, $\pm$C circuit of Fig 4.11(f) for simulating the supercapacitor D_1 and use the $\pm$R, $\pm$C circuit of Fig 4.12(a) for simulating the supercapacitors D_2 and D_4; the problem of simulating the supercapacitor D_3 will be considered later. The circuit of Fig 4.27(e) is obtained by replacing the supercapacitors D_1, D_2 and D_4, in Fig 4.27(d), by their corresponding $\pm$R, $\pm$C circuits. In the circuit of Fig 4.27(e) the values of capacitors C_{D_1}, C_{D_2} and C_{D_4} can be chosen arbitrarily but the circuit of Fig 4.27(f) is obtained if we choose $C_{D_1} = C_{D_2} = C_{D_4} = C_{s_n}$. In Fig 4.27(f) the negative shunt capacitor at node 2 can be combined with the series capacitor between nodes 1 and 2; this will have the effect of multiplying the filter transfer function by a factor of half.

Now let us consider the problem of simulating the supercapacitor D_3. We note from Fig 4.27(f) that D_3 appears as an isolated supercapacitor and thus there is no possibility of achieving cancellation of the positive and negative components if we use one of

the circuits of Fig 4.11 to simulate D_3. Therefore, if D_3 is simulated using one of the circuits of Fig 4.11 then a minimum of two NICs and three capacitors would be required; however, if D_3 is realised using an s^2-type PIC (say) terminated in a resistor, then two OP-AMPs and two capacitors only would be required. We shall use the latter method to show that the simulation method of this chapter, which uses NICs, and the well established simulation method, which uses PICs, can be advantageously combined in the same circuit.

The circuit in Fig 4.27(g) shows the realisation of the circuit of Fig 4.27(f) using four NICs and one PIC. Note that the circuit in Fig 4.27(g) requires six operational amplifiers and ten capacitors; however, since most of the capacitors in the circuit are coupled via resistors, it is necessary to have narrow tolerance capacitors. An alternative realisation of the circuit in Fig 4.27(g) is shown in Fig 4.27(h) which requires two more NICs but in this circuit all capacitors can have preferred values and wide manufacturing tolerances, provided the circuit is adjusted deterministically in the following way.

In Fig 4.27(h), the NIC having a scaling factor K_5 can be thought of as dividing the circuit into two parts. The circuit to the right hand side of NIC_5 can be divided into three subcircuits which are coupled via the PIC and NIC_6. Thus the capacitor(s) inside each of these circuits can have arbitrary values and tolerances provided we vary the resistors in each circuit accordingly such that the various time constants within each of these subcircuits are kept at their nominal values; the conversion factors of the PIC and NIC_6 are then changed to match the impedance levels of these three subcircuits. Let

us now look at the circuit to the left hand side of NIC_5. At the input end, the values of R_1 and R_3 are calculated as

$$R_1 = 3C_{s_n} R_{1_n} /(C_1+C_2+C_4)$$

$$R_3 = 3C_{s_n} R_{2_n} /(C_1+C_2+C_4)$$

The conversion factors K_1, K_2 and K_4 are chosen as: $K_1 = C_3/C_2$, $K_2 = C_5/C_4$ and $K_4 = C_6/C_5$. The values of R_2, R_4 and K_3 are calculated as: $R_2 = (C_{s_n}/C_3)^2 R_1 R_{D_1}/R_{1_n}$, $R_4 = (C_{s_n}/C_5)^2 R_1 R_{D_2}/R_{1_n}$ and $K_3 = C_5/C_4$. Finally, the conversion factor of NIC_5, which couples the two networks together, is calculated as: $K_5 = R_3 R_{3_n}/(R_{2_n} R_5 K_3)$.

As stated previously, active RC realisations of the filter in Fig 4.27(a) have also been derived in [36] and [17] with fifteen OP-AMPs and twelve capacitors, and twelve OP-AMPs and eight capacitors, respectively. If the above filter is realised by the full impedance scaling method, then five PICs (i.e. ten OP-AMPs) and eleven capacitors would be required.

4.7 Computed and measured results

In Section 4.6 we developed novel active RC circuits for simulating lowpass, highpass and bandpass filters. Some of these filter circuits have been simulated on the computer using a network analysis program, and a limited amount of practical work has also been under-taken in that some discrete component models have been constructed and their performances measured. In this section, we shall present the computed and the measured results for these filters.

The main purpose of the practical work that has been carried-out was two-fold; firstly to show that the sensitivity of these active RC circuits is low enough for the method to be practically viable; and secondly to show that these active RC circuits do not suffer from adverse effects e.g. high DC off-sets, instability, etc..

In the discrete component models, polystyrene capacitors and carbon film resistors were used throughout. The values of the components were selected, or were made-up by combinations, from the available standard values to be within $\pm$ 0.5 % of their corresponding nominal values; thus it was not necessary to tune the circuits. Also, the designs of the circuits were not compensated to take into account the effect of the finite gain bandwidth products of the OP-AMPs. All measurements were carried-out with 1 V_{RMS} input signal level.

As a first example a fifth order Chebyshev lowpass filter, with a cut-off frequency of 1 kHz and a passband ripple of 0.28 dB, was designed using the method illustrated in Fig 4.13; the active RC circuit is shown in Fig 4.28 and its nominal and measured component values are listed in Table 4.1. The element values of the prototype filter were obtained from [31]. The operational amplifiers used in the circuit were of type μA 741, which have typical f_T value of 1 MHz. Figs 4.29(a) and (b) show the computed passband and stopband responses, respectively, of the nominal design for ideal OP-AMPs (i.e. $f_T = \infty$) and for the case when OP-AMPs have f_T's of 1 MHz. The corresponding measured response curves of the discrete component model are shown in Figs 4.30(a) and (b).

As a second example a fifth order Chebyshev highpass filter with a cut-off frequency of 1 kHz and a passband ripple of 0.28 dB was designed using the method illustrated in Fig 4.20; the active RC circuit is shown in Fig 4.31 and its nominal and measured component values are listed in Table 4.2; the element values of the prototype highpass filter were obtained from the above lowpass prototype filter via the lowpass to highpass transformation. The OP-AMPs used in the circuit were again of type μA 741.

In the absence of capacitor C_p the discrete component model of Fig 4.31 was found to oscillate at a frequency of approximately 250 kHz. All the other remaining fifteen combinations of connecting the OP-AMP input terminals were explored but no stable circuit was found; so the following measurements were made with the OP-AMP input connections as shown in Fig 4.31 and with the stabilising capacitor C_p present. The stability of NIC circuits is discussed morefully in Chapter 5 and the reasons for the instability of this circuit will be discussed there in more detail.

Figs 4.32(a) and (b) show the computed passband and stopband responses, respectively, of the nominal design for the case of ideal OP-AMPs and for the case when OP-AMPs have f_T's of 1 MHz. The corresponding measured response curves of the discrete component model are shown in Figs 4.33(a) and (b).

As a third example an eight order elliptic bandpass filter, with a passband from 1 kHz to 1.4 kHz, passband ripple of 0.4 dB, stopband attenuation > 51.05 dB below 685 Hz and above 1.714 kHz, was designed using the prototype structure of Fig 4.27(c). The element values of the prototype structure are given in Table 4.3

and the active RC circuit is shown in Fig 4.34. The nominal and measured component values of the circuit are given in Table 4.4. The capacitor C_p and resistors R_{p_1} and R_{p_2} in Fig 4.34 are required to stabilise the circuit (the stability of NIC circuits is discussed in Chapter 5) and their values were determined practically.

The OP-AMPs used in the circuit of Fig 4.34 were of the type HA4741, which have typical f_T's of 3.5 MHz. The computed passband and stopband responses of the circuit are shown in Figs 4.35(a) and (b), respectively, and the measured response curves of the discrete component model are shown in Figs 4.36(a) and (b), respectively.

From above, we note that the computed and the measured results for the lowpass, the highpass and the bandpass filter are in good agreement and the small descrapencies which there are can be explained in terms of the tolerances on the components and non-ideal effects associated with the OP-AMPs (e.g. finite f_T's, etc.).

4.8 Sensitivity considerations of the active RC filter circuits

4.8.1 General

The main objective in designing active RC filters via the simulation of resistively terminated LC ladder filters is to obtain active RC circuits which retain the low sensitivity properties of their LC prototypes. Therefore, we shall now discuss the sensitivity of the active RC circuits designed by the new method described in this chapter.

The sensitivity of active RC filter circuits is extensively discussed in the literature and it often leads to considerable controversy as different authors use different criteria for evaluating the sensitivity. Hence an appropriate starting point for our discussion is to out-line the criterion which we shall use here to consider the sensitivity of the active RC circuits. In order to do this we begin by making the following observations.

Filters are usually designed to meet some required loss-frequency specification and the design procedure is often carried-out assuming the components to be ideal, i.e. free from any parasitic effects what-so-ever. In order to estimate whether a filter circuit will still meet its required loss-frequency specification (and hence to evaluate its practical viability) when there is some tolerance on the values of the components, it is essential that the designer should have some knowledge of the order of the sensitivity of the filter loss to changes in the component values and to the parasitics associated with the components. It is shown in Section 1.2.3 that resistively terminated LC ladder filters, which are designed to have maximum power transfer at the frequencies of minimum loss in the passband, have very low sensitivity in the passband to changes in the values of the reactive components.

The term "low sensitivity" is also often used in the literature in conjunction with active RC circuits which are obtained by simulating resistively terminated LC ladder filters; however, the use of the term low sensitivity in this context is not strictly true since active RC circuit always has more components and hence its over-all sensitivity must always be greater than the sensitivity of its LC ladder prototype. It is obviously to be expected that active RC circuits

obtained by different simulation methods will have different sensitivities. However, it must be remembered that sensitivity is by no means the sole criterion for judging whether a particular simulation method is practically feasible; other attributes of the simulation method such as ease of tuning, number of resistors, capacitors and amplifiers used in the realisation are also equally as important as the sensitivity of the circuit.

From the above general discussion we note that the problem of sensitivity arises from the fact that we have tolerances on the values of the components used to realise the filter circuit. There are basically two types of tolerances; firstly, the component values may differ from their respective nominal values due to manufacturing tolerances, and secondly the component values may change due to ageing and variations in the ambient conditions. These latter type of variations are usually referred to as "post adjustment" variations and they are generally very much smaller than the manufacturing tolerances. In the realisation of high precision filters it is always necessary to trim some components of the circuit in order to take-up the manufacturing tolerances on the values of the untrimmed components. Hence, since it has been shown that the components of the active RC circuits obtained by the new method can have wide manufacturing tolerances the main source of sensitivity is that due to the post-adjustment variation in the component values.

The sensitivity of active RC circuits is made-up of two contributions; one due to the passive components (i.e. resistors and capacitors) and the other due to the active components (i.e. finite f_T's of operational amplifiers). Here we shall only consider the

sensitivity due to the passive components; the problem of the active sensitivity will be examined in more-detail in Chapter 5.

It has been shown in Section 4.6 that for the active RC circuits derived by the present method the manufacturing tolerances on the values of the capacitors can be taken into account by trimming the resistors in the circuit. Thus the starting point in our discussion is that we assume that the circuit has been adjusted to have "ideal" characteristic at the time of manufacture. The typical values for the post-adjustment variation of thick-film resistors and ceremic chip capacitors are of the order of 28 parts per million per degree centigrade; hence a temperature variation of $\pm$ 40^{o}C would result in a $\pm$ 0.112 % variation in the component values.

It is important to note that the post-adjustment variations would mainly produce correlated changes in the component values, with some what smaller uncorrelated changes which result from the mis-match between the temperature coefficients of the components. The correlated changes in the resistors and capacitors of the circuit would result in variation of the RC products which would have a predominant effect on the cut-off frequency of the filter. On the other hand, the uncorrelated changes in the components would effect both the cut-off frequency and the passband ripple of the filter. Hence from the point of view of studying the sensitivity it is important to consider the changes in the components to be uncorrelated; indeed, this approach is adopted here.

Let us now consider how we shall interpret the sensitivity of the active RC circuits derived in this chapter. In order to show that these active RC circuits exhibit low sensitivity properties we shall

make use of two methods; in the first instant we shall interpret the effect of changes in the passive components of the active RC filter in terms of "equivalent prototypes" filters; however, later-on we shall also present some computed sensitivity results for two active RC lowpass filters.

4.8.2 Interpretation of sensitivity in terms of equivalent prototype circuits

The equivalent prototype filter circuit is obtained in the following way. A component (say Z_o) in the active RC circuit is changed by a finite amount (ΔZ) from its nominal value. We now trace back the steps which we followed to obtain the active RC structure and thus arrive at an LC network which is equivalent to the modified active RC network. Some of the elements of this equivalent prototype will directly correspond to the elements of the original prototype, except perhaps for a constant scaling of their values, while some of the reactive elements may become "lossy", i.e. they may have finite positive or negative Q-factors.

The basic principle of the above argument will now be illustrated by considering the sensitivity of one of the active RC lowpass circuits designed in Section 4.6.1.

Let us consider the prototype lowpass filter of Fig 4.13(a) and its active RC realisation of Fig 4.13(d), which is also shown in Fig 4.37(a) for convenience. In Fig 4.37(a) we note that the resistor R_s, between nodes 1 and 2, and the capacitors C_{1n}, C_{3n} and C_{5n} correspond directly to the similarly designated elements of the prototype LC filter of Fig 4.13(a). Moreover, any variation in the

values of capacitors C_{L_2} and C_{L_4} in Fig 4.37(a) can be interpreted by an equivalent variation in the values of inductors L_{2_n} and L_{4_n}, respectively, in Fig 4.13(a). Hence we have a one-to-one relationship between the following elements (R_{s_n} (between nodes 1 and 2), C_{1_n}, C_{L_2}, C_{3_n}, C_{L_4} and C_{5_n}) of the active RC filter and the following elements (R_{s_n}, C_{1_n}, L_{2_n}, C_{3_n}, L_{4_n} and C_{5_n}) of the original LC filter, respectively. Therefore the sensitivity of the filter response to these elements of the active RC filter is the same as the sensitivity to the corresponding elements of the low sensitivity LC filter.

Let us now consider the sensitivity of the shunt resistor at node 2 in Fig 4.37(a). In Fig 4.37(a), suppose we label the series resistor between nodes 1 and 2 as R_1 and the shunt resistor as R_2, where nominally $R_1 = R_2 = R_{s_n}$. Now, we can replace resistors R_1 and R_2 by a single series resistor of value R, where

$$R = \frac{R_1 R_2}{R_1 + R_2} \tag{4.6}$$

The effect of carrying-out this circuit modification multiplies the transfer function of the circuit by a constant factor G, where

$$G = 1 + \frac{R_1}{R_2} \tag{4.7}$$

Thus if we let the transfer function of the original circuit be T(s), then the transfer function, T′(s), of the modified circuit is given by

$$T'(s) = G\, T(s) \tag{4.8}$$

Using the identity given in equation (1.1) and equation (4.8), we obtain

$$S^{|T'(s)|}_{|T(s)|} = 1 \qquad S^{|T'(s)|}_{G} = 1 \tag{4.9}$$

Now, making use of the identity

$$S^{y}_{x} = S^{y}_{z}\, S^{z}_{x} \tag{4.10}$$

and the results of equation (4.9), we obtain the following:

$$S^{|T'(s)|}_{R_1} = S^{|T'(s)|}_{G}\, S^{G}_{R_1} = \frac{R_1}{R_1 + R_2} \tag{4.11}$$

$$S^{|T'(s)|}_{R_2} = S^{|T'(s)|}_{G}\, S^{G}_{R_2} = \frac{-R_2}{R_1 + R_2} \tag{4.12}$$

$$S^{|T'(s)|}_{R} = S^{|T'(s)|}_{G}\, S^{G}_{R} = S^{G}_{R} \tag{4.13}$$

In equations (4.11) and (4.12) if we note that nominally $R_1 = R_2 = R_{s_n}$, then $S^{|T'(s)|}_{R_1} = -S^{|T'(s)|}_{R_2} = \frac{1}{2}$. From this result we conclude that the sensitivity of the shunt resistor at node 2 in Fig 4.37(a) is equal in magnitude to the sensitivity of the series resistor between nodes 1 and 2 except that it has an opposite sign. But it has been shown above that the series resistor between nodes 1 and 2, in Fig 4.37(a), is directly equivalent to the source resistor in Fig 4.13(a). Therefore the above result together with the discussion on the sensitivity of LC filters to terminating resistors, presented in Section 1.2.3, leads us to the conclusion that the shunt resistor at node 2 in Fig 4.37(a) is analogous to the load resistor R_{L_n} of Fig 4.13(a).

It is interesting to note that if resistors R_1 and R_2 are replaced by a single resistor R, as stated above, then any change in the value of R can be represented by an equivalent simultaneous changes in the values of R_1 and R_2; the direction and magnitude of these changes will be same as the change in R (this follows directly from equation (4.6)). From equation (4.7) we note that if the values of R_1 and R_2 change by the same amount in the same direction then the value of G does not change and consequently S_R^G in equation (4.13) becomes zero and hence the first order sensitivity of the transfer function T'(s) to small changes in the value of R also becomes zero.

The above argument shows that we have one-to-one correspondence between the seven elements of the active RC circuit of Fig 4.37(a) (i.e. two resistors and five capacitors) and the seven elements of the prototype filter of Fig 4.13(a). Therefore these elements of the active RC circuit have the same low sensitivity properties as their counterparts in the passive circuit. Thus, we have now to investigate the sensitivity of the filter response to the remaining elements of the circuit in Fig 4.37(a); namely, the four resistors (i.e. the resistors connected to the right hand sides of the NICs) and the four conversion factors of the NICs. We shall first consider the sensitivity of the filter response to the remaining resistors and for this purpose we shall assume the NIC conversion factors to have their nominal values such that the circuit under consideration is equivalent to the circuit of Fig 4.37(b).

In Fig 4.37(b), let us now consider the effect of a finite change ΔR in the value of the resistor between nodes 2 and 2'; this change can be represented as shown in Fig 4.37(c). The circuit of Fig 4.37(d) is obtained by transforming the encircled T-networks in

Fig 4.37(c) into their equivalent Π-networks. In Fig 4.37(d) we note that if $\Delta R = 0$ then we obtain the original prototype circuit of Fig 4.13(a). The circuit of Fig 4.37(e) is obtained by using the Norton left-to-right "L" transformation on the encircled part of Fig 4.37(d). From the circuit of Fig 4.37(e) we note that the effect of having a change ΔR in the value of the resistor between nodes 2 and 2′ in Fig 4.37(b) is twofold; firstly, a part of the prototype network is impedance scaled, and secondly two reactive elements in the resulting structure have finite Q-factors.

Now, as stated above, if we assume that the circuit of Fig 4.37(a) is tuned at the time of manufacture, then ΔR is of the order of $\pm$ 0.112 % of the nominal value of the source resistance, R_{s_n}; hence the value of the impedance scaling factor $\emptyset^2$ in Fig 4.37(e) is very nearly unity. It is shown in Section 1.2.3 that the sensitivity of resistively terminated LC ladder filter to small changes in its component values is low, and hence the effect of impedance scaling in the circuit of Fig 4.37(e) will not drastically impair the low sensitivity properties of the circuit. At first sight it may be thought that the appearance of resistors R_p and R_s in Fig 4.37(e) may cause a serious deterioration in the sensitivity of the circuit but it is shown below that the effect of these resistors is not very serious.

From Fig 4.13(a) we note that capacitors C_{1_n} and C_{5_n} are associated with resistors R_{s_n} and R_{L_n}; we can therefore define Q-factors, Q_{C_1} and Q_{C_5}, given by $wC_{1_n}R_{s_n}$ and $wC_{5_n}R_{L_n}$, respectively; where w is the frequency in radians/s. In the original prototype LC filter all the reactive elements are free of any parasitics and hence their individual Q-factors are infinite. Let us now assume that

parasitic resistance appears in parallel with each capacitor and a parasitic resistance appears in series with each inductor of the prototype filter such that all the reactive components have finite Q-factors. LC filter designers are quite well accustomed to having inductors and capacitors of finite Q-factors in practical circuits. To them it is a well known fact that provided the Q-factors of the individual reactive components are very much greater (e.g. an order of magnitude) than the circuit Q-factors (i.e. Q_{C_1} and Q_{C_5} in the case under consideration here), then it is always possible to build practical circuits; this implies that the circuit still preserves its low sensitivity properties. Therefore, in order to estimate whether our active RC circuit also maintains the low sensitivity properties of its prototype, we would have to look at the typical circuit Q-factor values and the values of the Q-factors of the reactive components.

A search through filter tables [31] reveals that for equally terminated LC ladder Chebyshev lowpass filters, from order one through to fifteen and passband ripple values from 0.0004 dB to 1.2494 dB, the greatest value of the component Q-factor, at the passband edge frequency (i.e. w = 1 rads/s), is approximately 3.431. Therefore, in order to obtain a satisfactory response curve we require the Q-factors of the reactive components to be only greater than 50. However, it has been stated above that ΔR would be of the order of 0.112 % of the source resistance value, and hence the actual Q-factors of C_{1_n} and L'_{2_n} ($= \emptyset^2 L_{2_n}$) in Fig 4.37(e) would be greater than 800; thus giving an excellent response curve in practice. Therefore, by virtue of the above argument, we can conclude that the active RC circuit of Fig 4.37(c) still maintains the low sensitivity properties of its LC ladder prototype of Fig 4.13(a).

Let us now consider the effect of finite change, ΔR, in the value of the resistor between nodes 2′ and 3, in Fig 4.37(b); the circuit under consideration thus becomes as shown in Fig 4.38(a). The circuit of Fig 4.38(b) is obtained by transforming the encircled T-networks in Fig 4.38(a) into their equivalent Π-networks. The application of the Norton right-to-left "L" transformation to the encicled part in Fig 4.38(b) leads to the circuit of Fig 4.38(c). As before, from the circuit of Fig 4.38(c) the effect of the change ΔR can be seen to be two-fold; i.e. some elements of the original LC prototype are impedance scaled and two reactive components have finite Q-factors. Using the same argument as before, it can be shown that provided $\Delta R << R_{s_n}$ then the sensitivity of the filter response to changes in the value of the resistor between nodes 2′ and 3 in Fig 4.37(b) is expected to be low.

The equivalent circuits for finite changes in the values of resistors between node pairs 3, 3′ and 3′, 4 in Fig 4.37(b) can also be derived in the same way and these are shown in Figs 4.39(a) and (b), respectively. Again, the sensitivities of the circuits in Fig 4.39 are expected to low provided $\Delta R << R_{s_n}$.

Let us now consider what effect the variations in the NIC conversion factors will have on the transfer function of the circuit in Fig 4.37(a). This problem will be approached in the following manner.

We shall consider a finite change in the conversion factor of one NIC, while all other NICs and components in the circuit have their respective nominal values, and obtain an equivalent circuit on the same lines as above. For example, suppose the conversion factor of

NIC_1 in Fig 4.37(a) is K_1', while all other components of the circuit have their respective nominal values, then the circuit of Fig 4.37(a) becomes equivalent to the circuit of Fig. 4.40(a). By transforming the encircled T-networks in Fig 4.40(a) into their corresponding Π-networks we obtain the circuit shown in Fig 4.40(b). An equivalent representation of this circuit is shown in Fig 4.40(c) from which we note that the consequence of NIC_1 having a variation in its conversion factor can be interpretted as having two effects on the prototype structure. Firstly, some elements of the prototype structure are impedance scaled; and secondly, one reactive element has a finite Q-factor. Therefore, by the same argument as for the sensitivity of the resistors in Fig 4.37(a) (which have no counterparts in the LC prototype) the sensitivity of the filter response to variations in the conversion factor of NIC_1 are expected to be low provided the variation is small, i.e. $|K_1' - K_1| \ll K_1$, where K_1 is the nominal value of the conversion factor (which is equal to unity in the case of Fig 4.37(a)).

Now let us derive the equivalent circuit when the conversion factor of NIC_2 in Fig 4.37(a) is not equal to its nominal value of unity. The circuit in Fig 4.41(a) is obtained from the circuit of Fig 4.37(a) by assuming NIC_2 to have a conversion factor K_2', while all other components of the circuit have their respective nominal values. Fig 4.41(b) shows an equivalent representation of the circuit in Fig 4.41(a). Transformation of the encircled T-networks in Fig 4.41(b) into their equivalent Π-networks leads to the circuit shown in Fig 4.41(c). The circuit in Fig 4.41(d) is obtained by using the Norton right-to-left "L" transformation on the encircled part of the circuit in Fig 4.41(c). It is seen from Fig 4.41(d) that the

effect of NIC_2 having a variation in its conversion factor is to impedance scale some elements of the prototype filter and to make the Q-factor of one of the reactive element finite. By the same argument as for NIC_1 the sensitivity of the filter response to variations in the conversion factor of NIC_2 will be low, provided $|K_2' - K_2| \ll K_2$, where K_2 (=1) is the nominal value of the conversion factor of NIC_2.

In the same way as above, equivalent circuits for the case when NIC_3 and NIC_4 have variations in their respective conversion factors can also be derived and these are shown in Fig 4.42(a) and (b), respectively.

In the above discussion we have considered the sensitivity of only one active RC realisation of a fifth order all-pole lowpass filter; obviously, the sensitivity of other types of all-pole structures (lowpass, highpass or bandpass) can be considered in the same way. The above method can also be used to interpret the sensitivity of elliptic structures, but the equivalent circuits obtained are relatively more complex than those obtained for all-pole structures.

4.8.3 Computed results for the sensitivity of two active RC circuits

In the previous subsection, it has been shown that there exists a one-to-one relationship between some components of the active RC circuit and the components of the prototype LC filter. Equivalent circuits were developed in order to show that the sensitivity of the active RC filter circuit response to variations in the values of the components which do not have counterparts in the LC prototype filter are fairly low provided the component variations are small.

As a further verification of the argument presented above, we shall now present some computed results for the sensitivity of two active RC circuits; the first of these circuits being the circuit of Fig 4.28, which is obtained by simulating the floating inductors in the prototype filter of Fig 4.13(a); the second circuit is shown in Fig 4.43 and it is obtained by simulating the grounded supercapacitors which result when we carry-out impedance scaling on the prototype filter of Fig 4.17(a). Both of these lowpass filters are designed to have a cut-off frequency of 1 kHz and a passband ripple of 0.28 dB; the nominal component values for the circuits of Figs 4.28 and 4.43 are given in Tables 4.1 and 4.5, respectively.

The loss-frequency responses of the circuits in Figs 4.28 and 4.43 were computed for the nominal values of the components and when each component is changed individually by $\pm$ 2 % from its nominal value; the results are shown plotted in Figs 4.44 and 4.45, respectively. In Fig 4.44 the sensitivity curves marked by R_1, R_2, C_1, C_2, C_3, C_4 and C_5 correspond directly to the sensitivity curves of R_{s_n}, R_{L_n}, C_{1_n}, L_{2_n}, C_{3_n}, L_{4_n} and C_{5_n}, respectively, of Fig 4.13(a) whereas in Fig 4.45, the sensitivity curves marked by R_1, R_4, R_7, R_{10} and R_{13} correspond directly to the sensitivity curves of L_{1_n}, C_{2_n}, L_{3_n}, C_{4_n} and L_{5_n}, respectively, of Fig 4.17(a). On comparing the results in Figs 4.44 and 4.45, we make the following three observations.

Firstly, although both circuits have basically the same structure (e.g. each circuit can be considered as consisting of five RC subcircuits which are coupled by four NICs), the sensitivities of the corresponding elements in the two structures are not the same.

Secondly, the circuit in Fig 4.43 can be seen to exhibit the interesting and useful property that the gain at zero frequency is independent of all passive component values. An explanation for this is as follows. It can be shown that the source and the load resistors in Fig 4.17(a) are equivalently represented by the two capacitors forming the capacitive potential divider at the output of the filter in Fig 4.17(d). But these capacitors have been replaced by a single capacitor C_5, in Fig 4.43, which (it can easily be shown) has a zero small change sensitivity.

Thirdly, we note that for the active RC circuits developed in this chapter we can adjust the circuit to allow for the manufacturing tolerances as discussed in Section 4.6, and thus we are mainly interested in the effect of the post-adjustment variations of the components on the filter transfer function. Such variations are expected in practice to be of the order of $\pm$ 0.112 %; i.e. approximately twenty times lower than the variations assumed in Fig 4.44 and 4.45. Therefore the response variations likely to occur in practice are expected to be correspondingly lower than the response variations shown in Figs 4.44 and 4.45.

4.9 Conclusions

In this chapter a novel approach to the active RC simulation of LC ladder filters has been presented. A simple procedure has been used to obtain 2-port $\pm$R, $\pm$C subcircuits which simulate grounded and floating inductors and grounded and floating frequency dependent negative resistors, of the supercapacitor type. It has been shown that by viewing the basic $\pm$R, $\pm$C subcircuits in different ways,

many more $\pm$R, $\pm$C subcircuits can be obtained for simulating inductors and supercapacitors.

These $\pm$R, $\pm$C subcircuits can be realised by means of +R, +C circuits and current inverting type negative impedance converters. However, this approach of simulating the inductors (or supercapacitors) and then performing direct replacement of the simulated elements in the prototype structure is not very attractive since each simulated element requires rather a large number of components (both passive and active). The most novel feature of the approach presented here is the way in which the use is made of these $\pm$R, $\pm$C subcircuits in filter design such that the number of components required in the active realisation is comparable with other active RC simulation methods (e.g. the method of partial and full impedance scaling [5,6]).

The $\pm$R, $\pm$C subcircuits, although electrically port symmetrical, are structurally unsymmetrical, thus giving two possible active RC realisations per simulated element, depending on the orientation of the ports of the simulated element. This gives rise to 2^N different realisations of a prototype filter in which N elements are being simulated. This feature of versatility of the new design method has been illustrated by producing four designs of a fifth order all-pole lowpass filter in which two floating inductors are being simulated.

The generality of the new design method has been shown by designing both all-pole and elliptic filters with lowpass, highpass and bandpass characteristics. The circuits designed by the new method can be designed in most cases to have equal and preferred value capacitors and also these capacitors can have wide manufacturing

tolerances if we assume that the resistors in the circuit can be adjusted.

For the design of all-pole filters the number of OP-AMPs required for the circuits designed by the method of this chapter is less than or equal to the number that would be required if the same filter is realised by the complex impedance scaling methods. Some type of elliptic structures (e.g. lowpass) may require a larger number of OP-AMPs, especially if capacitors with preferred values and wide manufacturing tolerances are to be used.

In order to show that active RC circuits designed by the new method are practically feasible, some computed and measured results of discrete component models were presented in Section 4.7. A close agreement is obtained between the computed and the measured results.

In Section 4.8 the sensitivity aspects of the active RC circuits derived in this chapter were discussed. It is shown that there exists a one-to-one relationship between some elements of the active RC circuit and the elements of the prototype filter. Furthermore, it has also been shown that changes in components which have no counterparts in the LC prototype can be considered in terms of equivalent prototype circuits. Each element of this type usually has two effects on the equivalent prototype circuit; firstly, some elements of the equivalent prototype are impedance scaled; secondly, the Q-factors of some reactive elements in the equivalent prototype circuit become finite. If the changes in component values are fairly small then these two effects do not seriously deteriorate the sensitivity of the active RC circuits. This point has been illustrated by presenting some computed sensitivity results for two designs of an active RC lowpass filter.

C H A P T E R 5

A STUDY OF THE EFFECT OF FINITE GAIN-BANDWIDTH PRODUCT OF THE AMPLIFIER IN NEGATIVE IMPEDANCE CONVERTER CIRCUITS

5.1 Introduction

The design of active RC circuits is often carried-out assuming the active elements (i.e. operational amplifiers) to be ideal because the design procedure is then quite straight forward. However, due to the imperfections of the operational amplifiers (OP-AMPs) the characteristics of the practical circuit may deviate considerably from the characteristics for which the circuit was designed. The OP-AMPs suffer from various imperfections but the single most serious imperfection is generally the finite gain bandwidth product, f_T, of the OP-AMP.

In this chapter we shall consider the effect, on the filter response, of using OP-AMPs with finite f_T's to realise the NICs in the active RC networks derived in Chapter 4; in particular, a method of minimising the effect of finite f_T's in circuits which use NICs will be discussed in Section 5.2. The possibility of minimising the effect of finite f_T's in circuits which use OP-AMPs to realise NICs stems from the following argument.

The usual requirement of an NIC is that it should have the required conversion factor, which is a quantity exclusively given by a ratio of two impedances, i.e. the "NIC impedances"; hence the conversion factor of an NIC solely depends on the relative impedance levels of the NIC impedances. Thus we have at our discretion the choice of the absolute impedance level of the NIC impedances and we shall show in Section 5.2 that this parameter can be utilised to minimise the effect of finite f_T's in NIC circuits. The conversion factors of NICs used in the filter circuits of Chapter 4 are independent of frequency and hence the simplest form for the NIC

impedances is to choose them as resistances; however, we shall also show that the effect of finite f_T's can be reduced further by choosing the NIC impedances to be of more complex form (e.g. a parallel or a series combination of a resistor and a capacitor).

In section 5.3, the criterion developed in Section 5.2 to minimise the effect of finite f_T's will be applied to the three NIC all-pole 5th order highpass filter of Fig 4.21(c); the validity of the method will be shown by means of some computed results and also by means of some measured results for the discrete component model.

A discussion on the stability considerations of the circuits which use NICs is presented in Section 5.4. It is shown that the stability of a NIC can be conviently approached in a simple way by considering the amounts of feedback being applied to the inverting and the non-inverting terminals of the OP-AMP (realising the NIC) at zero and infinite frequencies. Furthermore, a method is discussed in some detail which can be used to stabilise inherently unstable NIC circuits.

In Section 5.4 the following definition is assumed for the stability of a circuit: A circuit is stable if for a bounded input the output of the circuit is also bounded. In our discussion, we shall assume that the input to the circuit is zero.

5.2 A method of minimising the effect of finite f_T's in NIC circuits

5.2.1 General

In Chapter 4 we developed active RC filter circuits which require negative impedance converters (NICs). As discussed in Chapter 4, a

NIC can be realised very simply by means of an OP-AMP and two impedances which we shall refer to here as the "NIC impedances"; the conversion factor of the NIC is given by the ratio of the NIC impedances. If the OP-AMP is assumed to be ideal then the design of a NIC is quite straight forward and we can arbitrarily choose the impedance levels of the NIC impedances as long as their ratio is equal to the required conversion factor. Inevitably, if the OP-AMPs suffer from finite gain bandwidth products (f_T's) then the transfer function of the filter circuit will be in error. In this section we shall describe a method of minimising the effect of finite f_T's in circuits which use OP-AMPs to realise NICs. In order to minimise the effect of finite f_T's we have basically two parameters at our disposal; namely, the impedance levels of the NIC impedances and the composition of NIC impedances (e.g. R, parallel RC, etc). It will become apparent later in the chapter that both of these parameters can be exploited advantageously to significantly reduce the errors, due to the effect of finite f_T's, in the response of the circuit. The basic principle on which the method of minimising the effect of finite f_T's is based is as follows.

Consider the general 2-port network shown in Fig 5.1(a) which contains NICs. Now, one approach of minimising the effect of finite f_T's would be to consider each NIC in turn to have finite f_T (while all the remaining NICs in the circuit are considered to be ideal) and to minimise the error in the transfer function of the circuit by appropriately choosing the impedance levels and/or the composition of the NIC impedances. In the following we shall adopt this type of minimisation strategy; however, before we proceed to obtain a suitable

objective function which is to be minimised, it is necessary to consider the following.

Suppose the network of Fig 5.1(a), which comprises NICs, has been obtained by the method of Chapter 4. Now if we consider one of the NICs inside the network of Fig 5.1(a) to be non-ideal then separating the non-ideal NIC from the network will divide the network into one of the three forms shown in Figs 5.1(b), (c) or (d). In particular, if Fig 5.1(a) is an all-pole filter then separation of the non-ideal NIC will exclusively divide the network into the form shown in Figs 5.1(b) or (c), whereas for elliptic filters anyone of the three forms shown in Figs 5.1(b) ⟶ (d) may be obtained. Note that the subnetworks N_A, N_B and N_C in Figs 5.1(b), (c) and (d) may also contain NICs but these NICs are considered to be ideal. For ease of reference, we shall refer to the non-ideal NIC in circuits of Figs 5.1(b), (c) and (d) as the "coupling", the "grounded" and the "bridged" NIC circuits, respectively.

In the coupling and the bridged NIC circuits of Figs 5.1(b) and (d) the input and the output nodes of the original network occur in subnetworks N_A and N_B, respectively; whereas, in the grounded NIC circuit of Fig 5.1(c) the input and the output nodes are located in the subnetworks N_A and N_C, respectively.

In Sections 5.2.2 and 5.2.3 we shall derive the objective functions for minimising the effect of finite f_T's for the coupling and the grounded NICs, respectively. The case of the bridged NIC is much more complicated and it is not considered here. Thus the method to be described here is applicable for minimising the effect of finite f_T's in all-pole structures.

5.2.2 Minimising the effect of finite f_T for coupling NICs

Let us consider the problem of minimising the effect of finite f_T for the case of the coupling NIC network of Fig 5.1(b), which is also shown in Fig 5.2(a). The voltage transfer function, T, of the circuit in Fig 5.2(a) is given by

$$T = \frac{V_o}{V_i} = \frac{V_o}{V_1} \cdot \frac{V_1}{V_i} \qquad (5.1)$$

From equation (5.1) we note that the partial transfer function term V_o/V_1 is given by the ratios of the impedances within the subnetwork N_B, in the circuit of Fig 5.2(a), and hence it is not affected by the non-ideal NIC. However the other partial transfer function term (i.e. V_1/V_i) in equation (5.1) is dependent on the ratios of the impedances within the networks N_A and N_B and also on the NIC parameters and hence it is affected by the non-ideal performance of the NIC. Thus the object of minimising the effect of the finite f_T of the coupling NIC on the overall transfer function can be achieved by minimising the effect of the finite f_T on the partial transfer function V_1/V_i in the circuit of Fig 5.2(a). This can be achieved in the following manner.

In the circuit of Fig 5.2(a) if the transfer function of the subnetwork N_A, with port 2 open circuit, is $T_{A_{oc}}$ and if the input impedance at port 2, with port 1 short circuit, is Z_A then using Thevenin's theorem the circuit of Fig 5.2(a) can be represented as shown in Fig 5.2(b). Note that Z_B in Fig 5.2(b) represents the input impedance at port 1, with port 2 open circuit, of the subnetwork N_B in Fig 5.2(a). Since the transfer function $T_{A_{oc}}$ is given by the ratio of the impedances within the subnetwork N_A, i.e. it is not

affected by the non-ideal NIC, then our objective function for optimisation becomes the transfer function of the circuit in Fig 5.2(b) (i.e. V_1/V_2). The circuit of Fig 5.2(c) is obtained by replacing the NIC in the circuit of Fig 5.2(b) by its OP-AMP realisation (see Fig 4.2(b)). In the following we shall assume that the open loop gain, A, of the OP-AMP is characterised by

$$A = \frac{A_o \, w_c}{s + w_c} \tag{5.2}$$

where A_o and w_c are the DC gain and the 3-dB frequency, respectively, of the OP-AMP and s is the complex frequency variable.

If the voltage transfer function of the circuit in Fig 5.2(c) is T_1 then by straight forward analysis it can be shown that

$$T_1 = \frac{V_1}{V_2} = \frac{1}{1 - Z_A/(kZ_B) + A^{-1}\,[Z_A/Z_1 + Z_A/(kZ_B) + Z_1/(kZ_B) + 1]} \tag{5.3}$$

where $k = Z_1/Z_2$ is the conversion ratio of the NIC assuming $A \longrightarrow \infty$.

Let the transfer function of the circuit in Fig 5.2(c) be T_o when the OP-AMP is ideal; then an expression for T_o can be obtained from equation (5.3) by letting $A \longrightarrow \infty$.

$$\text{i.e.} \quad T_o = \frac{1}{1 - Z_A/(kZ_B)} \tag{5.4}$$

Now, using equation (5.4) the expression for the transfer function T_1 (i.e. equation (5.3)) can be rewritten as

$$T_1 = \frac{T_o}{1 + A^{-1}\left[(2T_o - 1) + (T_o - 1)Z_1/Z_A + T_oZ_A/Z_1\right]} \tag{5.5}$$

Let us express equation (5.5) as follows

$$T_1 = \frac{T_o}{1 + A^{-1}E} \tag{5.6}$$

$$\text{where} \quad E = (2T_o - 1) + (T_o - 1)Z_1/Z_A + T_oZ_A/Z_1 \tag{5.7}$$

Suppose we form the objective function, F, as the ratio of the ideal transfer function T_o and the non-ideal transfer function T_1, then from equation (5.6) we obtain

$$F = \frac{T_o}{T_1} = 1 + A^{-1}E \tag{5.8}$$

In equation (5.8) we note that if $A \longrightarrow \infty$ (i.e. ideal OP-AMP), then value of $F \longrightarrow 1$. Thus the problem of minimising the effect of finite f_T reduces to that of making the term $A^{-1}E$ in equation (5.8) as small as possible compared with unity. For a given OP-AMP type, the range of values of the open loop gain, A, would be specified and hence this parameter cannot be used for minimising the objective function of equation (5.8). Therefore the only way of minimising the objective function is to make E (see equations (5.8) and (5.7)) as small as possible.

The values of the impedances within the subnetworks N_A and N_B and the value of the NIC conversion factor k, in Fig 5.2(a), are dictated by the specifications for which the circuit is designed and practical

considerations (e.g. the use of equal and preferred value capacitors); therefore T_o (see equation (5.4)) and Z_A in equation (5.7) are not free parameters and hence these cannot be considered for minimising E. From equation (5.7) we see that the only free parameter for minimising E is Z_1, the NIC impedance (note that the value of Z_2 is chosen as $Z_2 = Z_1/k$, where k is the conversion factor of the NIC). From equation (5.8) we note that if we can manage to make $E = 0$, then the objective function becomes equal to unity and hence the effect of finite f_T becomes zero —— which is a very desirable result. Let us now see if it is possible to make $E = 0$. Equating equation (5.7) equal to zero and solving for Z_1 gives

$$Z_1 = - Z_A \qquad \text{and} \qquad Z_1 = - Z_A T_o/(T_o - 1) = -kZ_B \tag{5.9}$$

The result given in equation (5.9) is very desirable and would totally eliminate the effect of the finite f_T but it must be remembered that the impedance Z_A represents the impedance of the subnetwork N_A (see Fig 5.2(a)) which may contain NICs, and hence it would not be very practicable to use extra NICs to realise the NIC impedances. Therefore it may not be possible to choose the NIC impedances in accordance with equation (5.9). In this situation a compromise solution may be found by evaluating the two expressions for Z_1, given in equation (5.9), over some frequency band in which it is desired to minimise the effect of the finite f_T and then see if these expressions can be approximated by choosing the NIC impedances to be of "simpler" forms (e.g. resistive, parallel or series combination of a resistor and a capacitor, etc.). In order to avoid the requirement of extra active devices it is necessary to restrict the NIC

impedances to have only positive component values; obviously this restriction will limit the possibility of achieving closer agreement between the desired expressions for the NIC impedances (see equation (5.9)) and the expressions obtained by choosing the NIC impedances to be of simpler form.

For practical purposes, we require the NIC impedances to have a small number of components; hence the simplest approach is to make the NIC impedances resistive. Observing the constraint that the NIC impedances should not be realised with extra NICs, we shall now show how to obtain the optimum value for the NIC impedances when they are chosen as resistors.

Suppose we arbitrarily choose the level of the NIC impedances and then compute the objective function, F, in equation (5.8) over some frequency band of interest (e.g. the passband of the filter) and determine the minimum and the maximum values (in dBs) of the objective function in this frequency range. Now, if we repeat the above exercise for other values of the NIC impedances then we can plot a graph of NIC resistor values against the difference in the minimum and the maximum values of the objective function; the optimum value for the NIC resistors can then be obtained from this graph.

In the case of NIC impedances being resistors we have only one degree of freedom, namely the value of the resistors. However if the NIC impedances comprise a parallel or a series combination of a resistor, R, and a capacitor, C, then we have two degrees of freedom for minimising the objective function. The values of R and C can be chosen optimally but the computational procedure will be more complex than in the previous case when the NIC impedances were purely

resistive. Since the NIC impedances are more complex in form then the need to find the optimum values of R and C may not be as critical as in the previous case; an explanation for this is as follows.

The impedances Z_A and Z_B in Fig 5.2 are composed of $\pm$R's and $\pm$C's. Equation (5.9) shows the form that the NIC impedances must take in order to totally eliminate the effect of the finite amplifier f_T. However, as stated previously, it is not practicable to choose the NIC impedances according to equation (5.9); instead we make an approximation and restrict the NIC impedances to be either purely resistive or a parallel or series combination of a resistor and a capacitor. A better approximation to equation (5.9) is achieved when the NIC impedances comprise a resistor and a capacitor than when they are chosen to be purely resistive and hence the error introduced into the transfer function by the finite f_T will be smaller in the former case than in the latter. If the values of the resistors and capacitors comprising the NIC impedances are chosen in a certain manner then the error resulting from the finite f_T may be such that it is not necessary to optimise the values of the NIC impedances. One way of choosing the values of R and C (which make-up the NIC impedance Z_1) would be to replace Z_1 in equation (5.9) by the parallel or the the series RC expression and then evaluate the modulus's of the left hand side and the right hand side expressions in equation (5.9), at two frequencies to obtain two simultaneous equations which can then be solved to give the values of R and C.

For the case when the NIC impedances comprise a parallel or a series combination of R and C, the following procedure can be used if it is desired to choose the values of R and C optimally. Suppose the value of C is chosen arbitrarily; then the value of R can be

determined by the method described above (for the case when NIC impedances are purely resistive) such that the objective function is minimised. Similarly, this procedure can be repeated for other values of C. The optimum values of R and C correspond to the condition which produces the smallest deviations in the objective function.

It should be noted that if the NIC impedance Z_1 is chosen as a parallel or a series combination of a resistor and a capacitor, then, since $Z_2 = Z_1/k$ (where k is the conversion factor of the NIC), it follows that the other NIC impedance must also be composed of a similar resistor-capacitor combination. One serious implication of this is that the spread between the capacitors used for the NIC impedances must be exactly equal to the conversion factor of the NIC —— this is very undesirable restriction if preferred value capacitors, with wide manufacturing tolerances, are to be used in the filter circuit.

5.2.3 Minimising the effect of finite f_T for grounded NICs

In this subsection we shall consider a method of minimising the effect of finite amplifier gain bandwidth product for the grounded NIC circuit of Fig 5.1(c), which is also shown in Fig 5.3(a). As stated previously, for this circuit the output node of the filter is contained within the subnetwork N_C. If the voltage at the output node is V_o then the transfer function, T, of the circuit is given by

$$T = \frac{V_o}{V_i} = \frac{V_o}{V_1} \frac{V_1}{V_i} \tag{5.10}$$

For the same reasons as stated previously for the coupling NIC in Section 5.2.2, it can be shown that the object of minimising the

effect of finite f_T on the overall transfer function can be achieved by minimising the effect of finite f_T on the partial transfer function term V_1/V_i in equation (5.10).

In Fig 5.3(a) if the transfer function of the circuit to the point marked "X", with the NIC and the subnetwork N_B disconnected, is $T_{A_{oc}}$ and if Z_A represents the impedance as seen from point "X", then using the Thevenin's theorem it can easily be shown that the circuit of Fig 5.3(a) can be equivalently represented by the circuit shown in Fig 5.3(b), where Z_B represents the impedance of subnetwork N_B seen by the NIC. Now the transfer function $T_{A_{oc}}$ is not affected by the non-ideal NIC and our objective function for minimisation becomes the transfer function of the circuit in Fig 5.3(b) (i.e. V_1/V_2). The circuit in Fig 5.3(c) is obtained by replacing the NIC in the circuit of Fig 5.3(b) by its OP-AMP realisation.

Assuming the open loop gain, A, of the OP-AMP to be given by equation (5.2) and designating the voltage transfer function of the circuit of Fig 5.3(c) as T_1 then it can be shown by straightforward analysis that

$$T_1 = \frac{V_1}{V_2} = \frac{1 - A^{-1}\,[1 + Z_1/(kZ_B)\,]}{1-Z_A/(kZ_B)-A^{-1}\,[1+Z_1/(kZ_B)+Z_A/Z_1+Z_A/(kZ_B)]} \qquad (5.11)$$

where k is the conversion ratio of the NIC and is given by $k = Z_1/Z_2$. If the transfer function of the circuit in Fig 5.3(c) is T_o when the OP-AMP is ideal then an expression for T_o can be obtained from equation (5.11) by letting $A \longrightarrow \infty$.

$$\text{i.e.} \quad T_o = \frac{1}{1 - Z_A/(kZ_B)} \tag{5.12}$$

Now, using equation (5.12), the expression for the transfer function T_1 in equation (5.11) can be rewritten as

$$T_1 = \frac{T_o \{1 - A^{-1} [1 + Z_1(T_o - 1)/(Z_A T_o]\}}{1 - A^{-1} [(2T_o - 1) + Z_1(T_o - 1)/Z_A + T_o Z_A/Z_1]} \tag{5.13}$$

Let us express equation (5.13) as follows

$$T_1 = \frac{T_o[1 - A^{-1}E_1]}{1 - A^{-1}E_2} \tag{5.14}$$

where $E_1 = 1 + Z_1(T_o - 1)/(Z_A T_o)$ (5.15)

$$E_2 = (2T_o - 1) + Z_1(T_o - 1)/Z_A + T_o Z_A/Z_1 \tag{5.16}$$

Suppose F is the objective function given by the ratio of the ideal transfer function T_o and the non-ideal transfer function T_1, then from equation (5.14) we obtain

$$F = \frac{T_o}{T_1} = \frac{1 - A^{-1}E_2}{1 - A^{-1}E_1} \tag{5.17}$$

We note that in equation (5.17) if $A \longrightarrow \infty$ (i.e. the OP-AMP is ideal), then $F \longrightarrow 1$; thus the essential condition for minimising the effect of the finite f_T is to make $|F| = 1$ over the frequency range of interest. From equation (5.17), we note that this condition can be satisfied over the entire frequency range if E_1 and E_2 can be

simultaneously made equal to zero. Therefore, equating equations (5.15) and (5.16) equal to zero and solving for Z_1 gives

$E_1 = 0$ if

$$Z_1 = - Z_A T_o/(T_o - 1) = - kZ_B \tag{5.18}$$

and $E_2 = 0$ if

$$Z_1 = - Z_A \quad \text{or} \quad Z_1 = - Z_A T_o/(T_o - 1) = -kZ_B \tag{5.19}$$

From equations (5.18) and (5.19) we note that E_1 and E_2 simultaneously become zero if Z_1 is chosen as in equation (5.18). Although this result is very desirable and would totally eliminate the effect of the finite f_T it should be remembered that it is not practicable if the NIC impedances comprise negative elements, since this would require the use of extra NICs. In this situation, a compromise solution may be found by evaluating the expression for Z_1, given in equation (5.18), over some frequency band (e.g. the passband of the filter) in which it is desired to minimise the effect of finite f_T, and then see if this expression can be approximated by choosing the NIC impedances to be of simpler form (e.g. resistive, parallel or series combination of a resistor and a capacitor, etc.). One obvious consequence of restricting the NIC impedances to have only positive component values is that it will limit the possibility of achieving a closer approximation between the desired expression of the NIC impedances (see equation (5.18)) and the expression obtained by choosing the NIC impedances to be of simpler form.

The procedure for minimising the objective function of the grounded NIC circuit of Fig 5.3(c) is exactly the same as for the coupling NIC circuit of Fig 5.2(c).

So far we have concentrated only on choosing the NIC impedances to minimise the effect of the finite amplifier gain bandwidth product. Let us now consider if the same desired effect can be achieved by some other means.

In the ideal transfer function of the circuit of Fig 5.3(c) (see equation (5.12)) if we replace the NIC conversion factor, k, by the ratio of the NIC impedances (i.e. Z_1 and Z_2), then we obtain

$$T_o = \frac{1}{1 - Z_A Z_2/(Z_B Z_1)} \qquad (5.20)$$

From equation (5.20) we note that if Z_B is replaced by Z_1 and Z_1 is replaced by Z_B, which is equivalent to interchanging the positions of the impedances Z_1 and Z_B in the circuit of Fig 5.3(c) as shown in Fig 5.3(d), then T_o is not affected by this modification. However, if the same modification is carried-out in equations (5.15) and (5.16), then E_1 and E_2 become independent of the NIC impedances and hence the effect of the finite f_T on the transfer function, T_1, in equation (5.14) will not be dependent on the level of the NIC impedances. In this case the value of the NIC impedances can be chosen arbitrarily and the effect of the finite f_T will only depend on Z_A, Z_B, k and the amplifier gain —— i.e. the parameters which are specified and hence cannot be chosen in order to minimise the effect of the finite f_T.

The impedance Z_B in the circuit of Fig 5.3(c) represents the input impedance of the subnetwork N_B. It can be shown that if the subnetwork N_B contains active devices (e.g. other NICs) then on interchanging the positions of the impedances Z_1 and Z_B the grounded terminal of the impedance Z_B should be connected to the output terminal of the OP-AMP in order to ensure that the OP-AMPs used in Z_B to realise the NICs still have one of their output terminal grounded.

The above method of interchanging impedances Z_1 and Z_B could also have been applied to the coupling NIC circuit of Fig 5.2(c) with similar results. However, in Fig 5.2, since the output node of the filter circuit is contained within the subnetwork N_B, then if impedances Z_1 and Z_B are interchanged, the required output will be the difference between the voltages at two nodes, neither of which is grounded. Hence, in order to obtain an output relative to ground, it would be necessary to use a differential amplifier, and this would increase the total number of OP-AMPs in the circuit. Therefore, this technique is not considered in the context of minimising the effect of finite f_T for the circuit of the coupling NIC.

It should be noted that the interchanging of the impedances Z_1 and Z_B can be interpreted as being equivalent to realising the negative impedance (i.e. $-Z_B$) by an amplifier of gain $(1 + k^{-1})$, as described in [78].

5.3 A computed example —— Minimising the effect of finite f_T's for a three NIC all-pole 5th order highpass filter

In this section, some of the ideas developed in the previous section for minimising the effect of finite f_T's for circuits using

NICs will be used to minimise the effect of finite f_T's of the three NIC all-pole 5th order highpass filter of Fig 4.21(c), which is also shown in Fig 5.4(a). Fig 5.4(b) shows the general realisation of the circuit in Fig 5.4(a) when the NIC impedances are chosen to be resistive (capacitors C_7 and C_8, shown in dashed line, in Fig 5.4(b) should be ignored at this stage). The nominal component values of the circuit in Fig 5.4(b) are given in Table 5.1 for the case when the filter is designed to have a cut-off frequency of 1 kHz and a passband ripple of 0.28 dB; note that the values of the NIC resistors (i.e. R_6, R_7, R_8, R_9, R_{10} and R_{11}), in the circuit of Fig 5.4(b), have been chosen arbitrarily.

The computed loss-frequency responses of the filter circuit in Fig 5.4(b) are shown in Fig 5.5 for the case of ideal OP-AMPs (i.e. $f_T = \infty$) and for the case when all OP-AMPs have a gain bandwidth product of 1 MHz. From the curves in Fig 5.5 we note that when the OP-AMPs are non-ideal the loss of the circuit starts to peak at high frequencies (this peaking is approximately 20 dB). We shall now show that a marked improvement in the non-ideal response of the filter circuit can be achieved by appropriately choosing the level and the type of the NIC impedances.

In the circuit of Fig 5.4 the NIC with a conversion factor k_1 is a coupling type NIC and hence in order to minimise the effect of finite f_T of the OP-AMP realising this NIC we need to minimise the effect of finite f_T on the transfer function of the circuit shown in Fig 5.6(a). The impedances comprising Z_A and Z_B, in Fig 5.6(a), are shown in Figs 5.6(b) and (c), respectively. Note that since we are considering the non-ideal effect due to NIC_1, in Fig 5.4(a), the other two NICs (i.e. NIC_2 and NIC_3) are at this stage considered to be

ideal. The objective function for the circuit of Fig 5.6(a) is the same as in equation (5.8) except that due to the connection of the OP-AMP input terminals the term "A^{-1}" is replaced by "$-A^{-1}$".

The graph in Fig 5.7 shows the plot of the modulus of the objective function against frequency, in the frequency range $0.5 \longrightarrow 50$ kHz, when the NIC impedances (i.e. Z_1 and Z_2) in Fig 5.6(a) are chosen as resistors of value 1 kOhms and the OP-AMP is assumed to have f_T value of 1 MHz. In the graph of Fig 5.7, we mark-off $|F_{max}|$ and $|F_{min}|$ and define $(|F_{max}| - |F_{min}|)$ as the "loss variation" caused by this particular value of the NIC impedances. Fig 5.8 shows the plot of the loss variation against values of the NIC resistors and we note that the minimum of the loss variation has a value of approximately 1.1 dB corresponding to a NIC resistor value of 541.25 Ohms; this gives the best result that can be achieved by choosing the NIC impedances as resistors.

Fig 5.9 shows the plot of $|F|$ against frequency for the case when the NIC impedances are chosen as a parallel combination of a resistor, R, and a capacitor, C, where R = 22.7201 kOhms and C = 2.89036 nF. In Fig 5.9 the loss variation in the frequency band from $0.5 \longrightarrow 50$ kHz has been reduced to approximately 0.34 dB.

Let us now consider minimising the effect of finite f_T for NIC_2 in the circuit of Fig 5.4(b). Since NIC_2 is a grounded NIC the equivalent circuit for minimising the effect of the finite f_T is as shown in Fig 5.10(a) and the equivalents of impedances Z_A and Z_B are shown in Figs 5.10(b) and(c), respectively. Note that in this case NIC_1 and NIC_3 are considered to be ideal. The objective function for the circuit of Fig 5.10(a) is given by equation (5.17). The graph in

Fig 5.11 shows the plot of the modulus of the objective function against frequency, over the frequency band 0.5 ⟶ 50 kHz, when the NIC impedances (i.e. Z_1 and Z_2 in Fig 5.10(a)) are chosen as resistors of value 1 kOhms and 3 kOhms and the OP-AMP is assumed to have an f_T value of 1 MHz. The "loss variation" caused by these particular values of the NIC impedances is approximately 2.5 dB. The plot of the loss variation against the value of the NIC impedance Z_1 is shown in Fig 5.12 and the minimum of the loss variation has a value of 0.777 dB corresponding to Z_1= 122.18 Ohms; thus this represents the best result that can be achieved by choosing the NIC impedances as resistors.

In the circuit of Fig 5.10(a) the NIC impedances can be chosen to be of more complex form (e.g. parallel combination of a resistor and a capacitor) in order to reduce further the loss variation. However, as explained in subsection 5.2.3, in the case of the grounded NIC circuit we have the option of interchanging the positions of the impedances Z_1 and Z_B. Fig 5.13 shows the loss variation plotted against the value of the NIC impedance Z_1 (when Z_1 is chosen to be resistive) for the case when the positions of impedances Z_1 and Z_B in Fig 5.10(a) have been interchanged. From Fig 5.13 we note that, as predicted in subsection 5.2.3, the value of the loss variation (= 0.272 dB) is independent of the value of Z_1.

In the circuit of Fig 5.4(a), the conversion factor of NIC_2 is 1/3; the conversion factor for this NIC can be made equal to unity by making the values of the resistor and the capacitor terminating NIC_2 equal to $R_3/3$ and $3C_4$, respectively. Fig 5.14 shows the loss variation plotted against the value of the NIC impedance Z_1 (when Z_1 is chosen to be resistive) for the case when the circuit of Fig 5.4

has been designed to make the conversion factor of NIC_2 equal to unity and when the positions of the impedances Z_1 and Z_B in the circuit of Fig 5.10(a) have been interchanged. We note from Figs 5.13 and 5.14 that although the amplitude of the objective function, for the case when the positions of the impedances Z_1 and Z_B in Fig 5.10(a) have been interchanged, is invariant with respect to the level of the NIC impedances it is certainly dependent on the value of the conversion factor of NIC_2.

In the circuit of Fig 5.4(b), NIC_3 is a coupling type of NIC and hence the procedure for minimising the effect of its finite f_T is exactly the same as described earlier for NIC_1. Fig 5.15 shows the "equivalent circuit" of NIC_3 for minimising the effect of finite f_T together with the equivalents of impedances Z_A and Z_B. The plot of the loss variation against the value of the NIC impedance Z_1 (when it is chosen as a resistor) is shown in Fig 5.16 from which we note that the minimum of the loss variation has a value of 0.053 dB corresponding to $Z_1 = 2.969$ kOhms. The value of the loss variation for the circuit of Fig 5.14(a) can be reduced further by choosing the NIC impedances to be of more complex form; however, this is not necessary because the non-ideal effects of NIC_1 and NIC_2 are comparatively larger than the non-ideal effect of NIC_3 and hence the error in the filter output of Fig 5.4(a) will be mainly due to NIC_1 and NIC_2.

The graph in Fig 5.17 shows the computed loss-frequency characteristics of the circuit in Fig 5.4(b) for the case when the NIC impedances are chosen in the following manner. The impedances of NIC_2 and NIC_3 are chosen optimally from the graphs of Figs 5.12 and 5.16, respectively; note that choosing the impedances of NIC_2 from Fig 5.12

implies that the positions of impedances Z_1 and Z_B in Fig5.10(a) (and their counterparts in Fig 5.4(b)) have been interchanged. The impedances of NIC_1 were chosen as a parallel combination of a resistor of value 22.7201 kOhms and a capacitor of value 2.89036 nF. The nominal component values of this "optimal" circuit are listed in Table 5.1. Comparison of the graph in Figs 5.17 with the graph in Fig 5.5 shows that the non-ideal performance of the NIC circuits can be significantly improved by appropriately selecting the level and/or the type of the NIC impedances.

In order to test the validity of the above method of reducing the effects of finite f_T's a discrete component model of the circuit in Fig 5.4(b) was built using polystyrene capacitors, carbon resistors and 741 type operational amplifiers, which have typical f_T value of 1 MHz. The measured component values of the discrete component model are given in Table 5.1. The measured passband and stopband responses of the filter are shown in Figs 5.18(a) and (b), respectively. These measured results are considered to be in good agreement with the corresponding computed response shown in Fig 5.17.

5.4 Stability consideration of NIC circuits

One of the main reasons for the mistrust of NIC circuits, felt by many circuit designers, is that in practice NIC circuits are often found to be unstable. A great deal has been published in the litrature [80,81,82] concerning the phenomena which give arise to this instability and some attempts have been made to develop a stability criterion for NIC circuits [83].

In this section we shall describe a simple method of determining the stability or the instability of NIC filter circuits derived in Chapter 4. It will also be shown that in cases where inherent instability is encountered the NIC circuit can be stabilised by adding some extra components to the circuit.

When discussing the stability of NIC circuits it is customary to talk in terms of the NIC ports being short-circuit stable (unstable) or open-circuit stable (unstable). The following discussion differs from others of its kind in an important respect that it does not employ these concepts; instead the stability of an NIC is interpretted in terms of the amounts of feedback being applied to the inverting and the non-inverting terminals of the OP-AMP used to realise the NIC.

Before we embark on a detailed discussion of stability, it is appropriate to state the definition of stability to be used here; which is as follows. A circuit is stable if for a bounded input the output of the circuit is also bounded; in particular, we shall assume that the input to the circuit is zero.

Consider the general 2-port network shown in Fig 5.19(a) which is realised using NICs. Now let us consider the stability properties of each NIC in turn; the remaining NICs of the circuit are considered to be ideal and stable for this purpose. If the NIC whose stability properties are being examined is "pulled-out" from the network of Fig 5.19(a) then the resulting network can be represented as shown in Fig 5.19(b). With $V_{in} = 0$, if Z_A and Z_B represent the impedances to ground from terminals 1 and 2, respectively, of network N′ in Fig 5.19(b) with the NIC disconnected then the network in Fig 5.19(b) can be equivalently represented as shown in Fig 5.19(c). The circuit

in Fig 5.19(d) is obtained by replacing the NIC in Fig 5.19(c) by its OP-AMP equivalent circuit in which Z_1 and Z_2 are the NIC impedances.

Suppose V_1, V_2 and V_o are the voltages at terminals 1, 2 and 3, respectively, in Fig 5.19(d). Now, if F_{b1} and F_{b2} represent the amount of feedback from terminal 3 to terminals 1 and 2, respectively, then it can easily be shown that

$$F_{b1} = \frac{V_1}{V_o} = [1 + Z_1/Z_A]^{-1} \tag{5.21}$$

$$F_{b2} = \frac{V_2}{V_o} = [1 + Z_2/Z_B]^{-1} \tag{5.22}$$

For the particular connection of the OP-AMP input terminals shown in Fig 5.19(d), we can classify F_{b1} and F_{b2} as the negative and the positive feedback factors, respectively.

Now, a very simple and sufficient condition for stability of the circuit in Fig 5.19(d) is that at any frequency the value of the positive feedback factor must always be less than the value of the negative feedback factor. Thus from above, for the circuit of Fig 5.19(d), we should have

$$F_{b1} > F_{b2} \qquad \text{for } 0 < w < \infty$$

$$\text{i.e. } [1 + Z_1/Z_A]^{-1} > [1 + Z_2/Z_B]^{-1} \tag{5.23}$$

Alternatively, it can be shown that equation (5.23) can be equivalently stated as

$$Z_A/Z_1 > Z_B/Z_2 \qquad (5.24)$$

for $0 < w < \infty$

It is relevant to point-out that Z_A and Z_B would in general be complex impedances whereas Z_1 and Z_2 may be complex or only real. Thus the stability condition expressed by equation (5.24) implies that the real and imaginary parts of Z_A/Z_1 must be greater than the real and imaginary parts of Z_B/Z_2 for $0 < w < \infty$.

Note that the stability condition for the case when terminals 1 and 2 in Fig 5.19(d) correspond to the non-inverting and the inverting terminals of the OP-AMP, respectively, is same as in equation (5.24) except that the inequality sign is reversed.

It is clear from above that the stability of a NIC circuit is influenced by the connection of the OP-AMP input terminals. Hence in order to design stable NIC circuits, we require a systematic procedure for determining the connection of the OP-AMP input terminals. One such systematic procedure would be to select the form that the NIC impedances are to have (e.g. resistive, parallel combination of a resistor and a capacitor, etc.), and then evaluate Z_A/Z_1 and Z_B/Z_2 for $0 < w < \infty$; the connection of the OP-AMP input terminals can then be selected depending on wether $Z_A/Z_1 > Z_B/Z_2$ or $Z_A/Z_1 < Z_B/Z_2$. However, if either of these conditions is not satisfied for the frequency range $0 < w < \infty$, then the above procedure must be repeated for a different impedance level and/or a different composition of the NIC impedances.

In general, impedances Z_A and Z_B will be formed from complicated RC networks and hence evaluation of Z_A/Z_1 and Z_B/Z_2 will have to be done computationally. Thus the above systematic procedure may not be feasible in practice because it would require large amount of computation. In order to considerably reduce the amount of computation required the following two step procedure may be more attractive from practical point of view.

In the first step we evaluate Z_A/Z_1 and Z_B/Z_2 at zero and infinite frequencies (note that this evaluation can be done by inspection, assuming the circuit capacitors to be open-circuit at zero frequency and short-circuit at infinite frequency); hence these simple and necessary conditions can be used to discard many unstable cases. The above two simple and necessary conditions are not sufficient to guarantee stability but the application of these conditions would considerably reduce the number of possible cases (which may be stable or unstable) such that these are sufficiently small in number to enable them to be tested in the second step via the systematic procedure proposed above.

It is relevant to point-out that the NIC filter circuits derived in Chapter 4 have been obtained from inherently stable passive ladder prototypes and hence are expected to be also "inherently stable". The question of instability is associated with the circuits used to realise the NICs. If the circuits used to realise the NICs can be guaranteed to be stable then the question of instability will not arise for the circuits of Chapter 4.

Practical experience suggests that the second step of the above two step method is seldom necessary and thus in virtually all the

cases the connection of the OP-AMP input terminals can be chosen without any great computational effort. We shall now illustrate the basic steps involved in choosing the connection of the OP-AMP input terminals by considering an example. Let us consider the 5th order all-pole highpass filter circuit of Fig 5.4(a) and let us suppose that we want to determine the connection of the OP-AMP input terminals for NIC_3. If NIC_3 in Fig 5.4(a) is replaced by an OP-AMP realisation the resulting circuit can be drawn in the form shown in Fig 5.19(d), where the equivalents of the impedances Z_A and Z_B are given in Figs 5.15(b) and (c), respectively. Making use of Table 5.1, we note that at zero and infinite frequency the values of impedance Z_B are infinite and 10.9308 kOhms, respectively, whereas the corresponding values of impedance Z_A are 6.0885 kOhms and zero, respectively. Therefore, if Z_1 and Z_2 are chosen as resistors then at zero and infinite frequency $Z_B/Z_2 > Z_A/Z_1$, and thus Z_B must be connected to the inverting terminal and Z_A must be connected to the non-inverting terminal of the OP-AMP. It can be shown by a similar reasoning as above that the connection of the OP-AMP input terminals for NIC_1 and NIC_2, for the case when the NIC impedances are chosen as resistors, are as shown in Figs 5.6(a) and 5.10(a), respectively. Furthermore, it can also be shown that the connection of the OP-AMP input terminals for NIC_1 is same as shown in Fig 5.6(a) even when the NIC impedances comprise a parallel combination of a resistor and a capacitor.

We have shown above how to connect the input terminals of the OP-AMPs realising NICs using very simplified conditions which are necessary but not sufficient to guarantee stability. However, it must be stressed that it has been found in some practical circuits that for the case when the impedances Z_A and Z_B tend to the same limit

(e.g. zero) at infinite frequency then even though the OP-AMP input terminal connection has been chosen to satisfy the condition at zero frequency, the circuit is found to be oscillatory. An obvious explanation of this phenomenon is that the stability condition is being violated at some finite frequency. In this situation the interchange of the OP-AMP input terminals would not lead to a stable circuit because the stability condition at zero frequency would be violated; hence the circuit is "inherently" unstable. Note that this implies that when impedances Z_A and Z_B are tending to the same limit we cannot make use of this information for predicting the stability of the circuit.

It has been found that an inherently unstable circuit can be stabilised by adding two resistors and one capacitor to the existing circuit in the following manner. Suppose we connect a resistor of value R in series with the impedance Z_A and connect a resistor of value R/k (where k is the conversion factor of the NIC) in series with the impedance Z_B. For the case of an ideal NIC this circuit modification does not have any effect on the filter transfer function as the extra added resistors cancel the effect of each other. Suppose we now connect a capacitor of value C in parallel with the NIC impedance connected to the inverting terminal of the OP-AMP. The value of C is chosen such that the frequency at which the impedance of this capacitor becomes significant is very much greater than the highest frequency of interest. This circuit modification has the effect of making Z_A/Z_1 and Z_B/Z_2 tend to different limits at infinite frequency.

The value of R can be calculated by computing the stability expression for the modified circuit or alternatively by studying the

practical circuit model for various values of R. The nominal value of C is not very critical and hence $\pm$ 10 % tolerance can be easily accomodated by taking account of this when choosing the value of the NIC impedances.

Let us now consider another case of instability which may arise in practice. The method of over-coming this type of instability will be illustrated by means of an example. Suppose our objective is to determine the connection of the OP-AMP input terminals for NIC_3 in the highpass filter circuit of Fig 4.31 (for this purpose we assume that the value of capacitor C_p is zero) which has been designed for the specification given in Section 4.7. If we assume that NIC_1, NIC_2 and NIC_4 in Fig 4.31 are ideal then the equivalent circuit for considering the stability of NIC_3 becomes as shown in Fig 5.20(a) with equivalents of impedances Z_A and Z_B as shown in Figs 5.20(b) and (c), respectively. Using the component values given in Table 4.2 and evaluating Z_A and Z_B at zero frequency gives Z_A= 6.971 kOhms and Z_B= ∞. Thus if the NIC impedances (i.e. Z_1 and Z_2) in Fig 5.20(a) are chosen as resistors then in order to satisfy the stability criterion the non-inverting terminal of the OP-AMP must be connected to impedance Z_A and the inverting terminal to impedance Z_B. However, at infinite frequency, Z_A= 0 and Z_B= -106.84 kOhms and in order to satisfy the stability criterion the connection of the OP-AMP input terminals must be reversed to the one stated above. This means that we cannot choose the connection of the OP-AMP input terminals such that the necessary stability conditions are satisfied simultaneously at zero and infinite frequency. Therefore the circuit of Fig 5.20(a) is "potentially" unstable; indeed, as stated in Section 4.7 the practical model of this circuit exhibited this instability behaviour.

The method of stabilising the circuit is to choose the OP-AMP input terminal connection such that the stability condition at zero frequency is satisfied (this amounts to making terminal 1 as the non-inverting terminal of the OP-AMP) and then connecting a capacitor in parallel with the resistive impedance Z_2. The effect of connecting a capacitor in parallel with Z_2 is that at infinite frequency the amount of feedback being applied to the non-inverting terminal approaches the value of zero, thus satisfying the stability condition simultaneously at zero and infinite frequency. The value of the "stabilising" capacitor should be kept as small as possible and should ideally be determined by ensuring that the stability criterion is valid over the entire frequency range.

We have described above various methods for stabilising potentially unstable NIC circuits. These methods may seem rather cumbersome but it must be stressed again that the majority of the circuits derived in Chapter 4 are perfectly stable and hence do not require these measures.

5.5 Conclusions

In this chapter a study of the effect of finite amplifier gain bandwidth product in negative impedance converter circuits was discussed and a method of reducing the effect of finite f_T was also presented. Furthermore, the stability properties of NIC circuits were examined in some detail and some methods of stabilising potentially unstable circuits were also discussed.

In Section 5.2 it was shown that the effect of finite f_T in NIC circuits can be reduced by appropriately choosing the composition and

the values of the NIC impedances. The basic principle of the method for reducing the effect of finite f_T is to consider the effect of each NIC in turn (the remaining NICs in the circuit being considered ideal) and to minimise the effect of the finite f_T of this NIC on the overall transfer function of the circuit. There are basically three positions in which an NIC can occur; viz, a coupling NIC, a grounded NIC and a bridged NIC. In Sections 5.2.2 and 5.2.3, respectively, the coupling and the grounded NICs were studied in detail and the corresponding objective functions for minimising the effect of finite f_T were also derived.

The expressions derived in Section 5.2 were used in Section 5.3 to minimise the effect of finite f_T's for the 5th order all-pole highpass filter circuit of Fig 4.21(c). Comparison of the initial loss-frequency response with the loss-frequency response of the filter in which the composition and the values of the NIC impedances are chosen optimally showed a marked improvement, thus providing a justification for the approach.

In Section 5.4 the stability properties of NIC circuits were discussed. The concept of viewing the stability of NIC circuits in terms of the amount of feedback being applied to the inverting and the non-inverting terminals of the OP-AMP realising the NIC was introduced. Some simple necessary (but not sufficient) conditions were stated which significantly simplify the predicting of the stability or the instability of an NIC circuit. Furthermore, some methods of stabilising, by the use of extra components, the inherently unstable NIC circuits were also described and illustrated by means of a practical example.

C H A P T E R 6

CONCLUSIONS

AND

DISCUSSION OF POSSIBLE FURTHER WORK

The objective of this work was to study methods of designing active RC filter circuits, which are suitable for microelectronic realisation, by simulation of low sensitivity LC filters. This objective has been fulfilled in the sense that two methods of designing active RC filters, i.e. the signal flow graph simulation method and the method of simulating the elements and the structure of LC filters, has been studied in detail and some new results have been obtained.

In the signal flow graph simulation approach, active RC circuits are used to "simulate" the mathematical relationships between the nodal voltages, the impedances of the branches and the currents in the branches of the prototype LC filter. In contrast, in the simulation of the elements and the structure of LC filters, active RC circuits are used to replace certain branches (e.g. the inductive branches) of the LC prototype (or an impedance scaled version of it).

In the signal flow graph approach to the simulation of LC filters, the signal flow graph can be manipulated such that the required transfer function is realised by second order sections which are coupled together with feedback loops. The use of the second order sections offers two main advantages. Firstly, the number of amplifiers required to realise a given filter is reduced considerably if the second order sections are realised with single amplifier biquadratic (SAB) circuits; this in turn eases the problems of DC power consumption and heat dissipation. Secondly, a considerable amount of work has been done in the past on the design and adjustment of second order circuits in general and SAB circuits in particular, which can be directly utilised in the practical implementation of active RC circuits designed by this approach. The above mentioned

possibility of using less amplifiers (usually N/2 OP-AMPs are required for an Nth order filter) is considered to be the single most important reason for designing low sensitivity active RC filters by the signal flow graph approach in preference to other simulation methods (e.g. the method of simulation of the elements and the structure of LC filters). Thus the work, described in this thesis, relating to this approach of designing active RC filters was restricted to using single amplifier biquadratic circuits. We shall now give a brief summary of the work presented in this thesis on the signal flow graph approach of designing active RC filters.

In Chapter 2 it was shown that if a SAB circuit (which has been designed assuming the OP-AMP to be ideal) is analysed by considering a typical non-ideal model for the OP-AMP then its characteristics deviate considerably from the nominal characteristics for which it was designed; for a given OP-AMP type, these deviations are increased as the operating frequency increases. This result suggested that in order to design SAB circuits for the realisation of high precision active RC filters the effects of the non-ideal OP-AMP must be taken into account at the design stage. Of the various non-ideal effects associated with OP-AMPs the one that is predominantly significant is the finite gain bandwidth product (f_T) of the OP-AMP.

The effect of finite f_T can be taken into account by predistorting the design of the SAB circuits. Two such predistortion methods were discussed in the context of SAB bandpass circuits. The approximate nature of the predistortion technique was high-lighted by considering the realisation of a sixth order leap-frog type feedback bandpass filter (with three predistorted SAB bandpass circuits) whose

characteristics showed significant errors in the passband of the filter even after predistortion.

As an alternative to the predistortion technique a method of fully compensating SAB circuits for effect of finite f_T was presented. This compensation method requires one additional resistor to be added to the existing SAB topology and it provides exact compensation for the finite f_T over the frequency range in which the gain of the OP-AMP can be modelled by a single pole roll-off. This compensation scheme was utilised for designing two Friend type SAB bandpass circuits and one Sallen and Key type SAB bandpass circuit which were subsequently used to realise the above mentioned sixth order bandpass filter. The computed response of the compensated filter circuit was in exact agreement with the nominal response.

Application of the above predistortion or the compensation methods to the design of SAB circuits results in non-linear design equations. For the Friend and the Sallen and Key type SAB bandpass circuits all the relevant design equations were derived in Chapter 2 and a method of numerically solving these non-linear equations was also presented.

In Chapter 3 the problem of minimising the sensitivity of multiple feedback filters to post-adjustment variations in the passive and the active elements was discussed in the context of the sixth order multiple feedback bandpass filter considered in Chapter 2. The basic principle of the sensitivity minimisation is that each SAB section in the multiple feedback configuration is designed such that the worst-case variations in the components of the SAB section has minimum effect on the overall filter response. In order to achieve

this an objective function which characterises some desirable features of the overall filter response was developed. A computer sensitivity analysis showed a very much smaller variation in the response of the optimised circuit compared with that of the previous un-optimised circuit, with respect to changes in the gain bandwidth product of the OP-AMPs. Some practical results for a discrete component model of one version of the optimised filter were also presented.

The realisation of active RC filters by simulation of the elements and structure of LC filters is dealt with in the latter part of this thesis (i.e. in Chapters 4 and 5). In the conventional approach to the realisation of active RC filters by this method, gyrators or positive impedance converters (PICs) are normally used as the basic active units. The work reported in this thesis on the realisation of active RC filters by simulation of the elements and the structure of LC filters differs from methods reported in the litrature in an important respect that it utilises negative impedance converters (NICs) as the basic active units. Active RC circuits which make use of NICs are regarded, by most workers in the field, with great suspicion and are often indiscriminantly labelled as "high sensitivity" circuits. One result which has emerged directly from the investigation reported in Chapter 4 has been to show that active RC networks which use NICs do not necessarily have high sensitivity. We shall now give a brief summary of the work presented in this thesis on the simulation of the elements and the structure of LC filters.

In Section 4.3 a simple procedure was used to generate 2-port $\pm R$, $\pm C$ subcircuits which simulate grounded and floating inductors and grounded and floating frequency dependent negative resistors of the

supercapacitor type. It was shown that these basic $\pm R$, $\pm C$ subcircuits can be looked upon in different ways to yield a multitude of $\pm R$, $\pm C$ subcircuits which simulate grounded and floating inductors and supercapacitors.

The most novel feature of the approach presented in Chapter 4 is the way in which the $\pm R$, $\pm C$ subcircuits are utilised in filter design such that the number of components required in the active RC realisation is comparable with other simulation methods (e.g. the method of partial and full impedance scaling).

An interesting feature of the $\pm R$, $\pm C$ subcircuits derived in Sections 4.3 and 4.4 is that while they are electrically port-symmetrical, their physical structures are port-unsymmetrical. Thus depending on the orientation of the ports of the simulated element there are two possible active RC realisations for a simulated element. This gives rise to 2^N different realisations of a prototype filter in which N elements are being simulated. However, some of these realisations may require a larger number of active and/or passive components than other methods and thus may not be practically attractive. On the other hand some of these realisations offer economy in the total number of components required, compared with other methods, and hence are very desirable.

The design examples of both all-pole and elliptic filters with lowpass, highpass and bandpass characteristics were given in Section 4.6 to illustrate the generality of this new design method. The circuits designed by this method can in most cases have equal and nominally preferred value capacitors and it is also feasible to use capacitors with wide manufacturing tolerances if the resistors in the

circuit are trimmable. These properties make the circuits attractive for hybrid thin-film or thick-film realisation.

For the design of all-pole filters the number of OP-AMPs required is less than or equal to the number that would be required if the same filter is realised by the complex impedance scaling methods. In the case of elliptic structures the number of OP-AMPs required may be larger, especially if capacitors with preferred values and wide manufacturing tolerances are to be used.

In order to show that active RC circuits designed by the new method are practically feasible some computed and measured results (of discrete component models) were presented in Section 4.7 for lowpass, highpass and bandpass filter characteristics.

The sensitivity aspects of the active RC circuits, obtained by the method of Chapter 4, were considered in Section 4.8 where it was shown that there exists a one-to-one relationship between the elements of prototype filter and some elements of the active RC circuit simulating the prototype. The sensitivities of the remaining elements in the active RC realisation, which do not have a one-to-one counterpart in the LC prototype, were interpretted by deriving "equivalent" prototype circuits. It was shown that changes in these elements usually has two effects on the equivalent prototype circuit; firstly, some elements in the equivalent prototype are changed in value; and secondly, the Q-factors of some reactive elements in the equivalent prototype circuit become finite. Due to the low sensitivity nature of the prototype LC filter these two effects do not deteriorate the sensitivity of the active RC circuits; this point was

illustrated by presenting computed sensitivity results for two realisations of an active RC lowpass filter.

In the first part of Chapter 5 a method of minimising the effect of amplifier finite gain bandwidth product in NIC circuits of the type derived in Chapter 4 was presented. It was shown that the effect of finite f_T on the transfer function of the filter can be considerably reduced by appropriately choosing the composition and/or the impedance level of the NIC impedances. This method was applied to a three NIC all-pole fifth order highpass filter to reduce the effect of finite f_T's. In Section 5.4 a discussion on predicting the stability or the instability of the active RC circuits derived in Chapter 4 was presented. The concept of viewing the stability of the NIC circuit in terms of the amount of feedback being applied to the inverting and the non-inverting terminals of the OP-AMP, realising the NIC, was adopted. Some simple necessary (but not sufficient) conditions were stated which significantly simplify the prediction of the stability or the instability of an NIC circuit. Also, some methods of stabilising, by the use of extra components, some inherently unstable NIC circuit were described.

——— o ——— o ———

In the discussion of possible further work, that arises out of the present work, it is felt that a detailed study of the following topics would of considerable interest.

In Chapter 2 a method of fully compensating lowpass and bandpass SAB circuits for the effect of finite f_T of the OP-AMP was presented. Consequently a criterion was developed in Chapter 3 for optimally designing the fully compensated Friend and the Sallen and Key type SAB bandpass circuits when these sections are used to realise a sixth order leap-frog feedback bandpass filter. It was found that for an optimum design the value of the closed loop gain for each SAB circuit can lie within a certain optimum band. It would be interesting to know how this optimum band is affected by the Q-factor and the resonance frequency of the SAB circuits.

In Chapter 3 it was shown that as far as variations in the f_T's are concerned the sensitivity of the optimised design is better than the sensitivity of the un-optimised design. However the optimum design was arrived at by considering changes in both the passive and the active elements of the circuit; hence in order to evaluate the improvement in performance a Monte-Carlo analysis including passive and active component parameter changes could be applied to the optimised and the un-optimised circuits.

In Chapter 4 a multitude of $\pm R$, $\pm C$ subcircuits for simulating floating and grounded inductors and supercapacitors were derived but it was found that only few of these $\pm R$, $\pm C$ subcircuits offer practical advantages. A major study is warranted to see if a circuit in which some elements are simulated by the $\pm R$, $\pm C$ subcircuits of

Chapter 4 can be advantageously combined with other element simulation methods to yield practically desirable active RC circuits.

The simulation method of Chapter 4 uses current inverting type NICs which suffer from potential instability; hence a development of novel, inherently stable, NICs would be very useful. This would almost certainly call for a departure from the conventional type of current inverting type NIC.

The versatility of the method of Chapter 4 was illustrated by designing filters with lowpass highpass and bandpass characteristics; however the range of operation was confined to low frequencies. In order for the method to be practically viable it must be possible to design filters at high frequencies. Inevitably as the frequency of operation is increased the non-ideal effects (i.e. the finite f_T's) of the OP-AMPs would dominate and the procedure described in Chapter 5 for minimising the effect of finite f_T's would become inadequate. Hence another fruitful area for further work would be to study, both theoretically and practically, methods of fully compensating the NICs for the effect of OP-AMP imperfections.

The dynamic range is a very important parameter of active RC filters and it has not been dealt with in this Thesis. Therefore another area for further work would be to determine the dynamic range of the active RC circuits proposed in this Thesis, and if necessary develop methods of improving it.

A P P E N D I X A

DERIVATION OF THE DESIGN EQUATIONS FOR CALCULATING THE RESISTOR VALUES OF THE THREE NIC LOWPASS FILTER CIRCUIT

In this Appendix we shall derive the design equations for calculating the values of the resistors of the lowpass filter which is realised using three NICs (see Fig 4.14) when the values of all the capacitors are known. In order to achieve our objective we proceed as follows.

Let us assume that the filter circuit under consideration is realisable as shown in Fig A.1(a) where the values of the capacitors C_1, C_2, C_3, C_4 and C_5 are known. The circuit of Fig A.1(b) is obtained by eliminating the NICs in the circuit of Fig A.1(a). In the circuit of Fig A.1(b) if the two encircled T-networks are transformed into their equivalent Π-networks under the assumptions:

$$R_2 = K_1 R_3 \tag{A.1}$$

$$\text{and} \quad R_5 = K_3 R_6 \tag{A.2}$$

then the circuit in Fig A.1(c) is obtained. Let us now assume that the "equivalent" prototype LC filter from which the active RC circuit of Fig A.1(a) was obtained is as shown in Fig A.1(d). The

characteristics of the"equivalent" prototype of Fig A.1(d) and the "original" prototype filter of Fig 4.13(a) must be identical, except that the impedance levels of the two circuits may not be equal. We can derive relationships between the impedances of the circuits of Figs A.1(d) and 4.13(a) by equating the quotient of any two impedances of the circuit in Fig A.1(d) with the quotient of the corresponding impedances of the circuit in Fig 4.13(a). The following six equations are obtained by following the above procedure; the subscript "p" denotes the elements of the original prototype filter, the values of which are known.

$$R_{s_1} C_1 = R_{s_p} C_{1_p} \tag{A.3}$$

$$K_1 C_2 R_3^2/R_{s_1} = L_{2_p}/R_{s_p} \tag{A.4}$$

$$R_{s_1} C_3/(K_1 K_2) = R_{s_p} C_{3_p} \tag{A.5}$$

$$K_1 C_4 R_5^2/R_{s_1} = L_{4_p}/R_{s_p} \tag{A.6}$$

$$R_{s_2} C_5 = R_{L_p} C_{5_p} \tag{A.7}$$

$$K_1 K_3 R_{s_2}/R_{s_1} = R_{L_p}/R_{s_p} \tag{A.8}$$

In order to obtain the active RC circuit of Fig A.1(a) from the equivalent prototype of Fig A.1(d), we would have to split-up the source and the load resistors in Fig A.1(d) and introduce three shunt resistors in parallel with the capacitor C_3/K_1K_2, as shown in Fig A.1(c). This gives rise to the following three equations

$$R_{s_1} = R_1R_2/(R_1+R_2) \tag{A.9}$$

$$R_{s_2} = R_6R_7/(R_6+R_7) \tag{A.10}$$

$$K_2R_4 = R_3R_5/(R_3+R_5) \tag{A.11}$$

Now, we have twelve unknowns (R_1, R_2, R_3, R_4, R_5, R_6, R_7, R_{s_1}, R_{s_2}, K_1, K_2 and K_3) in Fig A.1 but we have only eleven equations; hence we require another equation in order to be able to calculate the values of all the components in Fig A.1. The additional equation is obtained in the following manner.

In splitting-up R_{s_1} in Fig A.1(d) into a resistive potential divider, formed by R_1 and R_2 in Fig A.1(c), the output of the filter is multiplied by a loss factor, L_f (= $R_2/(R_1+R_2)$); therefore we can rewrite equation (A.9) as

$$R_1 = R_{s_1}/L_f \tag{A.12}$$

and $$R_2 = R_{s_1}/(1 - L_f) \tag{A.13}$$

also equation (A.10) can be rewritten as

$$R_7 = R_6R_{s_2}/(R_6 - R_{s_2}) \tag{A.14}$$

From equation (A.12), (A.13) and (A.14) we note that in order to ensure that values of resistors R_1, R_2 and R_7 are positive and finite, we must have $0 < L_f < 1$ and $R_6 > R_{s_2}$.

It can be shown, using equations (A.8), (A.2), (A.13), (A.1), (A.4) and (A.6), respectively, that the condition $R_6 > R_{s_2}$ is satisfied if

$$L_f > \{1 - (R_{s_p}/R_{L_p}) \ [L_{4_p} C_2/L_{2_p} C_4]^{1/2}\}$$

Therefore the range in which L_f can lie is

$$\{1 - (R_{s_p}/R_{L_p}) \ [L_{4_p} C_2/L_{2_p} C_4]^{1/2}\} < L_f < 1 \qquad (A.15)$$

In equation (A.15) R_{s_p}, R_{L_p}, L_{2_p} and L_{4_p} are the components of the original prototype filter and hence are specified by the characteristic for which the filter is designed. Hence the implication of equation (A.15) is that if the active filter circuit of Fig A.1(a) is to be designed for some specific value of the loss factor, L_f, then there is a maximum allowable spread between the capacitors C_2 and C_4. Thus by choosing an appropriate value of the loss factor, L_f, in equation (A.15), we can deterministically calculate the values of the unknowns in Fig A.1(a) using equations (A.1) ⟶ (A.14).

REFERENCES

[1] P.L. HAWKES, "Tantalum film circuits", Electronic Engineering, Vol. 38, pages 388-389, June 1966.

[2] P. KIRBY, "Thick film advances simplify complete hybrid module design", Electronic Engineering, Vol. 48, pages 35-38, March 1976.

[3] S.K. MITRA, "Analysis and Synthesis of Linear Active Networks", John Wiley, 1969.

[4] W. HEINLEIN and H. HOLMES, "Active Filters for Integrated Circuits —— Fundamentals and Design Methods", Prentice-Hall, 1974.

[5] W. SARAGA, "Active filters for communication", European Conference on Circuit Theory and Design, pages 218 - 227, 1978.

[6] W. SARAGA, D. HAIGH and R.G. BARKER, "A design philosophy for microelectronic active-RC filters", IEEE Proceedings, Vol. 67,pages 24 - 33, January 1979.

[7] W. SARAGA, D.G. HAIGH and R.G. BARKER, "Microelectronic active-RC channel bandpass filters in the frequency range 60 - 108 kHz for FDM SSB telephone systems", IEEE Trans. on Circuits and Systems, Vol. CAS - 25, pages 1022 - 1031, Dec. 1978.

[8] J.G. LINVILL, "RC active filters", IRE Proceedings, Vol. 42, pages 555 - 564, March 1954.

[9] T. YANAGISAWA, "RC active networks using current inversion type negative-impedance converters", IRE Trans. on Circuit Theory, Vol. CT - 4, pages 140 - 144, September 1957.

[10] W. SARAGA, "A contribution to active RC network synthesis", presented at the Symposium on Network Theory held at Cranfield Institute of Technology, Cranfield, England, September 21st, 1961 —— Reprinted by Pergamon Press 1963.

[11] R. JEFFERS and D.G. HAIGH, "Active RC lowpass filters for f.d.m. and p.c.m. systems", IEE Proceedings, Vol. 120, pages 945 - 953, September 1973.

[12] K.R. LAKER, R. SCHAUMANN and M.S.GHAUSI, "Multiple - loop feedback topologies for the design of low-sensitivity active filters", IEEE Trans. on Circuits and Systems, Vol. CAS - 26, pages 1 - 21, January 1979.

[13] D.J. PERRY, "New multiple feedback active RC network", Electronics Letters, Vol. 11, pages 364 - 365, August 1975.

[14] G. SZENTIRMAI, "Synthesis of multiple feedback active filters", Bell System Technical Journal, Vol. 52, pages 527 - 555, April 1973.

[15] J. GORSKI-POPIEL, "RC-active synthesis using positive immittance converters", Electronics Letters, Vol. 3, pages 381 - 382, August 1967.

[16] L.T. BRUTON, "Network transfer functions using the concept of frequency dependent negative resistance", IEEE Trans. on Circuit Theory, Vol. CT - 16, pages 406 - 408, August 1969.

[17] H.G. DIMOPOULOS and A.G. CONSTANTINIDES, "Linear transformation active filters", IEEE Trans. on Circuits and Systems, Vol. CAS - 25, pages 845 - 852, October 1978.

[18] F.E.J. GIRLING and E.F. GOOD, "The leapfrog feedback filter", Radar Research Establishment, RRE Memorandum No. 1176, Malvern, England, September 1955.

[19] F.E.J. GIRLING and E.F. GOOD, "Active filters —— The leapfrog or active ladder synthesis", Part 12, Wireless World, pages 341 - 345, July 1970.

[20] K.R. LAKER and M.S. GHAUSI, "A comparison of active multiple-loop feedback techniques for realising high order bandpass filters", IEEE Trans. on Circuits and Systems, Vol. CAS - 21, pages 774 - 783, November 1974.

[21] R.W. TURPIN and W. SARAGA, "Sensitivity comparison of three types of active RC circuits", Proceedings of IEEE International Symposium on Circuits and Systems, pages 114 - 117, Munich, 1976.

[22] H.J. ORCHARD, "Inductorless filters", Electronics Letters, Vol. 2, pages 224 - 225, June 1966.

[23] H.J. ORCHARD, "Loss sensitivities in singly and doubly terminated filters", IEEE Trans. on Circuits and Systems, Vol. CAS - 26, pages 293 - 297, May 1979.

[24] S.H. WUPPER and K. MEERKOTTER, "New active filter synthesis based on scattering parameters", IEEE Trans. on Circuits and Systems, Vol. CAS - 22, pages 594 - 602, 1975.

[25] G.C. TEMES and S.K. MITRA, "Modern Filter Theory and Design", John Wiley, 1973.

[26] L. WEINBERG, "Network Analysis and Synthesis", McGraw-Hill, 1962.

[27] A.I. ZVEREV, "Handbook of Filter Synthesis", John Wiley, 1967.

[28] W. SARAGA, "Minimum inductor or capacitor filters", Wireless Engineer, pages 163 - 175, July 1953.

[29] D.G. HAIGH, "On the simulation of LC filters by active RC networks", Ph.D. Thesis, Faculty of Engineering, University of London, England, 1976.

[30] J.K. SKWIRZYNSKI, "Design Theory and Data for Electrical Filters", Van Nostrand, 1965.

[31] R. SAAL, "Handbook of Filter Design", AEG Telefunken, 1979.

[32] G.SZENTIRMAI, "FILSYN : A general purpose filter synthesis program", IEEE Proceedings, Vol. 65, pages 1443 - 1458, October 1977.

[33] A.G.J. HOLT and M.R. LEE, "Sensitivity comparison of active cascade and inductance simulation schemes" IEE Proceeding, Vol. 119, pages 277 - 289, March 1972.

[34] D.G. HAIGH and R. JEFFERS, "The design of an audio frequency active RC bandpass filter for a specific engineering requirement", The Radio and Electronic Engineer, Vol. 42, pages 373 - 380, August 1972.

[35] W. SARAGA, "A contribution to the design of low sensitivity active networks", Proceedings of IEEE International Symposium on Circuits and Systems, pages 191 - 195, San Francisco, 1974.

[36] P.O. BRACKETT and A.S. SEDRA, "Direct SFG simulation of LC ladder networks with application to active filter design", IEEE Trans. on Circuits and Systems, Vol. CAS - 23, pages 61 - 67, February 1976.

[37] P.O. BRACKETT and A.S. SEDRA, "Filter Theory and Design : Active and Passive", Pitman, 1978.

[38] "Active Inductorless Filters", Edited by S.K. MITRA, IEEE Press, 1971.

[39] D.J. PERRY, "Reply to comment on new multiple feedback active RC network", Electronics Letters, Vol. 12, page 41, January 1976.

[40] R.L. ADAMS, "On reduced sensitivity active filters", Proceedings of 14th Midwest Symposium on Circuit Theory, pages 14.3-1/14.3-8, May 1971.

[41] K.R. LAKER, M.S. GHAUSI and J.J. KELLY, "Minimum sensitivity active (leapfrog) and passive ladder bandpass filters", IEEE Trans. on Circuits and Systems, Vol. CAS - 22, pages 670 - 677, August 1975.

[42] G. HURTIG, "III : The primary resonator block technique of filter synthesis", International Filter Symposium, page 82, April 1972.

[43] J. TOW, "Design and evaluation of shifted companion form (follow the leader feedback) active filters", Proceedings of IEEE International Symposium on Circuits and Systems, pages 656 - 660, San Francisco, 1974.

[44] K.R. LAKER and M.S. GHAUSI, "Minimum sensitivity multiple loop feedback bandpass active filters", Proceedings of IEEE International Symposium on Circuits and Systems, pages 458 - 461, April 1977.

[45] R.P. SALLEN and E.L. KEY, "A practical method of designing RC active filters", IRE Trans. on Circuit Theory, Vol. CT - 2, pages 74 - 85, March 1955.

[46] J.T. LIM "Improvement in or relating to active filter networks", British Patent Application No. 9657, 16 April 1971.

[47] J.J. FRIEND, "A single OP-AMP biquadratic filter section", IEEE International Symposium on Circuit Theory, Digest of Technical Papers, pages 179 - 180, 1970.

[48] T. DELYANNIS, "High Q-factor circuit with reduced sensitivity", Electronics Letters, Vol. 4, page 577, December 1968.

[49] J.J. FRIEND, C.A. HARRIS and D. HILBERMAN, "STAR: An active biquadratic filter section", IEEE Trans. on Circuits and Systems, Vol. CAS - 22, pages 115 - 121, February 1975.

[50] W.H. HOLMES, W.E. HEINLEIN and S. GRUTZMANN, "Sharp-cutoff low-pass filters using floating gyrators", IEEE Journal of Solid State Circuits, Vol. SC - 4, pages 38 - 50, February 1969.

[51] A.G.J. HOLT and J. TAYLOR, "Method of replacing ungrounded inductances by grounded gyrators" Electronics Letters, Vol. 1, page 105, Februeary 1965.

[52] A. ANTONIOU, "Realisation of gyrators using operational amplifiers, and their use in RC active network synthesis", IEE Proceedings, Vol. 116, pages 1838 - 1850, November 1969.

[53] R.H.S. RIORDAN, "Simulated inductors using differential amplifiers", Electronics Letters, Vol. 3, pages 50 - 51, February 1967.

[54] L.T. BRUTON, "Non-ideal performance of two-amplifier positive impedance converters", IEEE Trans. on Circuit Theory, Vol. CT - 17, pages 541 - 549, November 1970.

[55] L.T. BRUTON and A.B. HAASE, "High-frequency limitations of RC active filters containing simulated - L and FDNR elements", Circuit Theory and Applications, Vol. 2, pages 187 - 194, 1974.

[56] L.T. BRUTON and J.T. LIM, "High-frequency comparison of GIC - simulated inductance circuits", Circuit Theory and Applications, Vol. 2, pages 401 - 404, 1974.

[57] K. MARTIN and A.S. SEDRA, "Optimum design of active filters using the generalized immittance converter", IEEE Trans. on Circuits and Systems, Vol. CAS - 24, pages 495 - 503, September 1977.

[58] H.J. ORCHARD and A.N. WILSON, "New active gyrator circuit", Electronics Letters, Vol. 11, pages 261 - 262, 1974.

[59] C.E. SCHMIDT and M.S. LEE, "Multipurpose simulation network with single amplifier", Electronics Letters, Vol. 11, pages 9 - 10, 1975.

[60] W.T. RAMSEY, "Highpass and bandpass filters using a new single-amplifier simulated inductor", IEE Electronic Circuits and Systems, Vol. 2, pages 79 - 85, 1978.

[61] R.H. CHENG and J.T. LIM, "Single OP-AMP networks for shunt arms in ladder filters", Proceedings of IEEE International Symposium on Circuits and Systems, pages 313 - 316, 1977.

[62] H.J. ORCHARD and D.F. SHEAHAN, "Inductorless bandpass filters", IEEE Journal of Solid-State Circuits, Vol. SC - 5, pages 108 - 118, June 1970.

[63] J. VALIHORA, J.T. LIM and L.T. BRUTON, "The feasibility of active filtering in frequency division multiplex systems", Proceedings of IEEE International Symposium on Circuits and Systems, pages 121 - 125, April 1974.

[64] A.G.J. HOLT and R.L. LINGGARD, "Multi-terminal gyrator", IEE Proceedings, Vol. 117, pages 1591 - 1598, August 1970.

[65] L.T. BRUTON, "Frequency selectivity using positive impedance converter type networks", IEEE Proceedings, Vol. 56, pages 1378 - 1379, August 1968.

[66] A. BUDAK and D.M. PETRELA, "Frequency limitations of active filters using operational amplifiers", IEEE Trans. on Circuit Theory, Vol. CT - 19, pages 322 - 328, July 1972.

[67] P.O. BRACKETT and A.S. SEDRA, "Active compensation for high-frequency effects in OP-AMP circuits with applications to active RC filters", IEEE Trans. on Circuits and Systems, Vol. CAS - 23, pages 68 - 72, February 1976.

[68] A.M. SOLIMAN and M. ISMAIL, "Active compensation of OP-AMPs", IEEE Trans. on Circuits and Systems, Vol. CAS - 26, pages 112 - 117, February 1979.

[69] L.E. THOMAS, "The biquad: Part 1 —— Some practical design considerations", IEEE Trans. on Circuit Theory, Vol. CT - 18, pages 350 - 357, May 1971.

[70] A.M. SOLIMAN and M. ISMAIL, "Phase correction in two-integrator loop filters using a single compensating resistor", Electronics Letters, Vol. 14, pages 375 - 376, June 1978.

[71] H. WUPPER, "Extending the frequency range for some RC active filters", Proceedings of IEEE International Symposium on Circuits and Systems, pages 324 - 327, 1977.

[72] G.S. MOSCHYTZ, "Linear Integrated Networks —— Design", Bell Laboratories Series, 1975.

[73] P.E. FLEISCHER, "Sensitivity minimisation in a single amplifier biquad circuit", IEEE Trans. on Circuits and Systems, Vol. CAS - 23, pages 45 - 55, January 1976.

[74] J. Glover, "Lossless ungrounded inductor realisation", Electronics Letters, Vol. 12, pages 679 - 681, December 1976.

[75] D. PATRANABIS, M.P. TRIPATHI and S.B. ROY, "A new approach for lossless floating inductor realization", IEEE Trans. on Circuits and Systems, Vol. CAS - 26, pages 892 - 893, October 1979.

[76] D.J. PERRY, "Some uses of the circulator in filter networks", M.Sc. Thesis, Cranfield Institute of Technology, 1974.

[77] J.M. ROLLETT, "Improvements in or relating to electrical impedance networks", UK Patent No. 1238059, 7 July 1971.

[78] J. GORSKI-POPIEL, "RC active networks", Electronics Letters, Vol. 1, pages 288 - 289, December 1965.

[79] M.S. PIEDADE and M.M. SILVA, "Linear transformation active filters", IEE Proceedings, Part G, Vol. 128, pages 180 - 181, August 1981.

[80] J.D. BROWNLIE, "On the stability properties of a negative impedance converter", IEEE Trans. on Circuit Theory, Vol. CT - 13, pages 98 - 99, March 1966.

[81] A.F. SCHWARZ, "On the stability properties of a negative immittance convertor", IEEE Trans. on Circuit Theory, Vol. CT - 14, page 77, 1967.

[82] R.F. HOSKINS, "Stability of negative-impedance converters", Electronics Letters, Vol. 2, page 341, September 1966.

[83] A.C. DAVIES, "Large-signal characteristics and stability criteria of negative-impedance convertor circuits", Electronic Engineering, pages 536 - 541, September 1967.

[84] B. SINGH and W. SARAGA, "A novel approach to the active RC simulation of LC ladder filters", Proceedings of IEEE International Symposium on Circuits and Systems, pages 113 - 118, 1980.

SECTION	w_{oi}	Q_i	A_i
1	$\left[\frac{(1+C_1/C_3)}{C_1L_2}\right]^{1/2}$	$R_L\left[\frac{(1+C_1/C_3)C_1}{L_2}\right]^{1/2}$	$\frac{R_L}{R_s(1+C_1/C_3)}$
2	$\frac{1}{C_3R_L}$	——	1
3	$\left[\frac{(1+C_5/C_3)}{L_4C_5}\right]^{1/2}$	$R_L\left[\frac{(1+C_5/C_3)C_5}{L_4}\right]^{1/2}$	$\frac{1}{(1+C_5/C_3)}$

Table 1.1 Relationship between sectional parameters in Fig 1.6(i) and the components of the prototype filter of Fig 1.6(a).

SECTION	w_{oi}	Q_i	A_i
1	$[C_1L_1]^{-1/2}$	$R_s[C_1/L_1]^{1/2}$	$[L_1/C_1]^{1/2}/R_L$
2	$[C_2L_2]^{-1/2}$	∞	$R_L/[L_2/C_2]^{1/2}$
3	$[C_3L_3]^{-1/2}$	$R_L[C_3/L_3]^{1/2}$	$[L_3/C_3]^{1/2}/R_L$

$$w_{o1} = w_{o2} = w_{o3}$$

Table 1.2 Relationship between the sectional parameters in Fig 1.8(b) and the components of the prototype LC filter of Fig 1.8(a).

SECTION	w_{oi}	Q_i	A_i
1	15 kHz	47.8875	$4.1765\ 10^{-2}$
2	15 kHz	∞	$1.5198\ 10^{-2}$
3	15 kHz	47.8875	$4.1765\ 10^{-2}$

Table 2.1 The values of the sectional parameters of the multiple feedback bandpass filter of Fig 1.9(b). Centre Frequency = 15 kHz; Bandwidth = 500 Hz; Passband Ripple = 0.5 dB; $F_{12} = F_{23} = 1$; Midband Gain = 1.

COMPONENT	NOMINAL DESIGN	PREDISTORTED DESIGN	COMPENSATED DESIGN
C_1	1.0	1.0	1.0
C_2	1.0	1.0	1.0
R_1	0.807698	0.644309	0.645448
R_2	139.383	139.678	139.547
R_a	10.0	10.0	10.0
R_b	0.1	0.0787	0.0882362
R_3	0	0	0.160558

C-values in nano-Farads and R-values in kilo-ohms.

Table 2.2 Component values of the modified Friend SAB bandpass circuit of Fig 2.2(b). Centre Frequency = 15 kHz; Q-factor = 47.8875; f_T of OP-AMP = 1 MHz for the predistorted and compensated designs.

COMPONENT	NOMINAL DESIGN	PREDISTORTED DESIGN	COMPENSATED DESIGN
C_1	1.0	1.0	1.0
C_2	1.0	1.0	1.0
R_1	184.082	135.255	135.46
R_2	184.082	184.364	184.245
R_3	0.613607	0.45085	0.451533
R_a	0.1	0.08455	0.0911956
R_b	10.0	10.0	10.0
R_4	0	0	0.160605

C-values in nano-Farads and R-values in kilo-Ohms.

Table 2.3 Component values of the modified Sallen and Key SAB bandpass circuit of Fig 2.3(b). Centre Frequency = 15 kHz; Q-factor = ∞; f_T of OP-AMP = 1 MHz for the predistorted and compensated designs.

COMPONENT	NOMINAL DESIGN	PREDISTORTED DESIGN	COMPENSATED DESIGN
C_{11}	1.0	1.0	1.0
C_{12}	1.0	1.0	1.0
R'_{1a}	256.589	204.684	205.046
R'_{1b}	256.589	204.684	205.046
R'_{1c}	0.812814	0.648391	0.649537
R_{12}	139.383	139.678	139.547
R_{13}	0	0	0.160558
R_{1a}	10.0	10.0	10.0
R_{1b}	0.1	0.0787	0.088236
C_{21}	1.0	1.0	1.0
C_{22}	1.0	1.0	1.0
R'_{2a}	705.12	518.089	518.875
R'_{2b}	705.12	518.089	518.875
R'_{2c}	385.214	283.038	283.467
R_{22}	184.082	184.364	184.245
R_{23}	0.613607	0.45085	0.451533
R_{24}	0	0	0.160605
R_{2a}	0.1	0.08455	0.0911956
R_{2b}	10.0	10.0	10.0
C_{31}	1.0	1.0	1.0
C_{32}	1.0	1.0	1.0
R'_{3a}	256.589	204.684	205.046
R'_{3b}	0.810247	0.646343	0.647486
R_{32}	139.383	139.678	139.547
R_{33}	0	0	0.160558
R_{3a}	10.0	10.0	10.0
R_{3b}	0.1	0.0787	0.0882362

C values in nano-Farads and R values in kilo-Ohms

Table 2.4 Component values of the multiple feedback bandpass filter circuit of Fig 2.8. Centre Frequency = 15 kHz; Bandwidth = 500 Hz; Passband Ripple = 0.5 dB; $F_{12} = F_{23} = 1$; Midband Gain = 1. f'_Ts of OP-AMPs = 1 MHz for the predistorted and compensated designs.

COMPONENT CHANGED	f_T	R_1	R_2	C_1	C_2	R_3	R_a	R_b
NEGATIVE CHANGE IN RESONANCE FREQUENCY	-	+	+	+	+	-	-	+
NEGATIVE CHANGE IN Q-FACTOR	-	+	-	+	-	+	+	-
NEGATIVE CHANGE IN GAIN FACTOR	-	+	-	+	-	+	+	-
POSITIVE CHANGE IN RESONANCE FREQUENCY	+	-	-	-	-	+	+	-
POSITIVE CHANGE IN Q-FACTOR	+	-	+	-	+	-	-	+
POSITIVE CHANGE IN GAIN FACTOR	+	-	+	-	+	-	-	+

Table 3.1 A Table showing the direction of component changes required to produce a positive or a negative change in the Resonance Frequency, the Q-factor and the Gain-factor for the modified Friend SAB bandpass circuit of Fig 2.2(b).

COMPONENT CHANGED	f_T	R_1	R_2	C_1	C_2	R_3	R_4	R_a	R_b
NEGATIVE CHANGE IN RESONANCE FREQUENCY	-	+	+	+	+	+	-	+	-
NEGATIVE Q-FACTOR	+	+	+	-	+	-	-	+	-
NEGATIVE CHANGE IN GAIN FACTOR	+	+	+	-	+	-	-	+	-
POSITIVE CHANGE IN RESONANCE FREQUENCY	+	-	-	-	-	-	+	-	+
POSITIVE Q-FACTOR	-	-	-	+	-	+	+	-	+
POSITIVE CHANGE IN GAIN FACTOR	-	-	-	+	-	+	+	-	+

Table 3.2 A Table showing the direction of component changes required to produce a positive or a negative change in the Resonance Frequency and the Gain-factor and to produce a positive or a negative Q-factor for the modified Sallen and Key SAB bandpass circuit of Fig 2.3(b).

COMPONENT	VALUE
C_{11}	1.0
C_{12}	1.0
R'_{1a}	277.601
R'_{1b}	277.601
R'_{1c}	3.03836
R_{12}	35.4632
R_{13}	0.185681
R_{1a}	10.0
R_{1b}	1.66684
C_{21}	1.0
C_{22}	1.0
R'_{2a}	922.583
R'_{2b}	922.583
R'_{2c}	187.212
R_{22}	24.701
R_{23}	4.43891
R_{24}	0.223148
R_{2a}	4.02099
R_{2b}	10.0
C_{31}	1.0
C_{32}	1.0
R'_{3a}	277.601
R'_{3b}	3.00547
R_{32}	35.4632
R_{33}	0.185681
R_{3a}	10.0
R_{3b}	1.66684

C-values in nano-Farads and R-values in kilo-Ohms

Table 3.3 Component values of the optimised design of the circuit in Fig 3.10.

COMPONENT	NOMINAL VALUES	MEASURED VALUES
C_{11}	10.0	10.06
C_{12}	10.0	10.17
R'_{1a}	55.522	56.75
R'_{1b}	55.522	56.94
R'_{1c}	0.30055	0.3002
R_{12}	3.5463	3.439
R_{13}	0.018568	0.02037
R_{1a}	10.0	10.04
R_{1b}	1.6668	1.714
C_{21}	10.0	10.12
C_{22}	10.0	9.963
R'_{2a}	46.129	48.19
R'_{2b}	46.129	47.85
R'_{2c}	31.509	33.56
R_{22}	2.4701	2.487
R_{23}	0.44389	0.4297
R_{24}	0.022315	0.2416
R_{2a}	4.021	3.943
R_{2b}	10.0	10.16
C_{31}	10.0	9.996
C_{32}	10.0	10.19
R'_{3a}	55.522	57.19
R'_{3b}	0.29893	0.2995
R_{32}	3.5463	3.464
R_{33}	0.018568	0.02006
R_{3a}	10.0	10.13
R_{3b}	1.6668	1.622

C-value in nano-Farads and R-values in kilo-Ohms.

Table 3.4 Nominal and measured component values of the discrete component model of the circuit in Fig 3.10.

COMPONENT	NOMINAL VALUE	MEASURED VALUE
C_1	23.173	23.18
C_2	20.802	20.81
C_3	36.335	36.37
C_4	20.802	20.80
C_5	23.173	23.17
R_1	10.0	9.99
R_2	10.0	10.03
R_3	10.0	9.96
R_4	10.0	9.96
R_5	10.0	10.05
R_6	10.0	9.98
R_7	10.0	9.98
R_8	10.0	10.07
R_9	10.0	9.99
R_{10}	10.0	9.99
R_{11}	10.0	10.07
R_{12}	10.0	10.01
R_{13}	10.0	10.01
R_{14}	10.0	10.08

C-values are in nano-Farads and R-values are in kilo-Ohms

Table 4.1 Nominal and measured component values of the discrete component model of the circuit in Fig 4.28.

COMPONENT	NOMINAL VALUE	MEASURED VALUE
C_1	20.0	20.01
C_2	10.0	10.00
C_3	10.0	10.01
C_4	10.0	10.01
C_5	10.0	10.01
C_p	0	0.047
R_1	10.931	10.92
R_2	10.0	10.07
R_3	10.0	10.08
R_4	12.177	12.16
R_5	10.0	10.17
R_6	10.0	10.17
R_7	6.971	6.966
R_8	10.0	10.13
R_9	10.0	10.14
R_{10}	12.177	12.16
R_{11}	10.0	10.10
R_{12}	10.0	10.08
R_{13}	10.931	10.95

C-values are in nano-Farads and R-values are in kilo-Ohms

Table 4.2 Nominal and measured component values of the discrete component model of the circuit in Fig 4.31.

COMPONENT	NOMINAL VALUE
R_{sn}	3.0 Ohms
L_{1n}	29.49 μH
C_{1n}	0.626 mF
L_{2n}	1.2687 mH
C_{2n}	63.79 μF
L_{3n}	309.38 μH
C_{3n}	40.837 μF
L_{4n}	90.412 μH
C_{4n}	9.6593 μF
L_{5n}	124.76 μH
L_{6n}	202.49 μH
L_{7n}	1.7791 mH

Table 4.3 Nominal component values of the prototype LC filter of Fig 4.27(c).

COMPONENT	NOMINAL VALUE	MEASURED VALUE
C_1	10.0	10.0
C_2	10.0	9.999
C_3	10.0	9.997
C_4	10.0	9.999
C_5	10.0	9.999
C_6	10.0	9.999
C_7	10.0	9.996
C_8	10.0	10.0
C_9	10.0	9.997
C_{10}	10.0	9.997
C_p	0	0.04732
R_{p1}	0	6.879
R_{p2}	0	6.869
R_1	10.0	9.95
R_2	10.0	9.953
R_3	187.8	187.9
R_4	0.983	0.9833
R_5	42.29	42.29
R_6	10.0	10.06
R_7	10.0	10.06
R_8	19.137	19.14
R_9	10.0	9.99
R_{10}	10.0	9.99
R_{11}	10.313	10.33
R_{12}	3.0137	3.017
R_{13}	4.1587	4.162
R_{14}	6.7497	6.744
R_{15}	12.251	12.27
R_{16}	12.251	12.25
R_{17}	12.251	12.22
R_{18}	59.303	59.42
R_{19}	10.0	10.03
R_{20}	10.0	10.04
R_{21}	2.8978	2.90

C-values are in nano-Farads and R-values are in kilo-Ohms.

Table 4.4 Nominal and measured component values of the discrete component model of the circuit in Fig 4.34.

COMPONENT	NOMINAL VALUE
C_1	10.0
C_2	10.0
C_3	10.0
C_4	10.0
C_5	10.0
R_1	23.173
R_2	10.0
R_3	10.0
R_4	20.802
R_5	10.0
R_6	10.0
R_7	36.335
R_8	10.0
R_9	10.0
R_{10}	20.802
R_{11}	20.0
R_{12}	10.0
R_{13}	11.587

C-values are in nano-Farads and R-values are in kilo-Ohms.

Table 4.5 Nominal component values of the circuit of Fig 4.43.

COMPONENT	NOMINAL VALUE UNOPTIMISED DESIGN	NOMINAL VALUE OPTIMISED DESIGN	MEASURED VALUE OPTIMISED DESIGN
C_1	10.0	10.0	9.957
C_2	10.0	10.0	10.04
C_3	10.0	10.0	10.04
C_4	10.0	10.0	10.05
C_5	20.0	20.0	20.02
C_6	10.0	10.0	10.02
C_7	0	2.89036	2.890
C_8	0	2.89036	2.889
R_1	5.4654	5.4654	5.485
R_2	24.354	24.354	24.35
R_3	10.457	10.457	10.46
R_4	6.0885	6.0885	6.112
R_5	10.931	10.931	10.93
R_6	1.0	22.7201	22.53
R_7	1.0	22.7201	22.51
R_8	1.0	2.0	1.992
R_9	3.0	6.0	5.999
R_{10}	1.0	3.0	3.002
R_{11}	2.0	6.0	6.001

C-values are in nano-Farads and R-values are in kilo-Ohms.

Table 5.1 Nominal and measured component values of the discrete component model of the circuit in Fig 5.4(b).

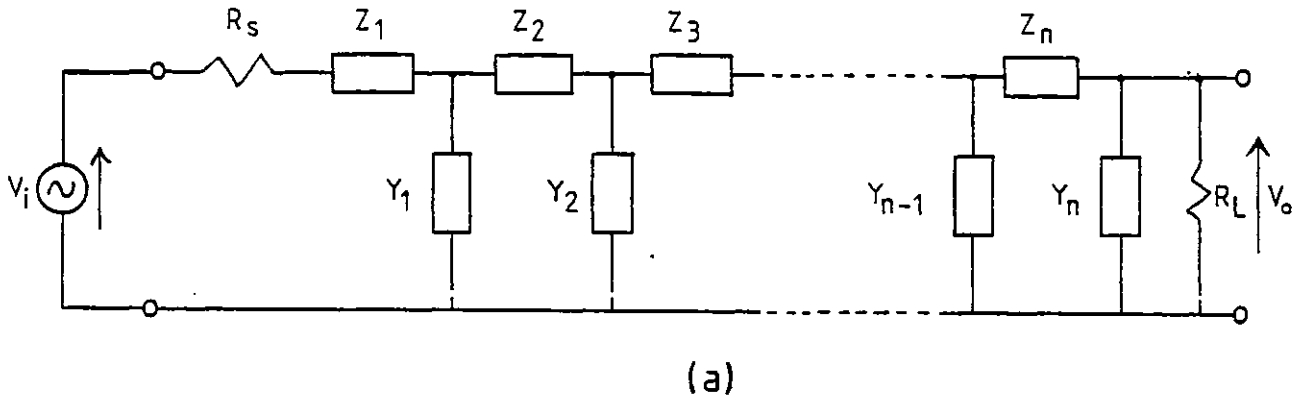

(a)

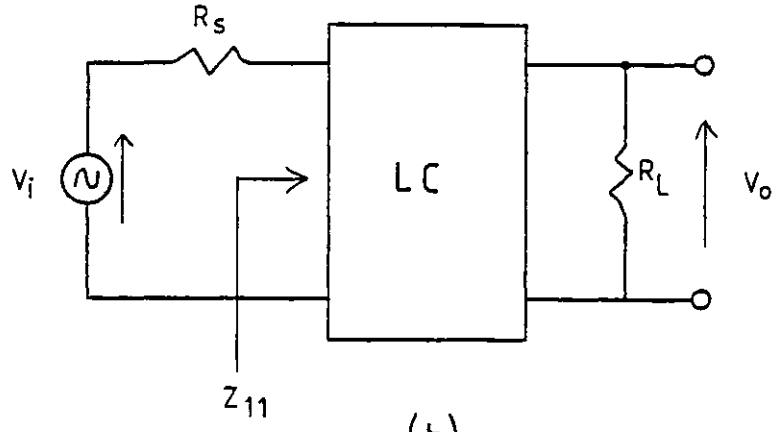

(b)

Fig 1.1 Resistively terminated LC ladder filters.
(a) General form of an LC ladder filter structure.
(b) Schematic diagram of an LC ladder filter.

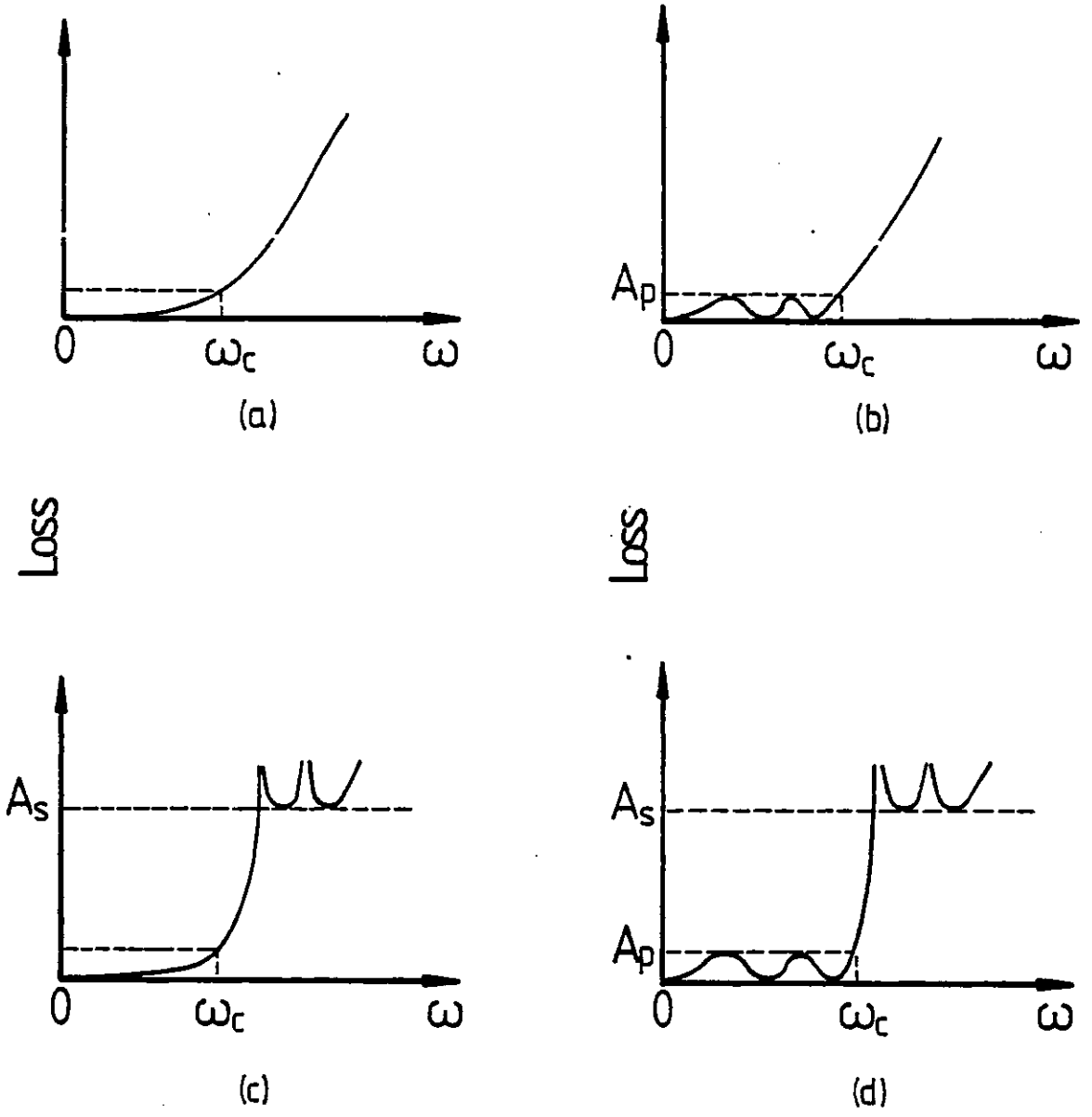

Fig 1.2 Basic types of loss-frequency curves for lowpass filters. (a) Butterworth response. (b) Chebyshev response. (c) Inverted Chebyshev response. (d) Elliptic response.

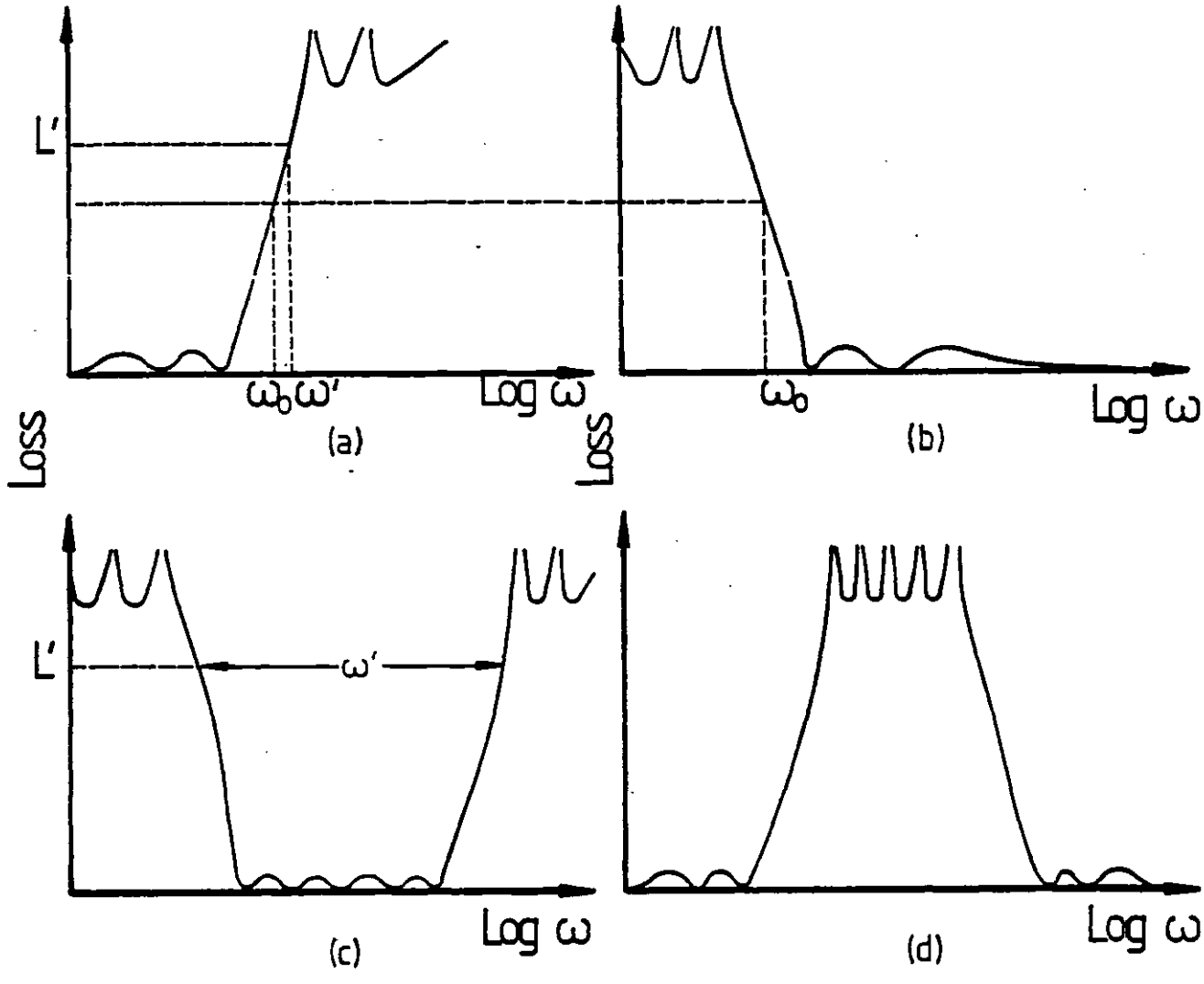

Fig 1.3 Basic filter response types derivable via transformations from lowpass filter response.
(a) Lowpass filter response. (b) Highpass filter response.
(c) Bandpass filter response. (d) Bandstop filter response.

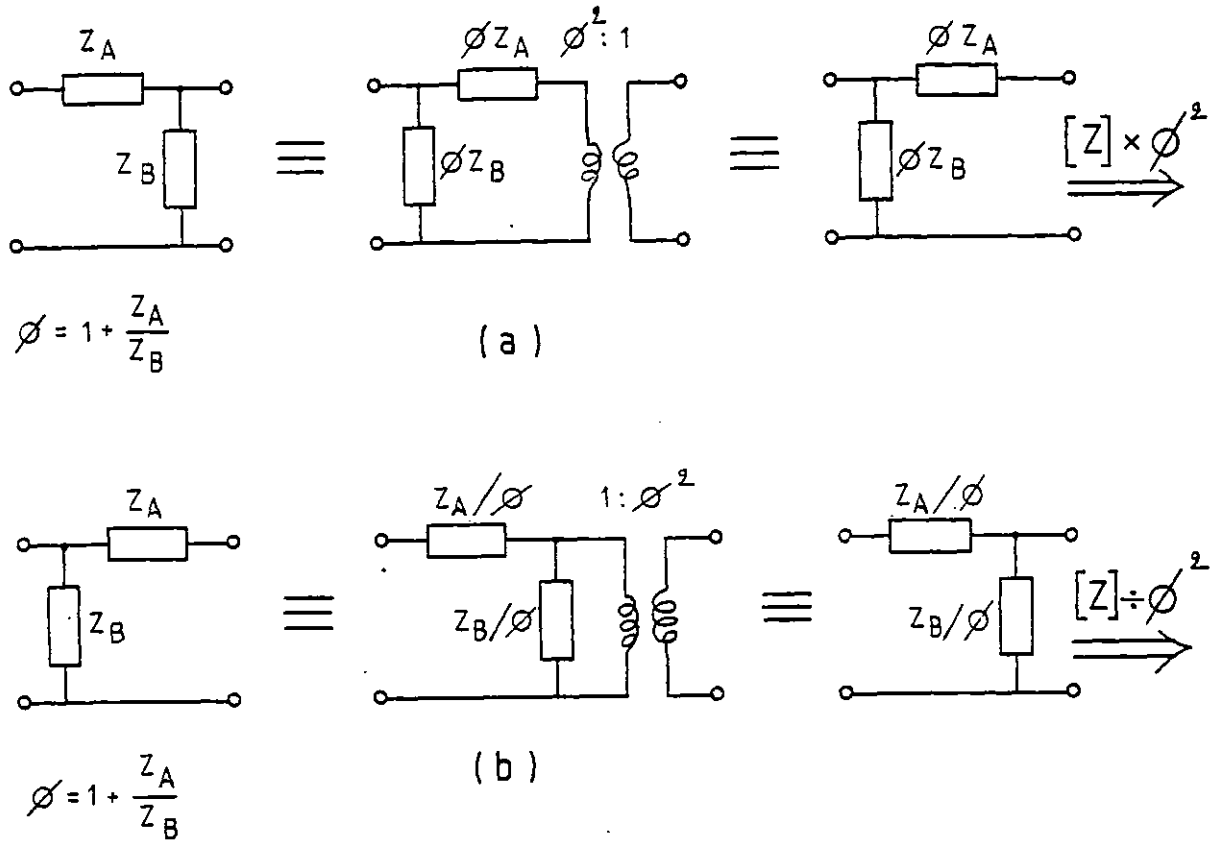

Fig 1.4 Norton transformations.
(a) General left-to-right "L" transformation. (b) General right-to-left "L" transformation.

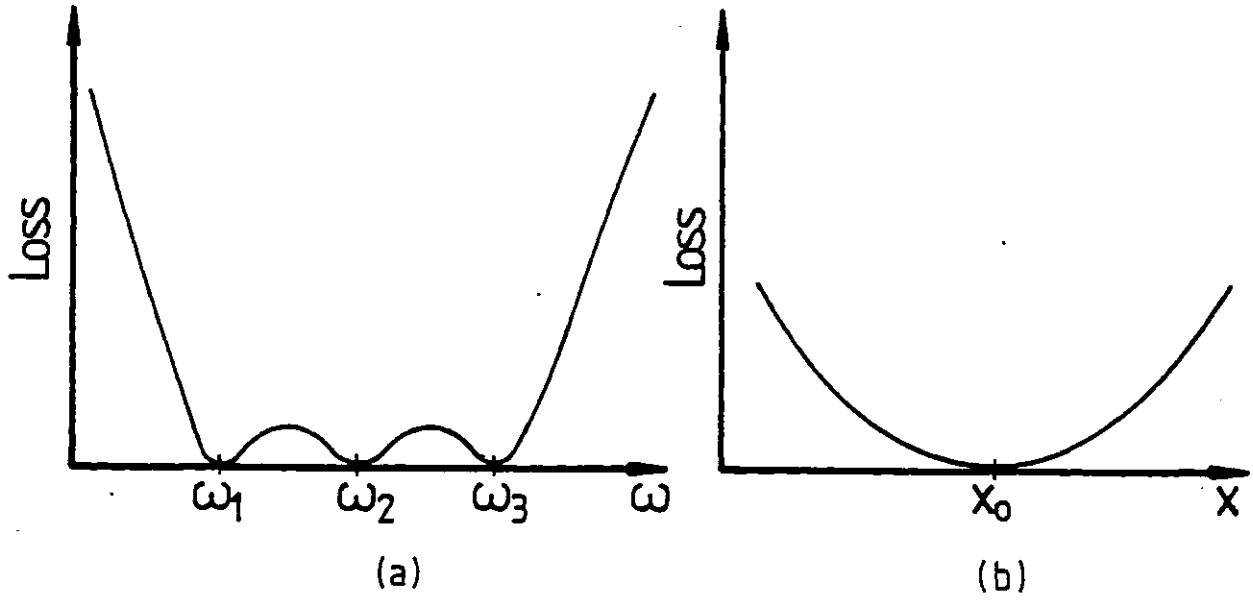

Fig 1.5 Sensitivity charateristics of resistively terminated LC ladder filters.
(a) Equiripple filter characteristic. (b) Loss variation versus component change.

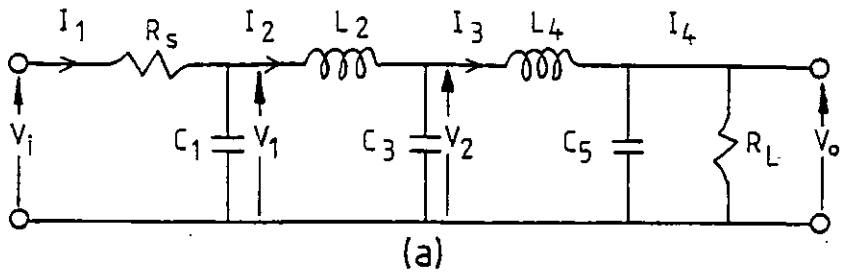

(a)

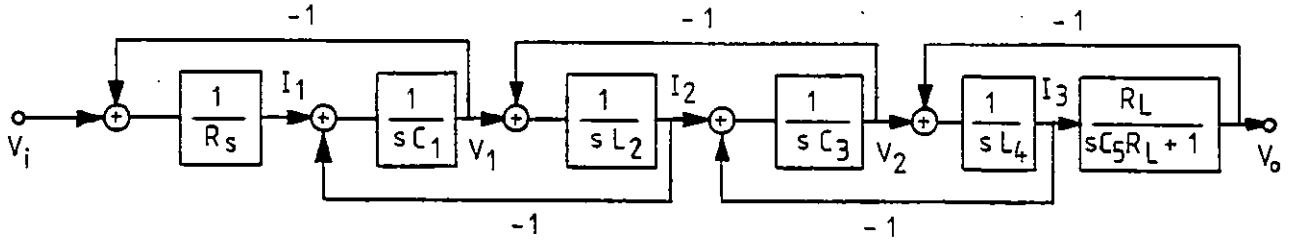

(b)

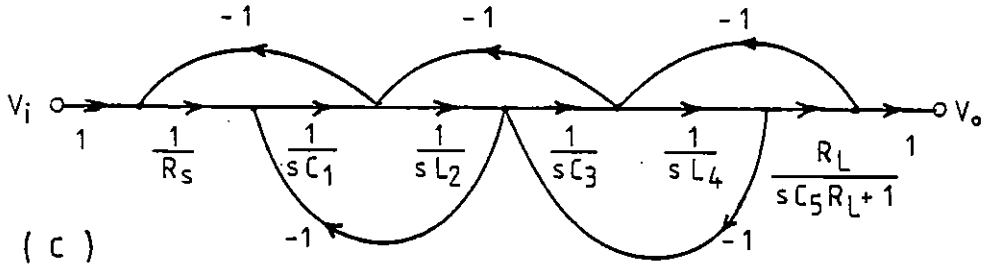

(c)

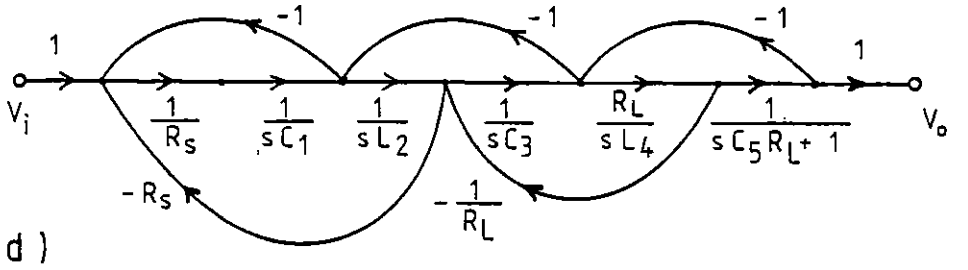

(d)

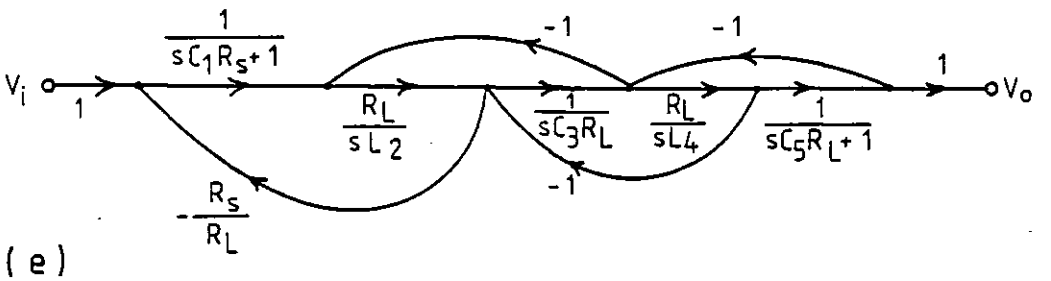

(e)

Fig 1.6 (Continued on next page).

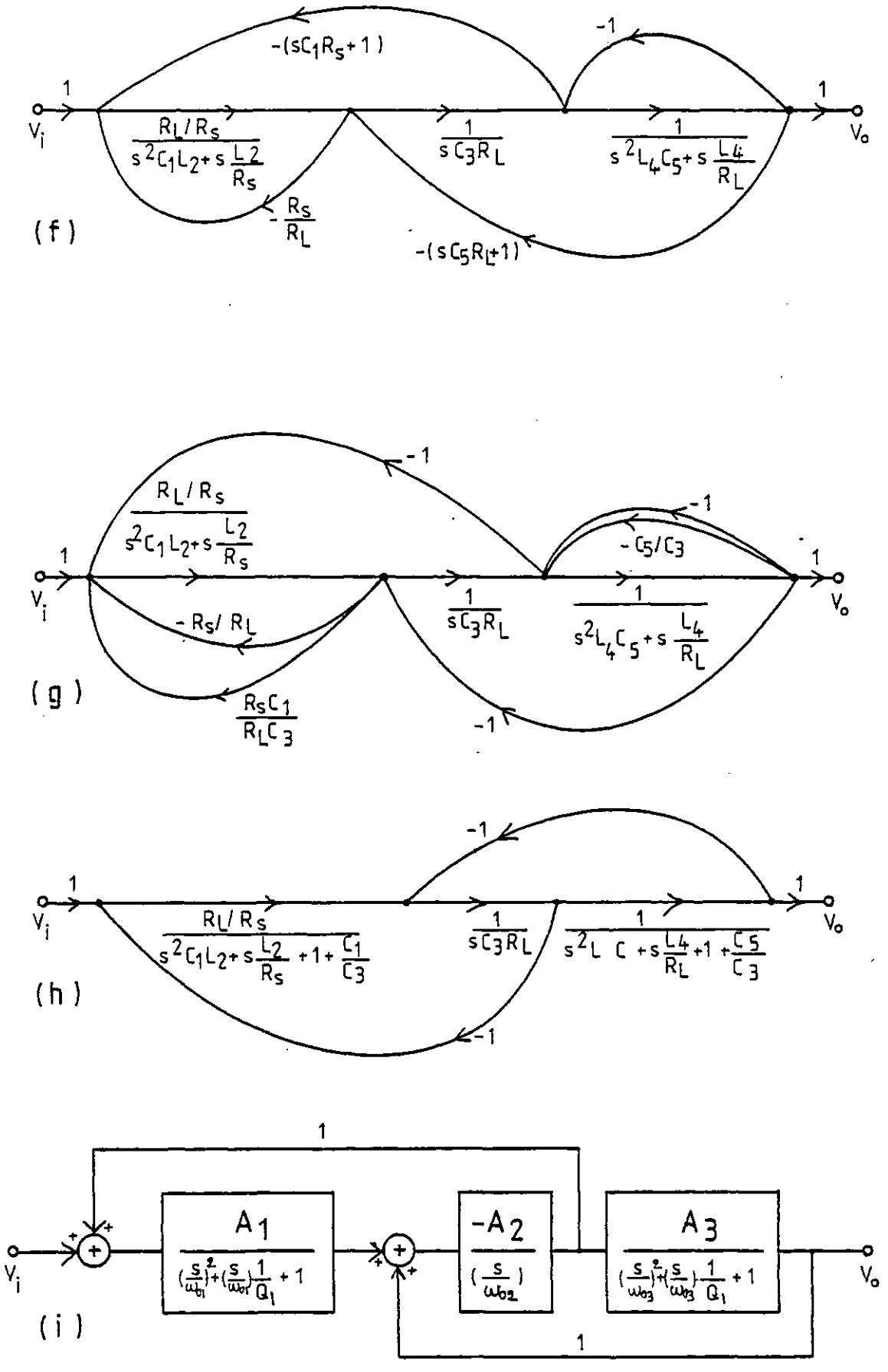

Fig 1.6 Signal flow graph simulation of LC ladder filters.
(a) Fifth order all-pole lowpass LC prototype filter.
(b) Signal flow block diagram representation of equations (2.14). (c) ⟶ (i) Derivation of the required leap-frog feedback structure by manipulation of the signal flow graph.

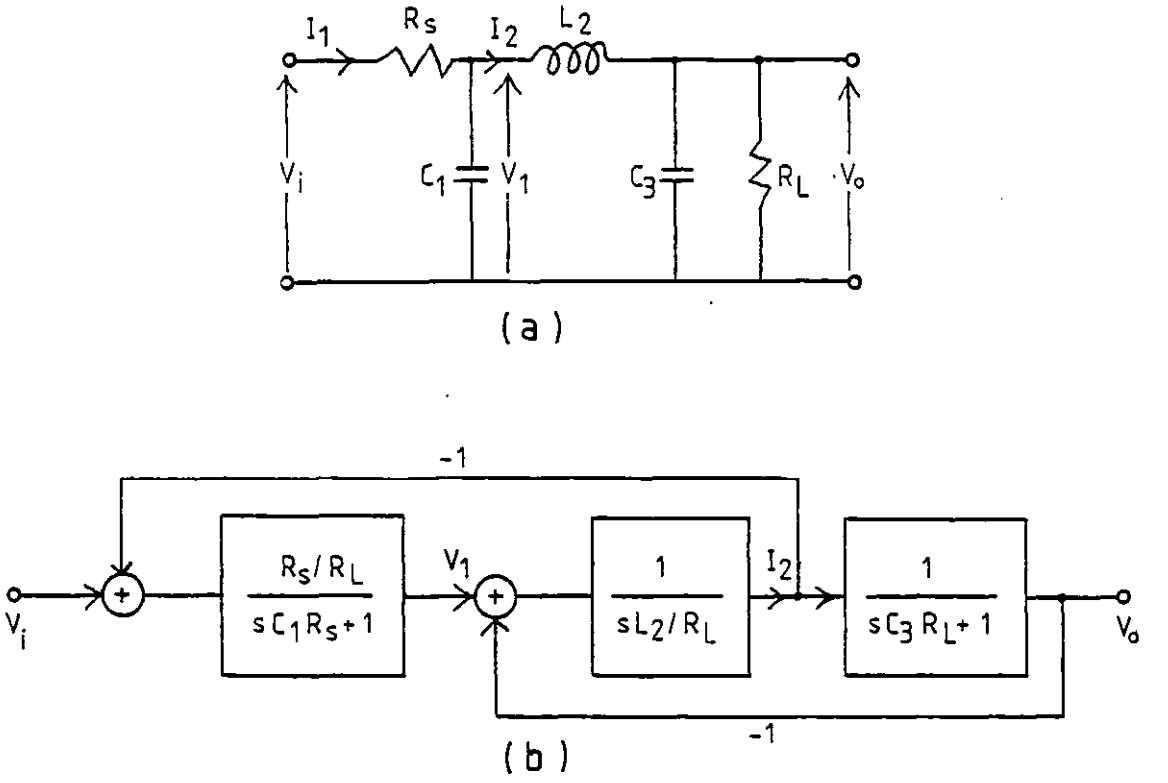

Fig 1.7 Third order lowpass LC filter and its leap-frog feedback equivalent.

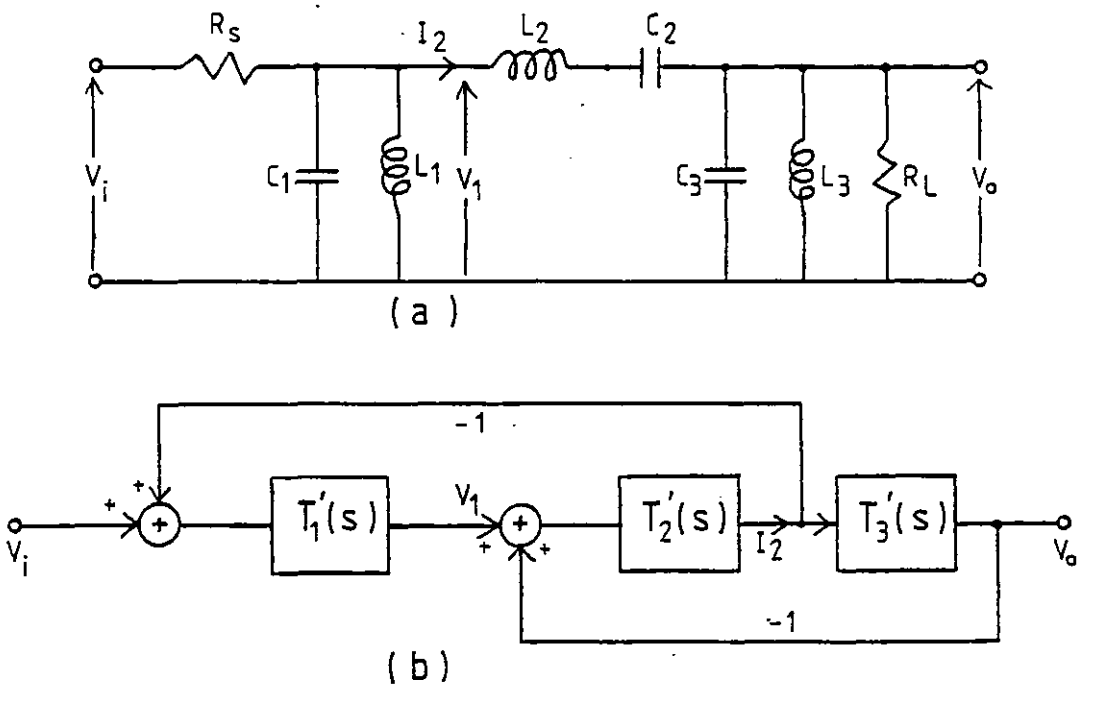

Fig 1.8 Sixth order bandpass LC filter and its equivalent leap-frog feedback stucture.

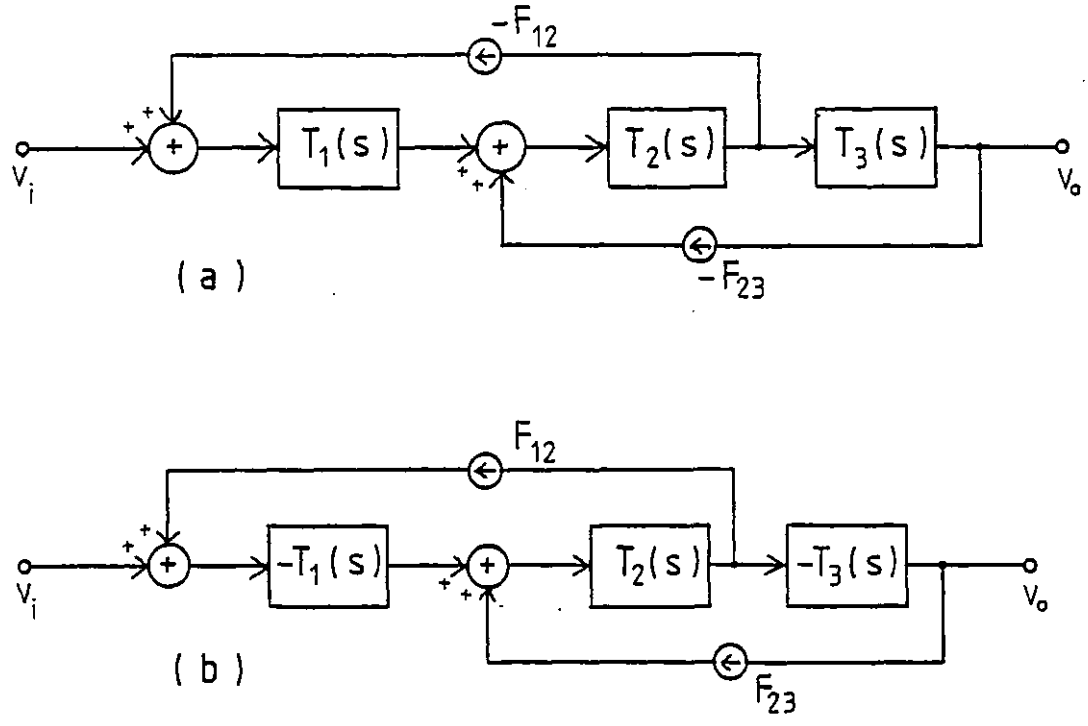

Fig 1.9 (a) Leap-frog feedback realisation of the LC filter in Fig 1.8(a) using non-unity feedback factors.
(b) Equivalent structure of (a) with non-negative feedback factors.

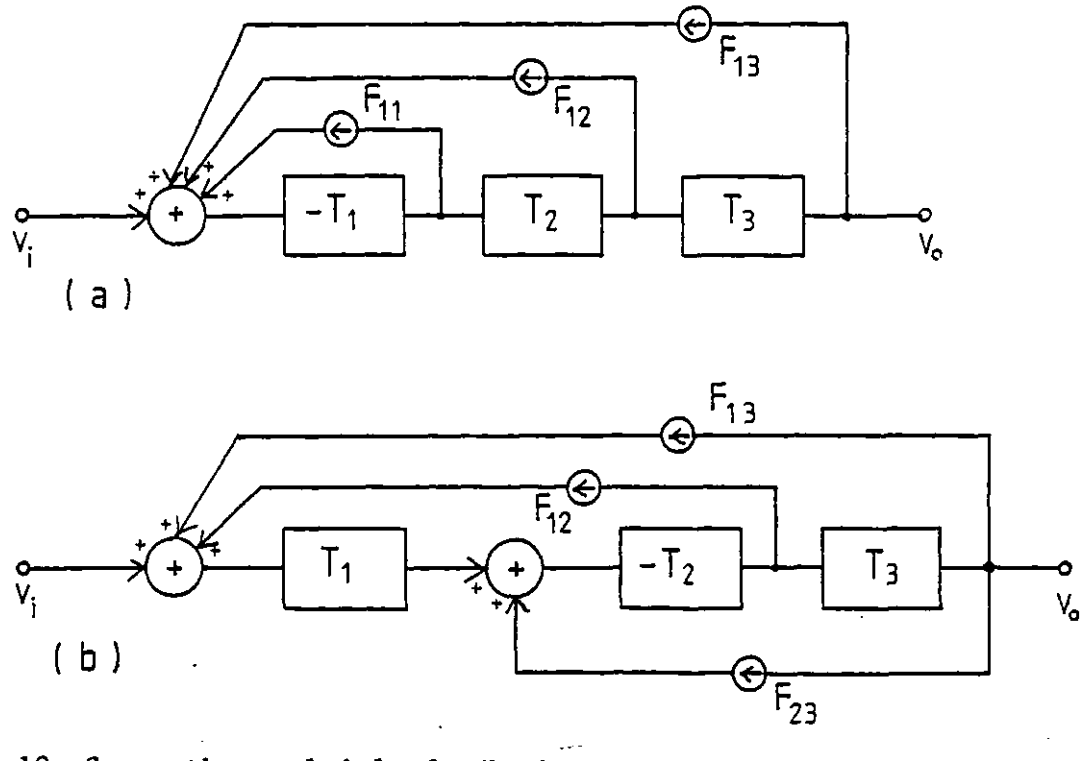

Fig 1.10 Some other multiple feedback topologies.
(a) Follow-the-leader feedback topology. (b) Minimum sensitivity feedback topology.

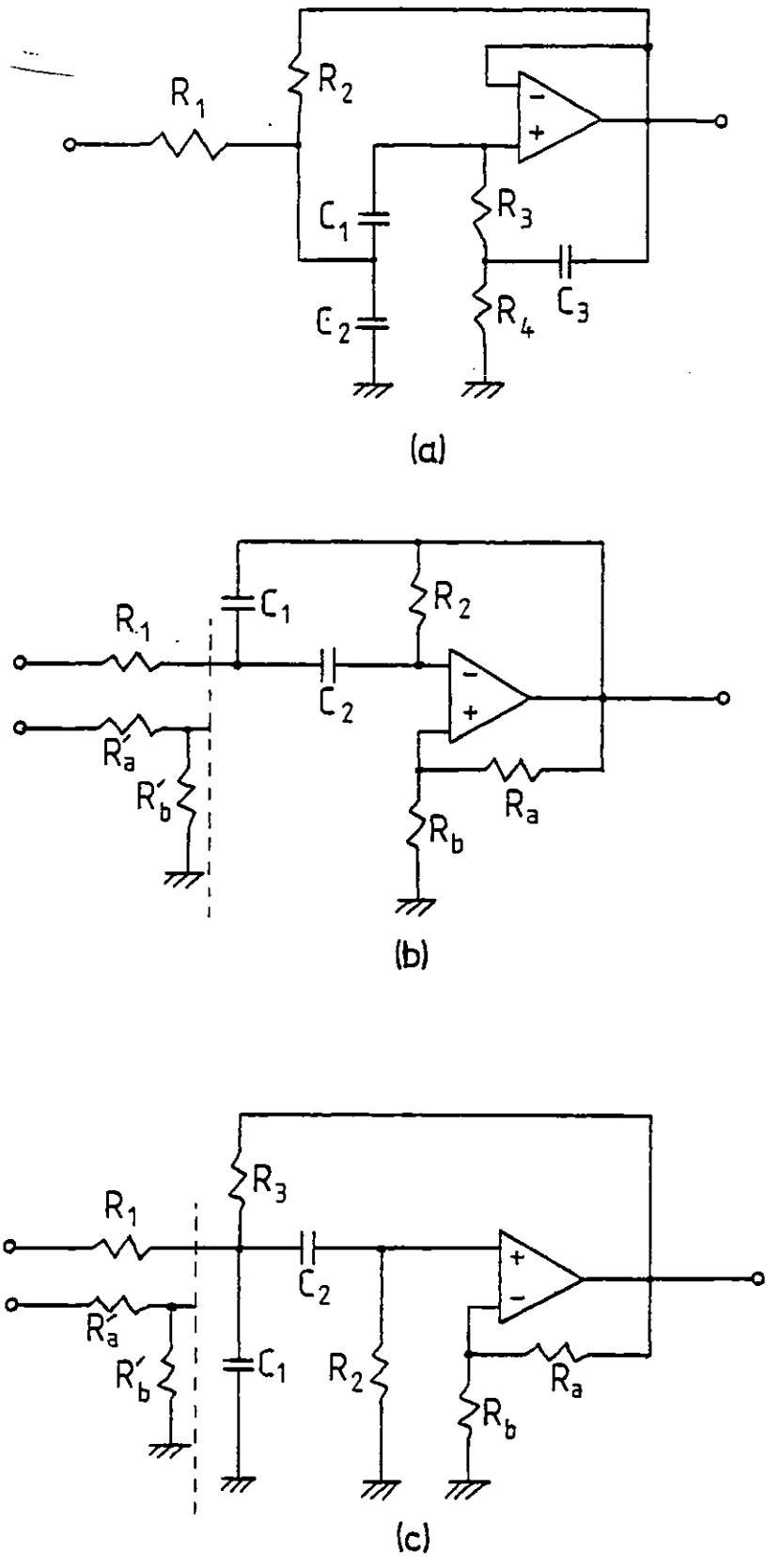

Fig 1.11 Some single amplifier biquadratic (SAB) bandpass circuits. (a) SAB Lim bandpass section. (b) SAB Friend bandpass section. (c) SAB Sallen and Key bandpass section.

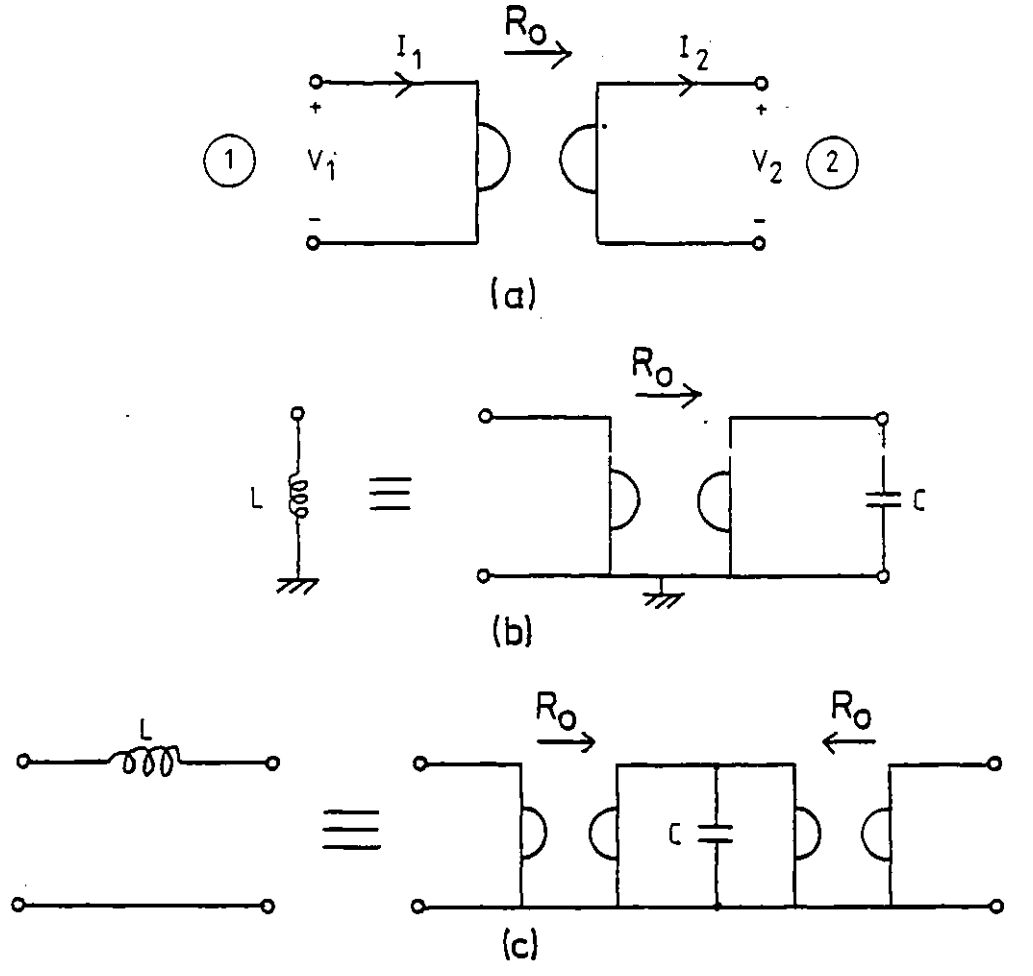

Fig 1.12 Gyrators and their usage for simulating inductors. (a) Symbolic representation of a gyrator. (b) Simulation of a grounded inductor. (c) Simulation of a floating inductor.

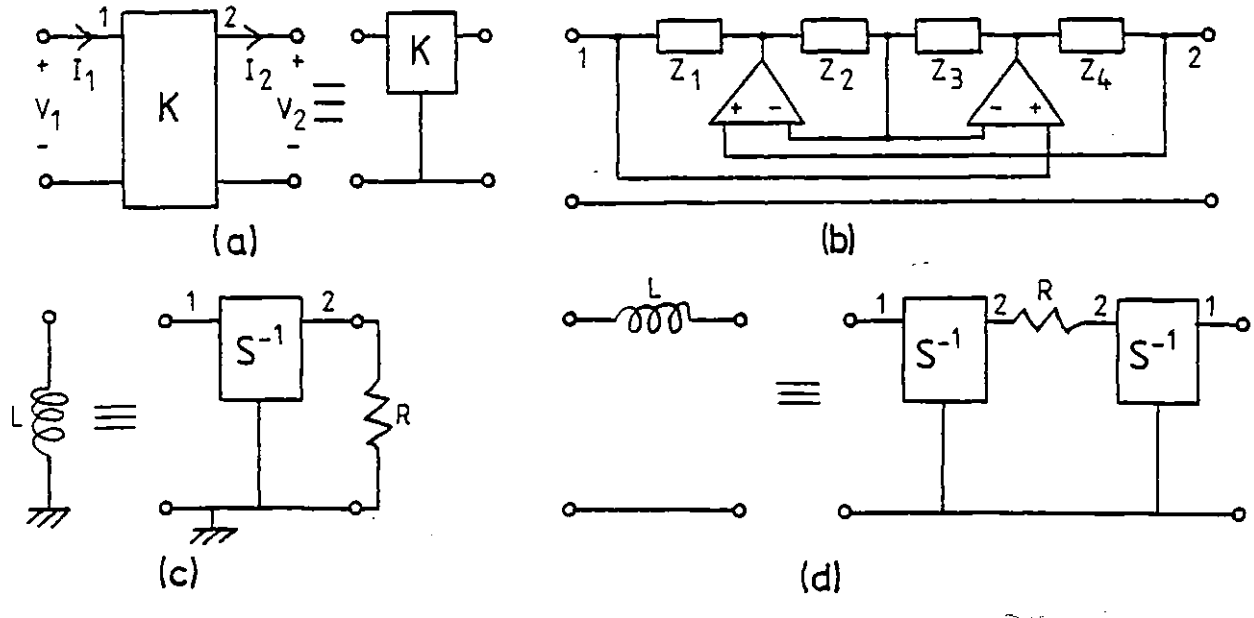

Fig 1.13 Positive impedance converter (PIC) and its usage for simulating inductors. (a) Symbolic representation of a PIC. (b) Circuit realisation of PIC. (c) Simulation of a grounded inductor. (d) Simulation of a floating inductor.

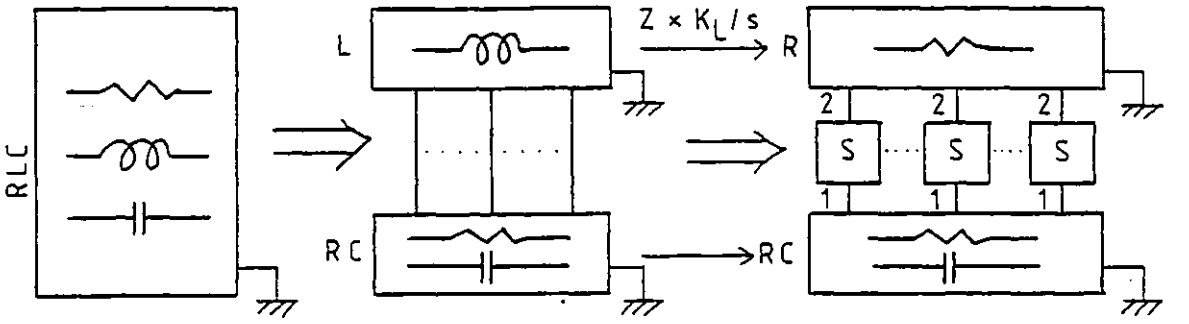

Fig 1.14 Basic principle of the Gorski-Popiel's method of simulating RLC filters.

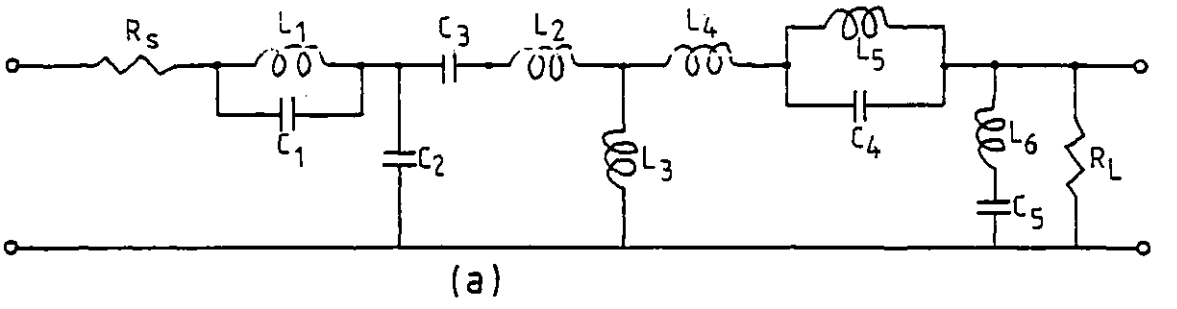

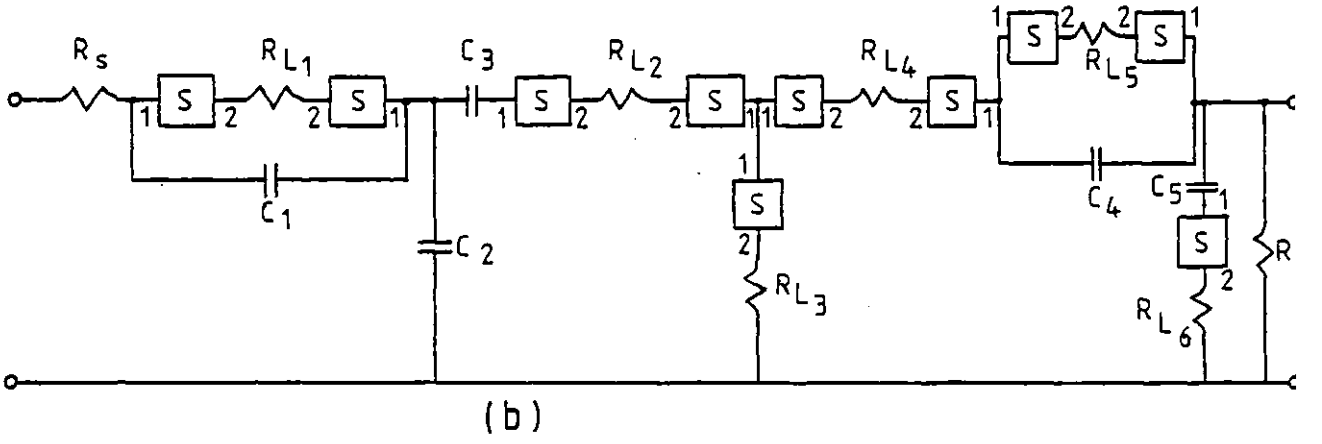

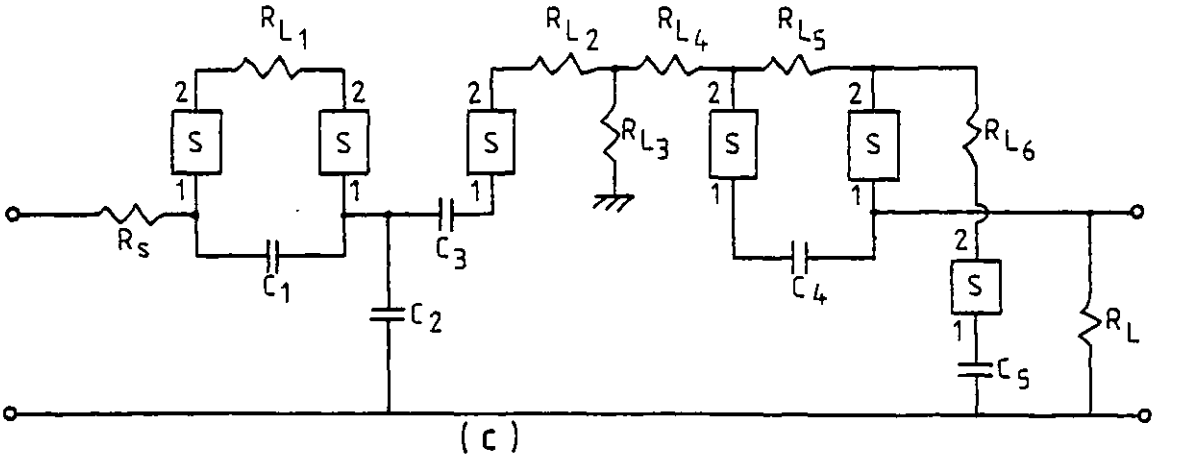

Fig 1.15 Design example of simulating RLC filters by inductor simulation methods.
(a) RLC - prototype filter. (b) Active RC realisation of (a) by simulating each inductor individually. (c) Active RC realisation of (a) using the Gorski-Popiel's method.

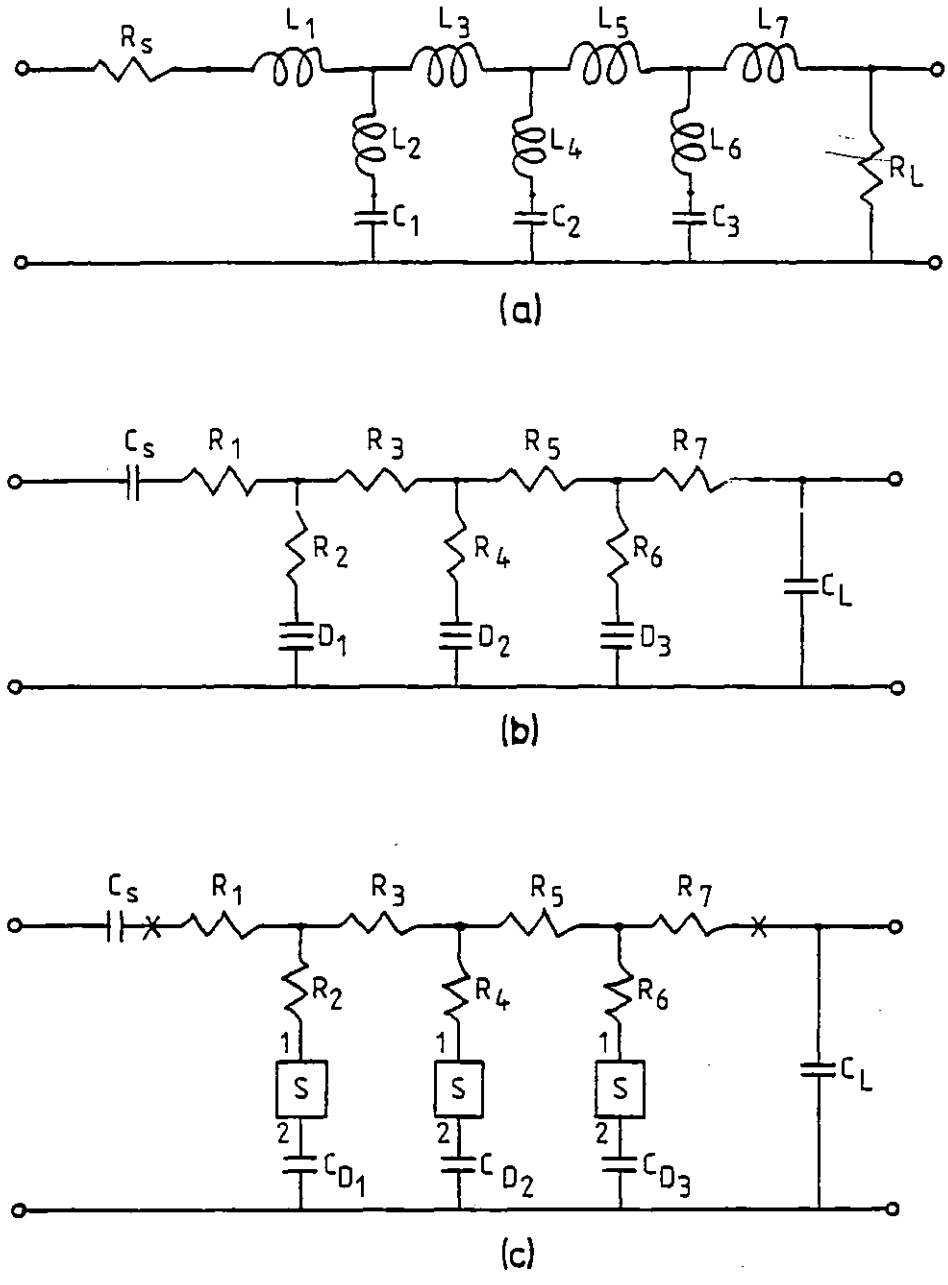

Fig 1.16 Bruton's method of simulating RLC filters.
(a) Prototype filter. (b) Impedance scaled version of the prototype filter. (c) Active RC realisation of the circuit in (b) using s-type FICs.

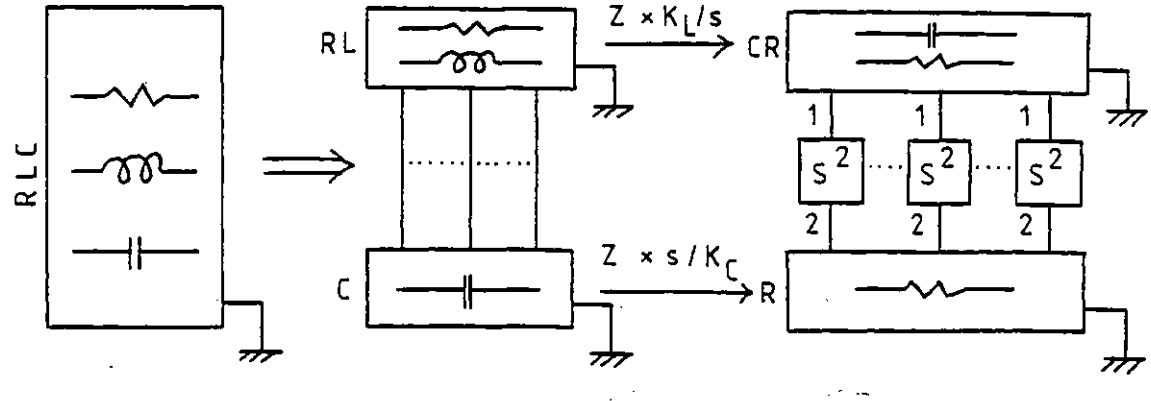

Fig 1.17 Basic principle of the full impedance scaling method of simulating RLC filters.

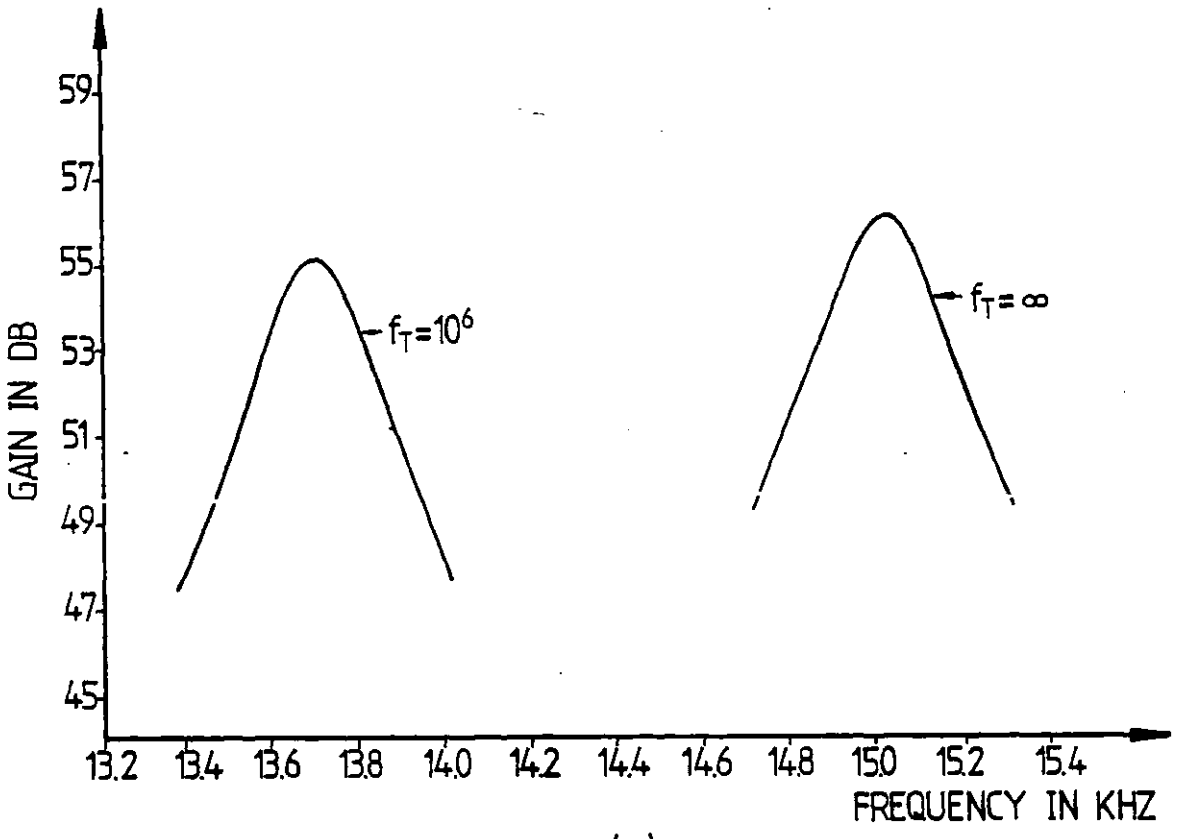

(a)

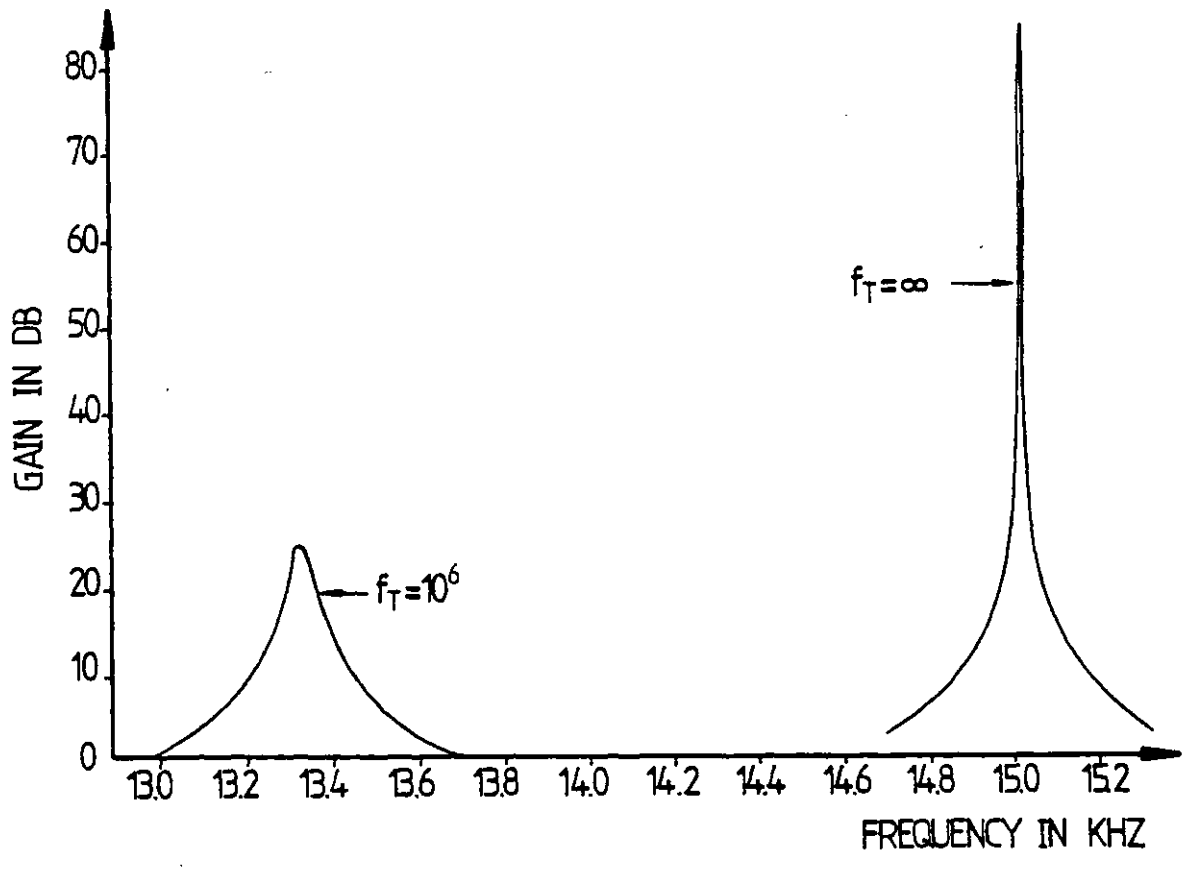

(b)

Fig 2.1 Effect of finite amplifier gain bandwidth product. (a) Friend SAB bandpass circuit designed for f_r = 15 kHz, Q_r = 47.8875 assuming the OP-AMP to be ideal. (b) Sallen and Key SAB bandpass circuit designed for f_r = 15 kHz, Q_r = ∞ assuming the OP-AMP to be ideal.

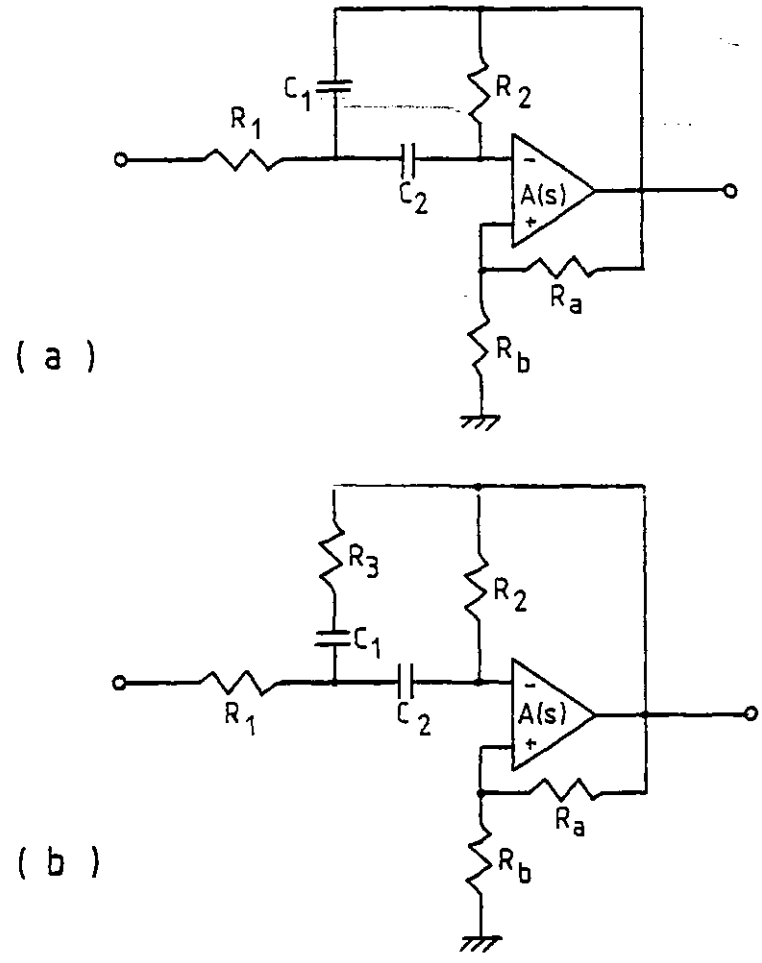

Fig 2.2 (a) Friend SAB bandpass circuit.
(b) Compensated Friend SAB bandpass circuit.

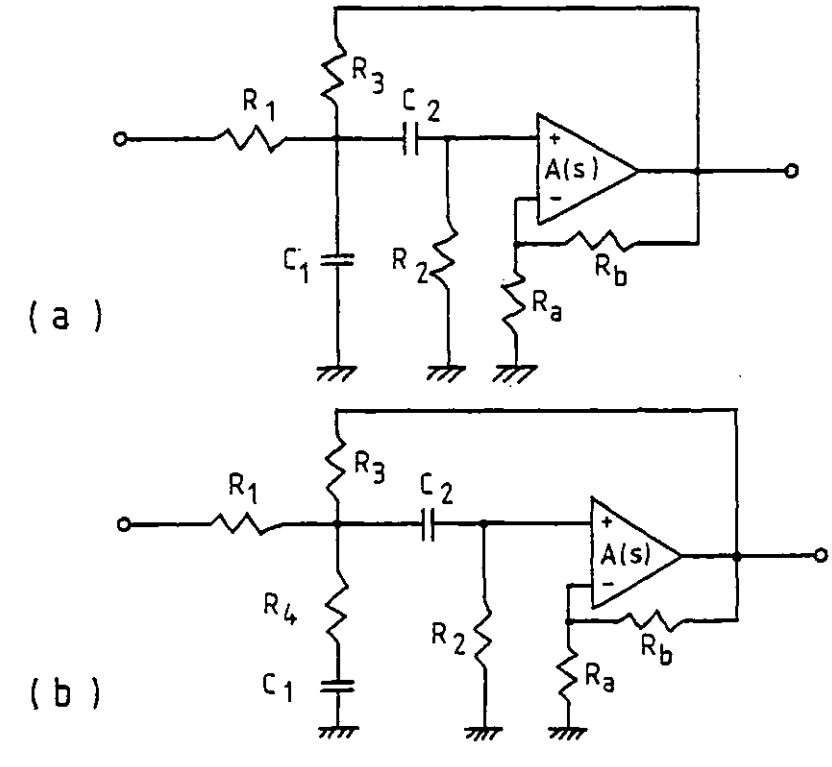

Fig 2.3 (a) Sallen and Key SAB bandpass circuit.
(b) Compensated Sallen and Key SAB bandpass circuit.

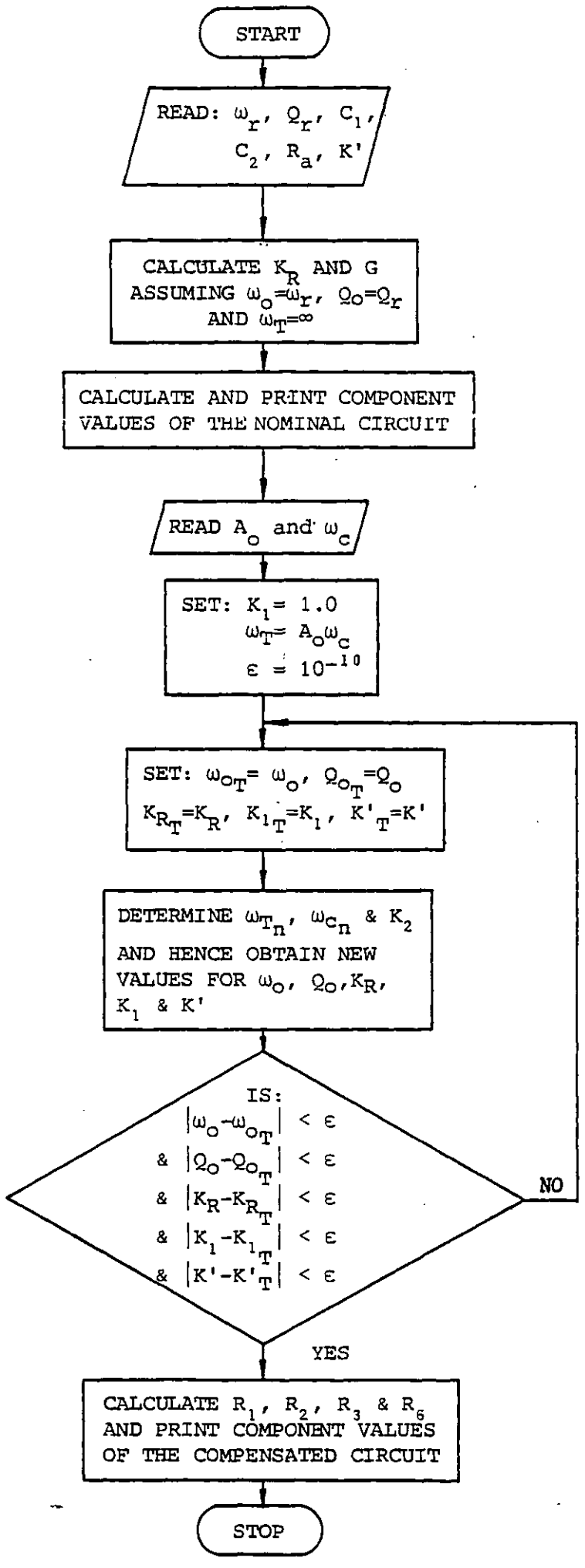

Fig.2.4 Flow chart of the computer program for designing the Friend circuit of Fig.2.2(b).

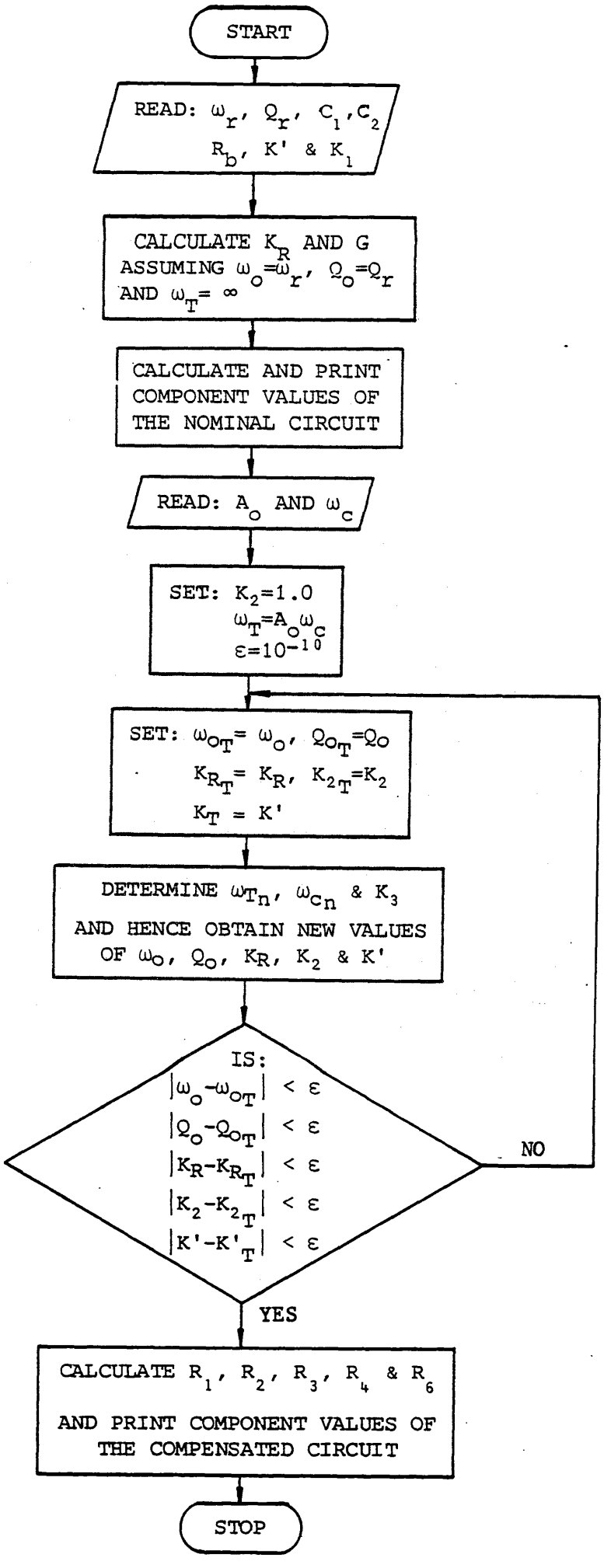

Fig. 2.5 Flow chart of the computer program for designing the Sallen and Key circuit of Fig.2.3(b).

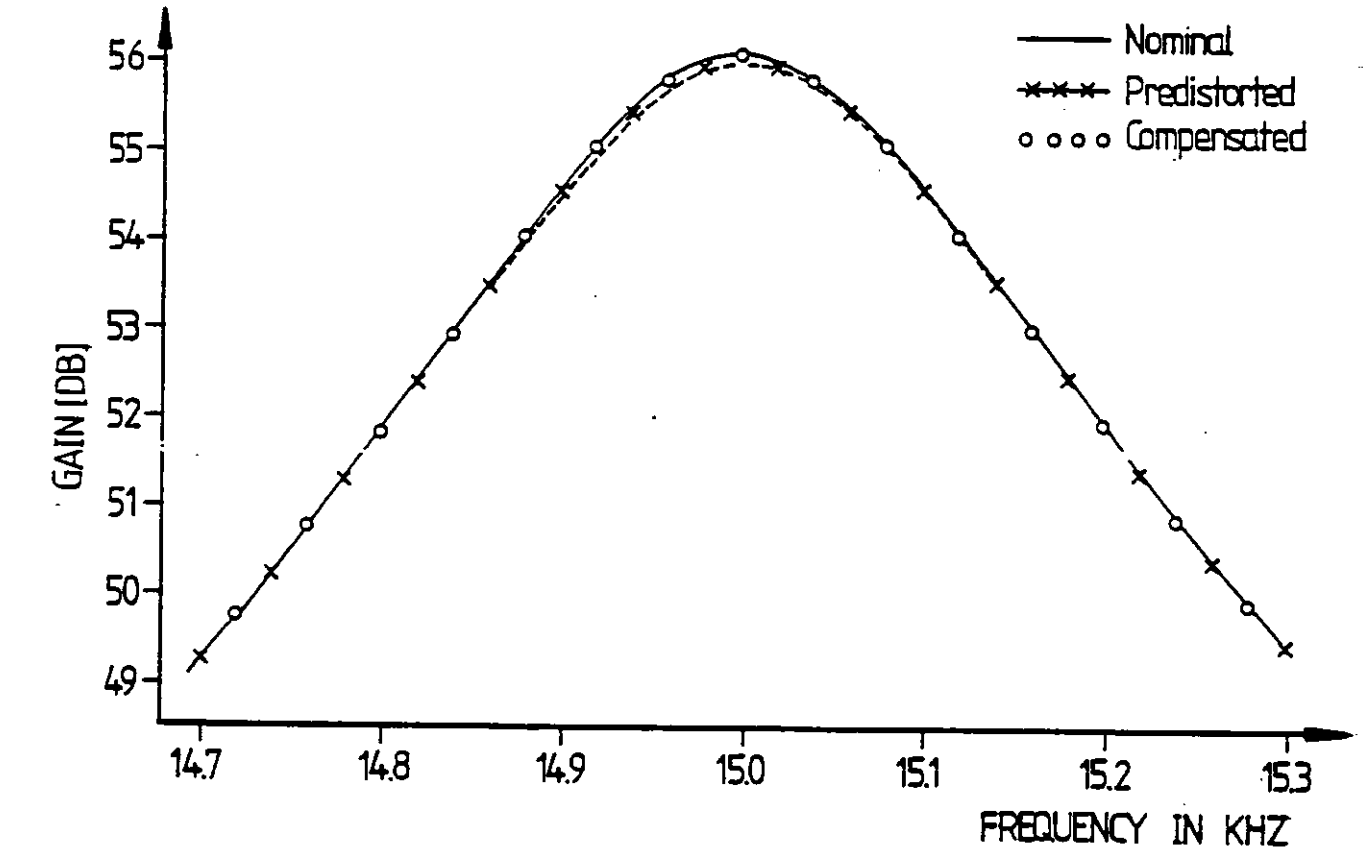

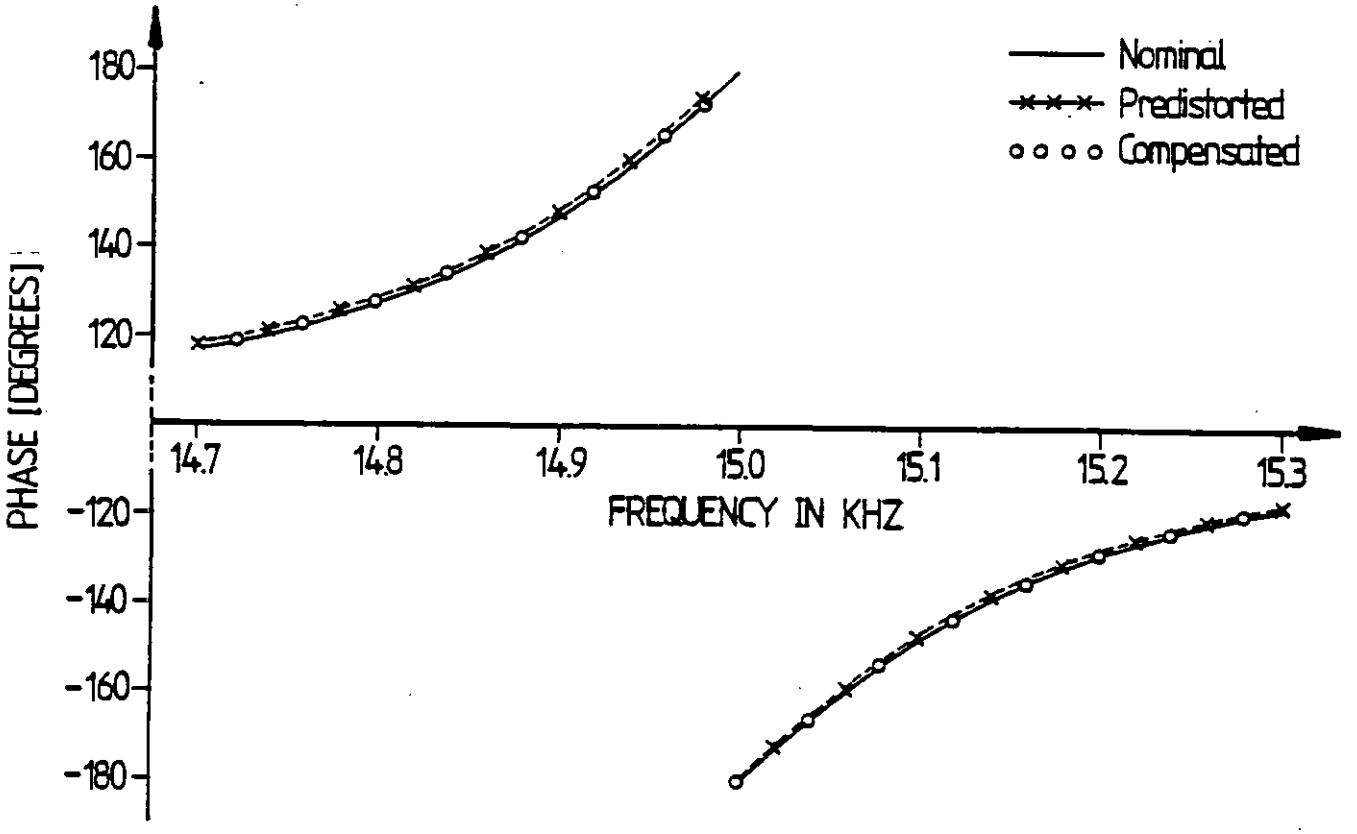

Fig 2.6 Comparison of the results of the nominal, predistorted and compensated designs of the Friend SAB bandpass circuit.

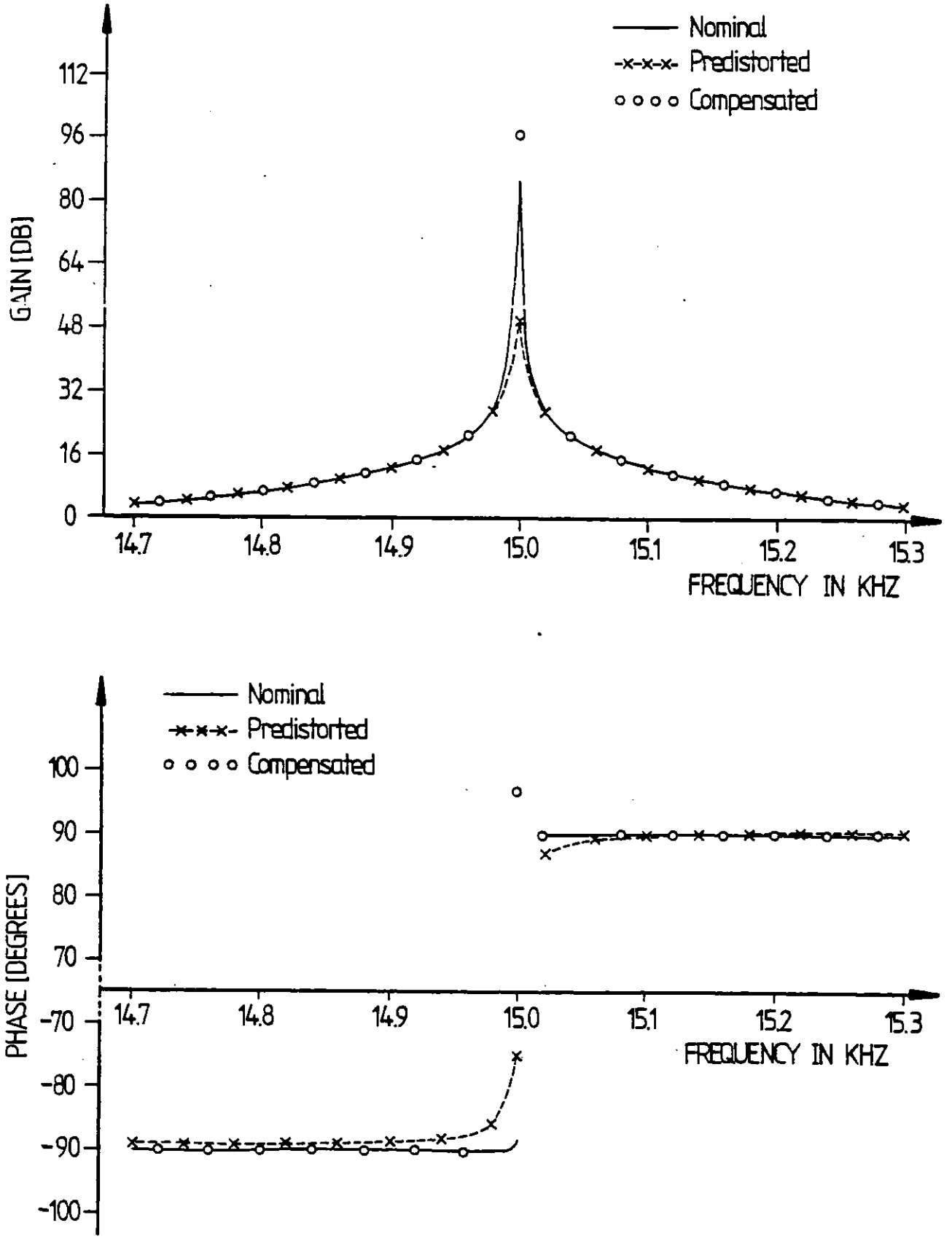

Fig 2.7 Comparison of the results of the nominal, predistorted and compensated designs of the Sallen and Key SAB bandpass circuit.

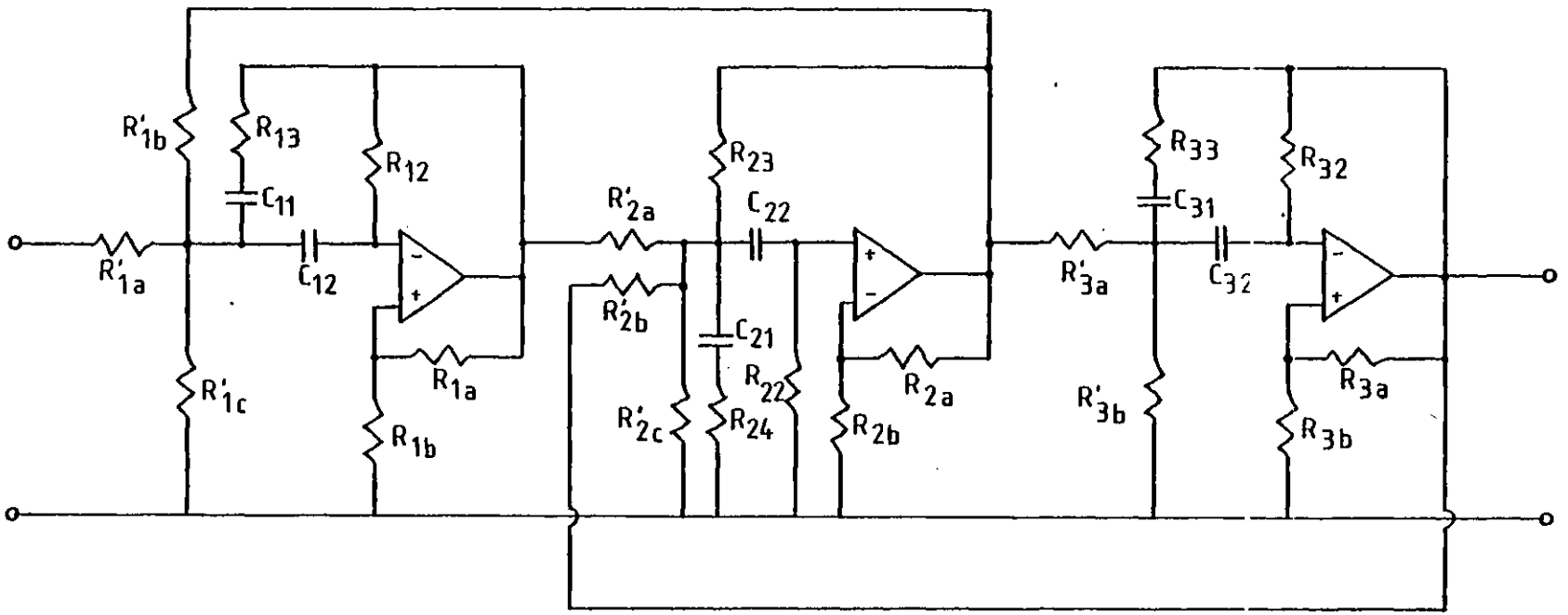

Fig 2.8 Sixth order multiple feedback bandpass filter.

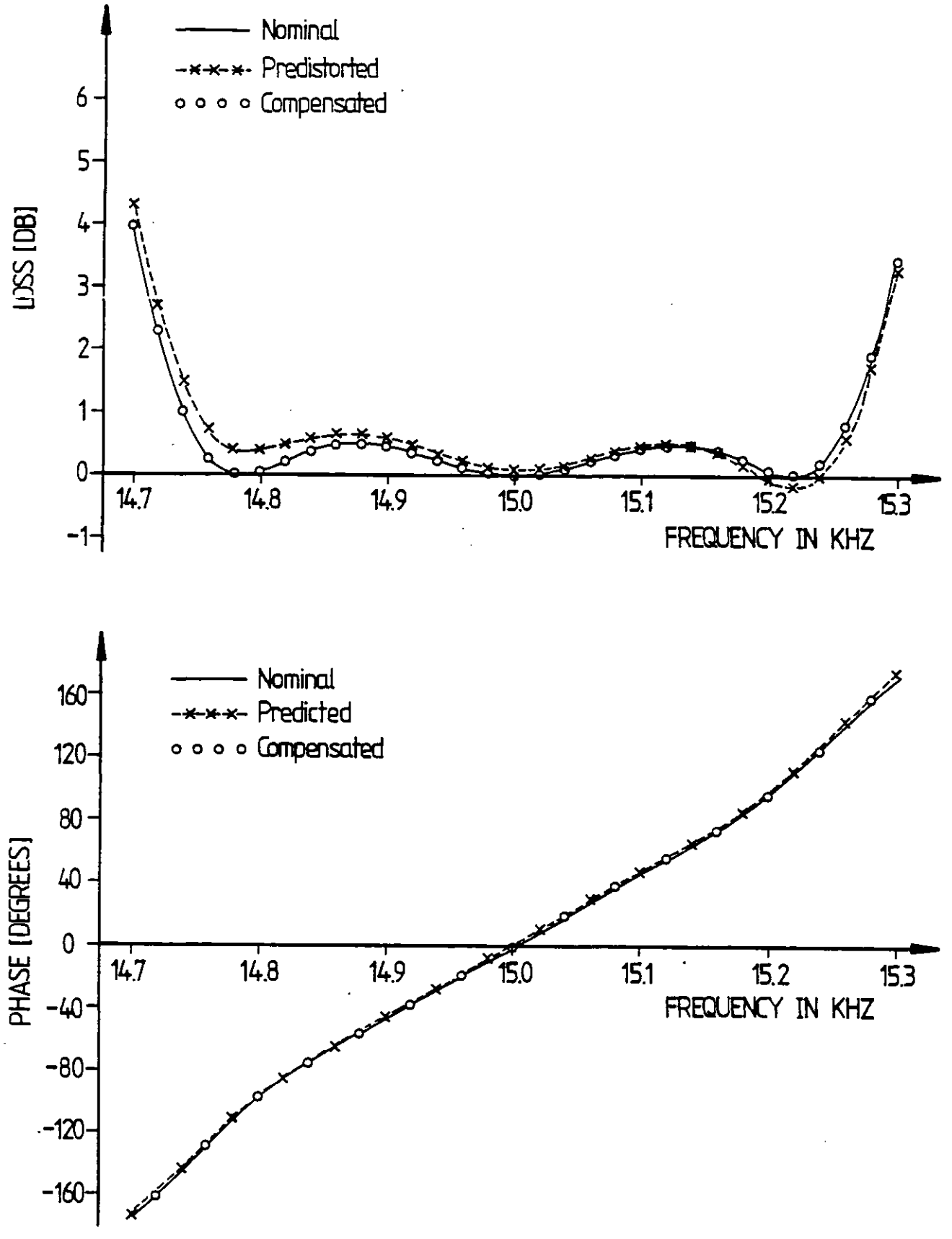

Fig 2.9 Comparison of the results of the nominal, predistorted and compensated designs of the multiple feedback filter of Fig 2.8.

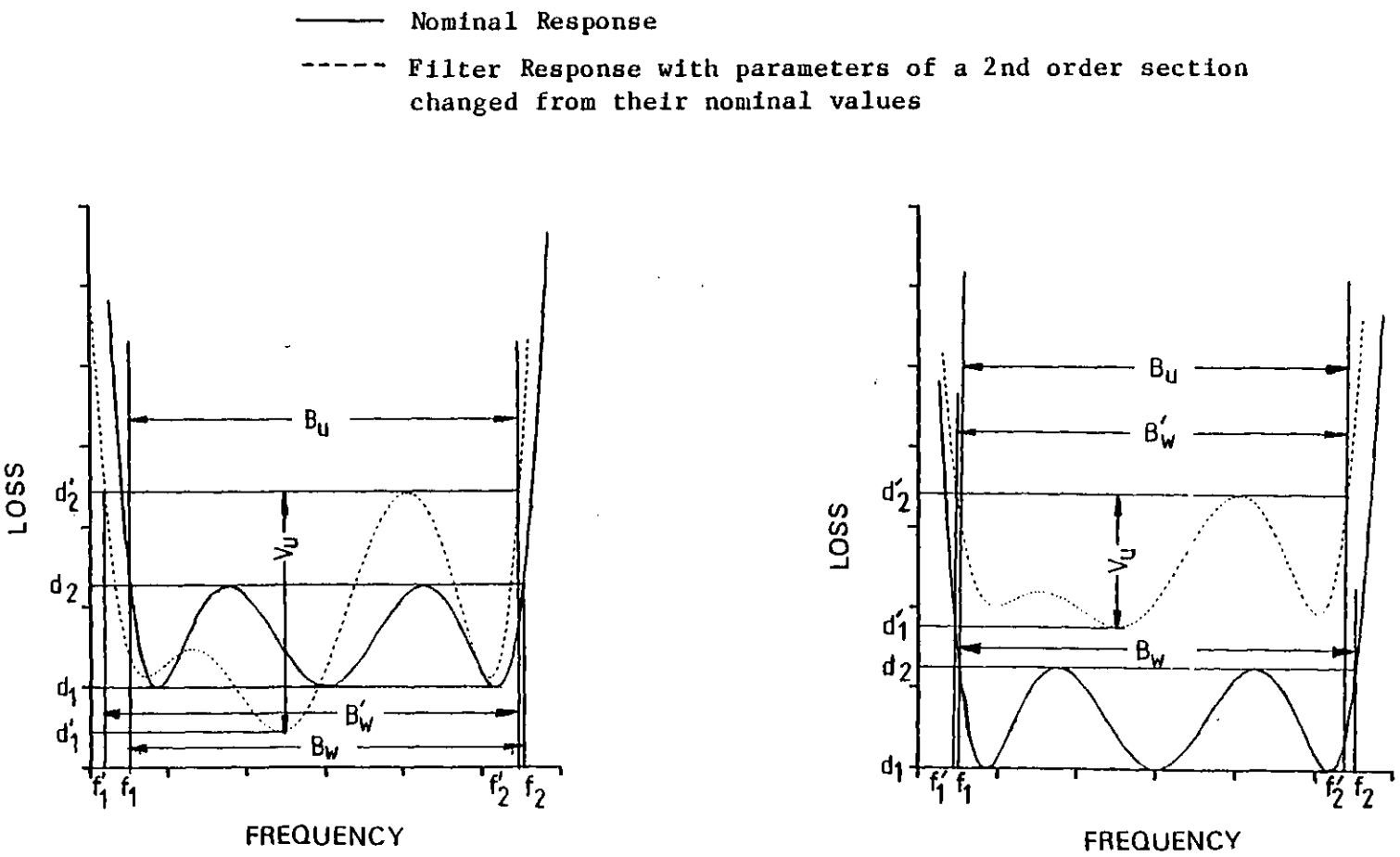

Fig 3.1 Determination of reduction in useful bandwidth and variation of loss in useful bandwidth.

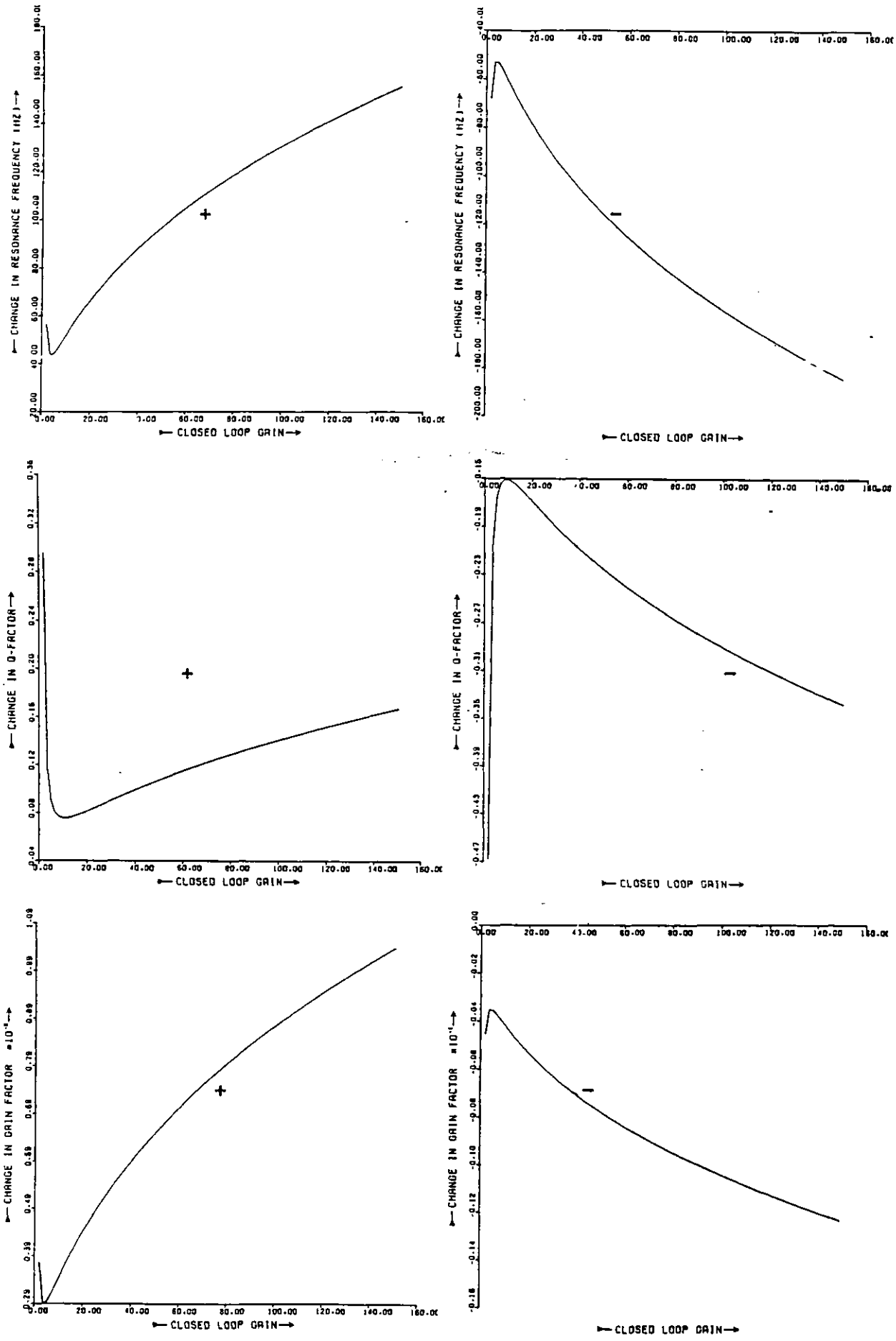

Fig 3.2 Changes produced in the resonance frequency, the Q-factor and the gain factor of the Friend circuit of Fig 2.2(b) when the f_T of the OP-AMP is changed by $\pm$ 10 %.

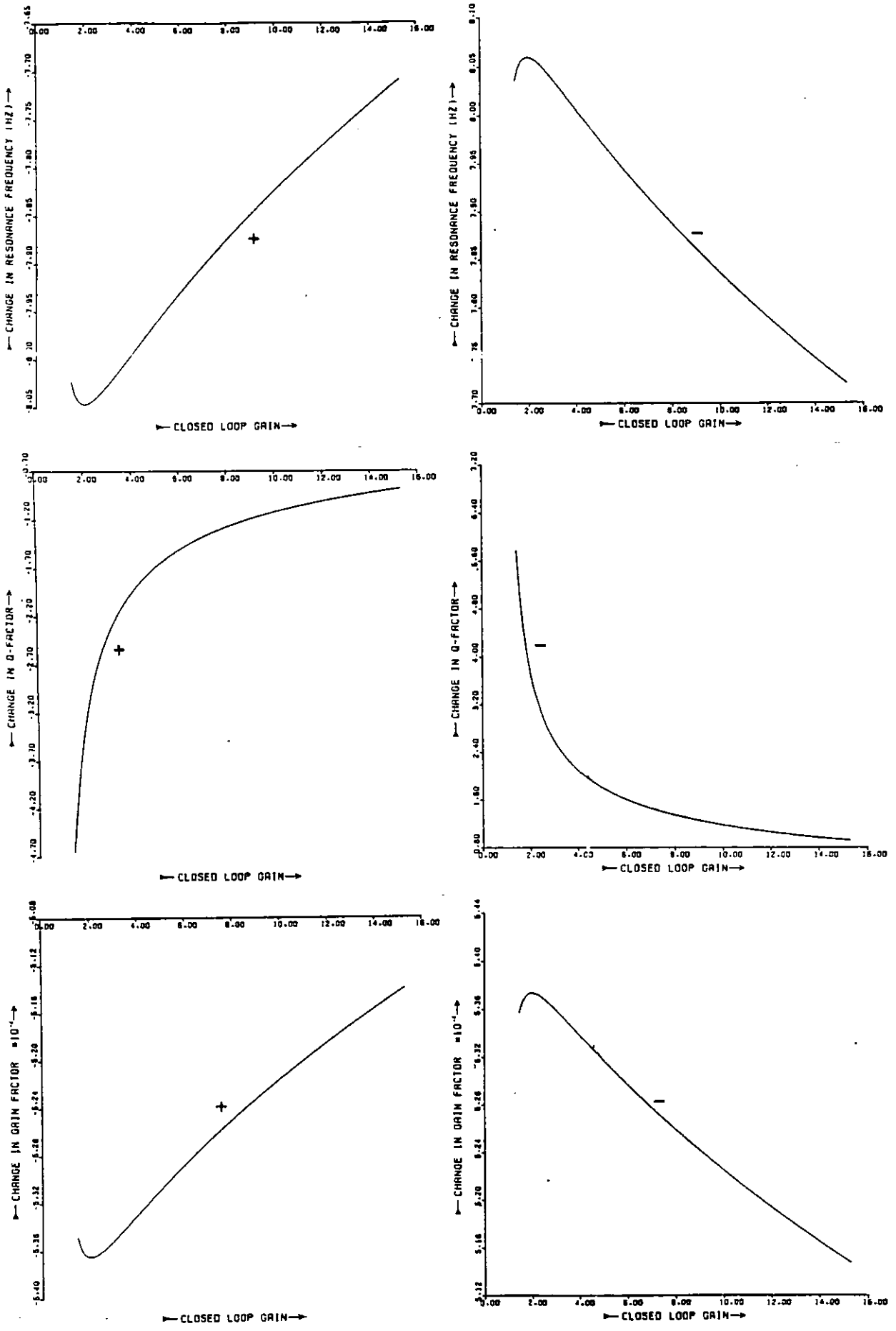

Fig 3.3 Changes produced in the resonance frequency, the Q-factor and the gain factor of the Friend circuit of Fig 2.2(b) when the value of resistor R_1 is changed by $\pm$ 0.112 %.

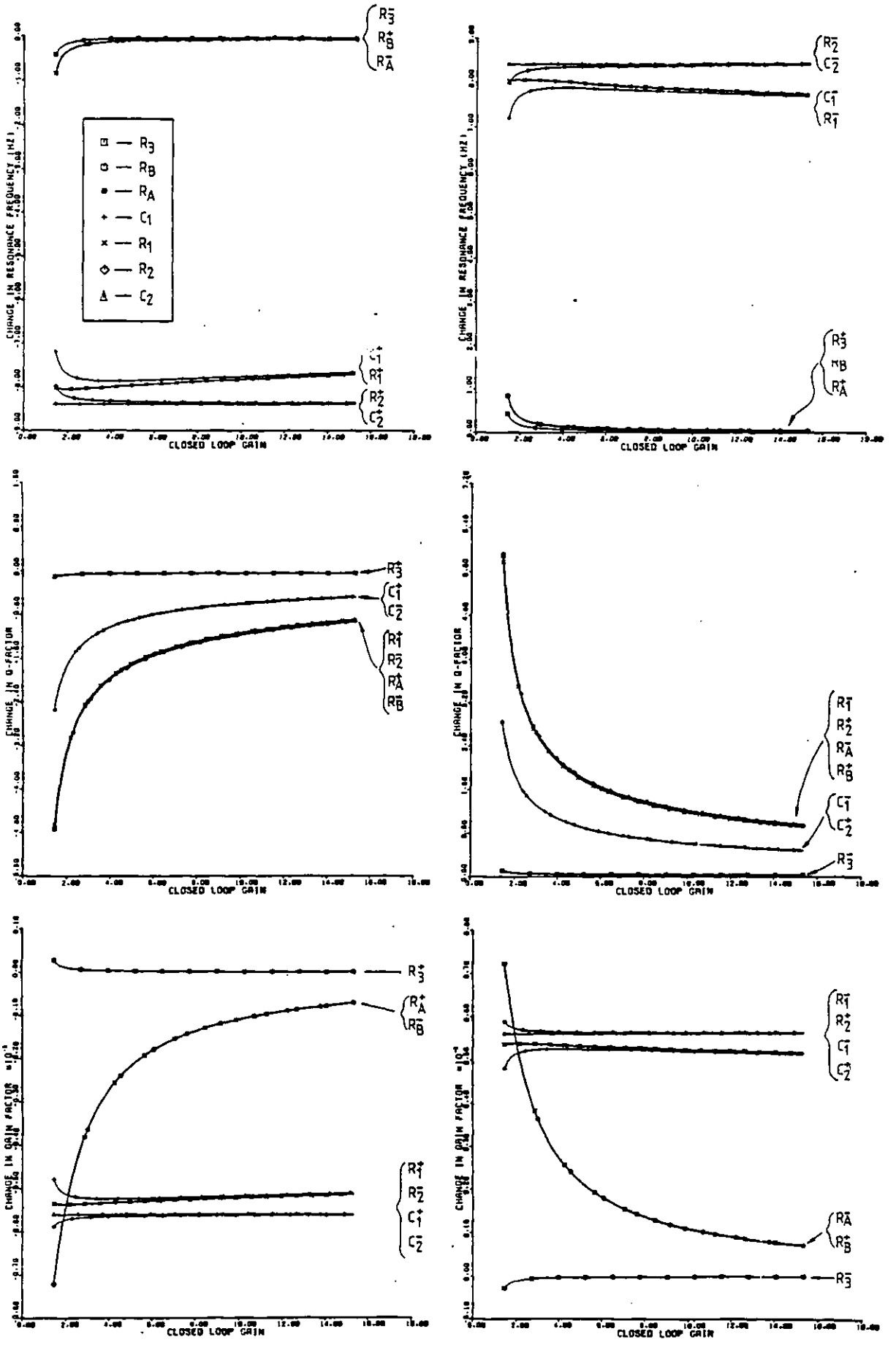

Fig 3.4 Changes produced in the resonance frequency, the Q-factor and the gain factor of the Friend circuit of Fig 2.2(b) when all the passive components of the circuit are varied, individually, by $\pm$ 0.112 % (R_1^+ implies + 0.112 % change in R_1, etc.).

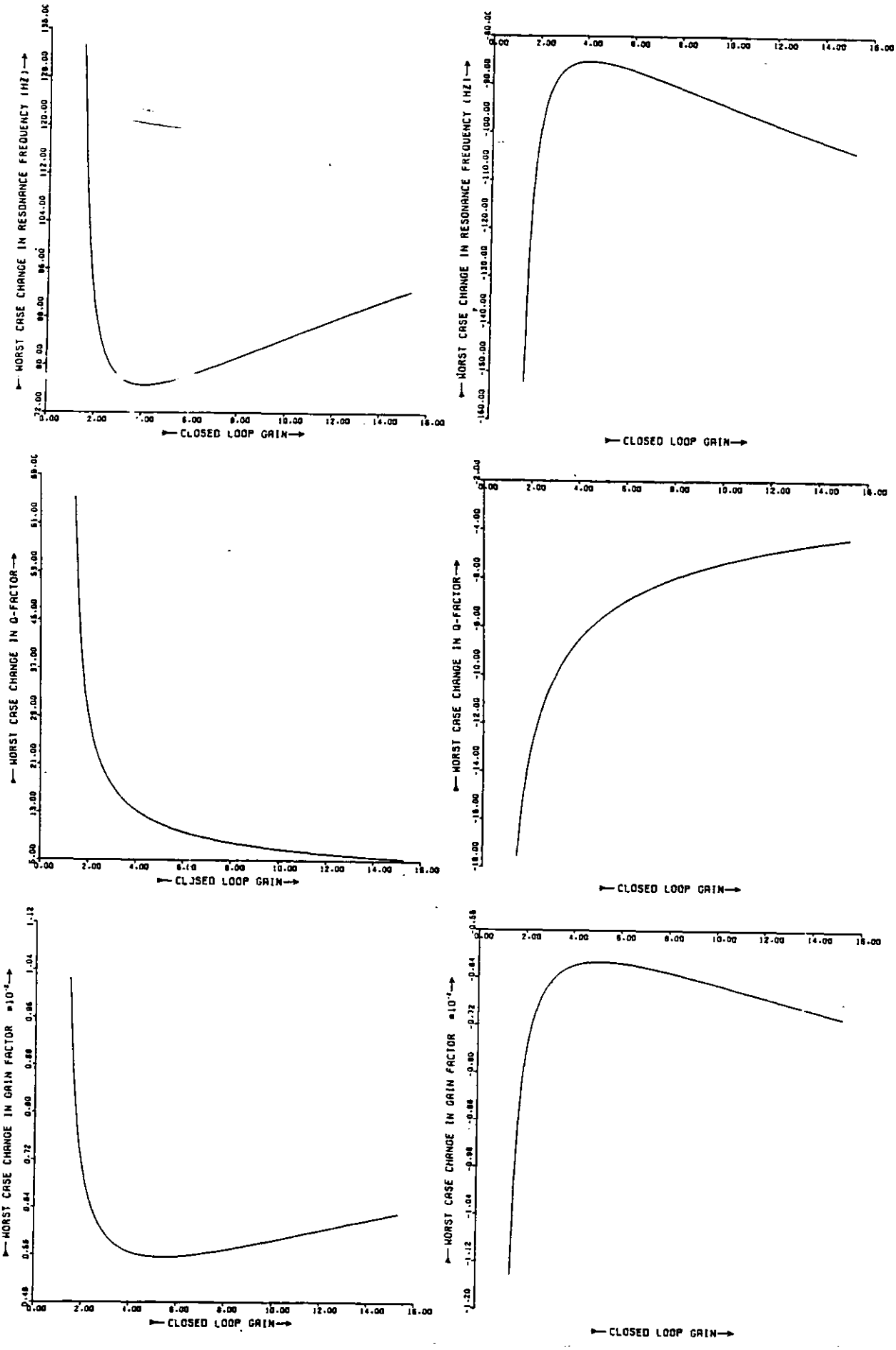

Fig 3.5 The worst case changes produced in the resonance frequency, the Q-factor and the gain factor when the passive components of the circuit of Fig 2.2(b) are varied by $\pm$ 0.112 % and the f_T of the OP-AMP is varied by $\pm$ 10 % according to Table 3.1.

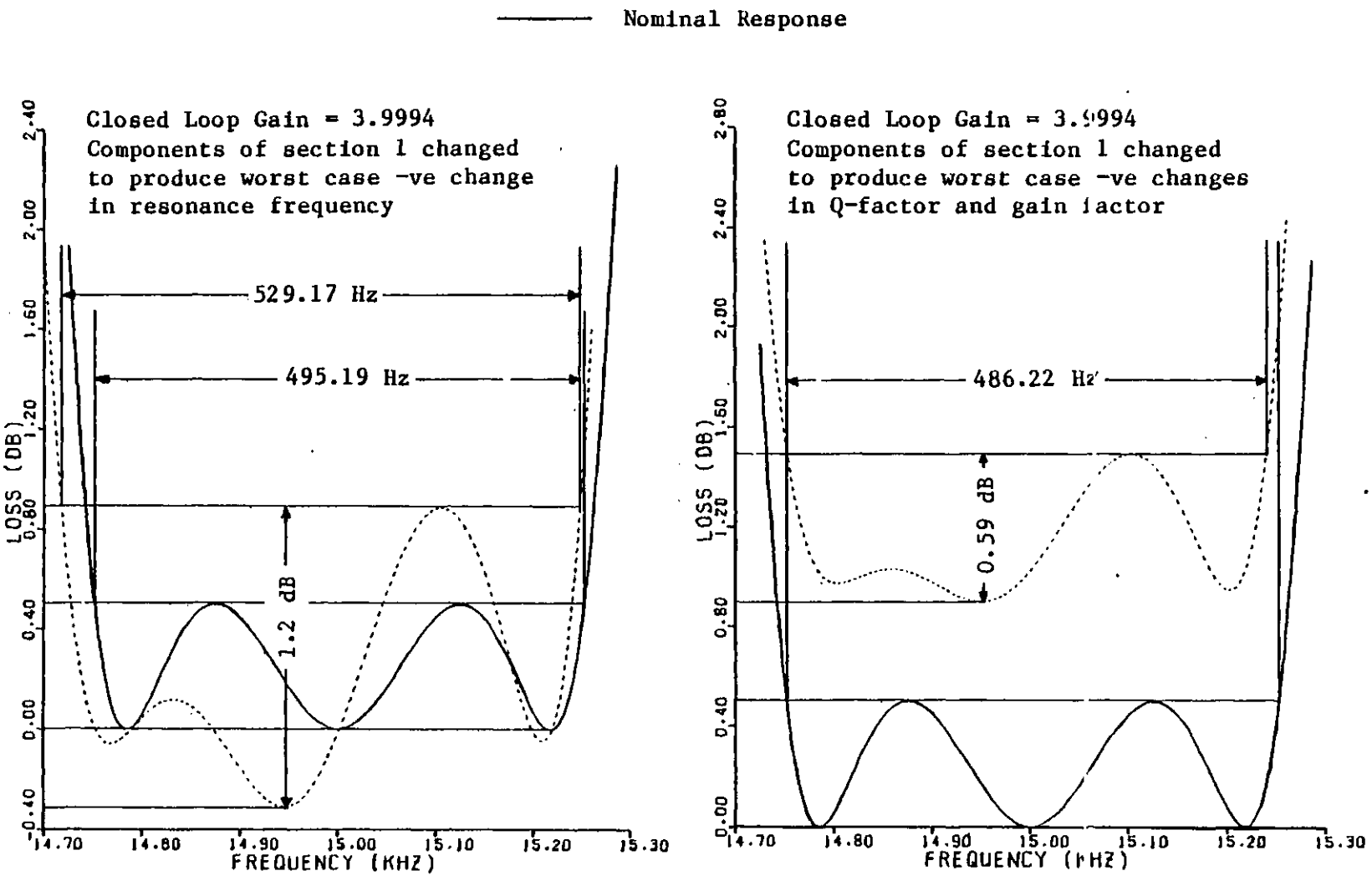

Fig 3.6 Typical graphs for determining reduction in useful bandwidth and variation of loss in useful bandwidth.

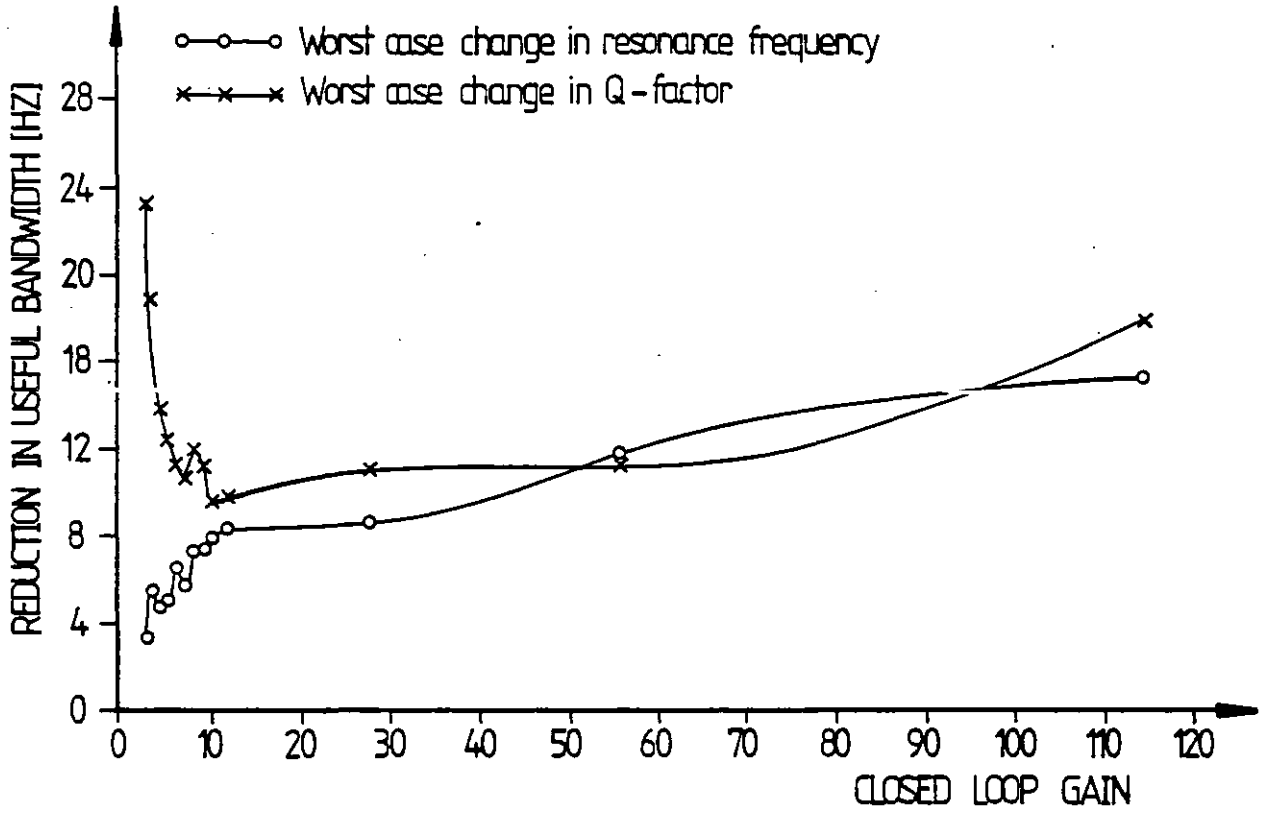

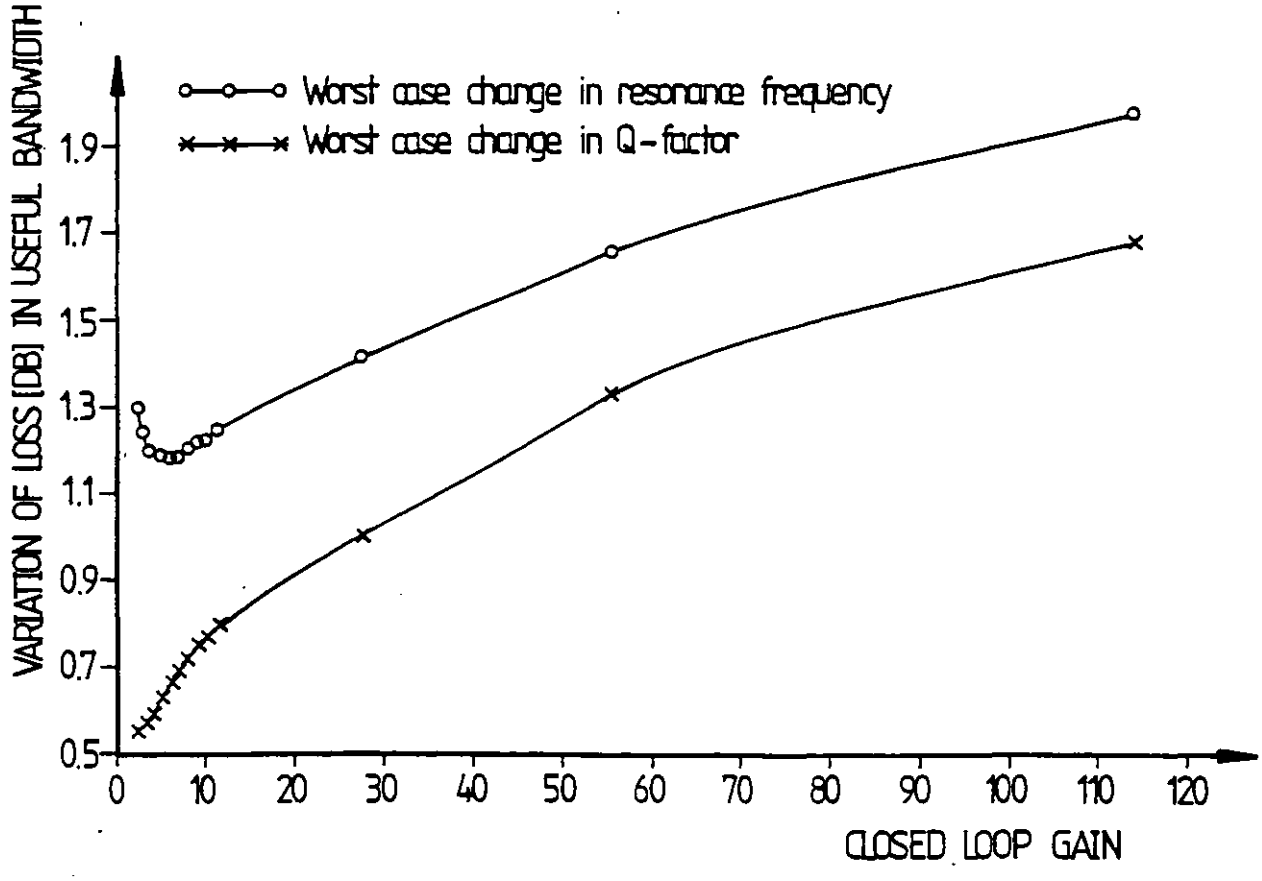

Fig 3.7 Plots of reduction in useful bandwidth and variation of loss in useful bandwidth against closed loop gain for the Friend SAB bandpass circuit realising the 1st second order section in Fig 2.8.

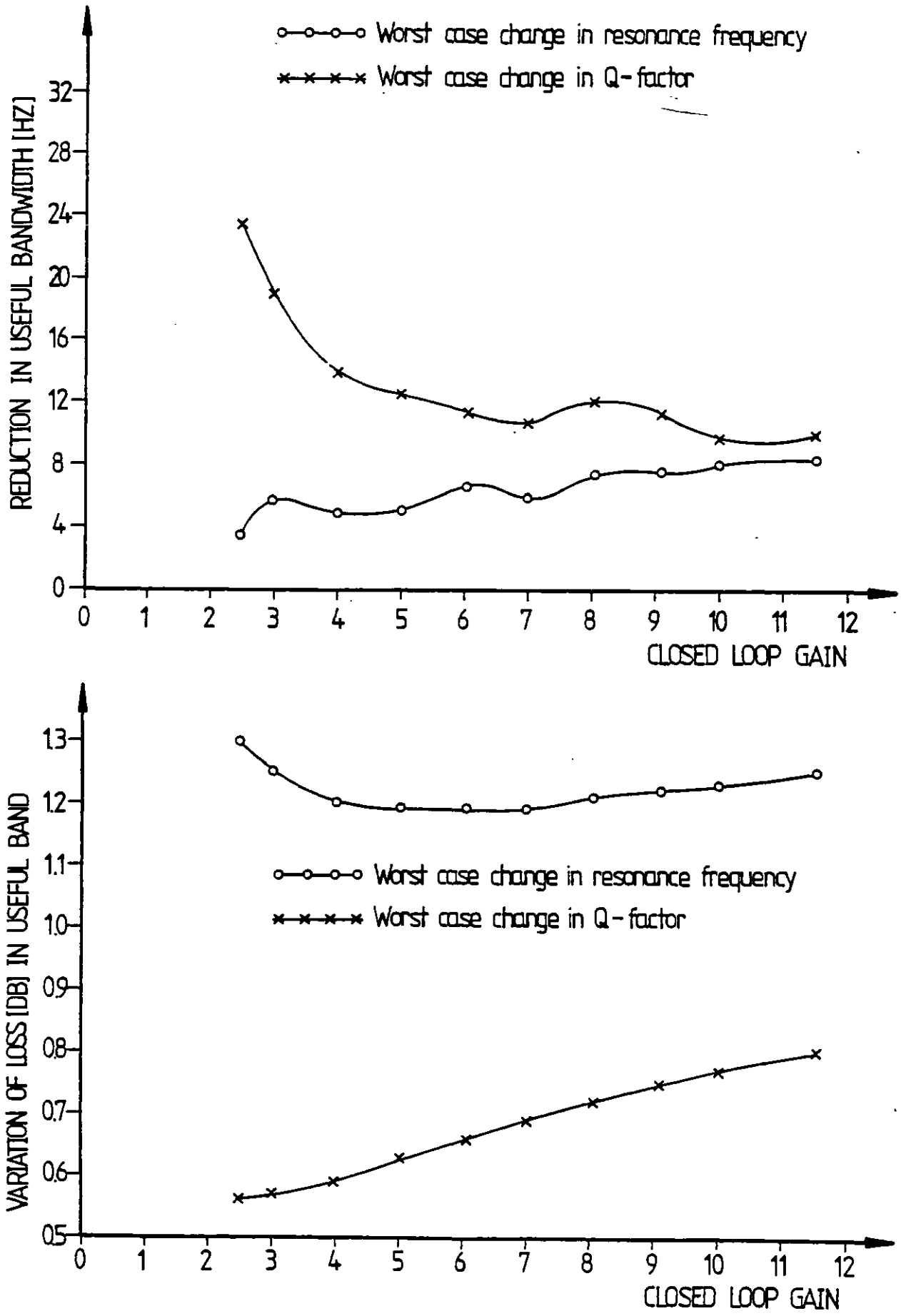

Fig 3.8 Expanded version of the plots in Fig 3.7.

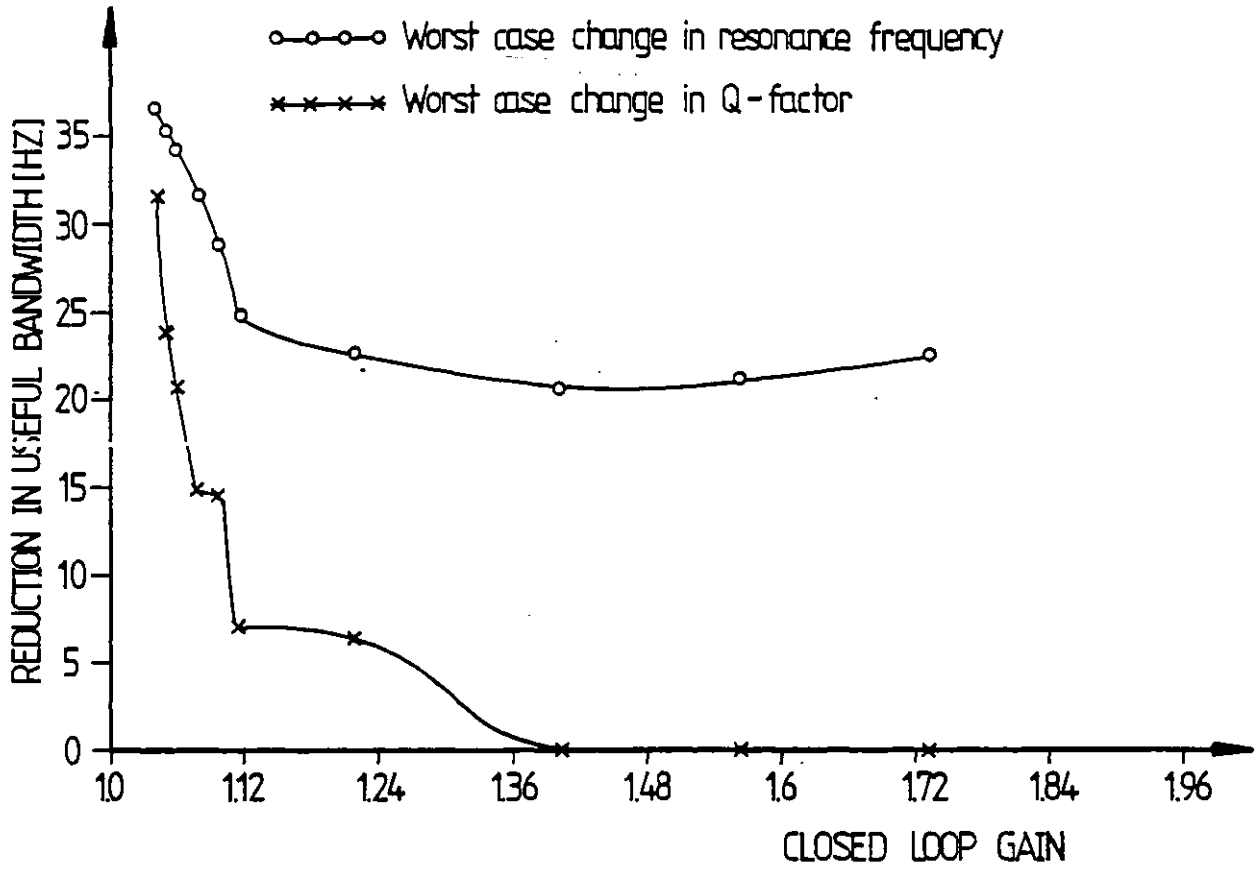

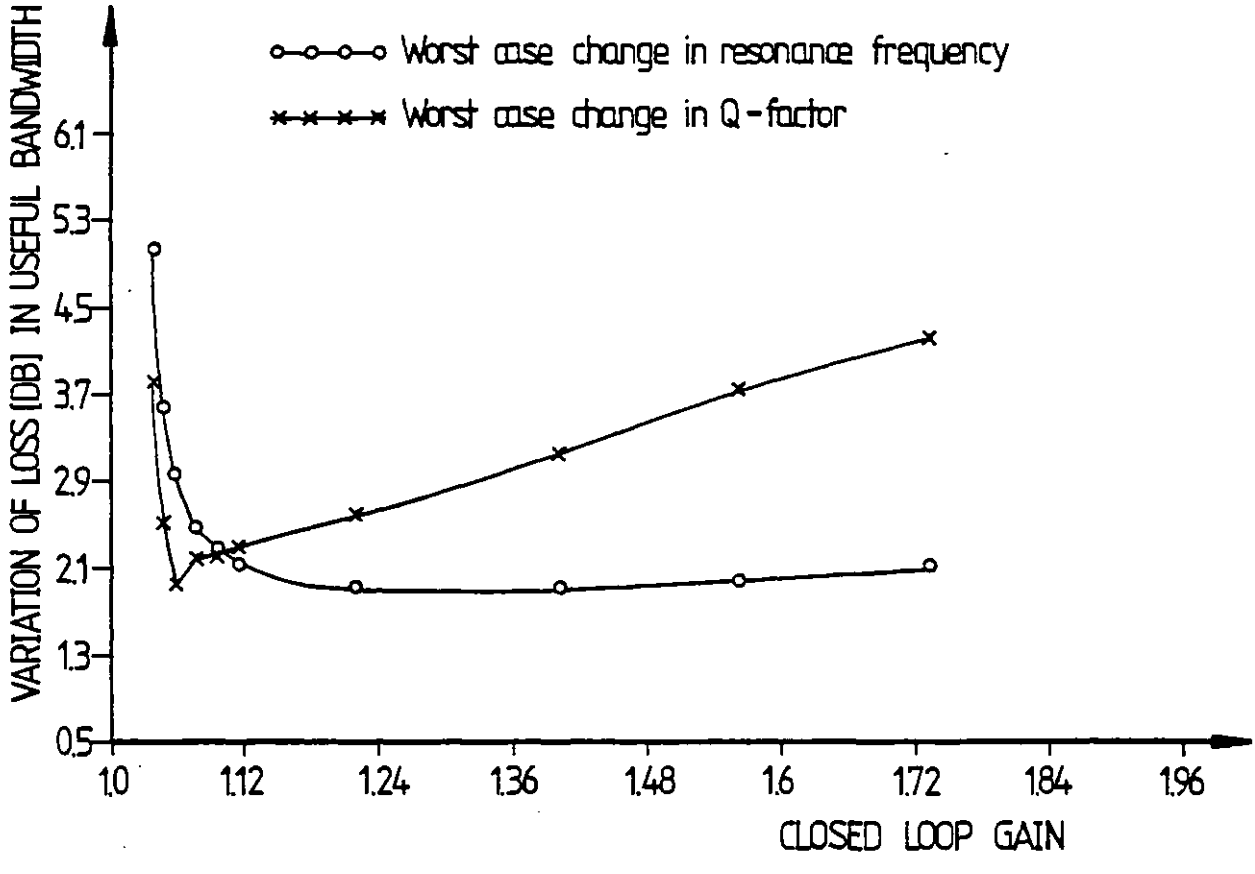

Fig 3.9 Plots of reduction in useful bandwidth and variation of loss in useful bandwidth against closed loop gain for the Sallen and Key SAB bandpass circuit realising the 2nd second order section in Fig 2.8.

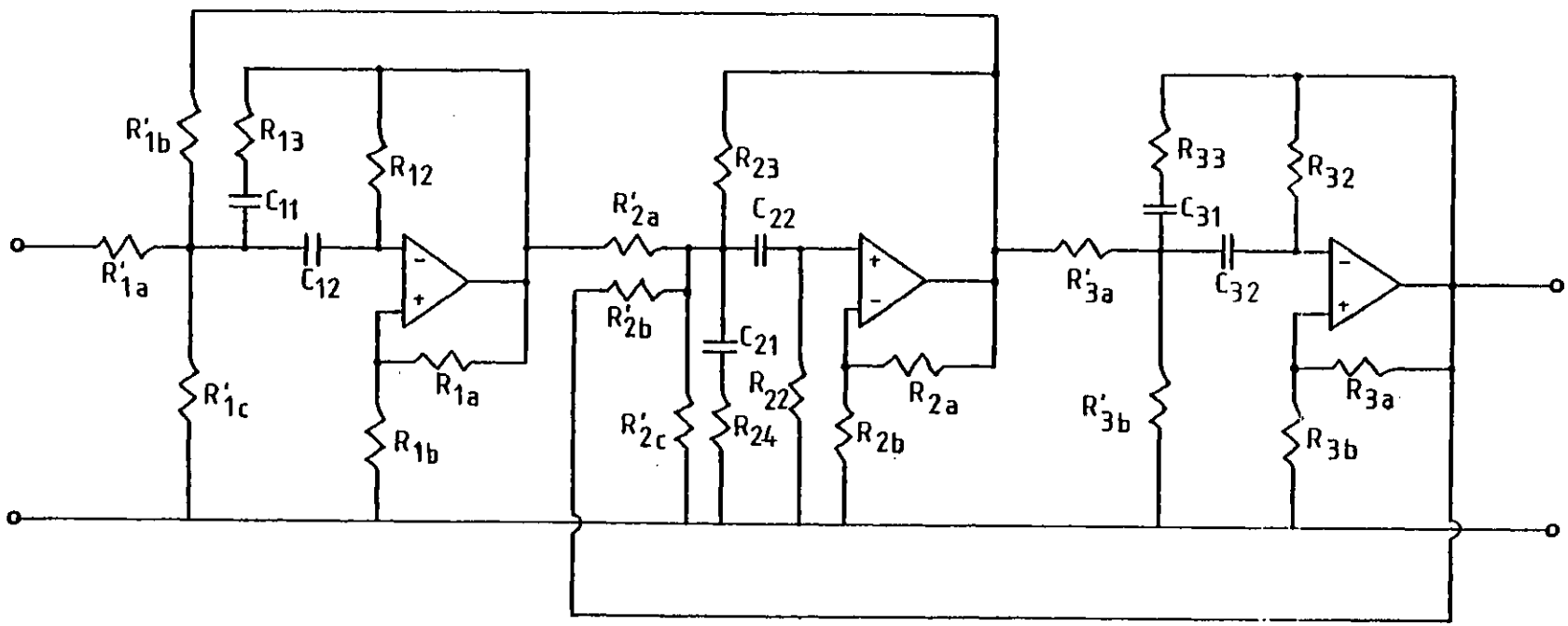

Fig 3.10 Sixth order multiple feedback bandpass filter.

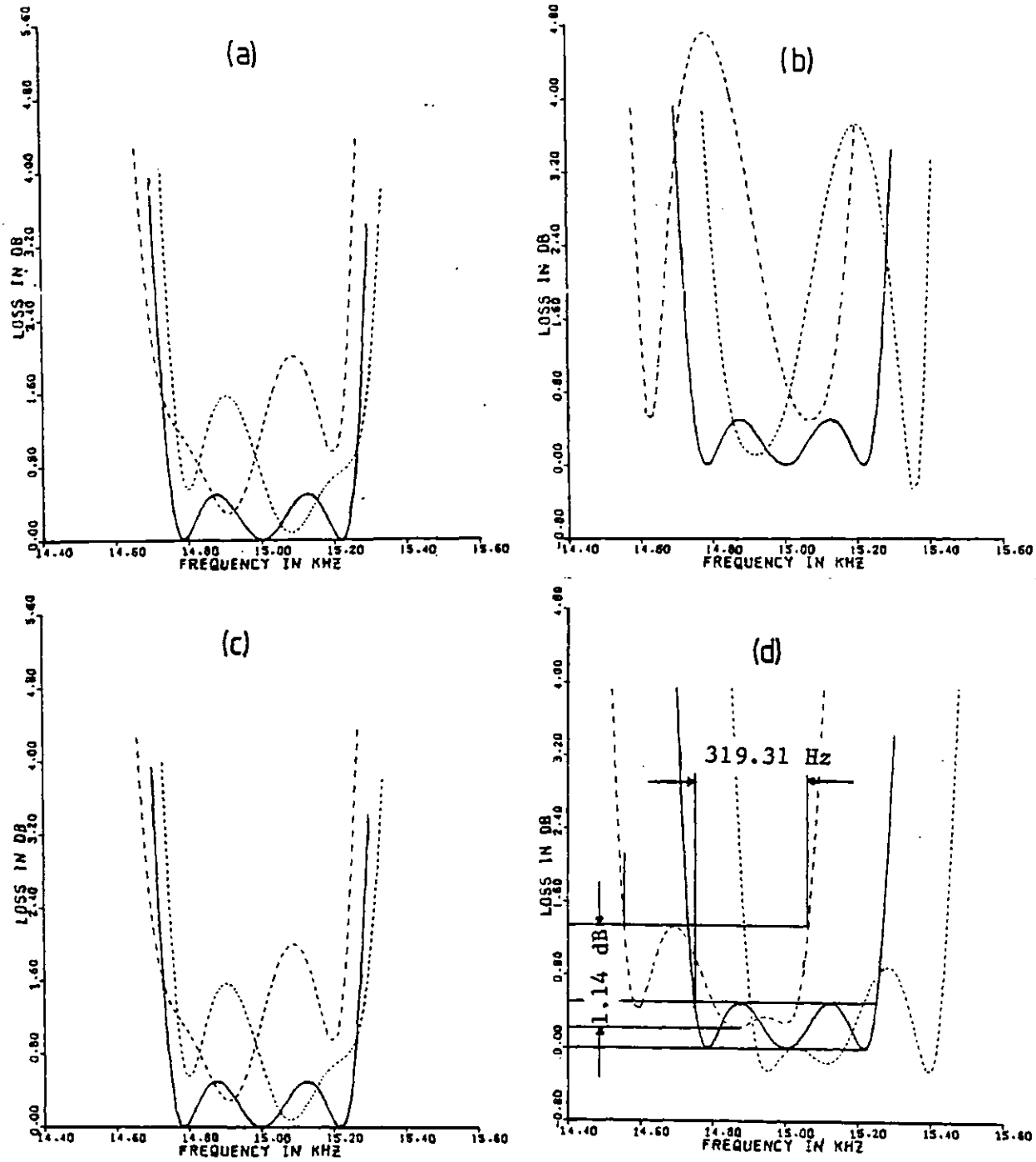

Fig 3.11 Effect of f_T variation on the frequency response of the un-optimised design of the 6th order bandpass filter. (a) f_T of OP-AMP one changed by $\pm$ 10 %. (b) f_T of OP-AMP two changed by $\pm$ 10 %. (c) f_T of OP-AMP three changed by $\pm$ 10 %. (d) f_Ts of all three OP-AMPs changed by $\pm$ 10 %.

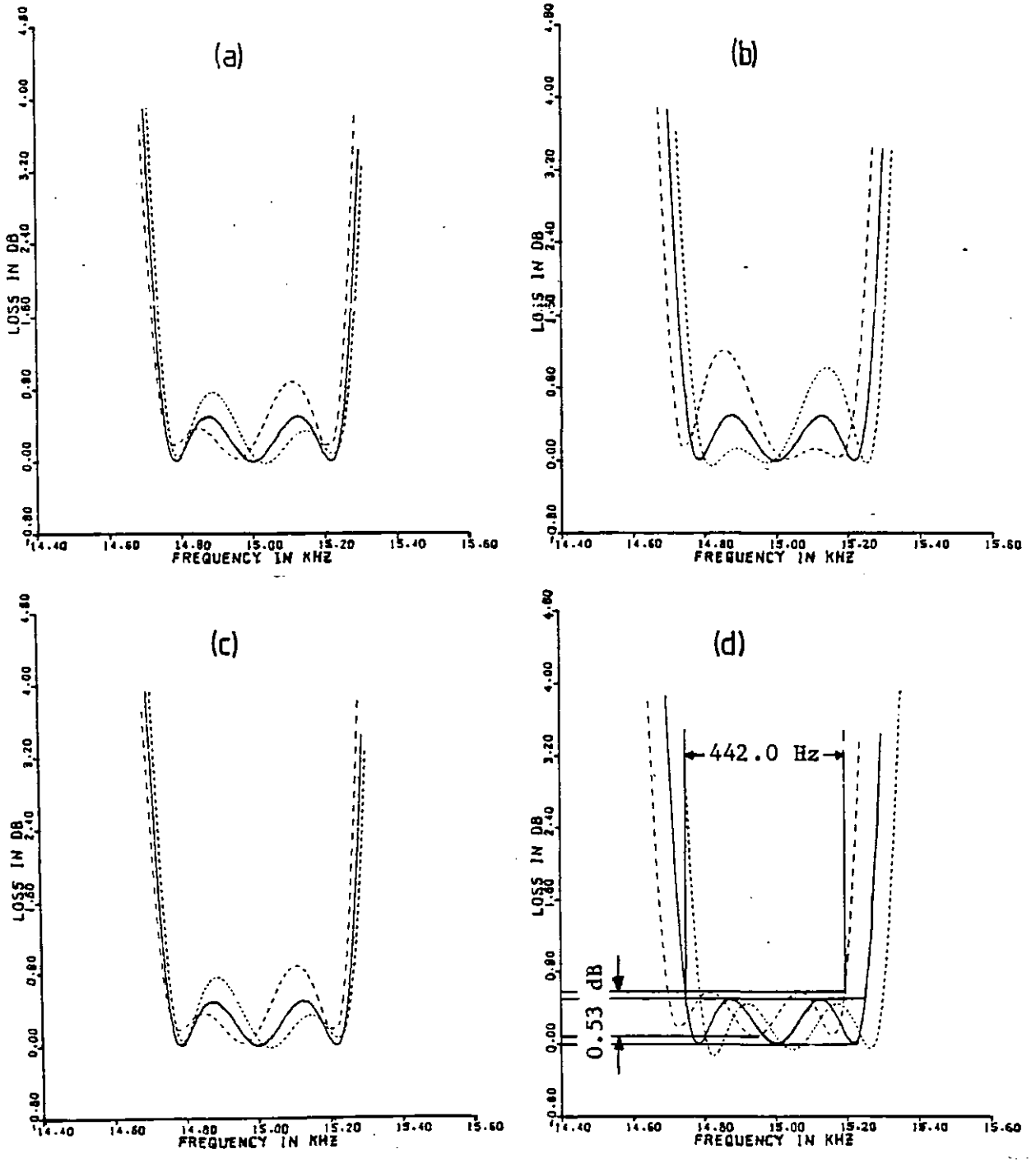

Fig 3.12 Effect of f_T variation on the frequency response of the optimised design of the 6th order bandpass filter. (a) f_T of OP-AMP one changed by $\pm$ 10 %. (b) f_T of OP-AMP two changed by $\pm$ 10 %. (c) f_T of OP-AMP three changed by $\pm$ 10 %. (d) f_T's of all three OP-AMPs changed by $\pm$ 10 %.

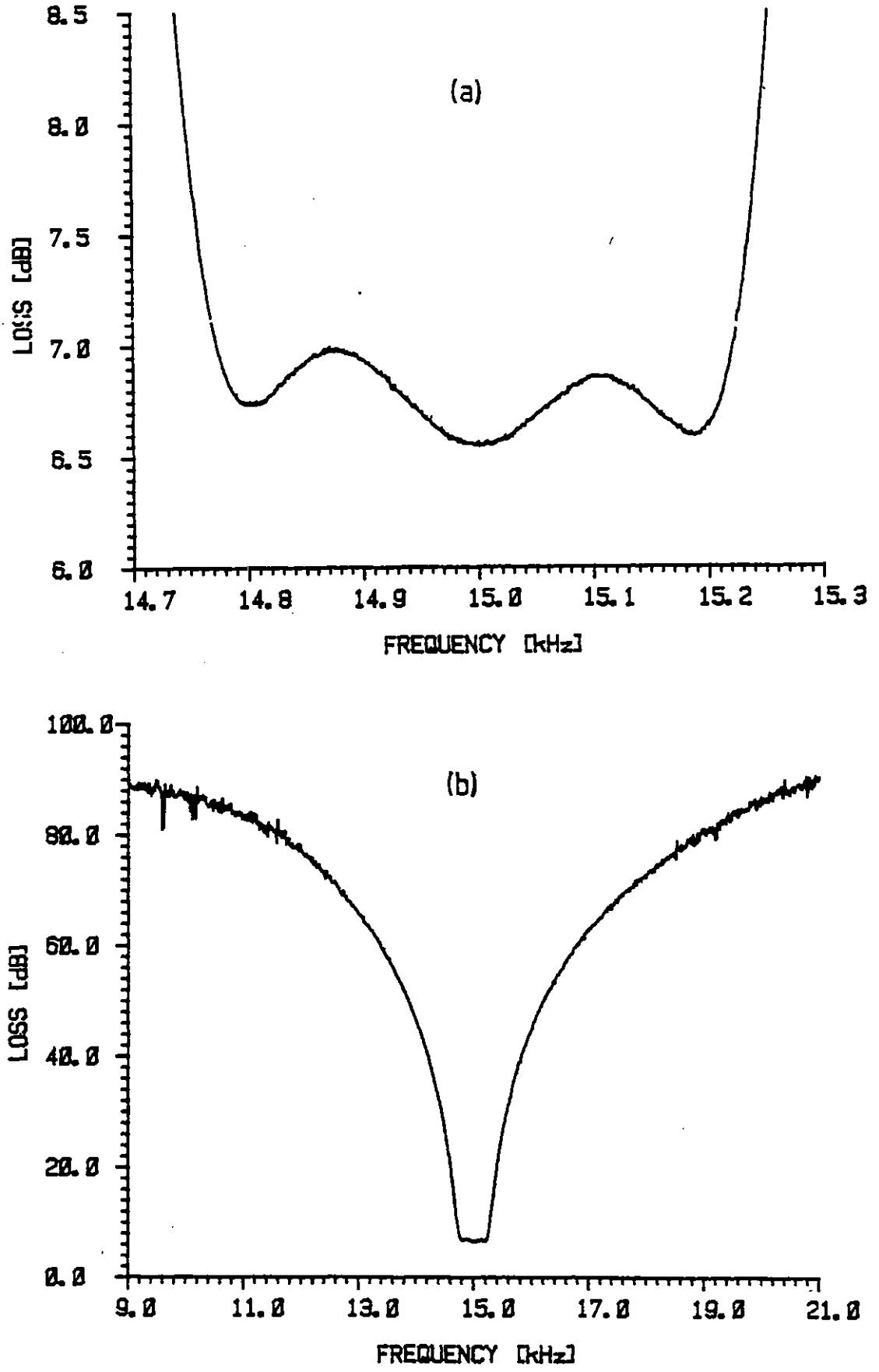

Fig 3.13 Measured frequency responses of the discrete component model of the 6th order multiple feedback filter of Fig 3.10.
(a) Passband response. (b) Stopband response.

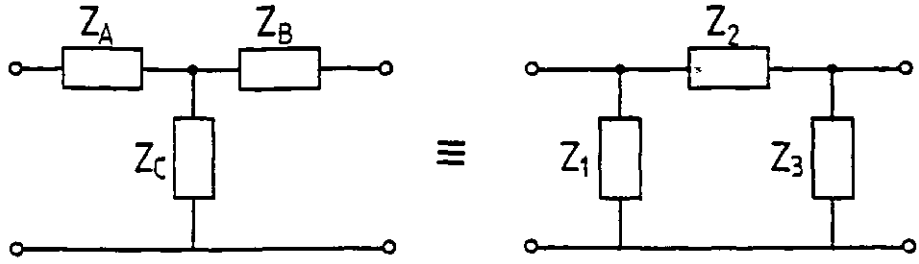

Fig 4.1 Equivalent star-delta networks.

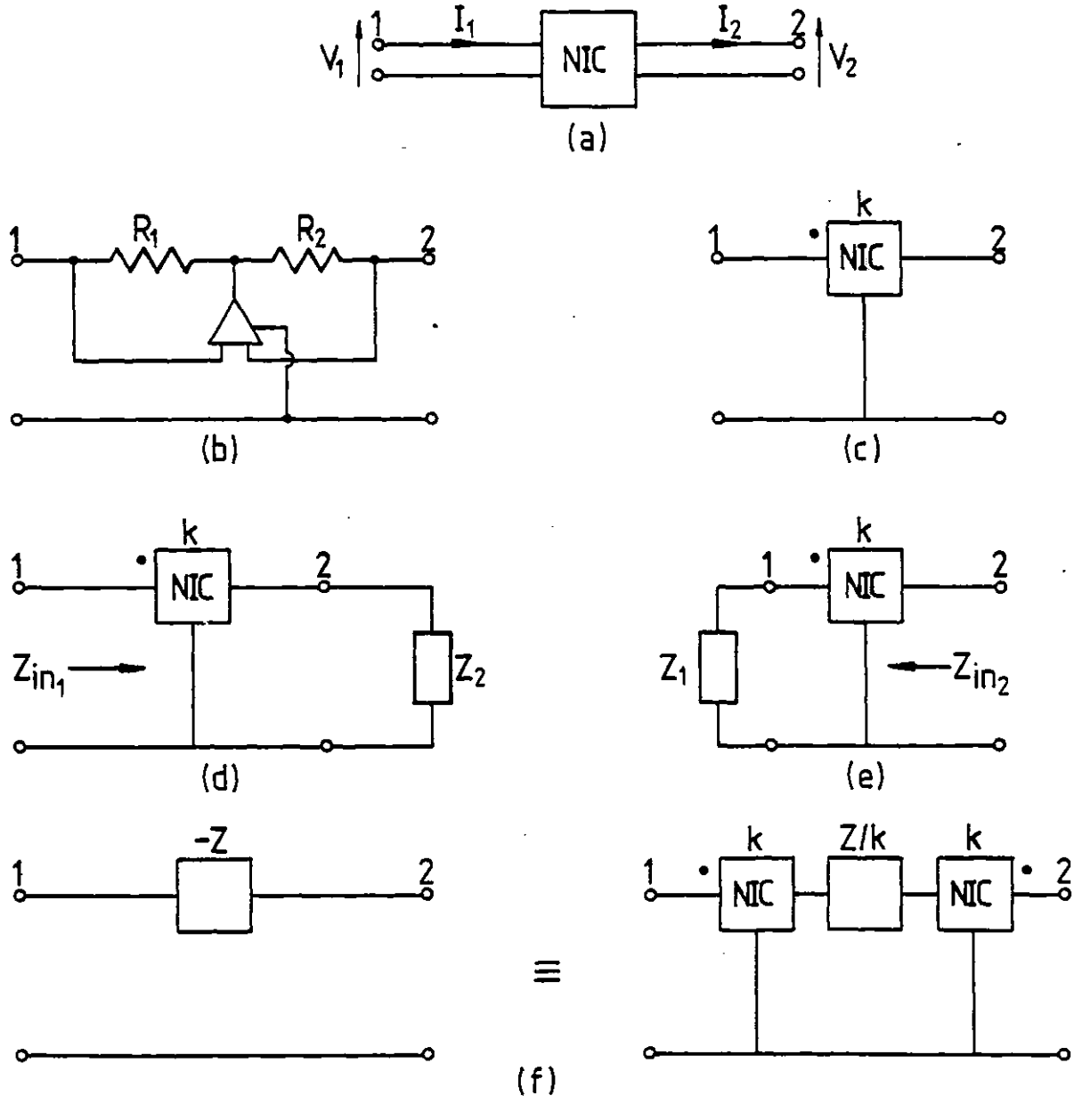

Fig 4.2 Definition and properties of Negative Impedance Converter (NIC) circuit.
(a) Schematic diagram of NIC circuit. (b) Realisation of an NIC circuit. (c) Symbolic representation of an NIC circuit. (d) NIC terminated at port 2. (e) NIC terminated at port 1. (f) Realisation of a floating negative impedance using NICs.

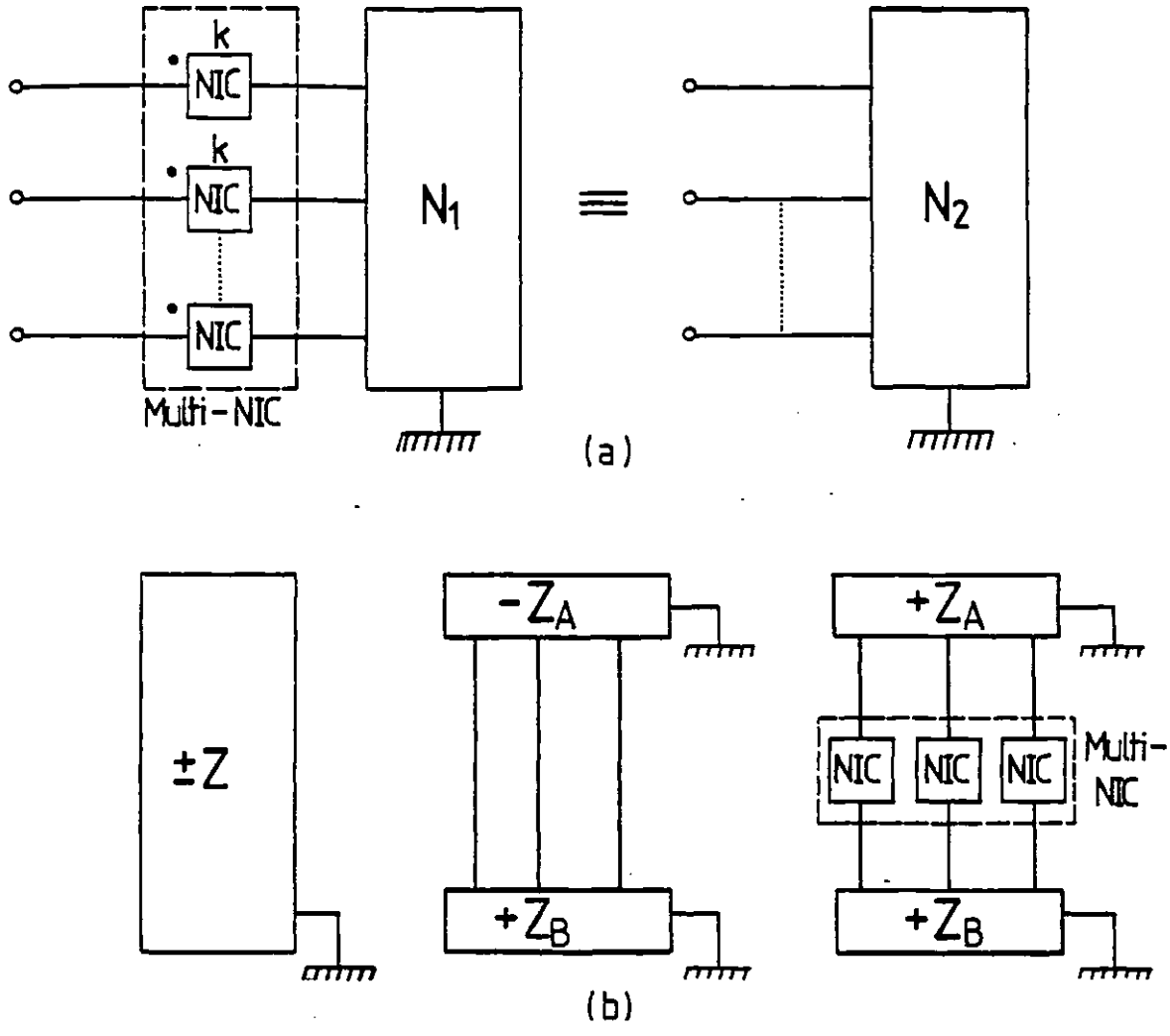

Fig 4.3 Some uses of NICs.
(a) Multi-NIC terminated in a network N_1. (b) Realisation of a network containing positive and negative impedances with positive impedances and a multi-NIC .

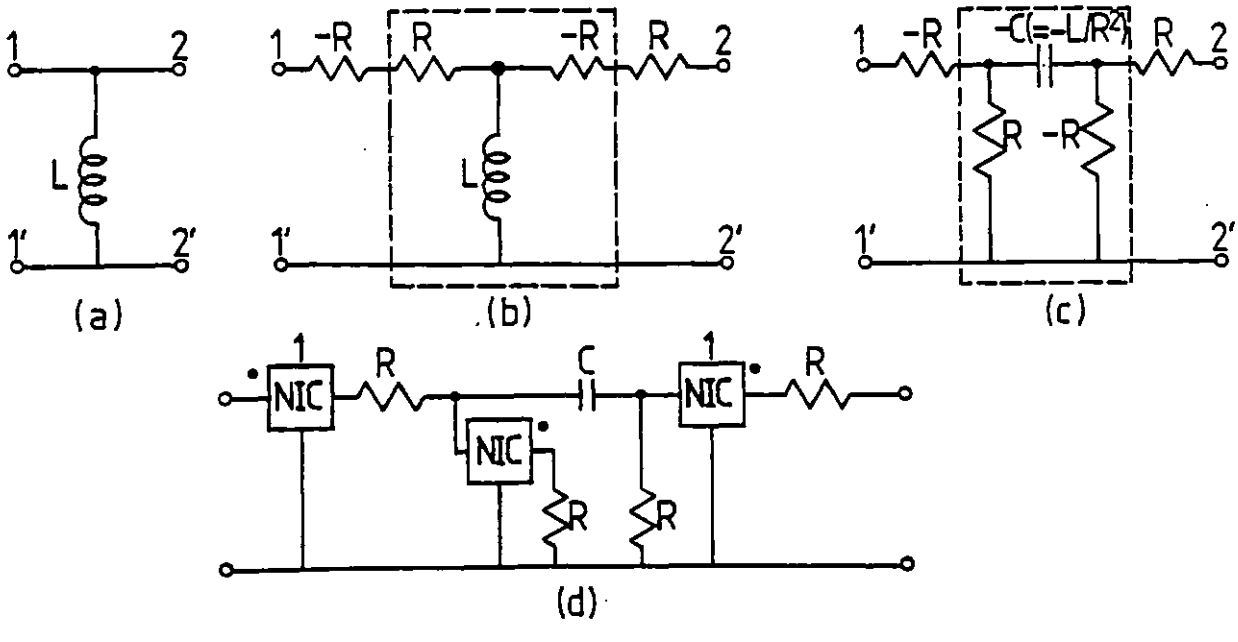

Fig 4.4 Equivalent grounded inductor 2-ports.

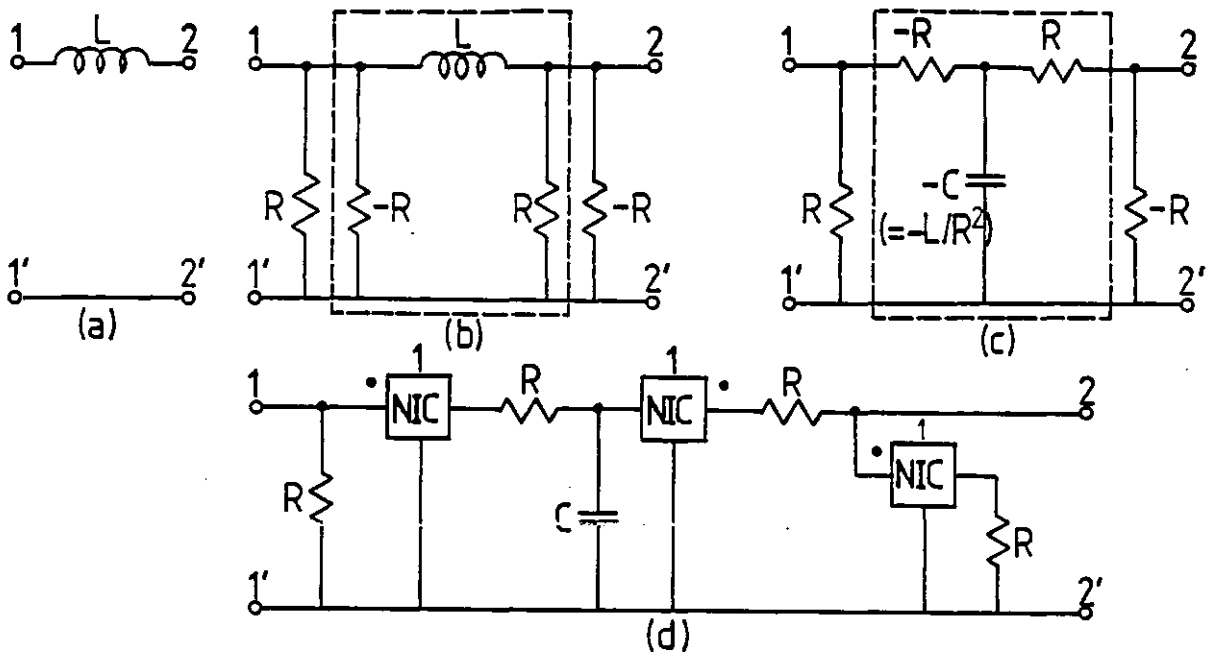

Fig 4.5 Equivalent floating inductor 2-ports.

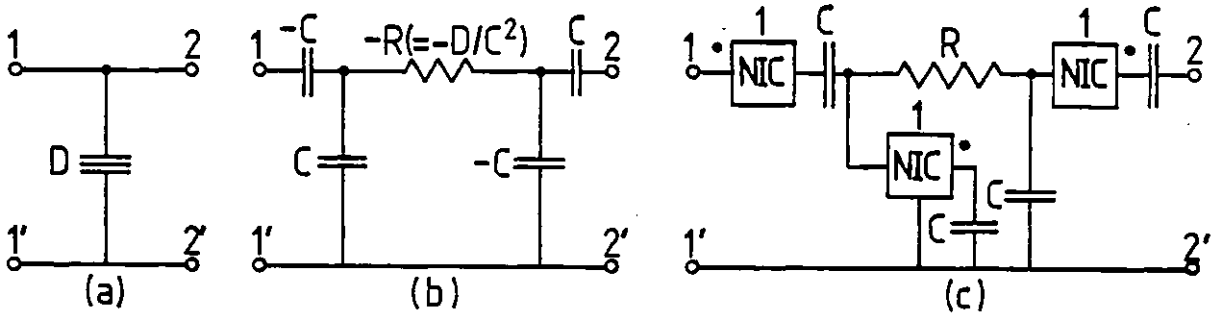

Fig 4.6 Equivalent grounded supercapacitor 2-ports.

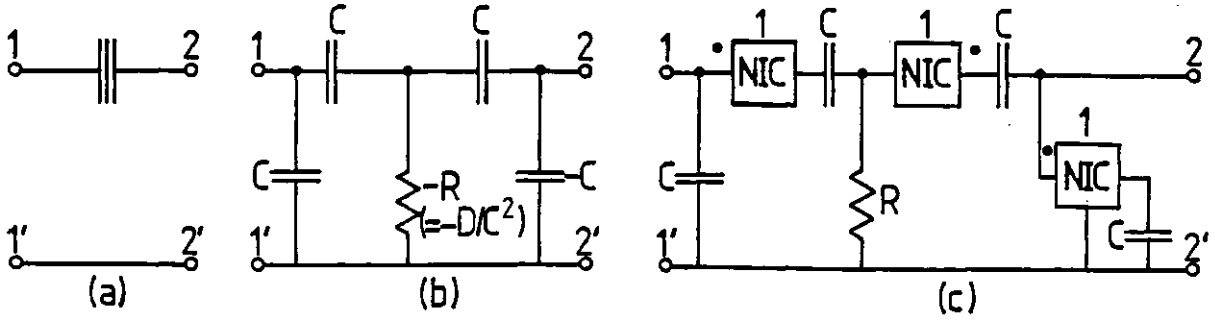

Fig 4.7 Equivalent floating supercapacitor 2-ports.

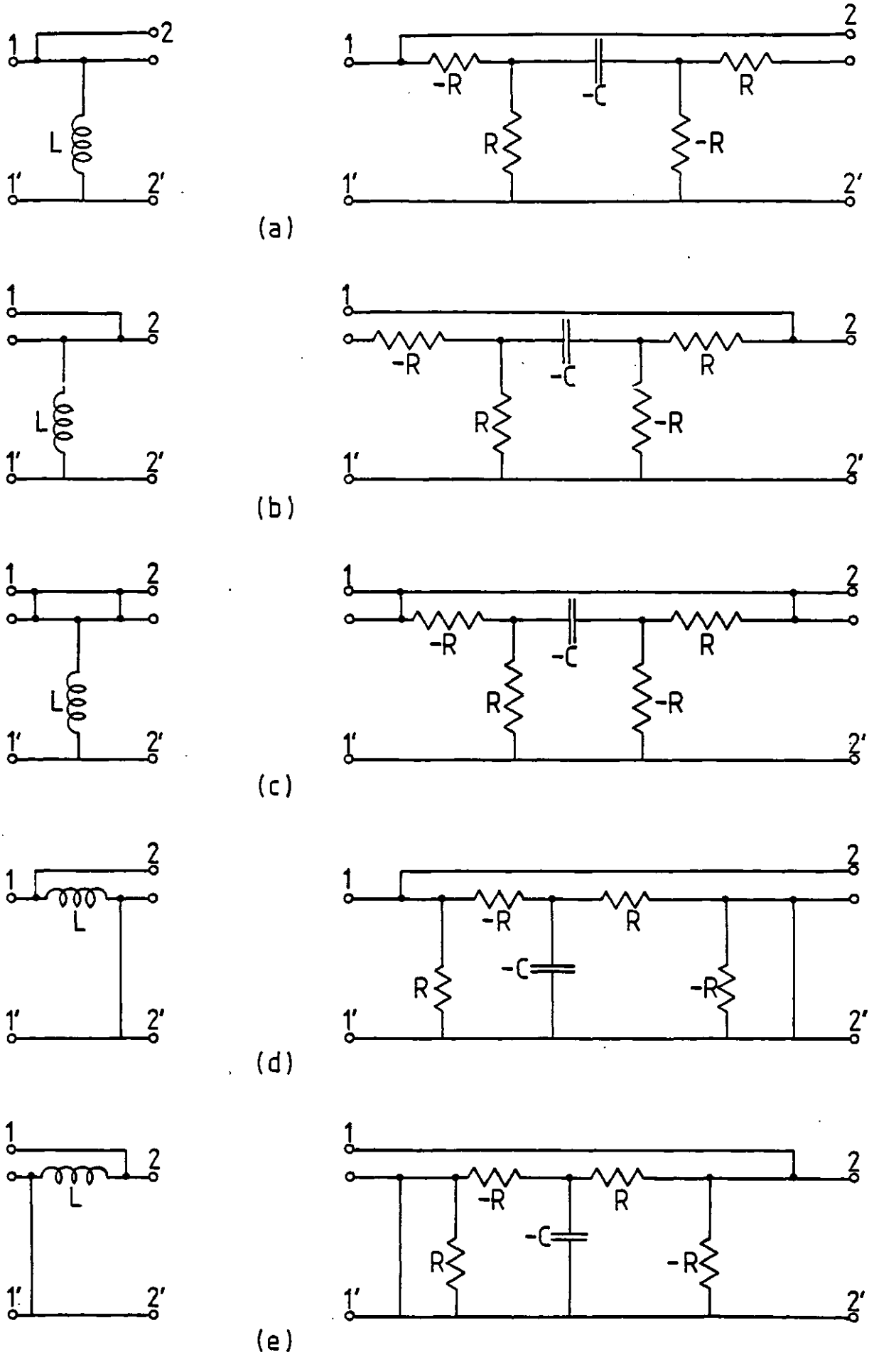

Fig 4.8 Derivation of the $\pm R$, $\pm C$ circuits for simulating grounded inductors by "terminal modification" in Figs 4.4 and 4.5.

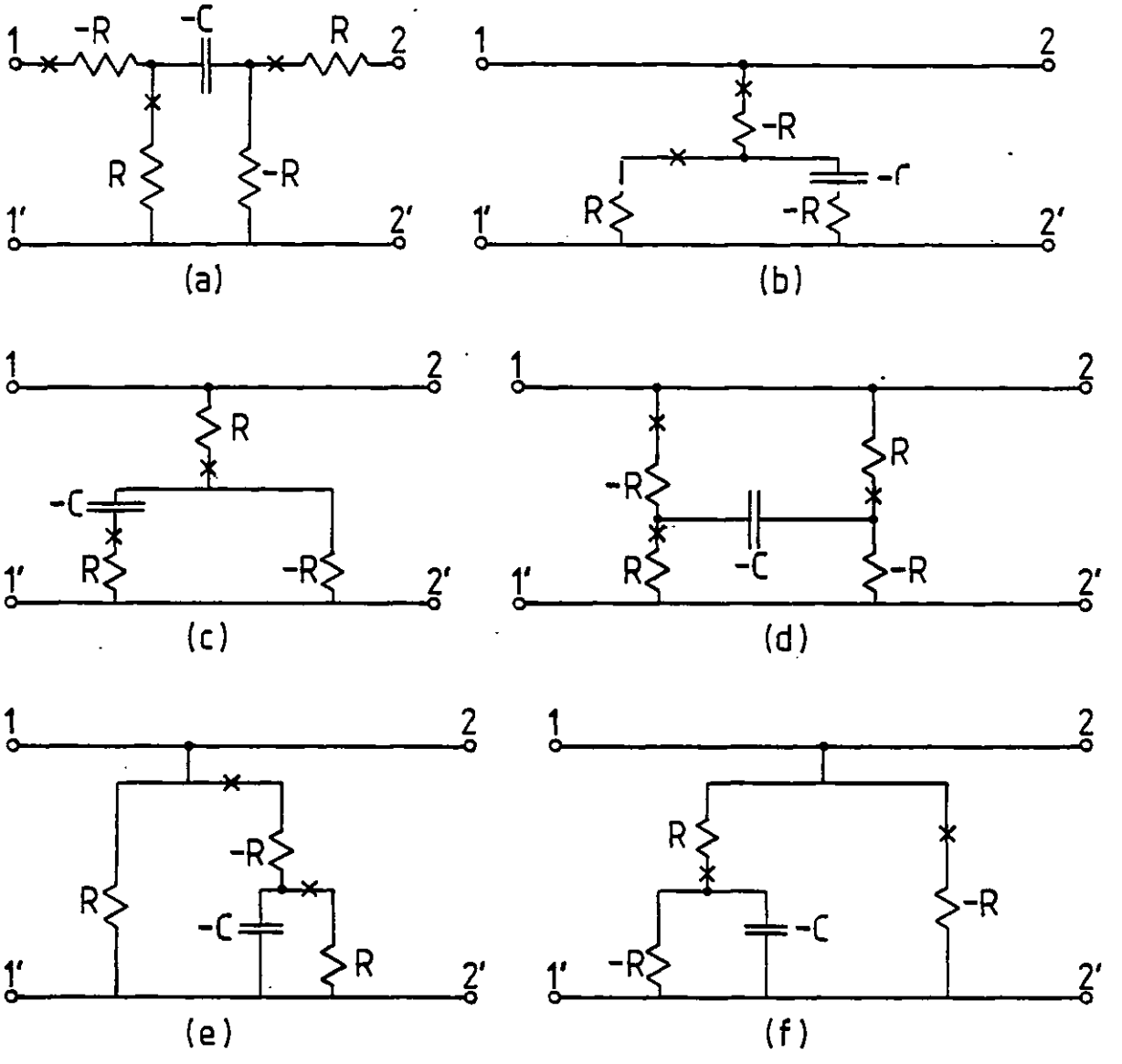

Fig 4.9 A set of $\pm R$, $\pm C$ circuits for simulating grounded inductors.

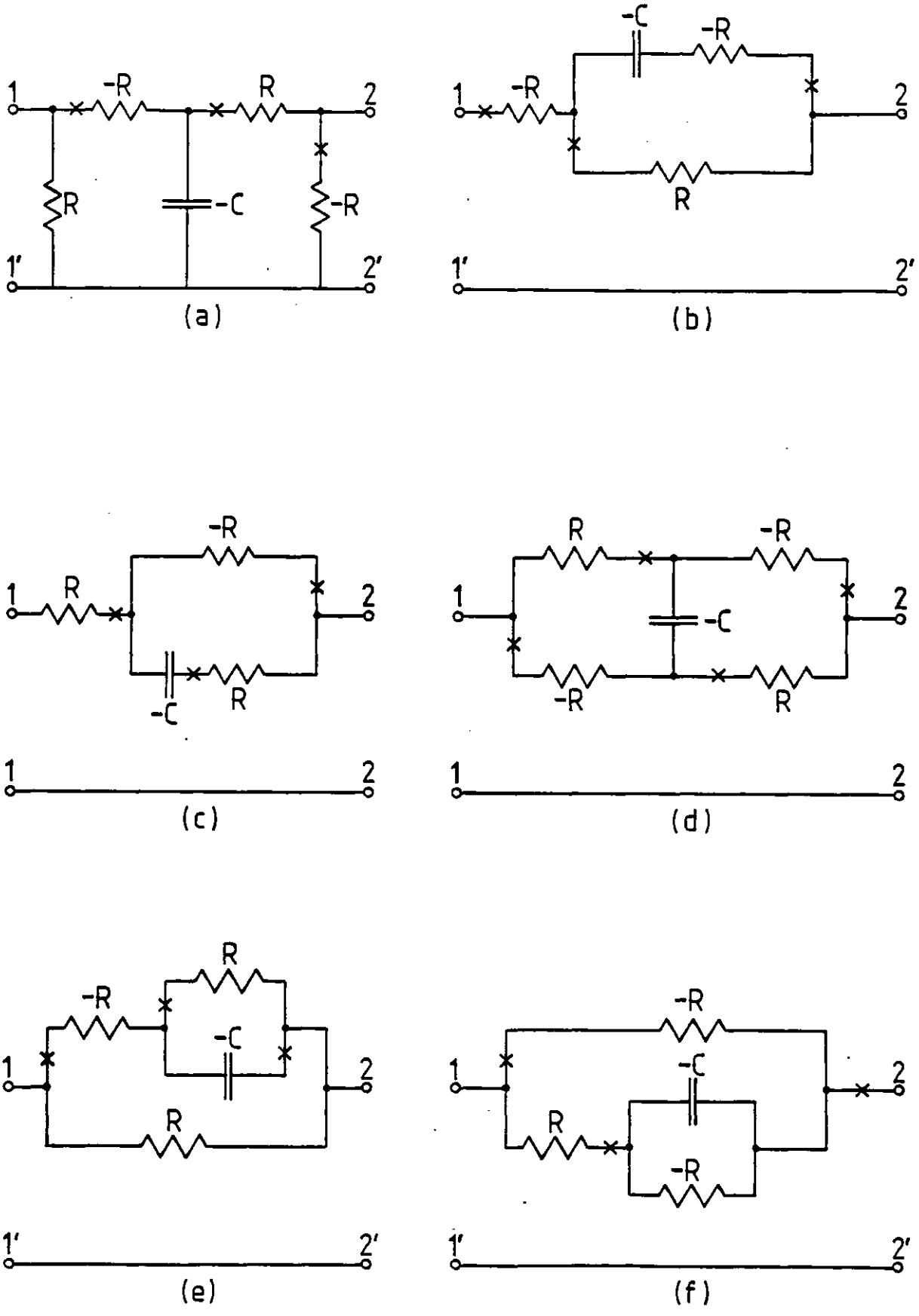

Fig 4.10 A set of $\pm$R, $\pm$C circuits for simulating floating inductors.

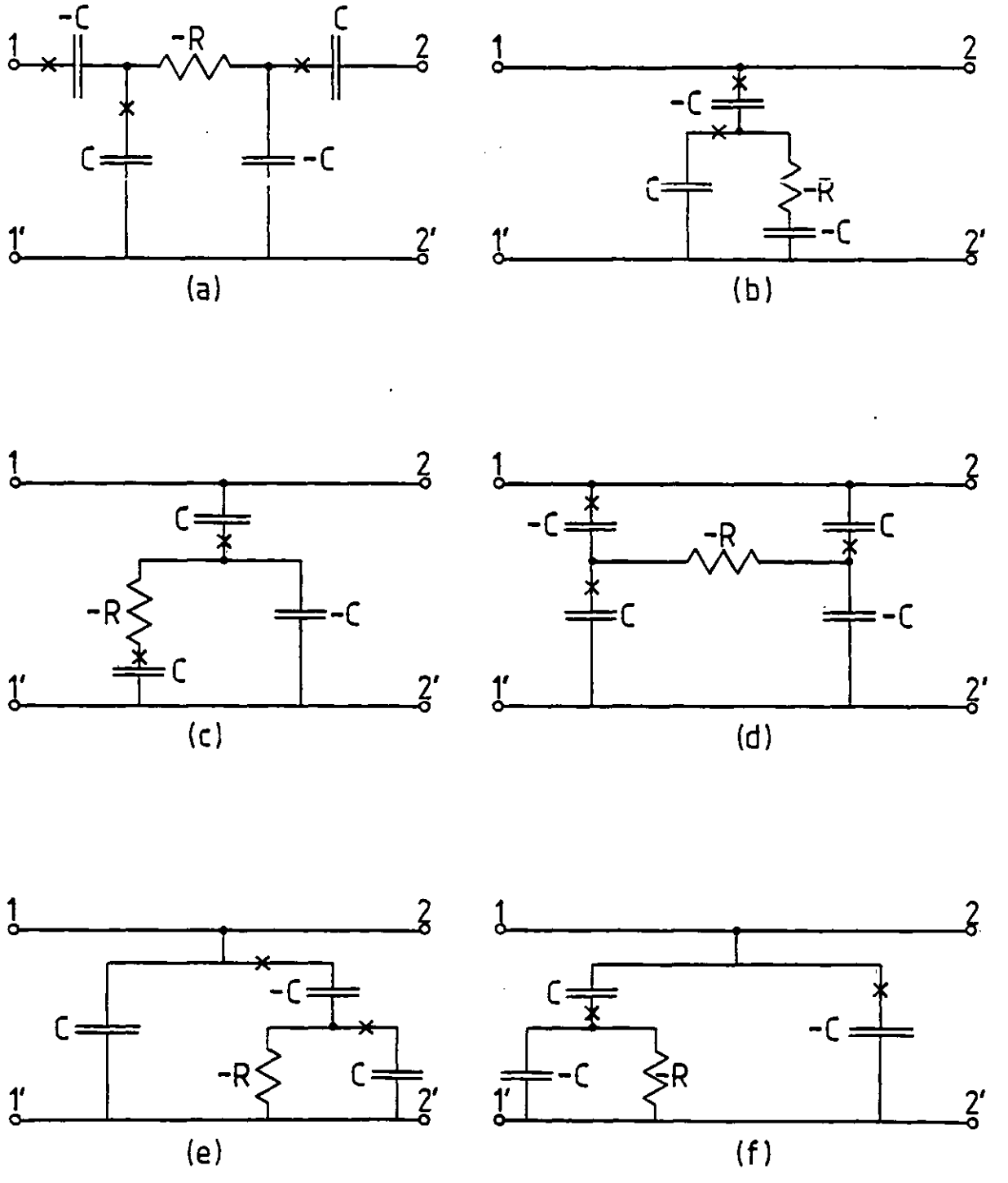

Fig 4.11 A set of $\pm R$, $\pm C$ circuits for simulating grounded supercapacitors.

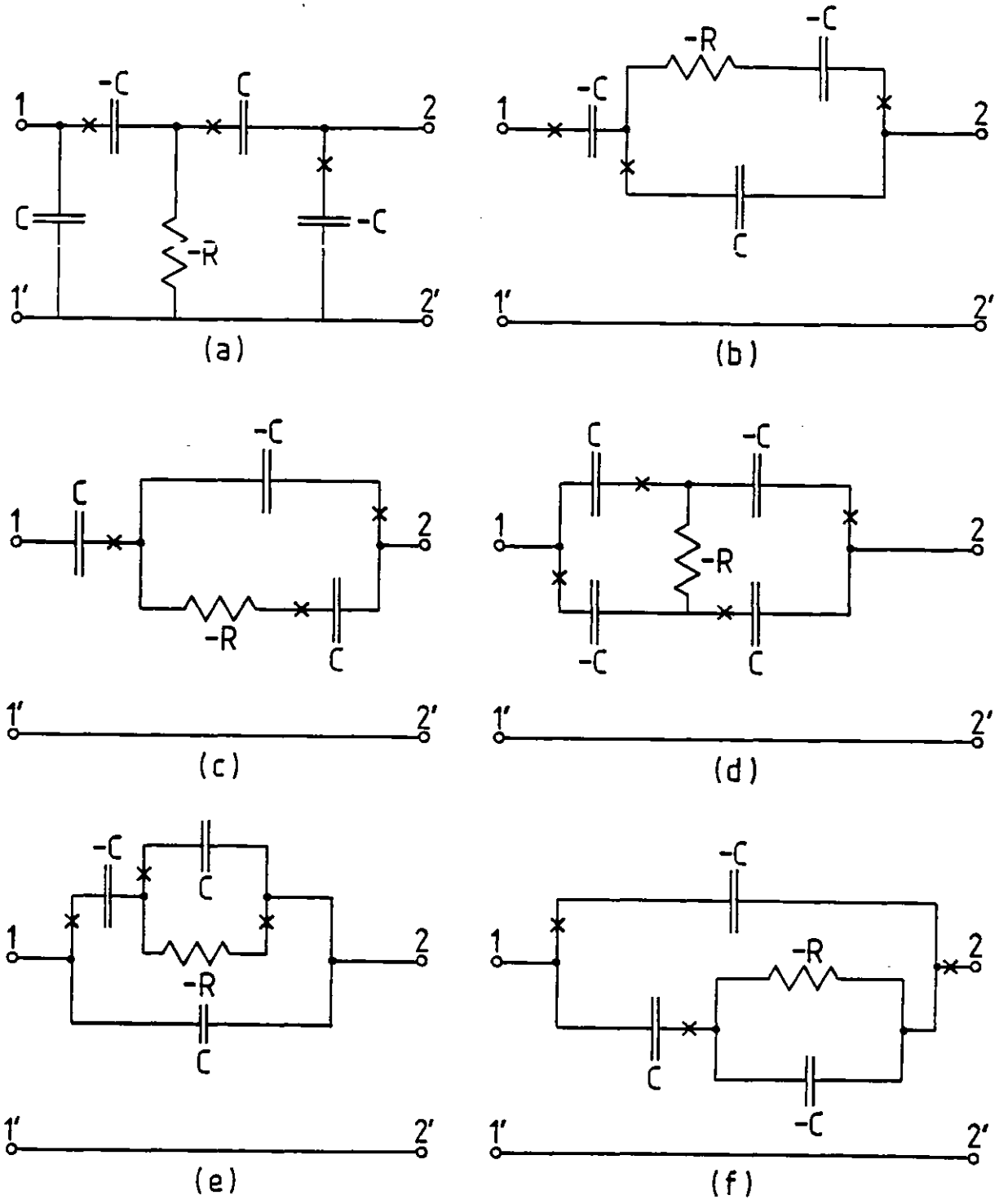

Fig 4.12 A set of $\pm R$, $\pm C$ circuits for simulating floating supercapacitors.

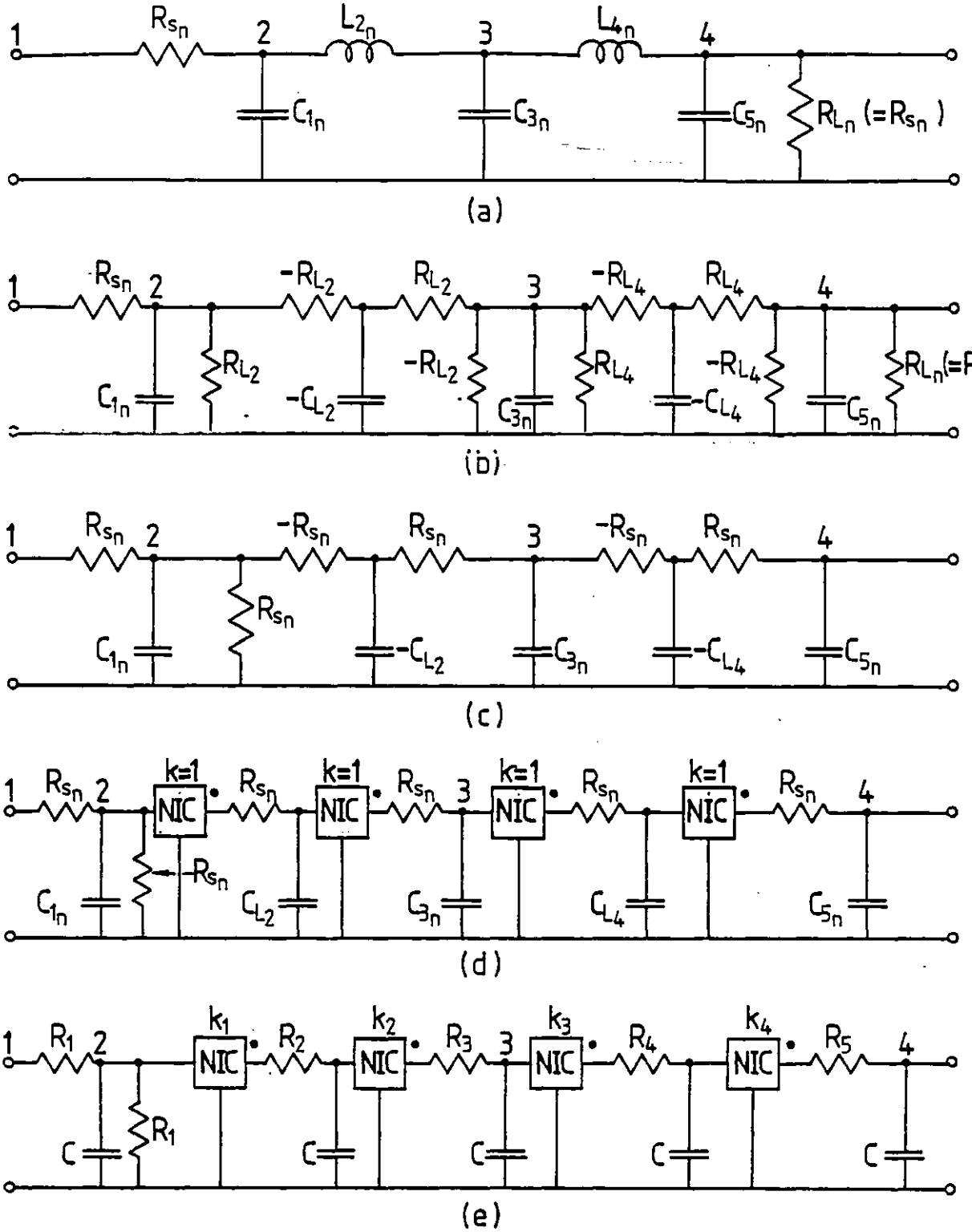

Fig 4.13 Active RC realisation of a 5th order all-pole lowpass filter by simulating the inductors —— Method 1.
(a) 5th order all-pole LC prototype filter. (b) Equivalent circuit of (a) obtained by substituting the $\pm R$, $\pm C$ circuit of Fig 4.5(c) for inductors L_{2_n} and L_{4_n} in (a).
(c) Equivalent circuit of (a) obtained by choosing $R_{L_2} = R_{L_4} = R_{s_n}$ in (b). (d) Active RC realisation of the circuit in (c) using NICs. (e) Active RC realisation of the circuit in (c) with equal value capacitors.

$CR_1 = C_{1_n} R_{s_n}$; $CR_2 = C_{L_2} R_{s_n}$; $CR_3 = C_{3_n} R_{s_n}$; $CR_4 = C_{L_4} R_{s_n}$;
$k_1 = R_1/R_2$; $k_2 = R_2/R_3$; $k_3 = R_3/R_4$; $k_4 = R_4/R_5$.

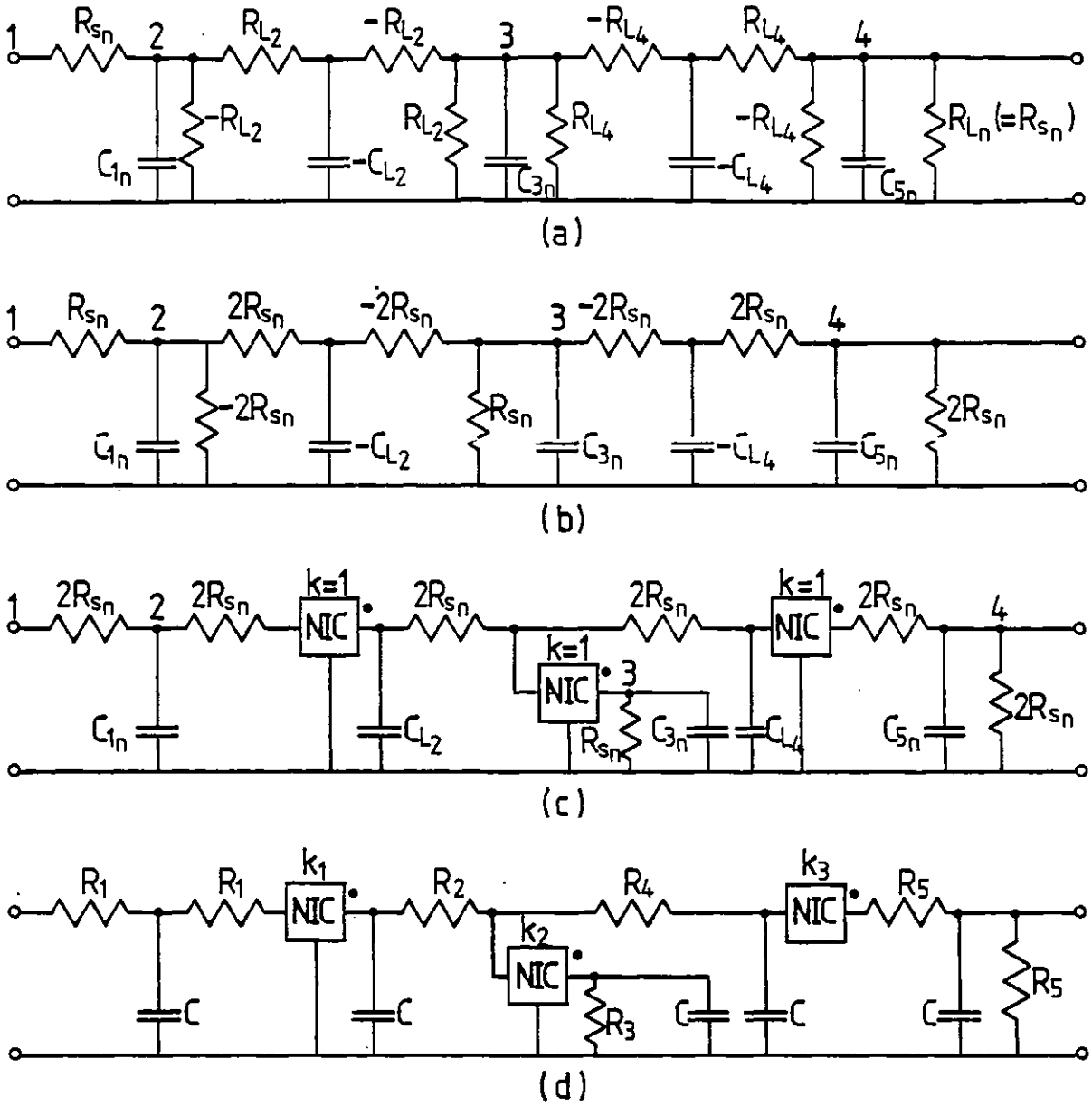

Fig 4.14 Active RC realisation of a 5th order all-pole lowpass filter by simulating inductors in the prototype filter —— Method 2.
(a) $\pm$RC equivalent of Fig 4.13(a) obtained from Fig 4.13(b) by interchanging the ports of the $\pm$R, $\pm$C circuit simulating the inductor L_{2_n}. (b) Circuit obtained by choosing $R_{L_2} = R_{L_4} = 2R_{s_n}$ in (a). (c) Active RC realisation of the circuit in (b) using NICs of unity scaling factor. (d) Active RC realisation of the circuit in (b) using equal value capacitors.

$R_1C = 2R_{s_n}C_{1_n}$; $R_2C = 2R_{s_n}C_{L_2}$; $R_3C = R_{s_n}C_{3_n}$; $R_4C = 2R_{s_n}C_{L_4}$;
$R_5C = 2R_{s_n}C_{5_n}$; $K_1 = R_1/R_2$; $K_2 = R_2R_4/\{R_3(R_2+R_4)\}$; $K_3 = R_4/R_5$.

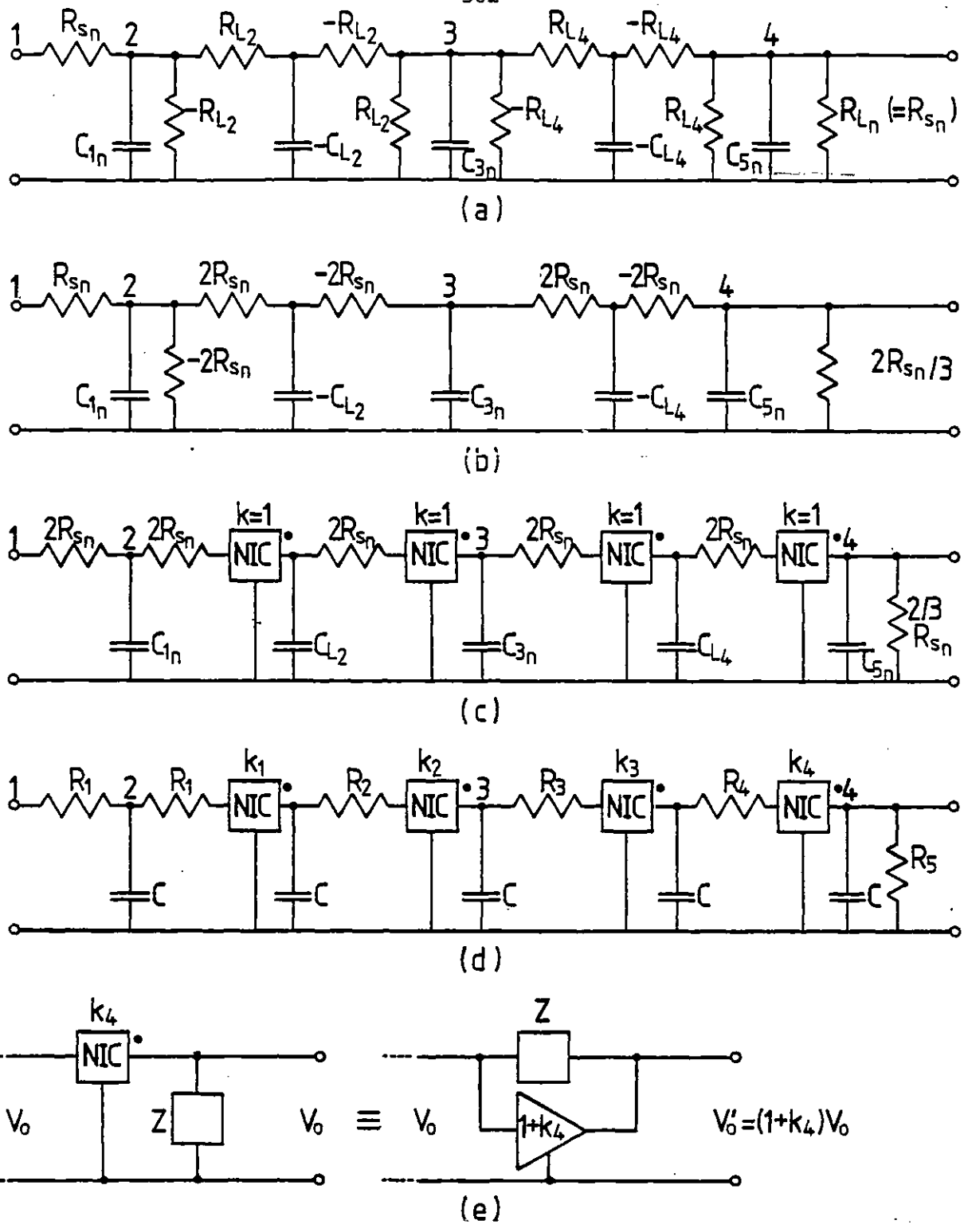

Fig 4.15 Active RC realisation of the 5th order all-pole lowpass filter of Fig 4.13(a) by simulating the inductors —— Method 3.
(a) $\pm$RC equivalent of Fig 4.13(a) obtained from Fig 4.14(a) by interchanging the ports of the $\pm$R, $\pm$C circuit simulating the inductor L_{4_n}. (b) Circuit obtained by choosing $R_{L_2} = R_{L_4} = 2R_{s_n}$ in (a). (c) Active RC realisation of the circuit in (b) using NICs of unity scaling factor. (d) Active RC realisation of the circuit in (b) using equal value capacitors. (e) Alternative scheme for realising the shunt impedance at node 4 in (a).

$R_1C = 2R_{s_n}C_{1_n}$; $R_2C = 2R_{s_n}C_{L_2}$; $R_3C = 2R_{s_n}C_{3_n}$; $R_4C = 2R_{s_n}C_{L_4}$;
$R_5C = 2R_{s_n}C_{5_n}/3$; $K_1 = R_1/R_2$; $K_2 = R_2/R_3$; $K_3 = R_3/R_4$; $K_4 = R_4/R_5$.

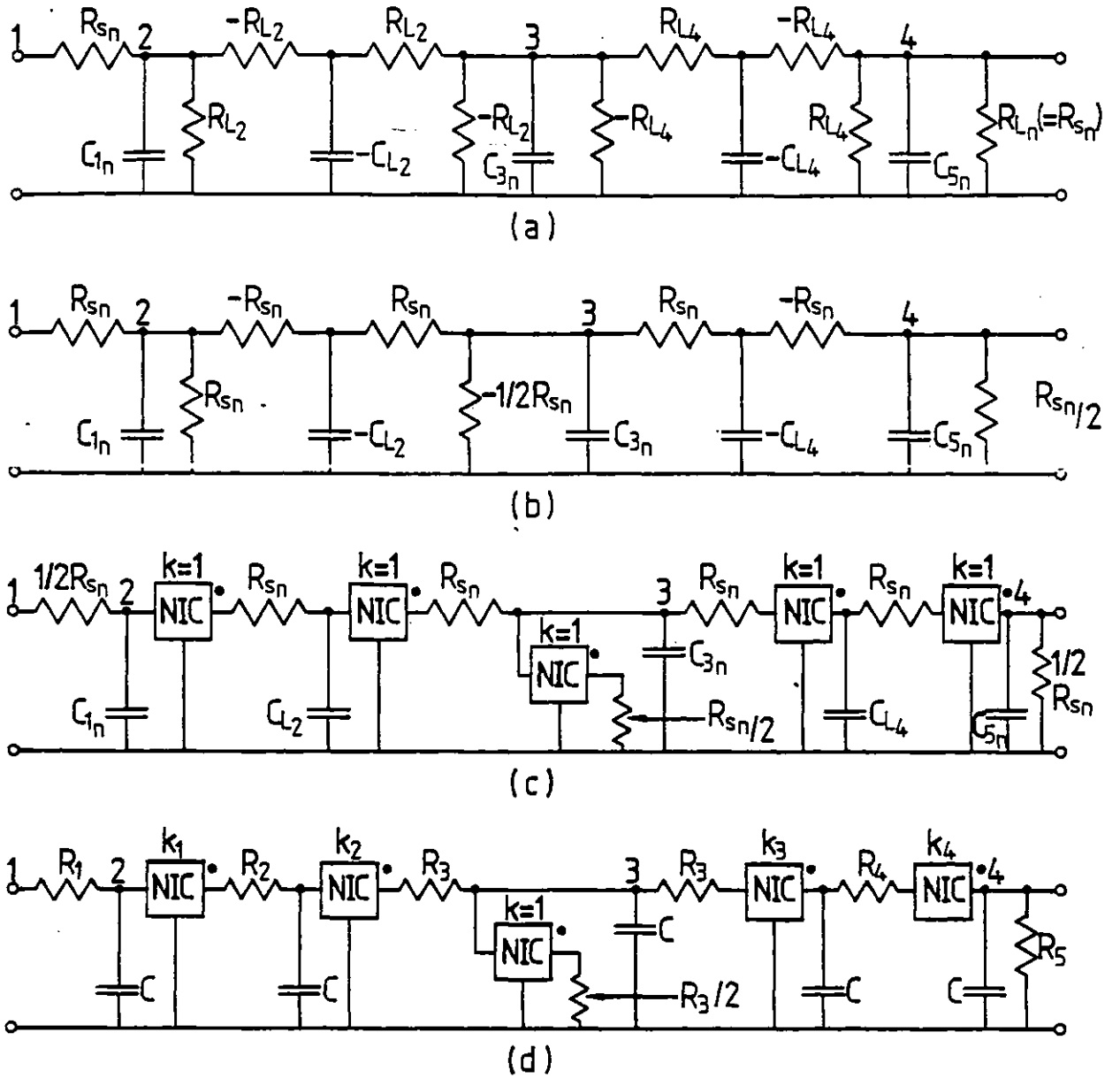

Fig 4.16 Active RC realisation of the 5th order all-pole lowpass filter of Fig 4.13(a) by simulating the inductors —— Method 4.
(a) $\pm$RC equivalent circuit of Fig 4.13(a) obtained from Fig 4.13(b) by interchanging the ports of the $\pm$R, $\pm$C circuit simulating inductor L_{4_n}. (b) Circuit obtained by choosing $R_{L_2} = R_{L_4} = R_{s_n}$ in (a). (c) Active RC realisation of the circuit in (b) using NICs of unity scaling factor. (d) Active RC realisation of the circuit in (b) using equal value capacitors.

$R_1C = R_{s_n} C_{1_n}/2$; $R_2C = R_{s_n} C_{L_2}$; $R_3C = R_{s_n} C_{3_n}$; $R_4C = R_{s_n} C_{L_4}$;
$R_5C = R_{s_n} C_{5_n}/2$; $K_1 = 2R_1/R_2$; $K_2 = R_2/R_3$; $K_3 = R_3/R_4$; $K_5 = R_4/2R_5$.

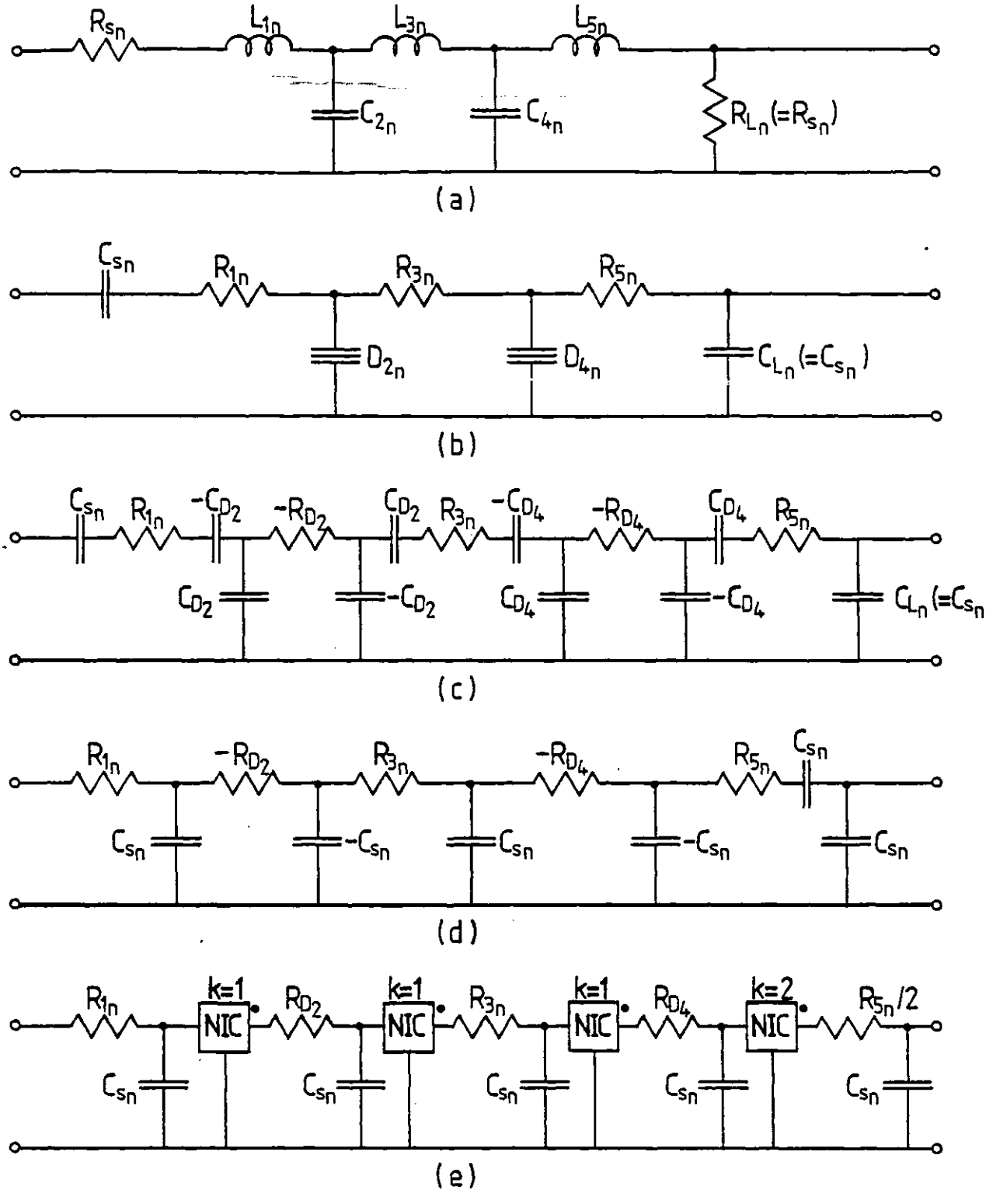

Fig 4.17 Active RC realisation of a 5th order all-pole lowpass filter by simulating grounded supercapacitors.
(a) Prototype LC filter. (b) Impedance scaled version of the prototype filter. (c) Circuit obtained by replacing grounded supercapacitors in (b) by their $\pm R$, $\pm C$ equivalent circuit of Fig 4.6(b). (d) Circuit obtained by choosing $C_{D_2} = C_{D_4} = C_{s_n}$ in (c). (e) Active RC realisation of (d) using NICs and equal value capacitors.

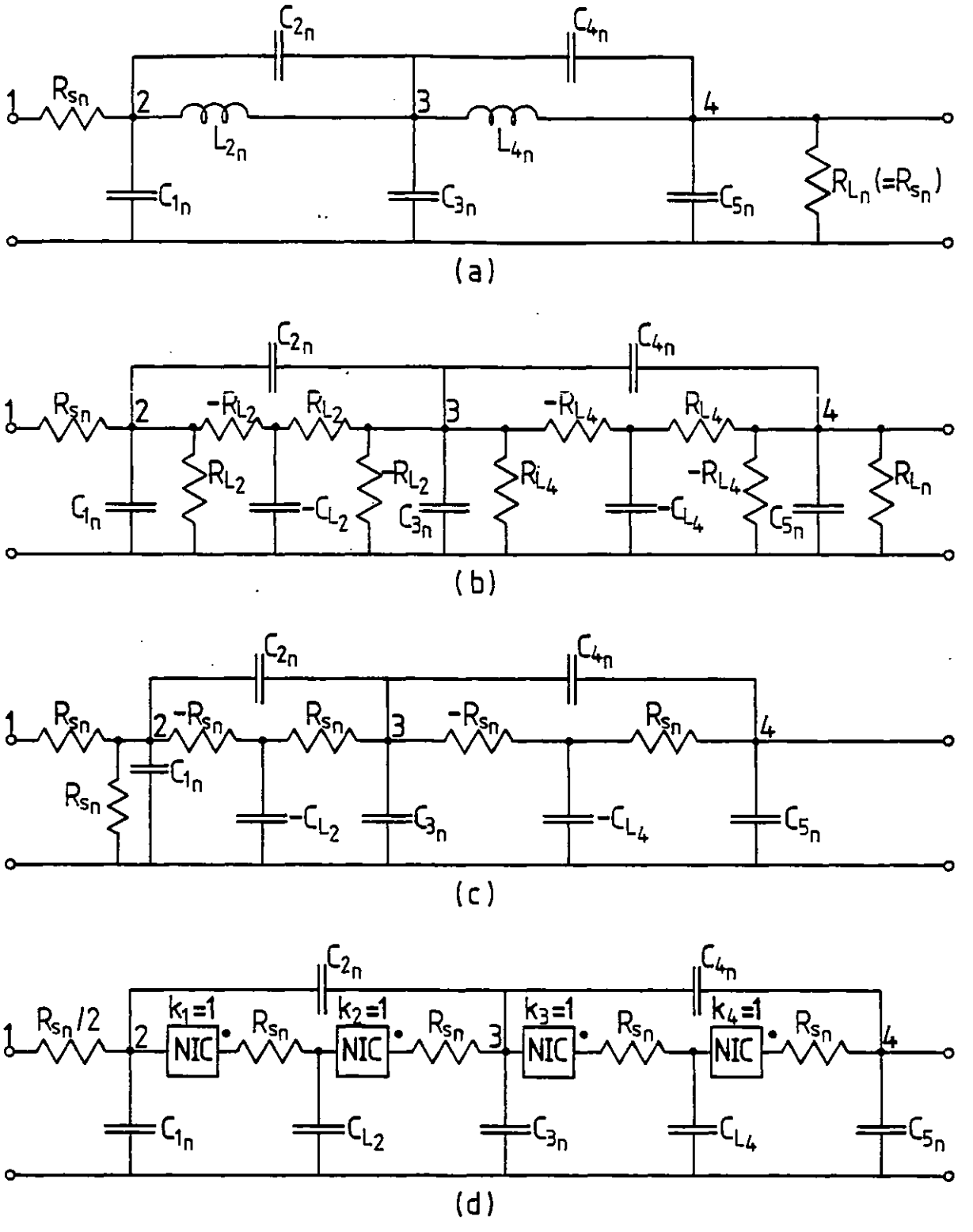

Fig 4.18 Active RC realisation of a 5th order elliptic lowpass filter.
(a) Prototype filter circuit. (b) Circuit obtained from (a) by replacing each inductor by its $\pm R$, $\pm C$ equivalent circuit. (c) Circuit obtained by choosing $R_{L_2} = R_{L_4} = R_{s_n}$ in (b). (d) Active RC realisation of (c) using NICs of unity scaling factors.

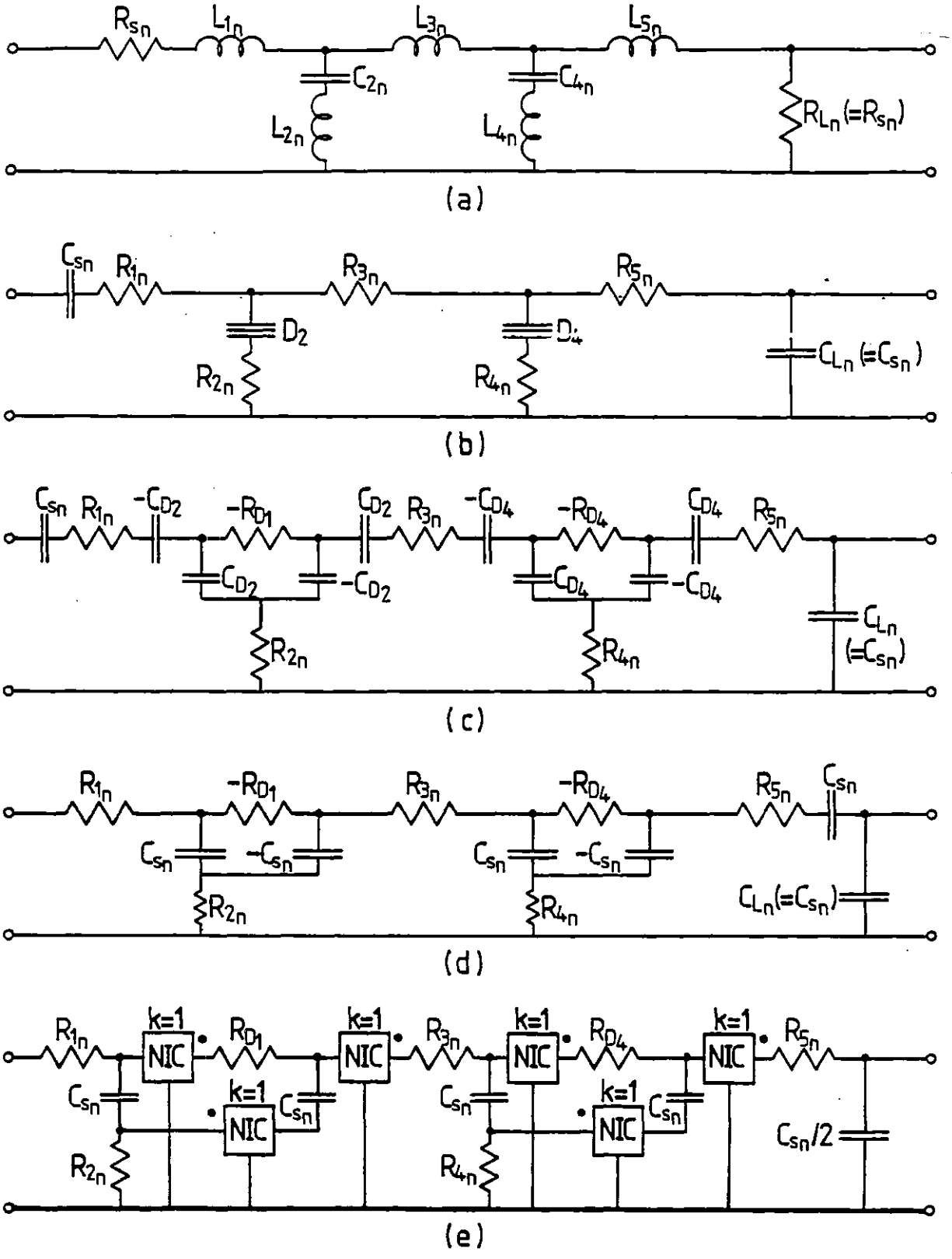

Fig 4.19 Alternative active RC realisation of a 5th order elliptic lowpass filter.
(a) Prototype filter circuit. (b) Impedance scaled version of the prototype filter. (c) Circuit obtained from (b) by replacing each supercapacitor by its $\pm R$, $\pm C$ equivalent circuit. (d) Circuit obtained by choosing $C_{D_2} = C_{D_4} = C_{s_n}$ in (c). (e) Active RC realisation of the circuit in (d) using equal value capacitors.

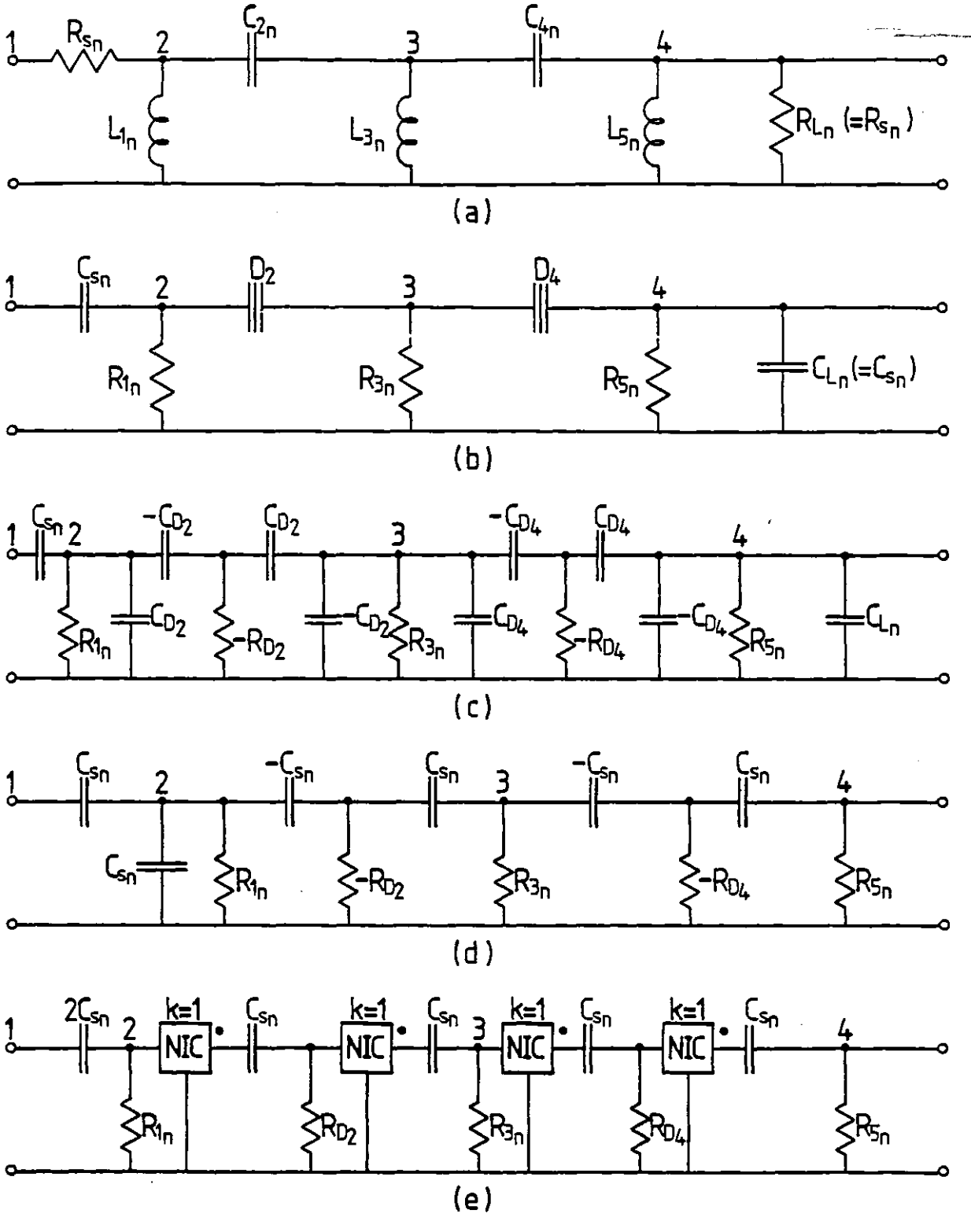

Fig 4.20 Active RC realisation of a 5th order all-pole highpass filter.
(a) Prototype filter circuit. (b) Impedance scaled version of the prototype filter. (c) Circuit obtained from (b) by replacing each supercapacitor by its $^{+}_{-}R$, $-^{+}C$ equivalent circuit. (d) Circuit obtained by choosing $C_{D_2} = C_{D_4} = C_{s_n}$ in (c). (e) Active RC realisation of the circuit in (d) using NICs of unity scaling factors.

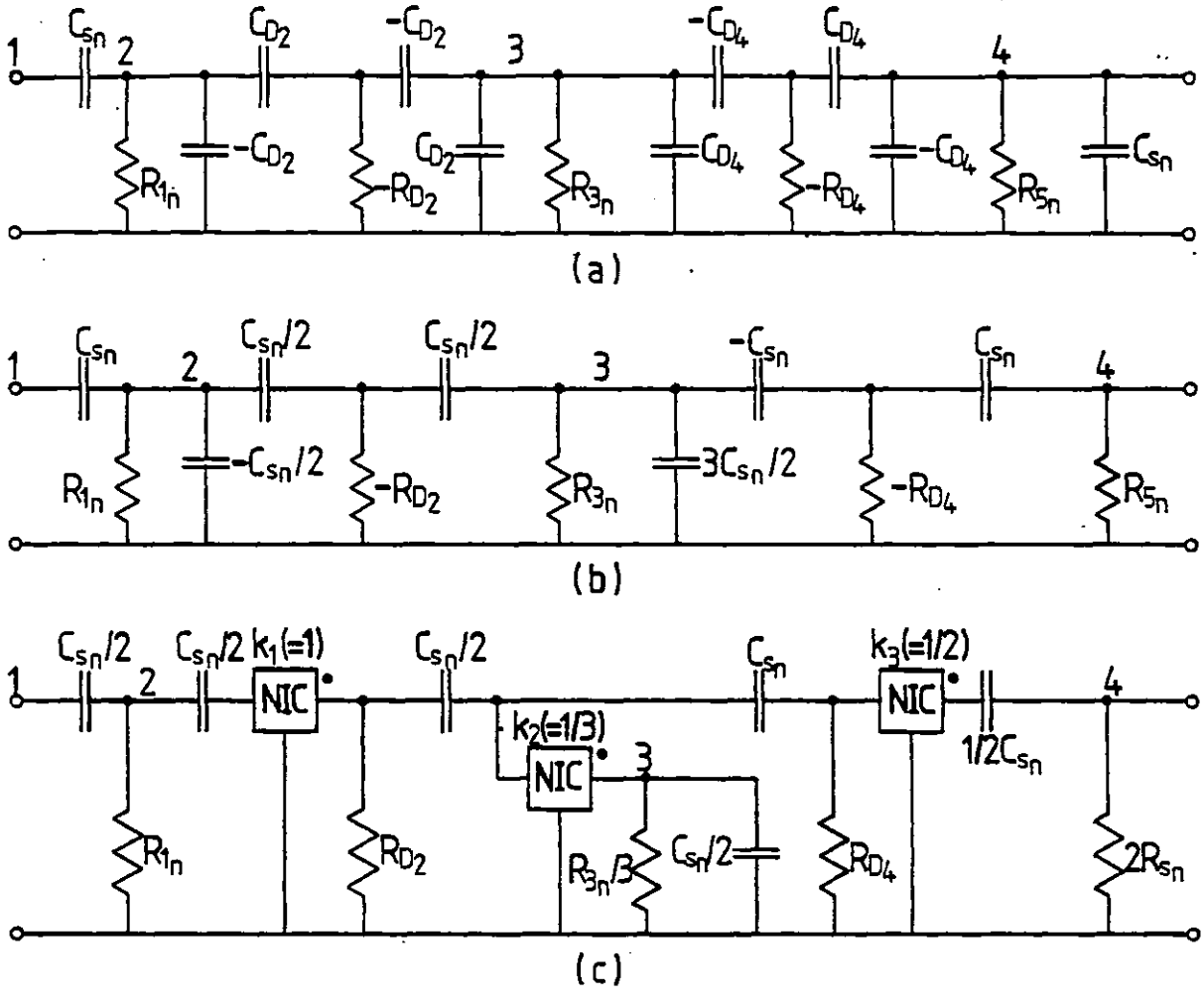

Fig 4.21 Active RC realisation of a 5th order all-pole highpass filter of Fig 4.20(a).
(a) $\pm$RC equivalent of Fig 4.20(b) obtained from Fig 4.20(c) by interchanging the ports of the $\pm$R, $\pm$C circuit simulating supercapacitor D_2. (b) Circuit obtained by choosing $C_{D_2} = C_{s_n}/2$ and $C_{D_4} = C_{s_n}$ in (a). (c) Active RC realisation of the circuit in (b) using NICs.

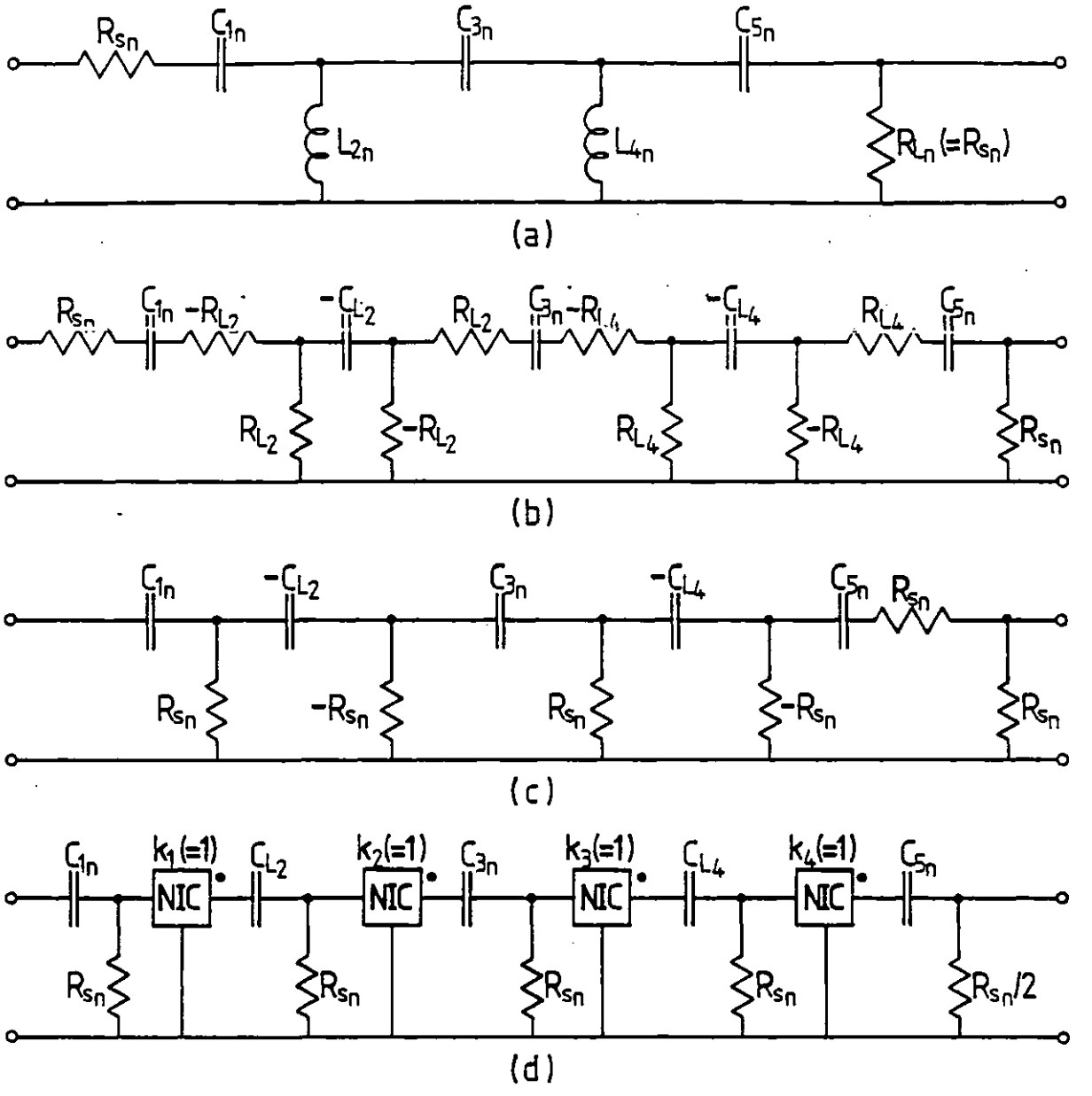

Fig 4.22 Active RC realisation of a 5th order all-pole highpass filter by simulating grounded inductors.
(a) Prototype LC filter. (b) Circuit obtained by replacing grounded inductors in (a) by their $\pm R$, $\pm C$ equivalent circuits (see Fig 4.4(c)). (c) Circuit obtained by choosing $R_{L_2} = R_{L_4} = R_{s_n}$ in (b). (d) Active RC realisation of (c) using NICs of unity scaling factors.

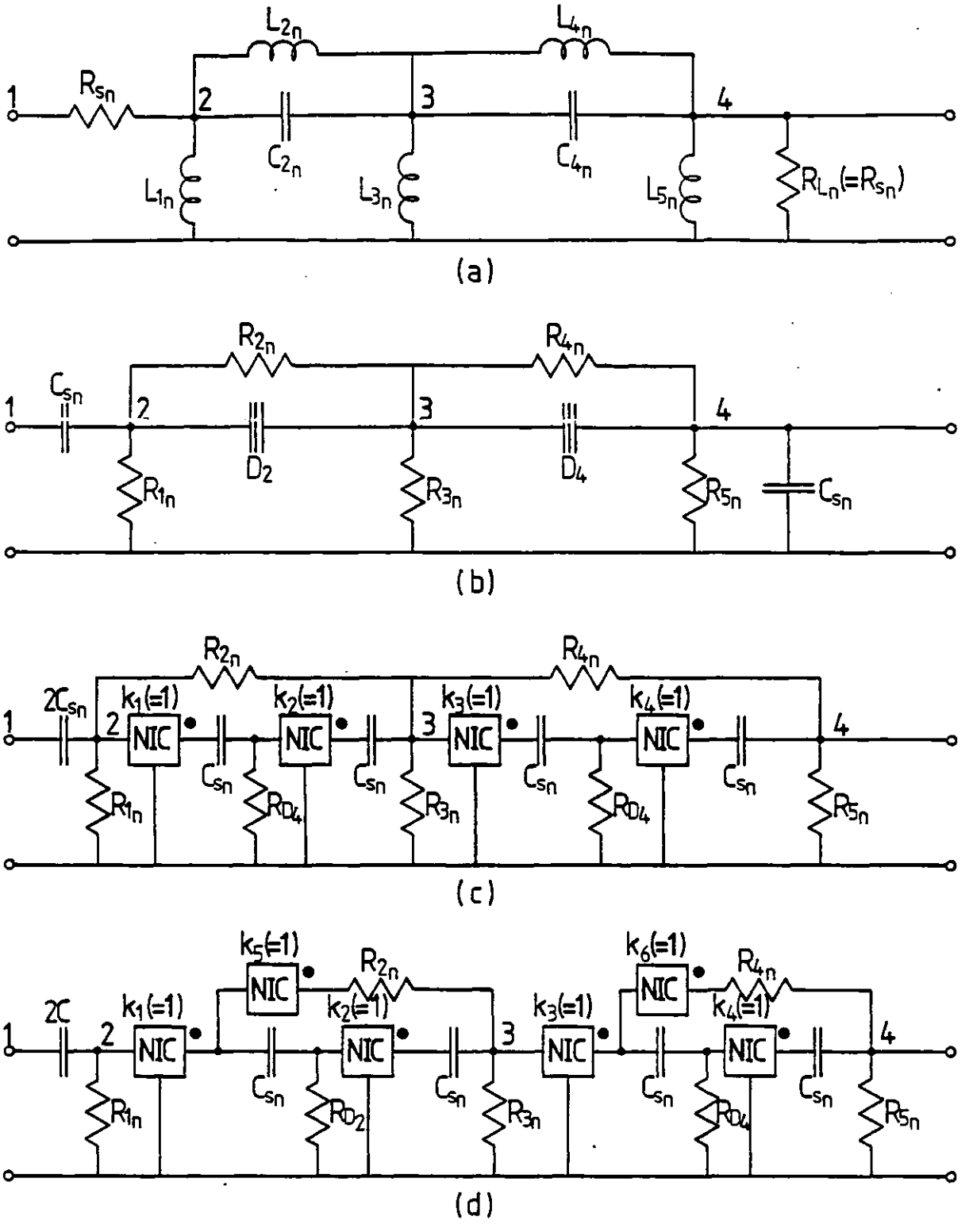

Fig 4.23 Active RC realisation of a 5th order elliptic highpass filter.
(a) Prototype LC filter. (b) Impedance scaled version of (a). (c) Active RC realisation of (b) which requires narrow tolerance capacitors. (d) Alternative realisation of (b) which allows the use of wide tolerance capacitors.

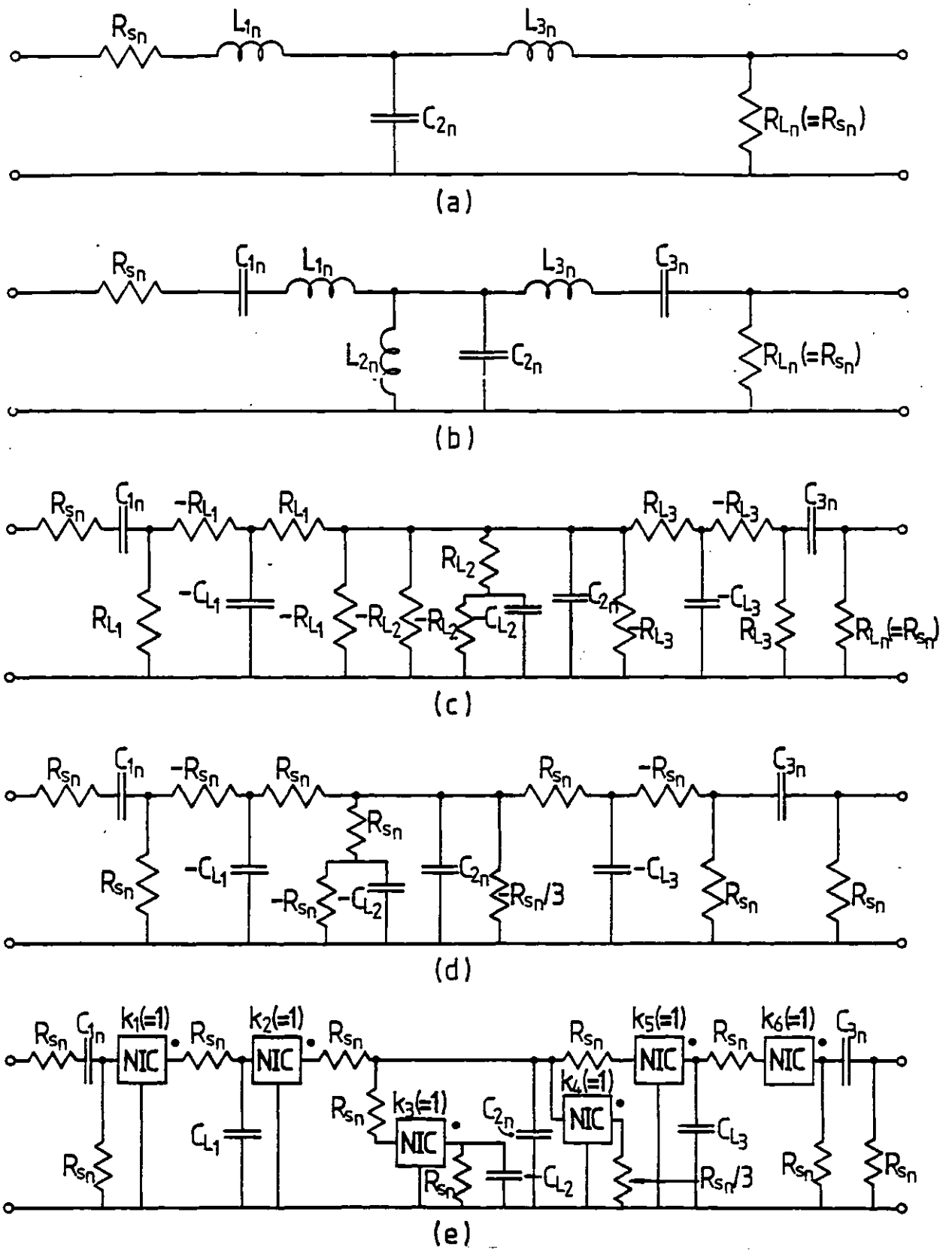

Fig 4.24 Active RC realisation of a 6th order all-pole bandpass filter.
(a) Prototype lowpass LC filter. (b) Prototype bandpass LC filter obtained from (a) by lowpass to bandpass transformation. (c) Circuit obtained from (b) by replacing inductors L_{1_n} and L_{3_n} by the $\pm R$, $\pm C$ circuit of Fig 4.5(c) and replacing inductor L_{2_n} by the $\pm R$, $\pm C$ circuit of Fig 4.4(c). (d) Circuit obtained by choosing $R_{L_1} = R_{L_2} = R_{L_3} = R_{s_n}$ in (c). (e) Active RC realisation of (d) using NICs of unity scaling factors.

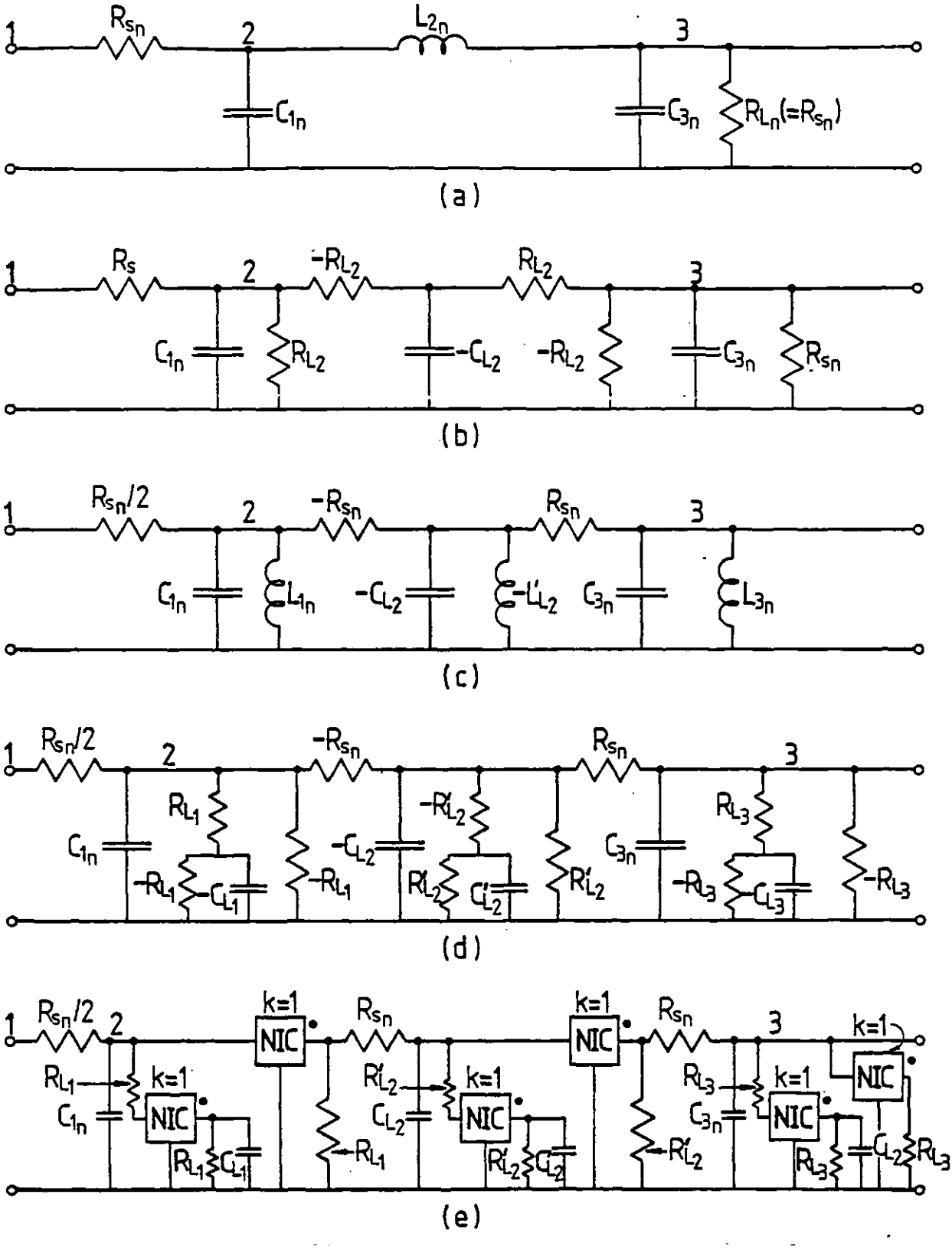

Fig 4.25 Alternative active RC realisation of the 6th order all-pole bandpass filter.
(a) Prototype lowpass LC filter. (b) Active RC realisation of (a) obtained by replacing inductor L_{2_n} by its $\pm R$, $\pm C$ equivalent circuit of Fig 4.5(c). (c) Circuit obtained by applying the lowpass to bandpass transformation to the circuit in (b) in which R_{L_2} has been chosen as $R_{L_2} = R_{s_n}$.
(d) Circuit obtained by replacing each grounded inductor in (c) by its $\pm R$, $\pm C$ equivalent circuit of Fig 4.8(e).
(e) Active RC realisation of (d) using NICs of unity scaling factors.

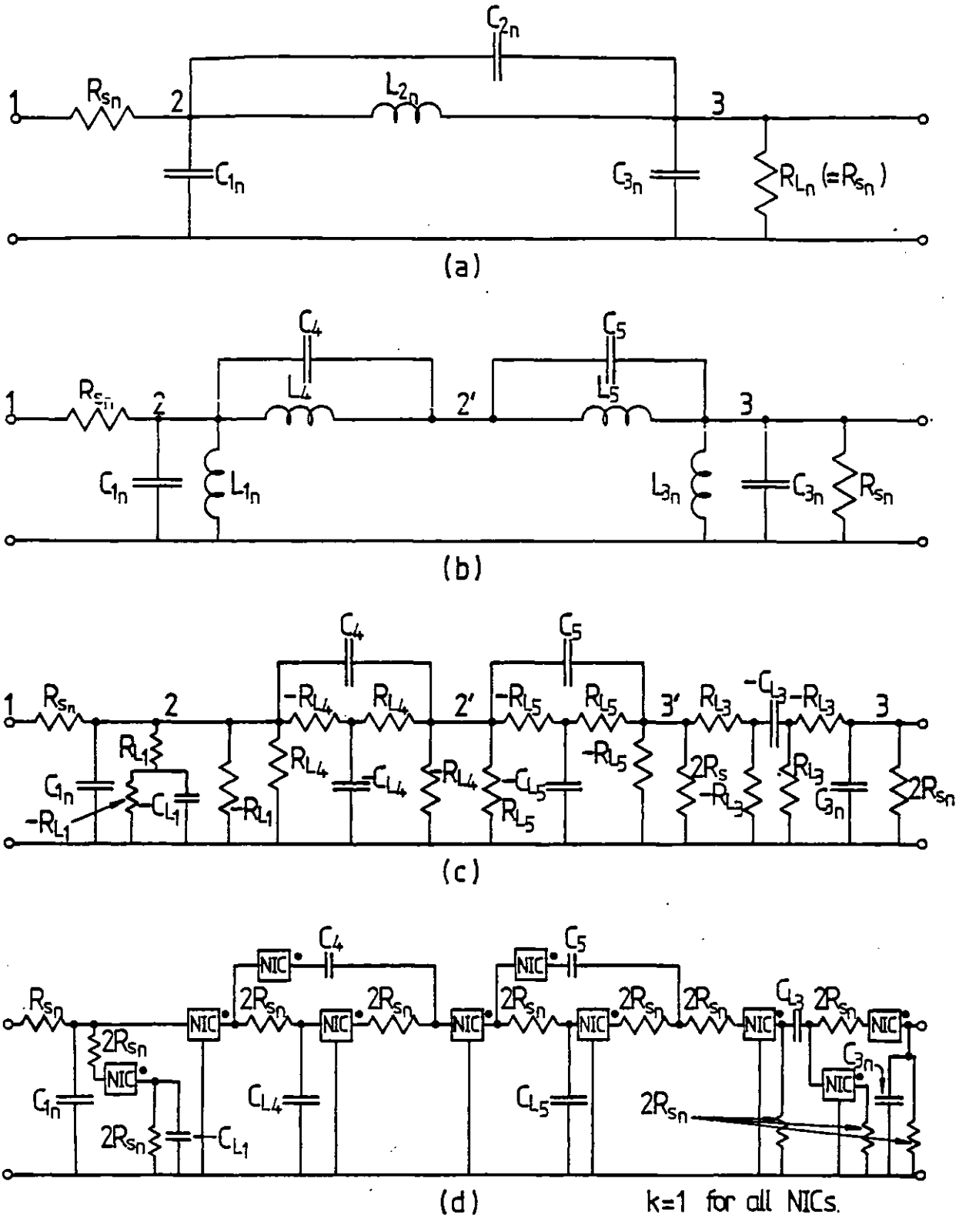

Fig 4.26 Active RC realisation of a 6th order elliptic bandpass filter.
(a) Prototype lowpass LC filter. (b) Prototype bandpass LC filter, obtained from (a) by applying the lowpass to bandpass transformation and arranged into a more suitable form. (c) Circuit obtained from (b) by replacing inductor L_{1_n} by its $\pm R$, $\pm C$ equivalent circuit of Fig 4.8(e), inductors L_4 and L_5 by their $\pm R$, $\pm C$ equivalent circuit of Fig 4.5(c) and inductor L_{3_n} by its $\pm R$, $\pm C$ equivalent circuit of Fig 4.4(c). (d) Active RC realisation of the circuit in (c) using NICs of unity scaling factors, when $R_{L_1} = R_{L_3} = R_{L_4} = R_{L_5} = 2R_{s_n}$.

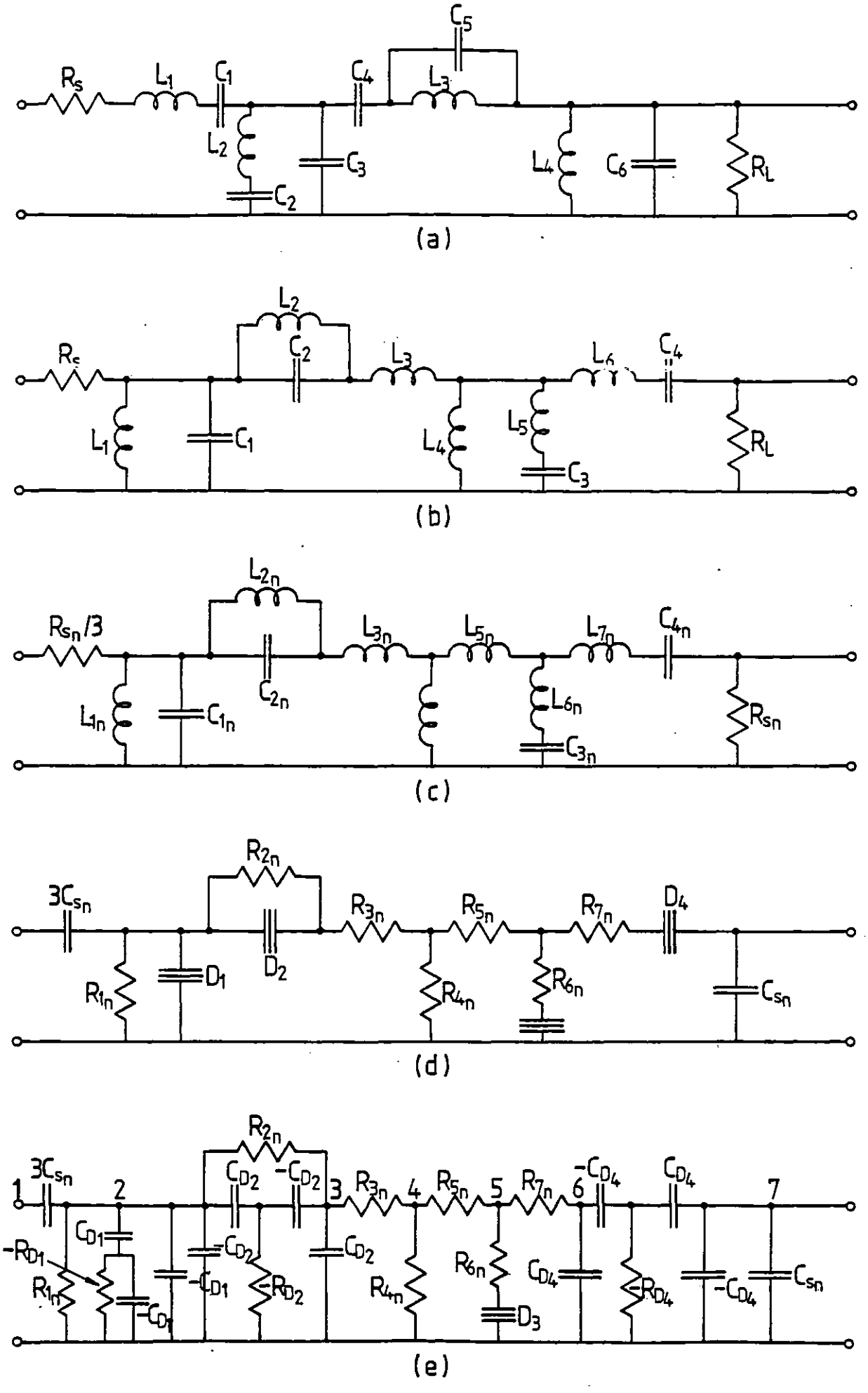

Fig 4.27 (Continued on next page)

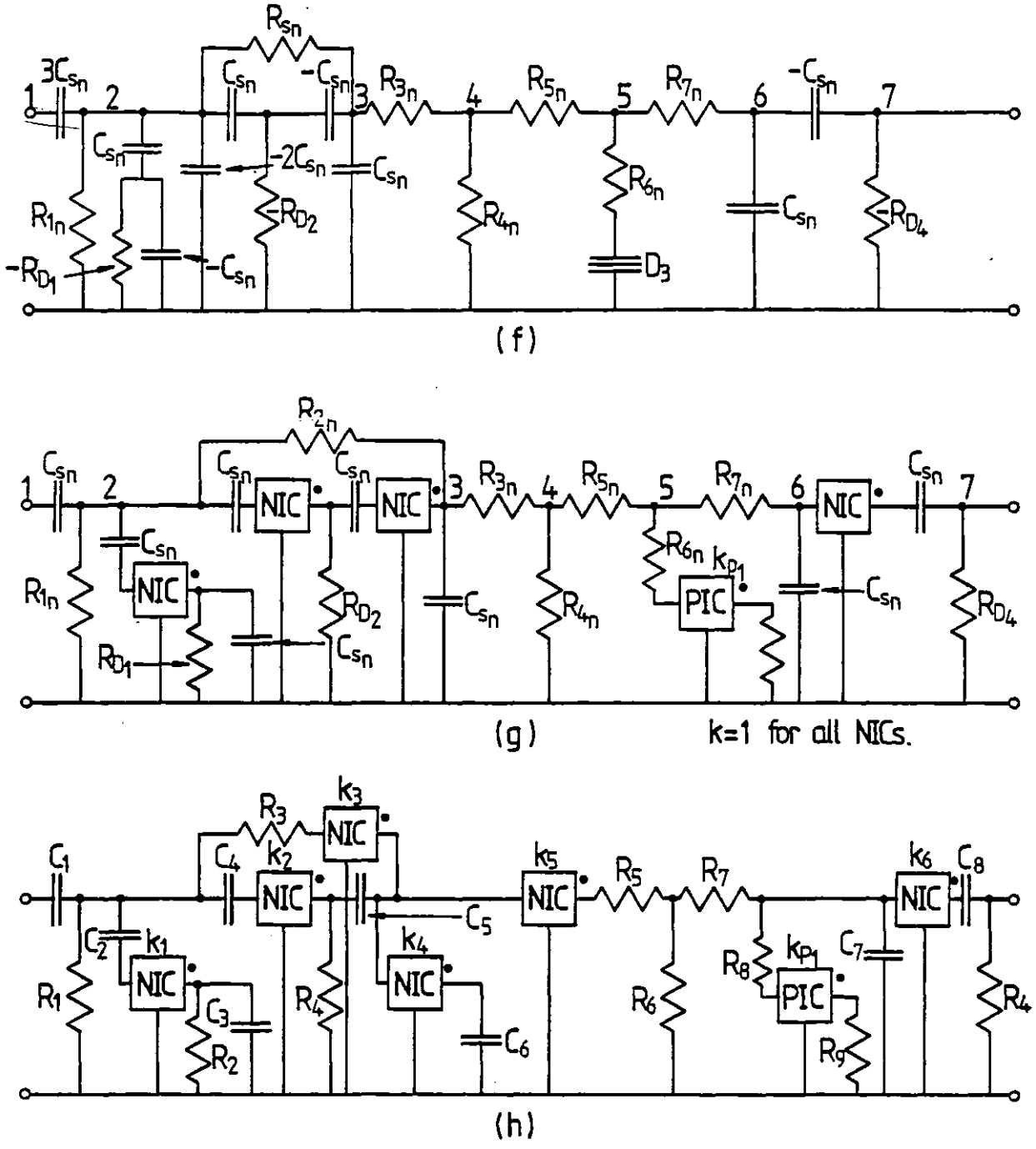

Fig 4.27 Active RC realisation of an 8th order elliptic bandpass filter.
(a) Prototype LC filter. (b) Dual circuit of (a). (c) Modified form of the filter circuit in (b) —— obtained by applying Norton transformations. (d) Complex impedanced scaled version of (c). (e) Circuit obtained from (d) by replacing D_1 by its $\pm R$, $\pm C$ equivalent circuit of Fig 4.6(b) and by replacing D_2 and D_4 by their $\pm R$, $\pm C$ equivalent circuit of Fig 4.7(c). (f) Circuit obtained by choosing $C_{D_1} = C_{D_2} = C_{D_4} = C_{s_n}$ in (c).
(g) Active RC realisation of the circuit in (f) using NICs and one PIC. (h) Active RC realisation of the circuit in (g) which allows the use of wide tolerance capacitors with deterministic adjustment procedure.

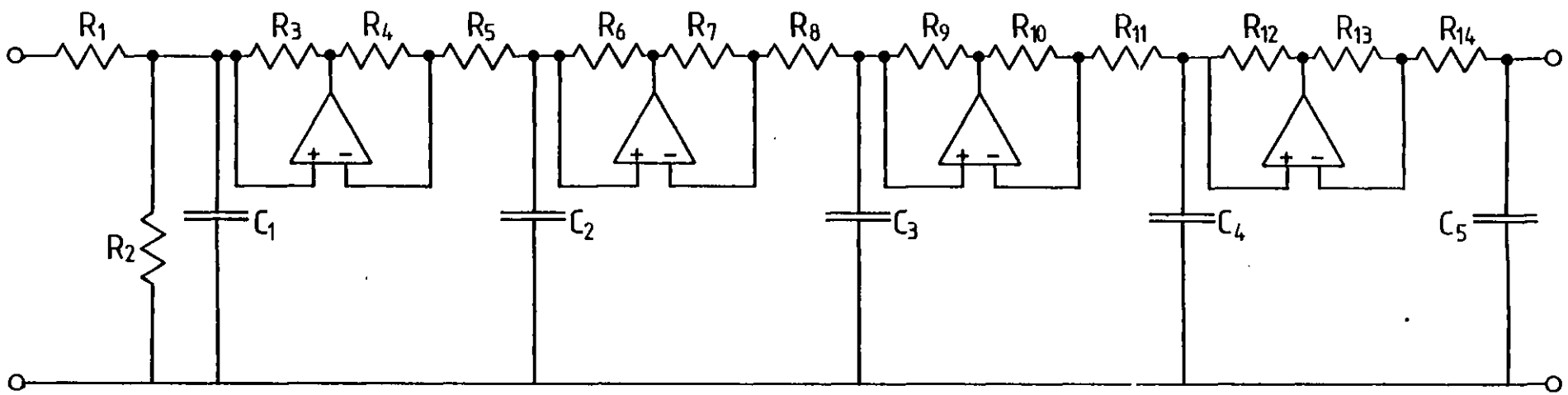

Fig 4.28 Active RC realisation of a 5th order all-pole Chebyshev lowpass filter.

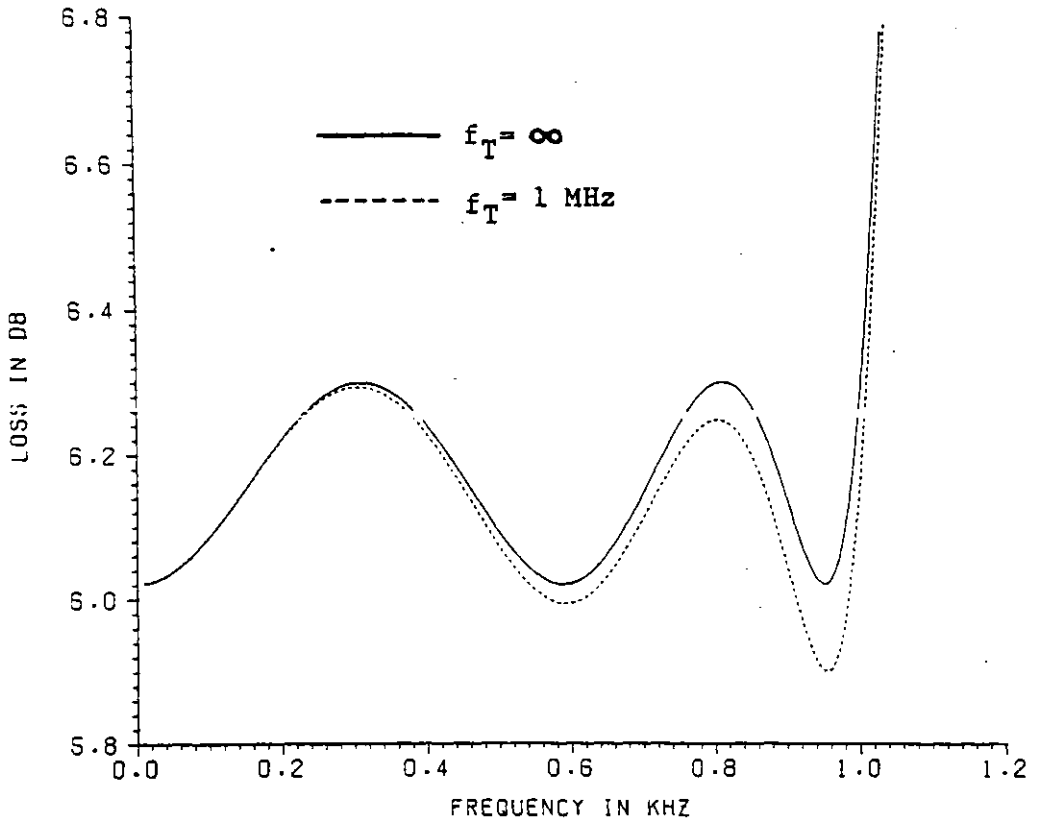

(a)

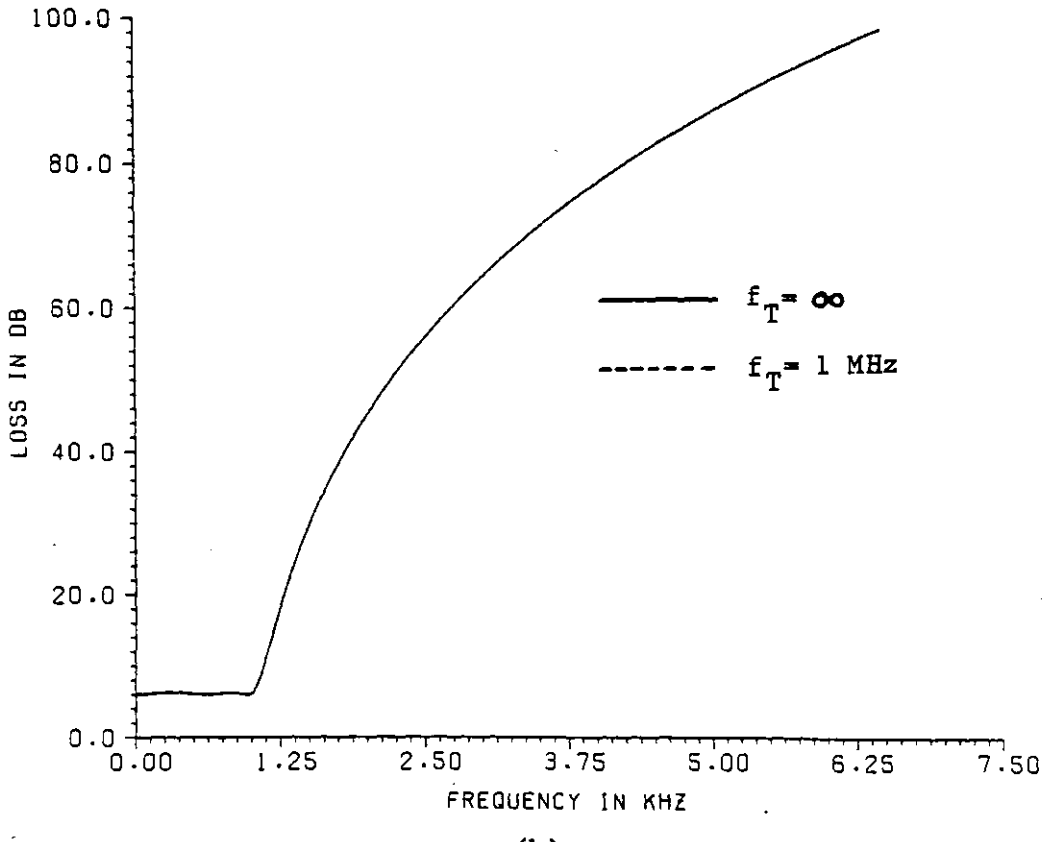

(b)

Fig 4.29 Computed response curves of the circuit in Fig 4.28. (a) Passband response. (b) Stopband response.

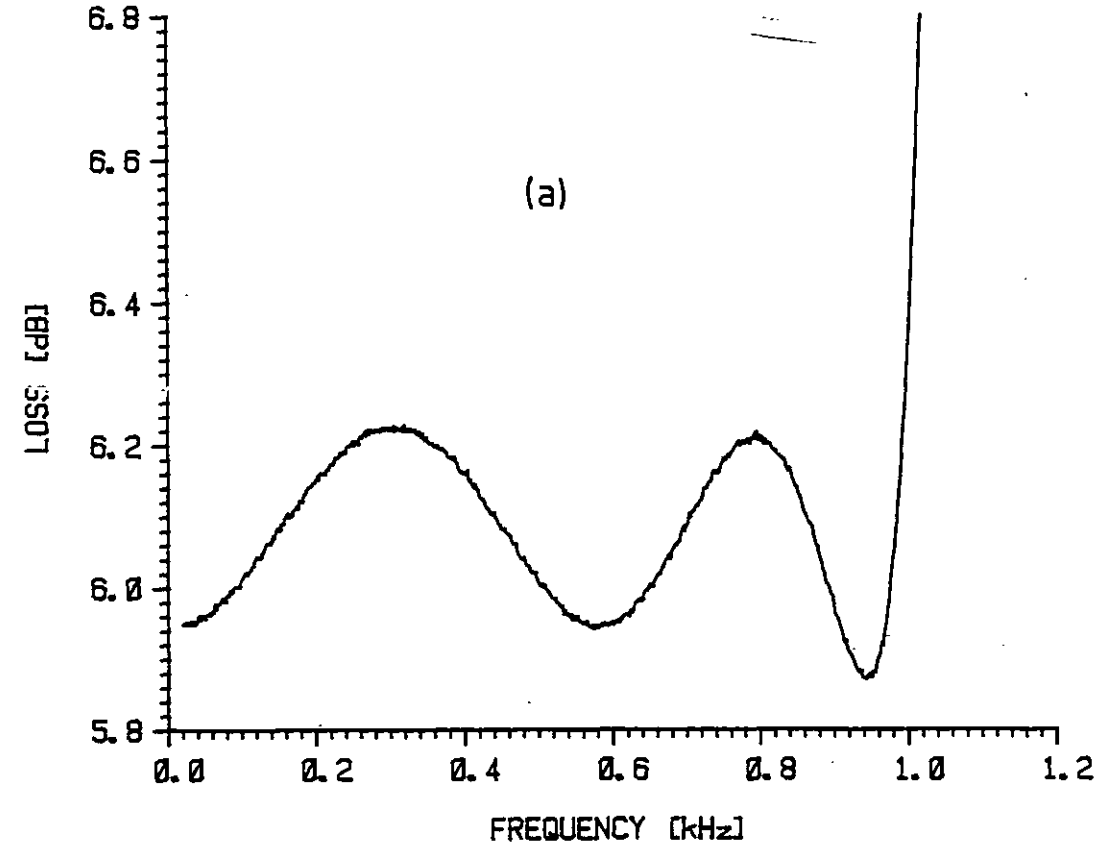

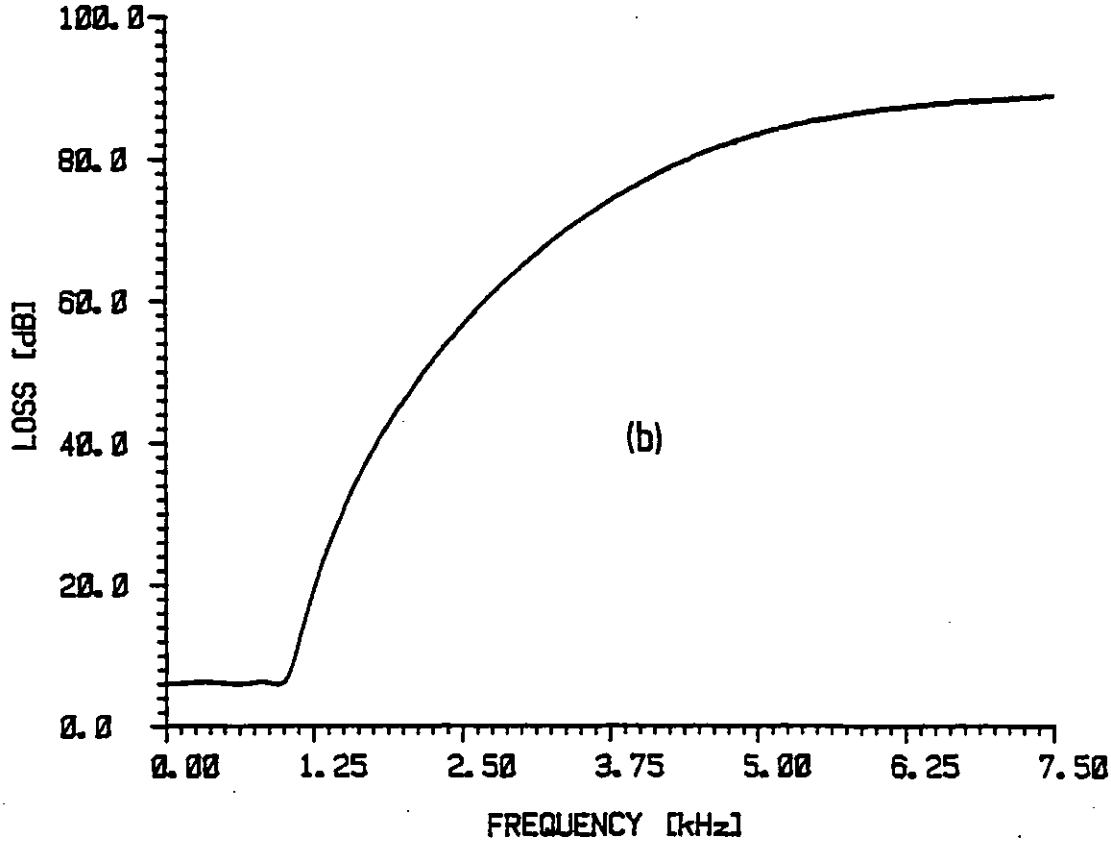

Fig 4.30 Measured response curves of the circuit in Fig 4.28.
(a) Passband response. (b) Stopband response.

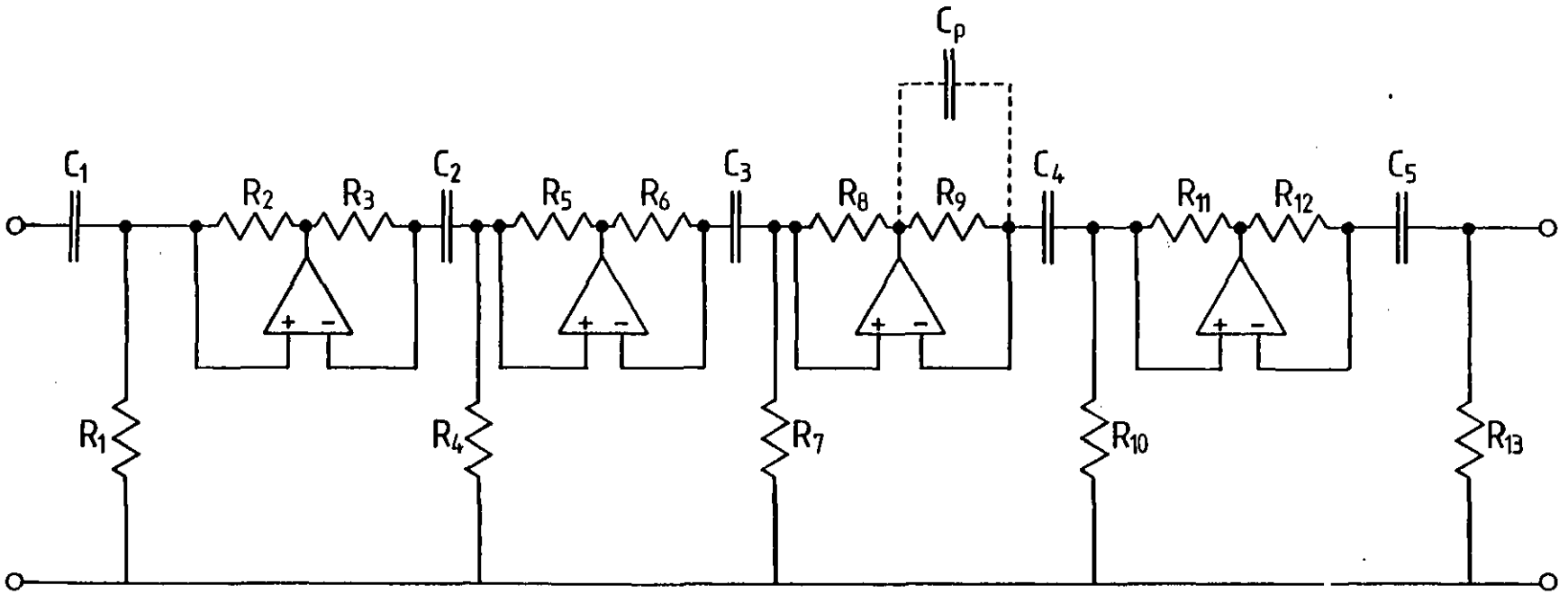

Fig 4.31 Active RC realisation of a 5th order all-pole Chebyshev highpass filter.

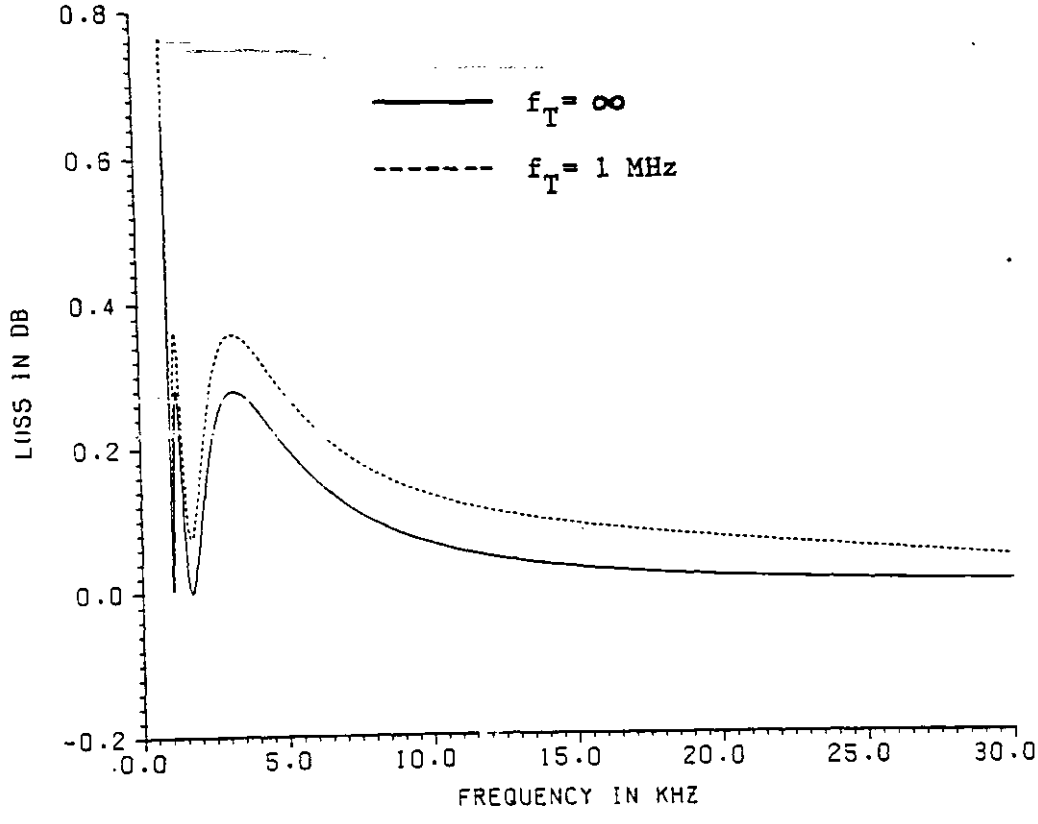

(a)

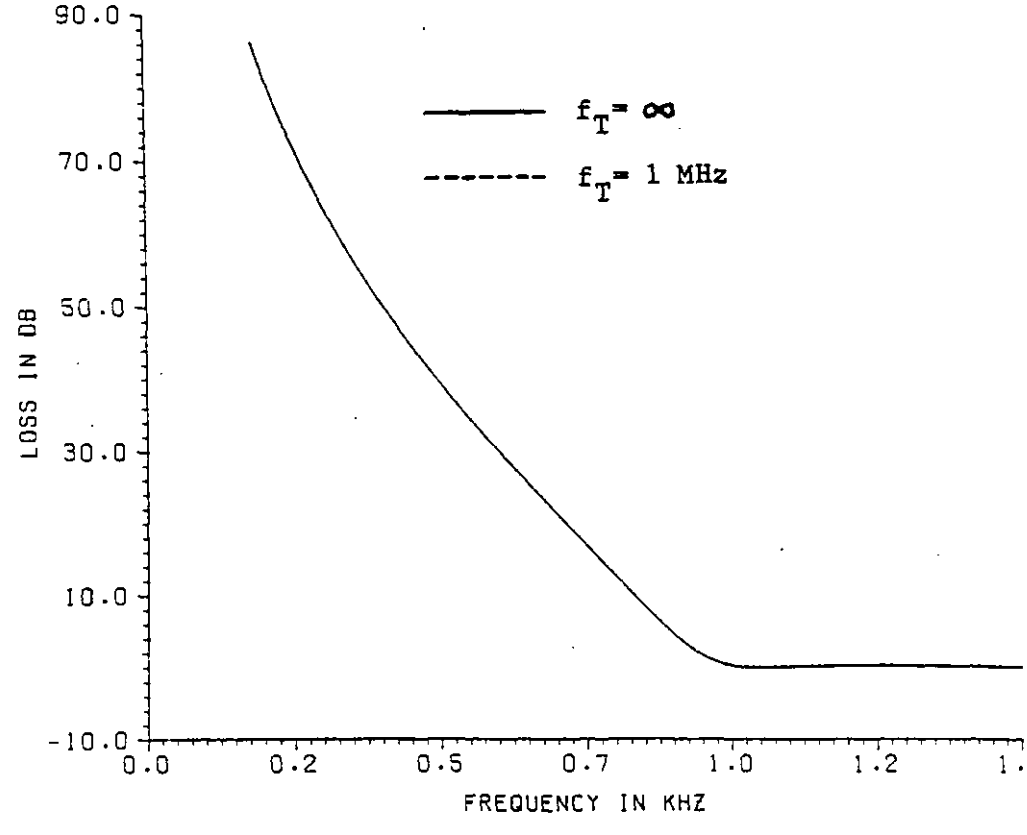

(b)

Fig 4.32 Computed response curves of the circuit in Fig 4.31. (a) Passband response. (b) Stopband response.

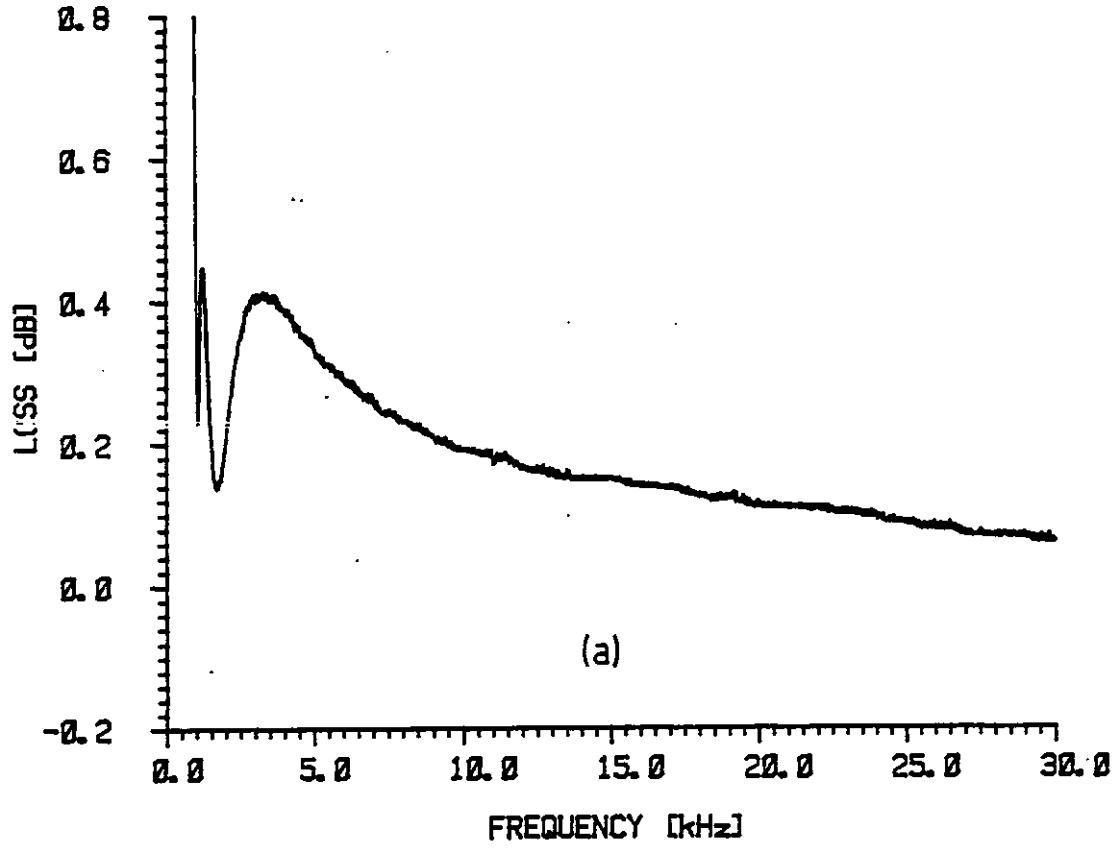

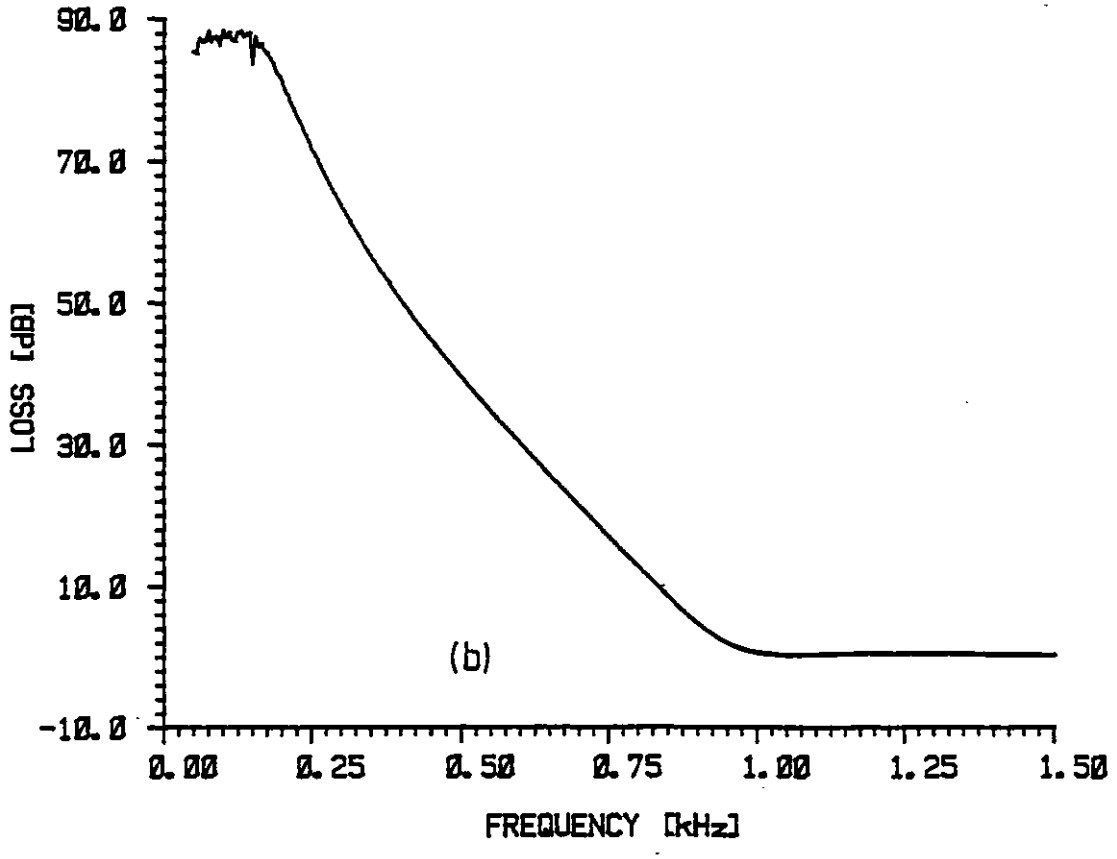

Fig 4.33 Measured response curves of the circuit in Fig 4.31. (a) Passband response. (b) Stopband response.

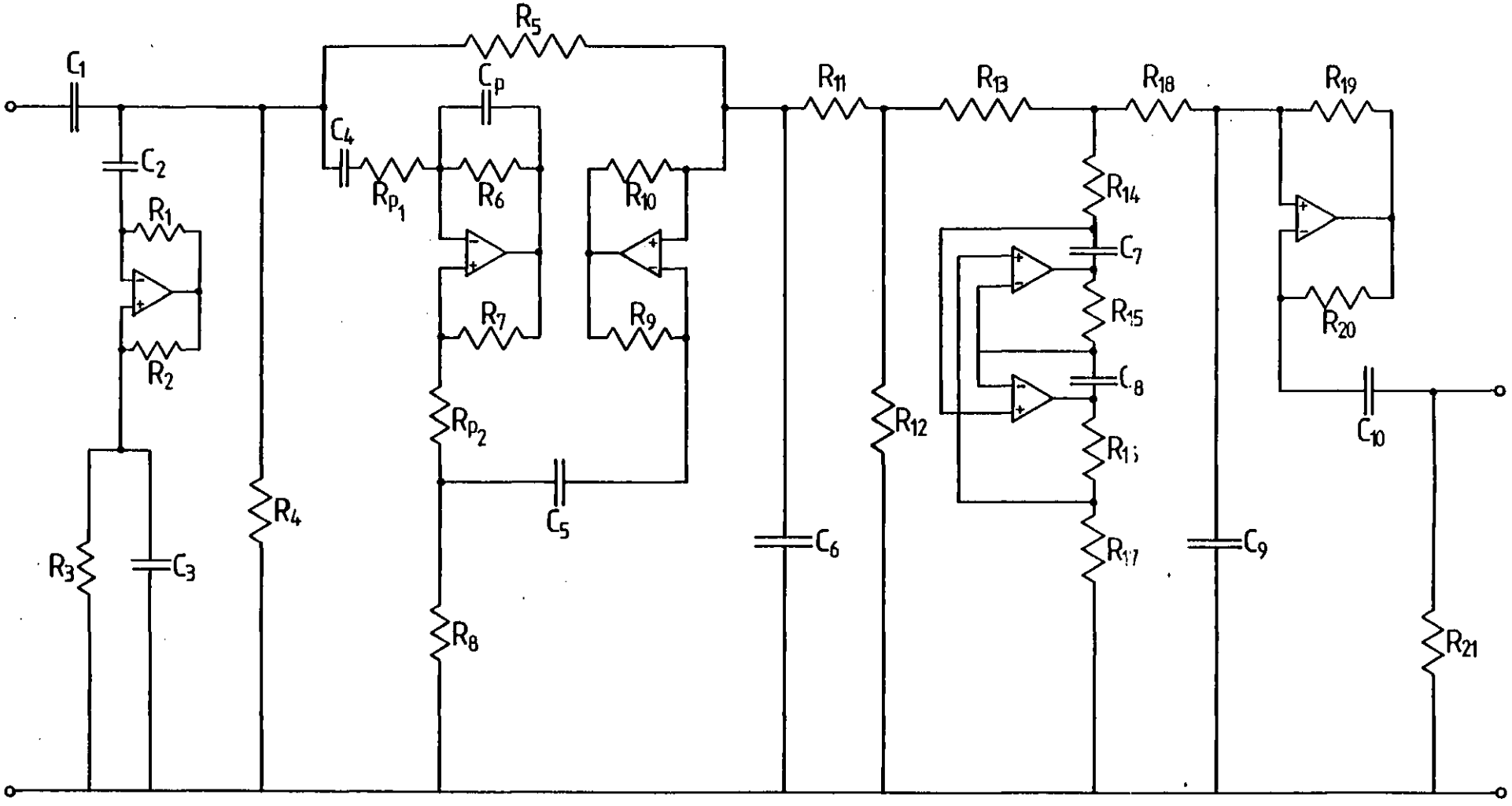

Fig 4.34 Active RC realisation of an 8th order elliptic bandpass filter.

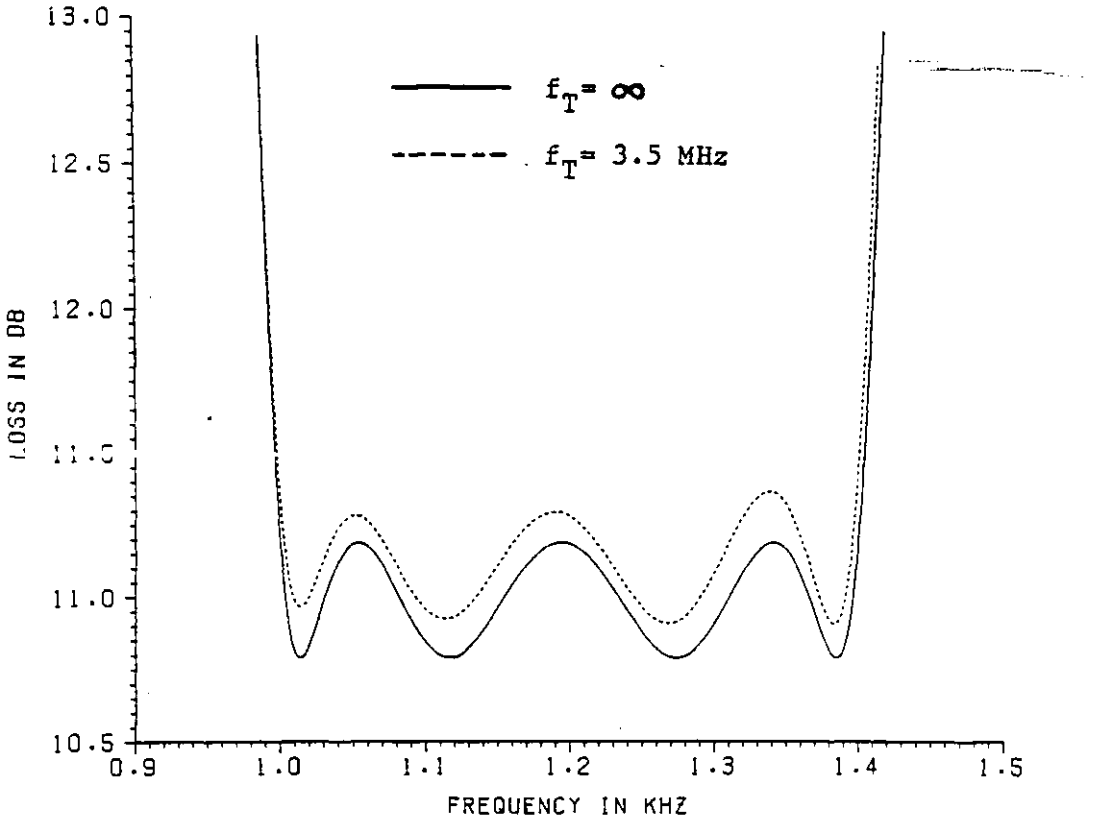

(a)

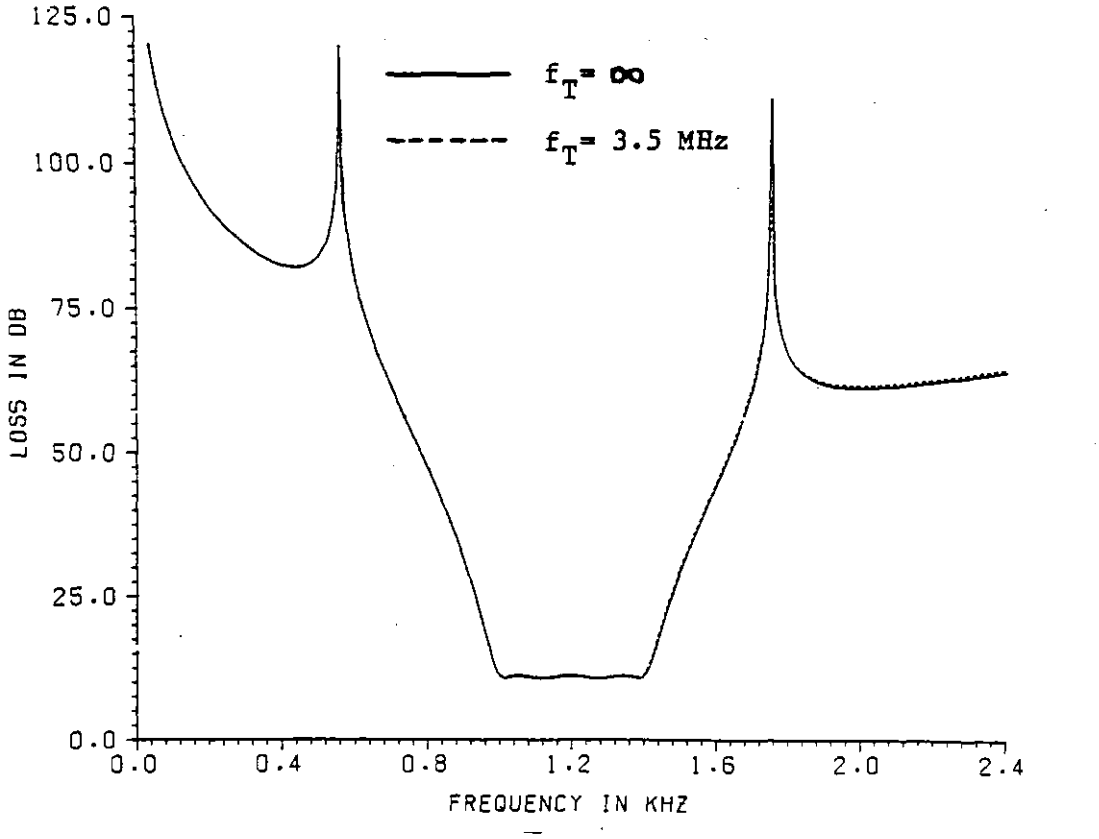

(b)

Fig 4.35 Computed response curves of the circuit in Fig 4.34. (a) Passband response. (b) Stopband response.

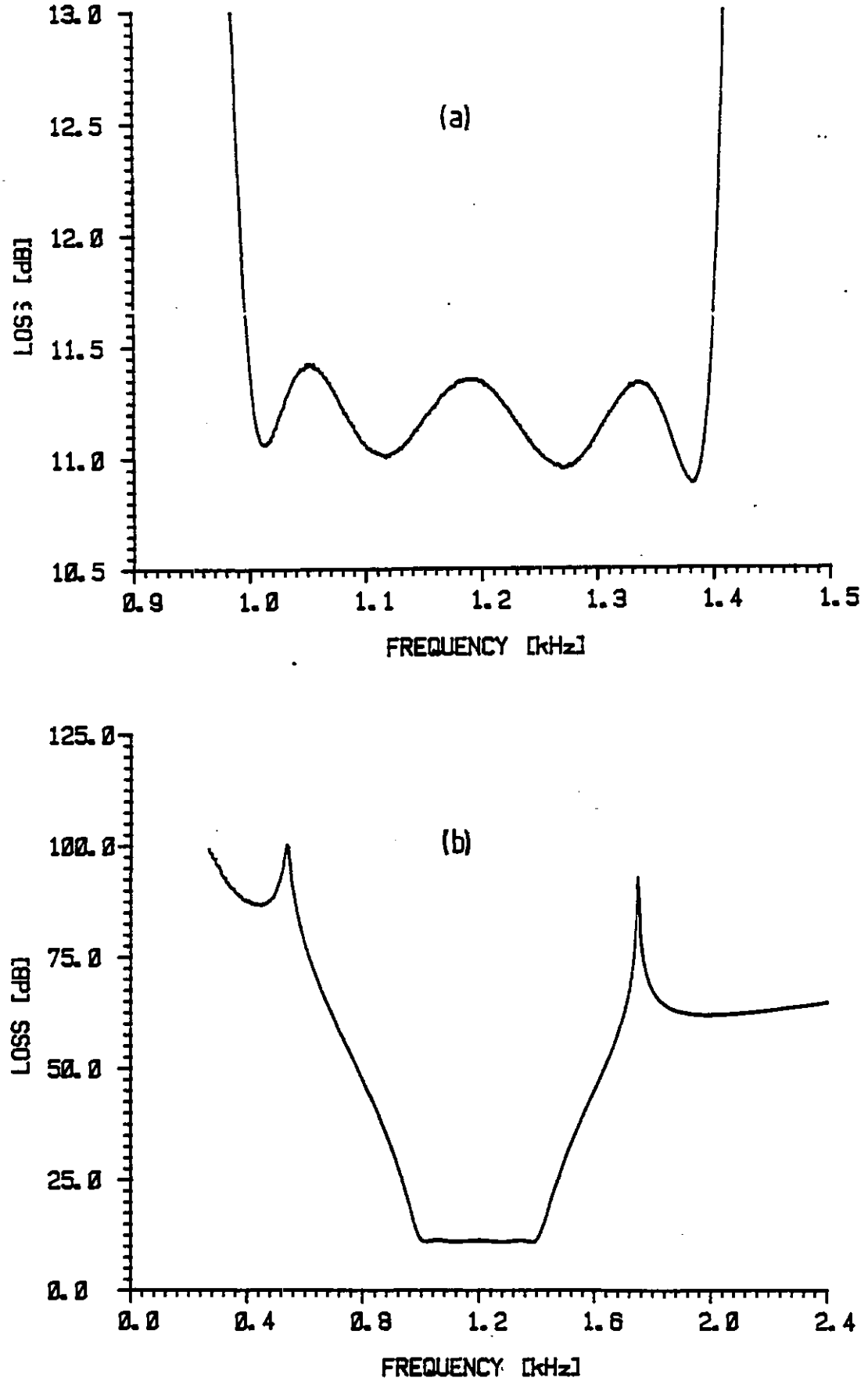

Fig 4.36 Measured response curves of the circuit in Fig 4.34.
(a) Passband response. (b) Stopband response.

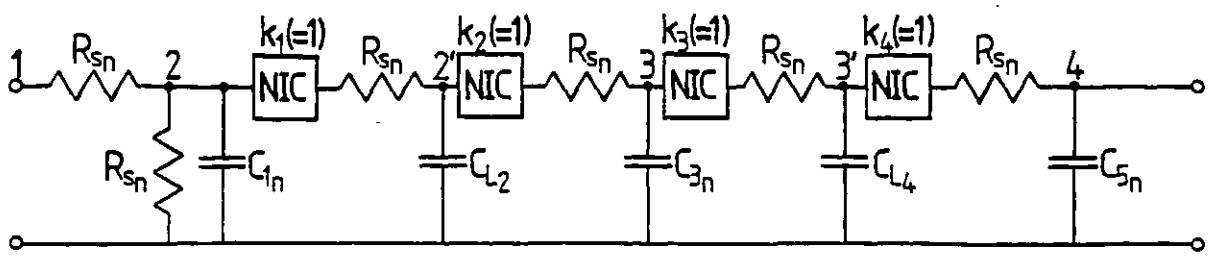

(a)

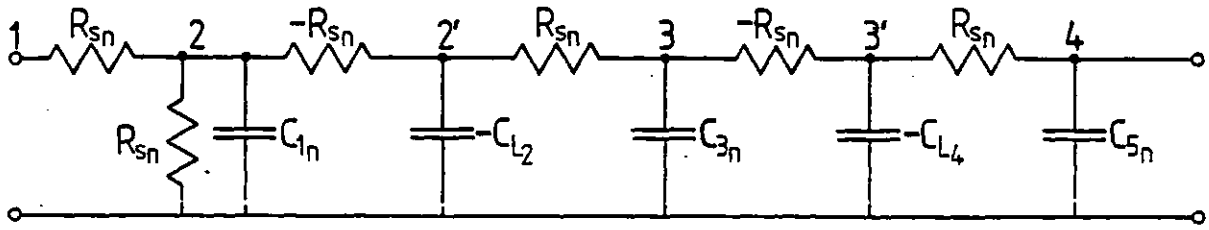

(b)

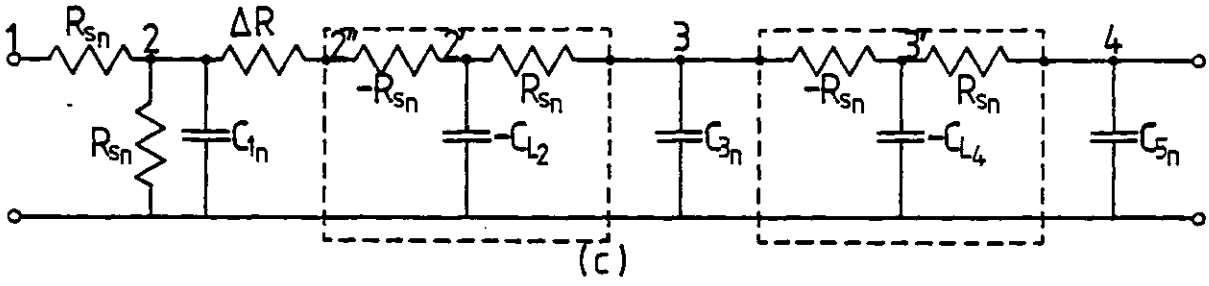

(c)

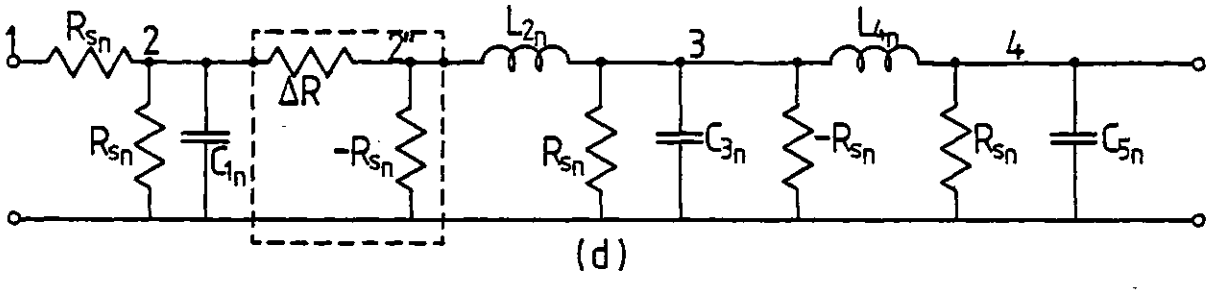

(d)

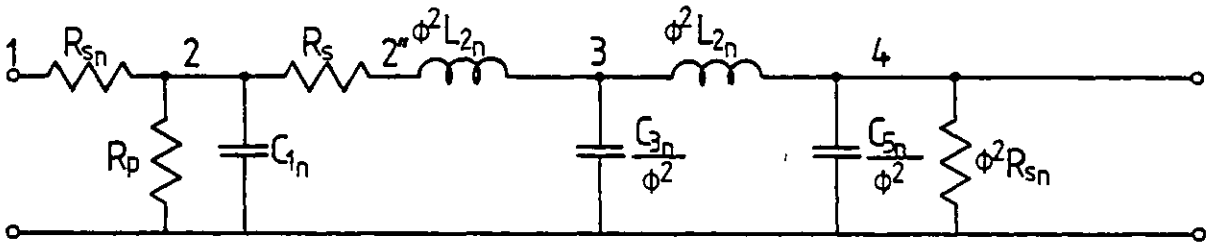

(e) $\Phi = 1 - \frac{\Delta R}{R_{sn}}$; $R_s = \Phi . \Delta R$; $R_p = \frac{-\Phi}{1-\Phi} R_{sn}$

Fig 4.37 (a) Active RC realisation of a 5th order lowpass filter obtained from Fig 4.13(d). (b) Circuit obtained from (a) assuming the NICs to have nominal conversion factors. (c) Circuit obtained by considering the value of the resistor between nodes 2 and 2' in (b) to be changed by an amount ΔR. (d) Circuit obtained from (c) by transforming the encircled T-networks into their equivalent Π-networks. (e) Circuit obtained by applying Norton transformations to the encircled part in (d).

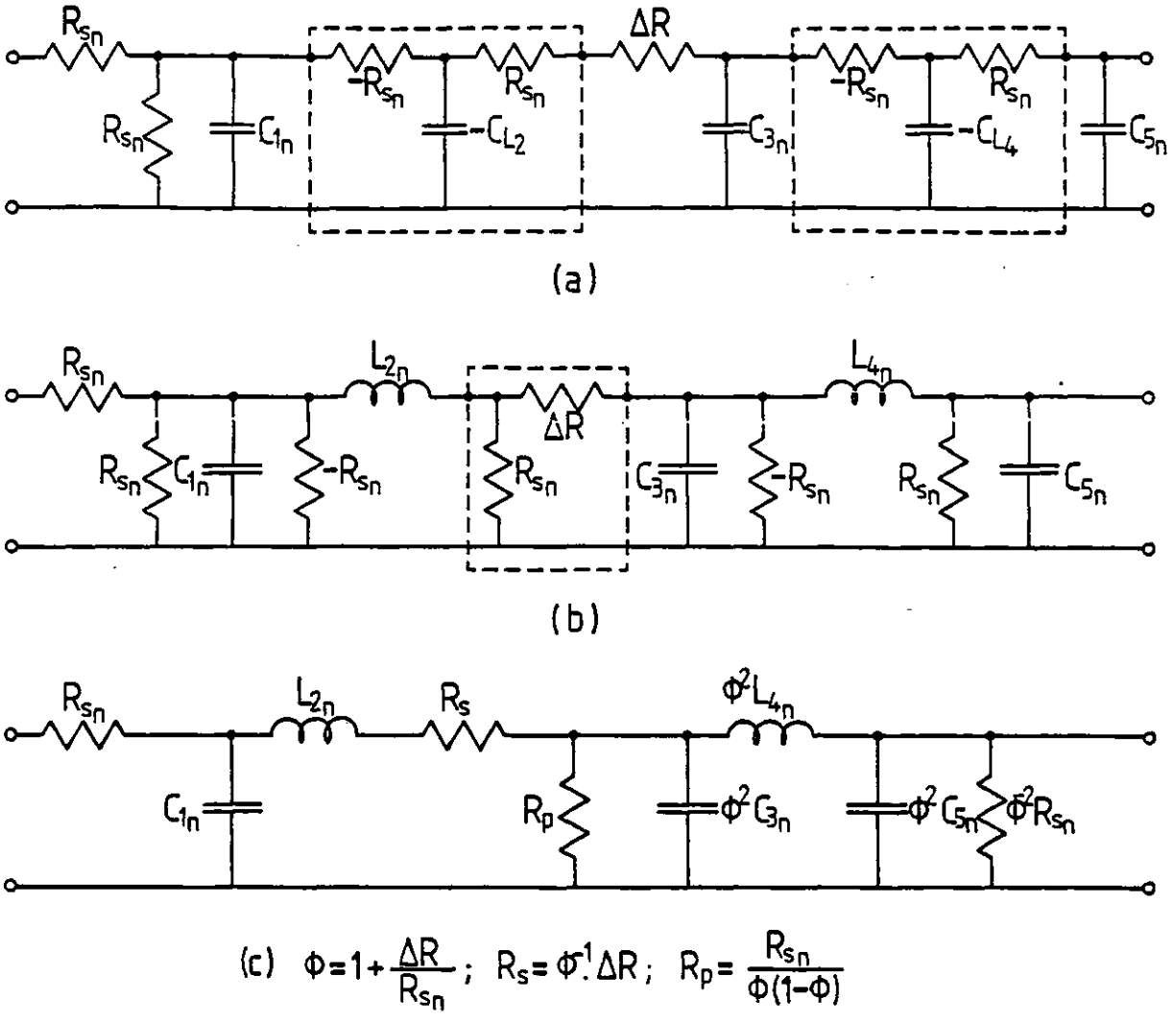

Fig 4.38 (a) Circuit obtained by considering the value of the resistor between nodes 2′ and 3 in Fig 4.37(b) to be changed by an amount ΔR. (b) Circuit obtained from (a) by transforming the encircled T-networks into their equivalent Π-networks. (c) Circuit obtained by applying Norton transformations to the encircled part in (b).

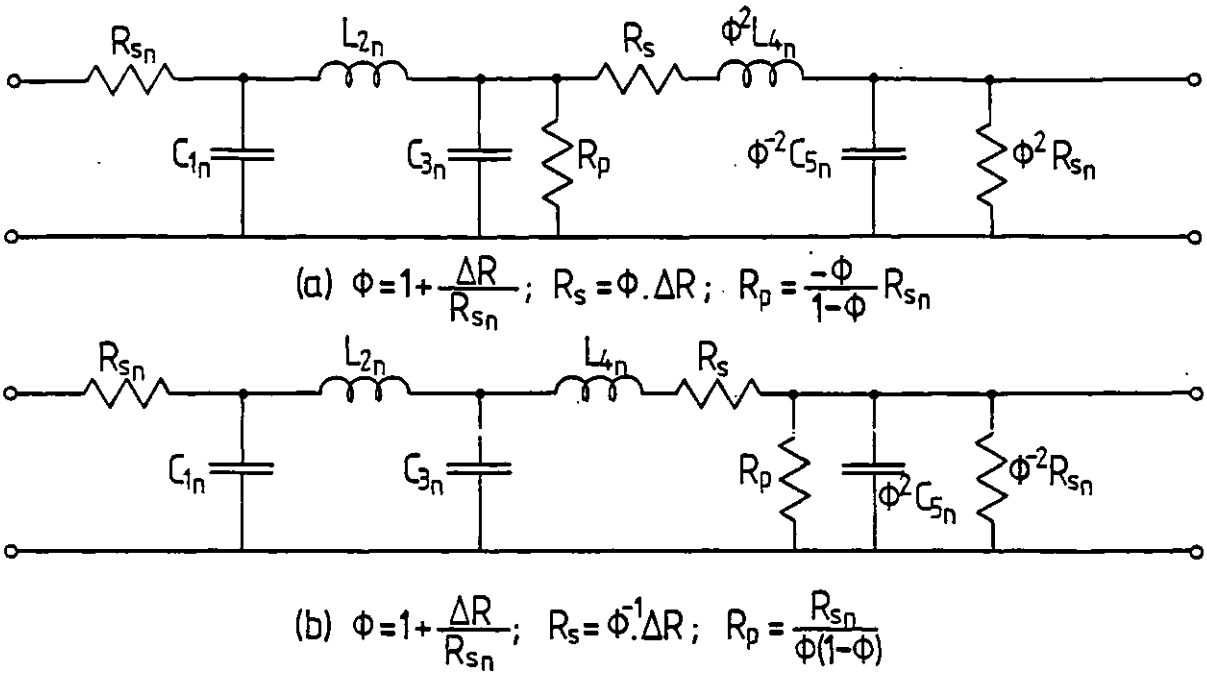

Fig 4.39 · (a) Equivalent circuit obtained by considering the value of the resistor between nodes 3 and 3´ in Fig 4.37(b) to be changed by an amount ΔR. (b) Equivalent circuit obtained by considering the value of the resistor between nodes 3´ and 4 in Fig 4.37(b) to be changed by an amount ΔR.

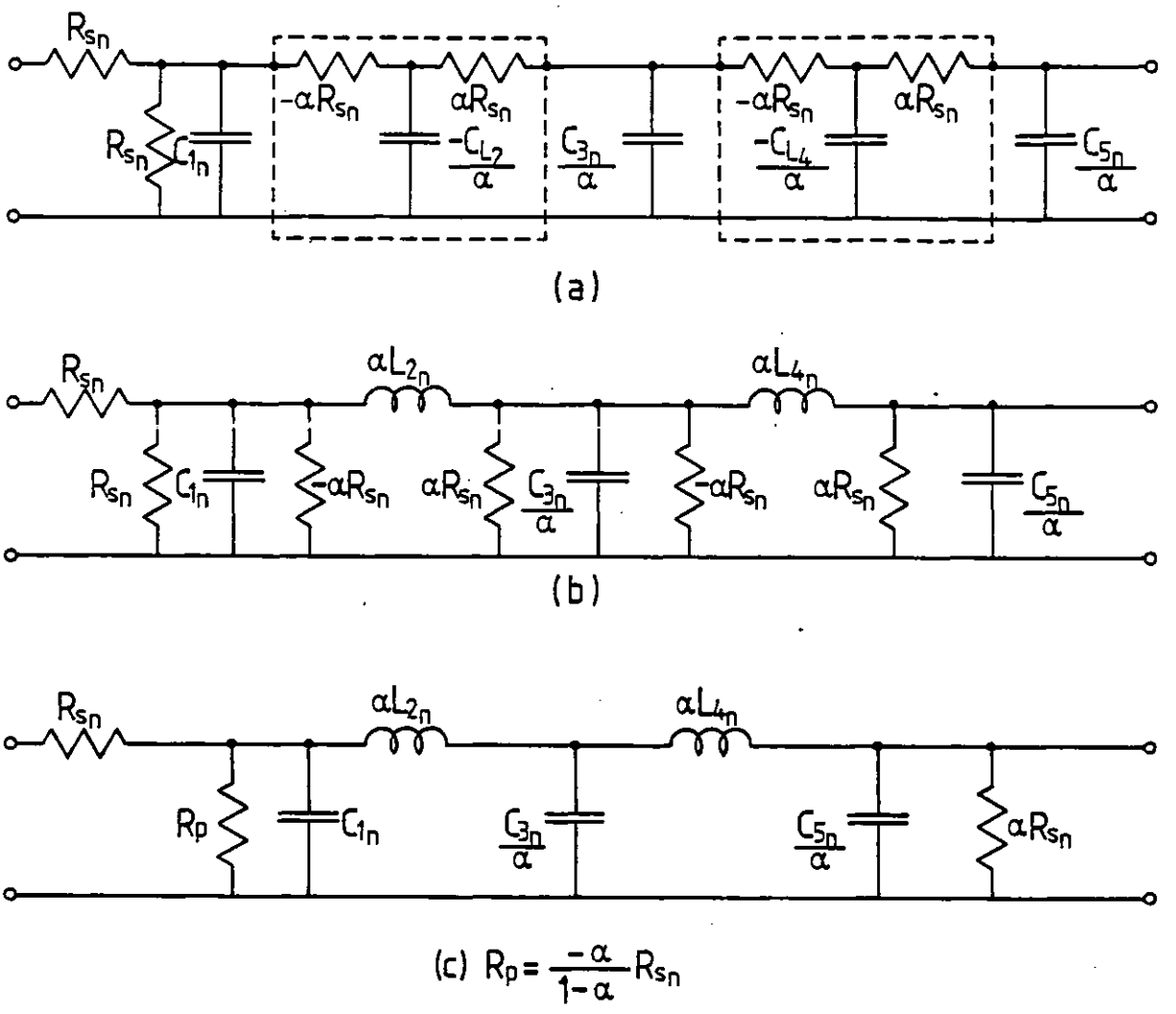

Fig 4.40 (a) Circuit obtained from Fig 4.37(a) assuming NIC_1 to have a conversion factor α while all other components have their nominal values. (b) Circuit obtained from (a) by transforming the encircled T-networks into their equivalent Π-networks. (c) An alternative representation of the circuit in (b).

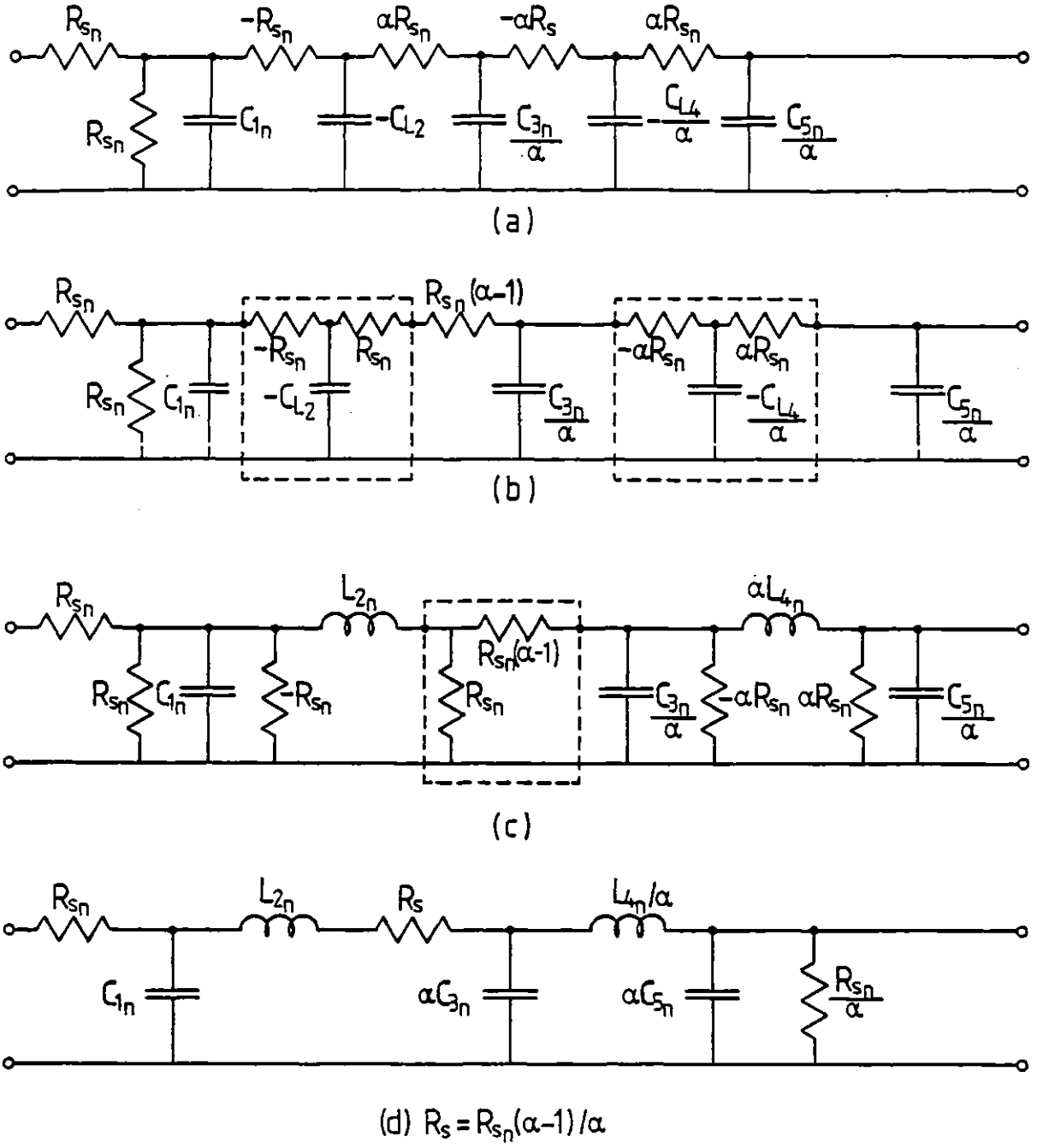

Fig 4.41 (a) Circuit obtained from Fig 4.37(a) assuming NIC_2 to have a conversion factor α while all other components have their nominal values. (b) An alternative representation of the circuit in (a). (c) Circuit obtained from (b) by transforming the encircled T-networks into their equivalent Π-networks. (d) Circuit obtained by applying the Norton transformations to the encircled part in (c).

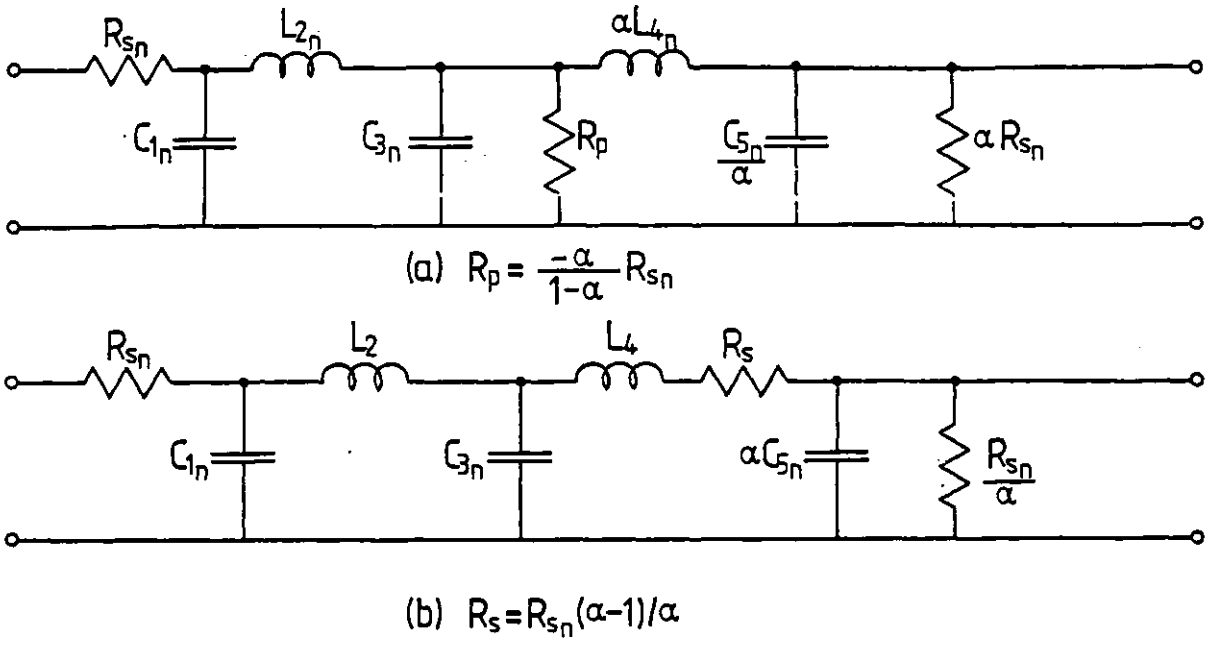

Fig 4.42 (a) Equivalent circuit obtained by considering the conversion factor of NIC_3 in Fig 4.37(a) to be α instead of its nominal value. (b) Equivalent circuit obtained by considering the conversion factor of NIC_4 in Fig 4.37(a) to be α instead of its nominal value.

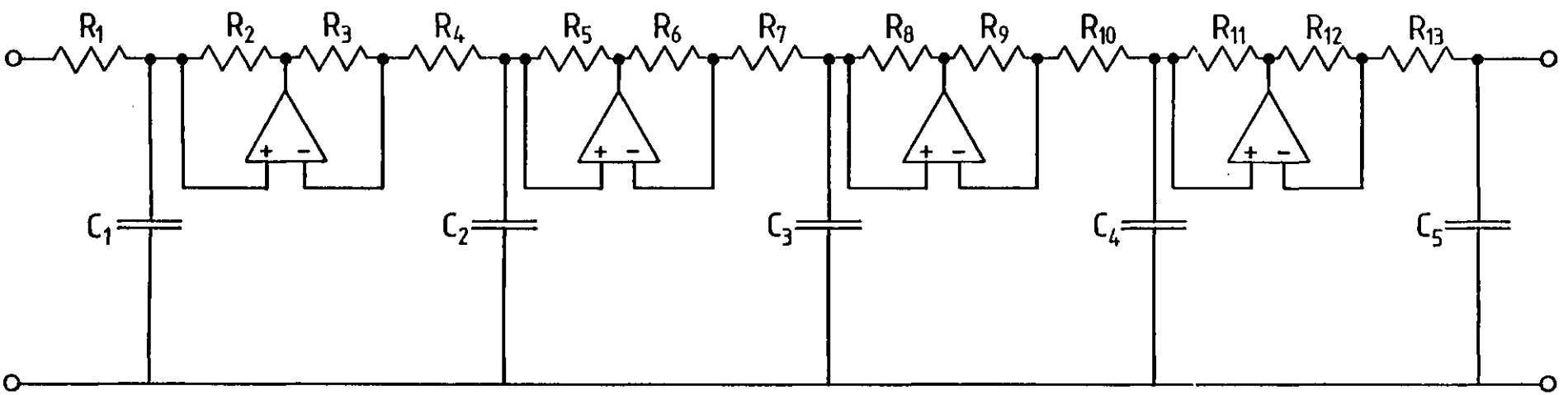

Fig 4.43 Active RC realisation of the 5th order lowpass filter of Fig 4.17(a).

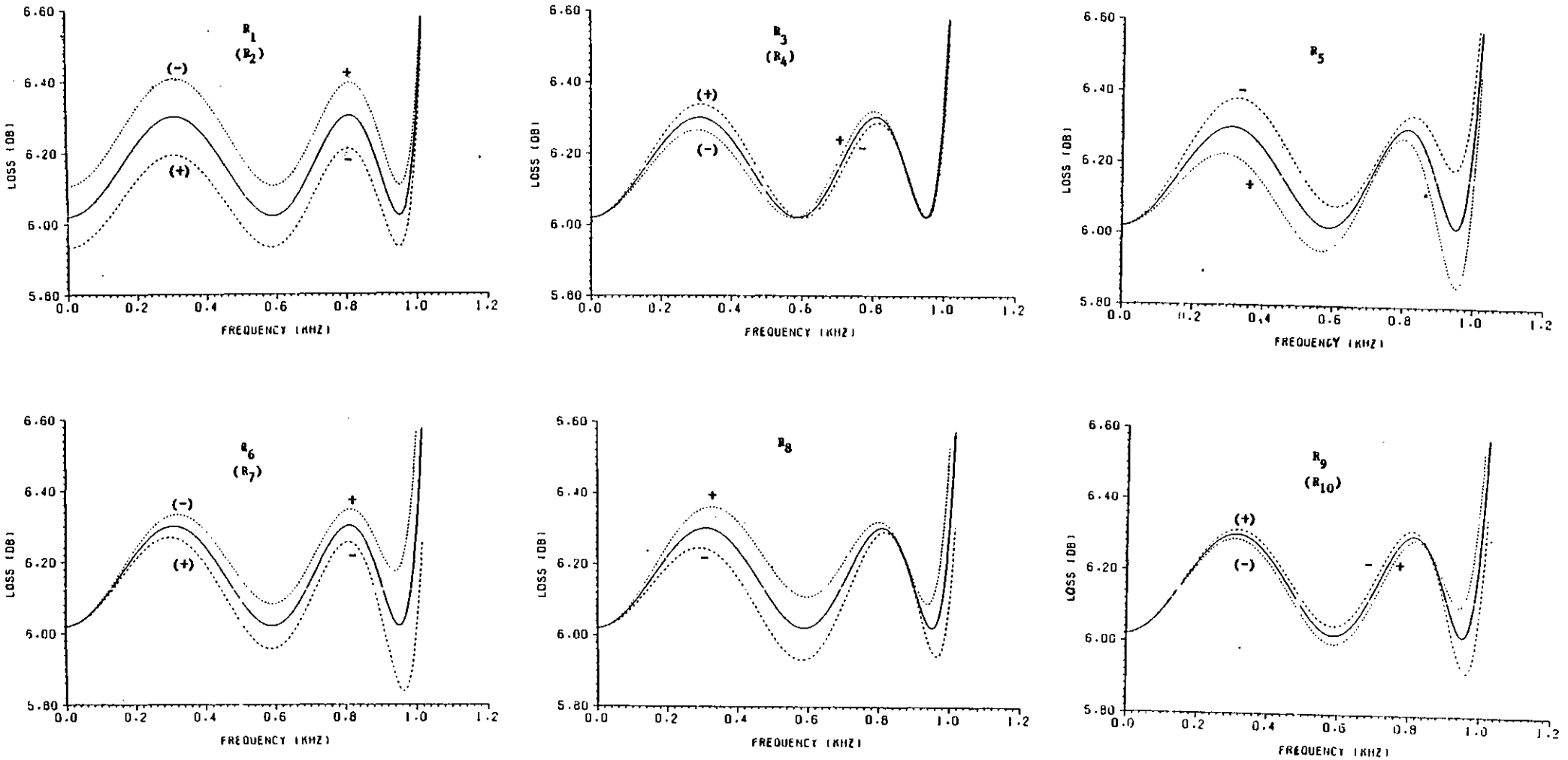

Fig 4.44 (Continued on next page)

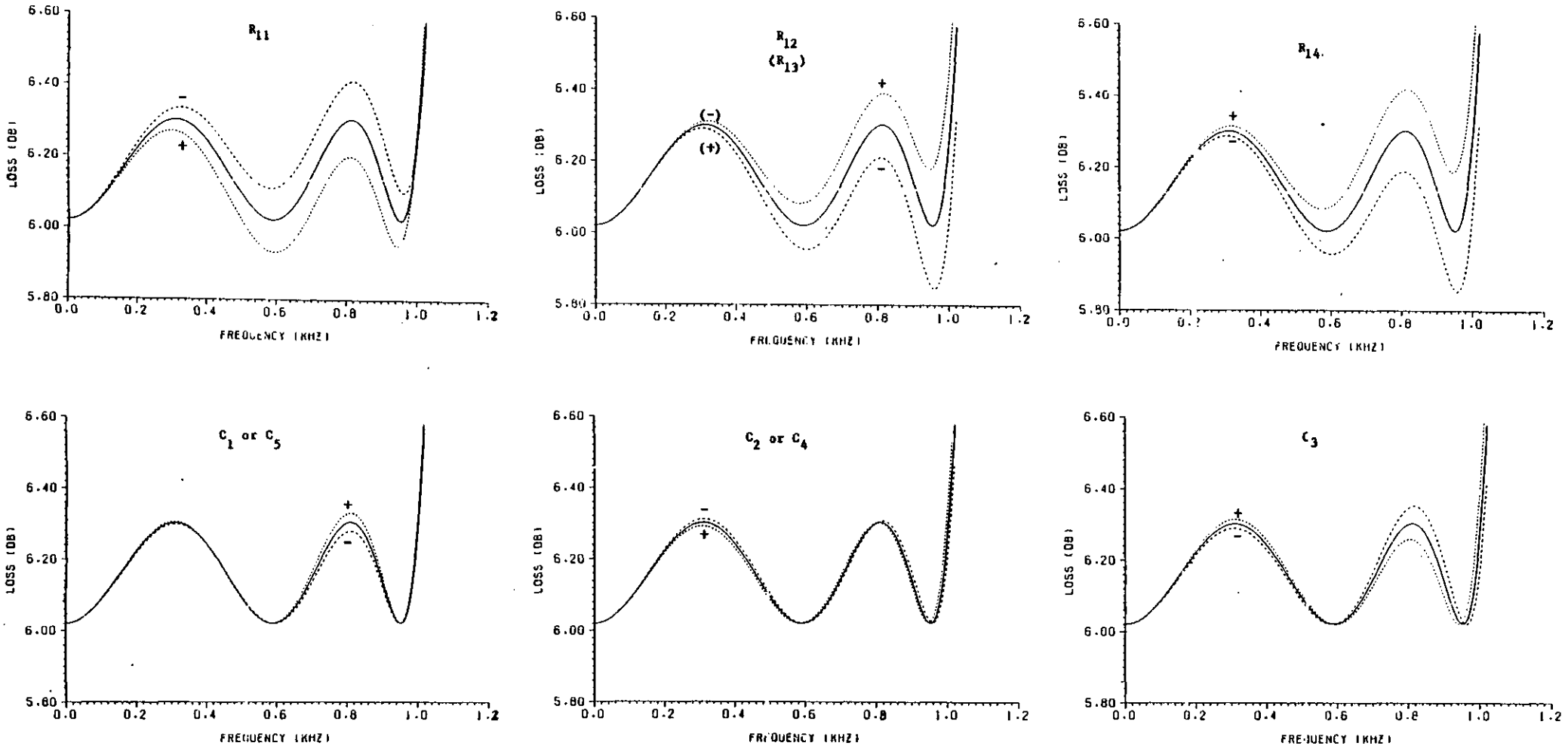

Fig 4.44 Effect of individually changing each component of the circuit in Fig 4.28 by $\pm$ 2 % from its nominal value.

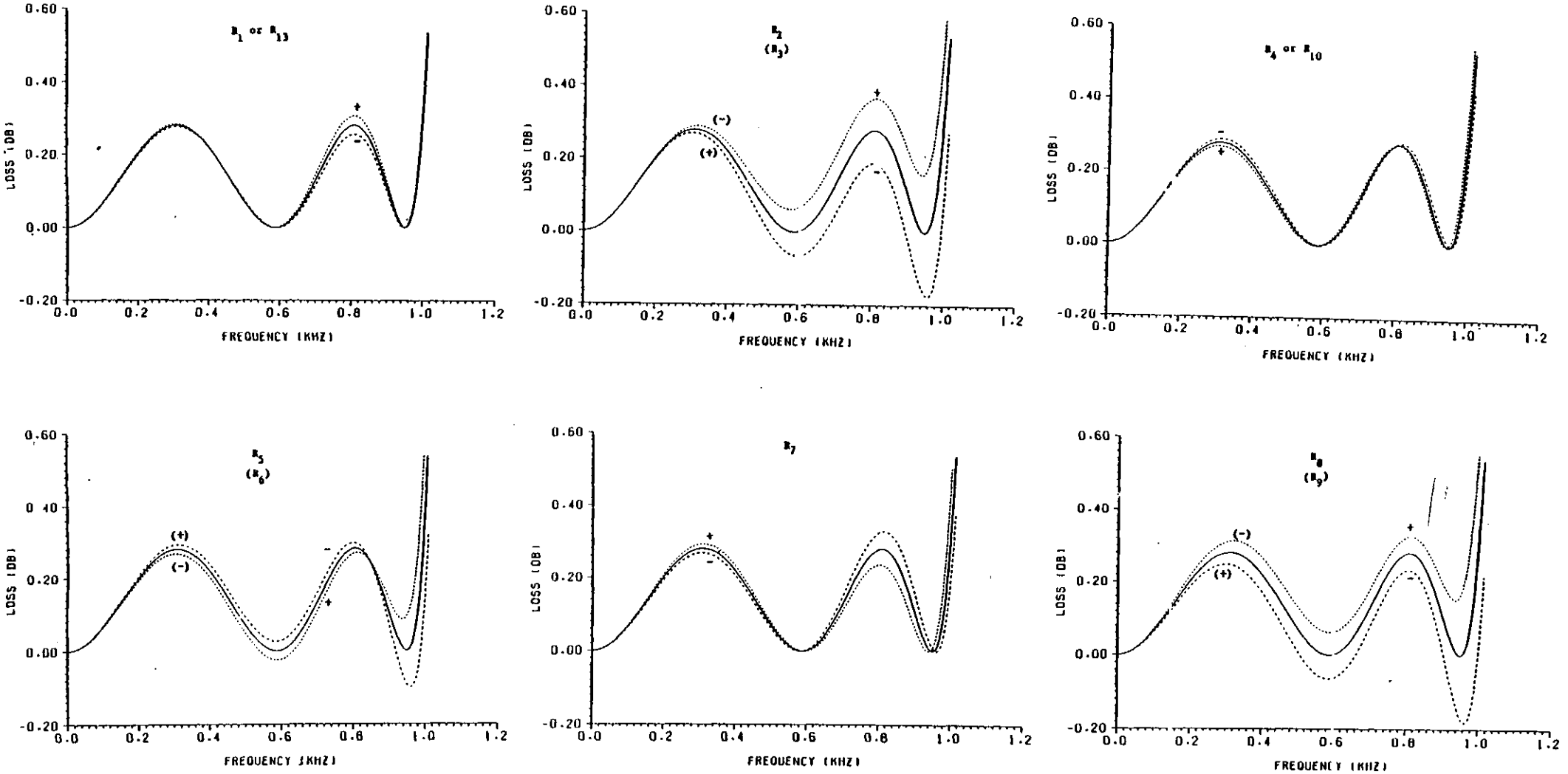

Fig 4.45 (Continued on next page)

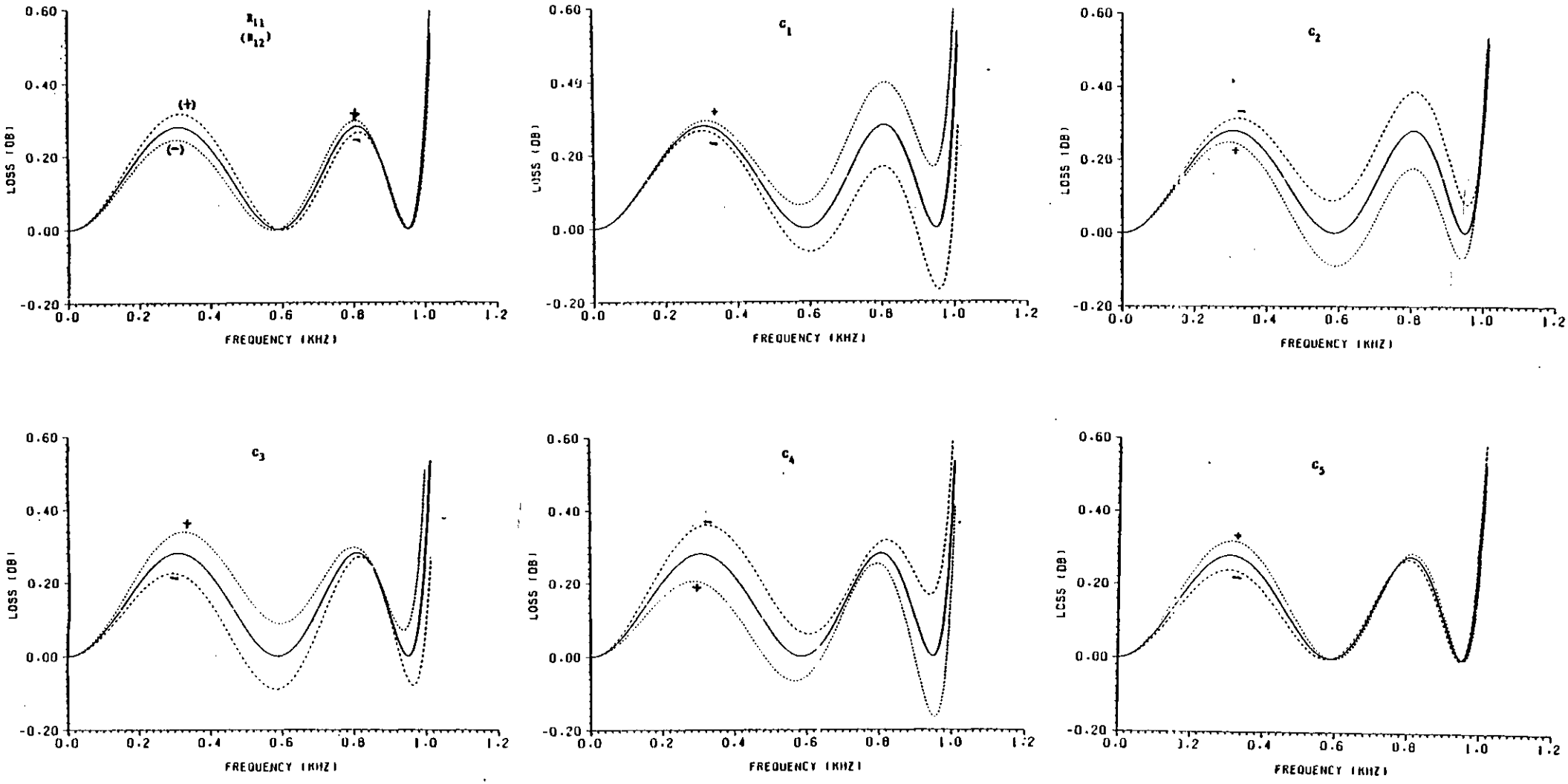

Fig 4.45 Effect of individually $\pm$ changing each component of the circuit in Fig 4.43 by $\pm$ 2 % from its nominal value.

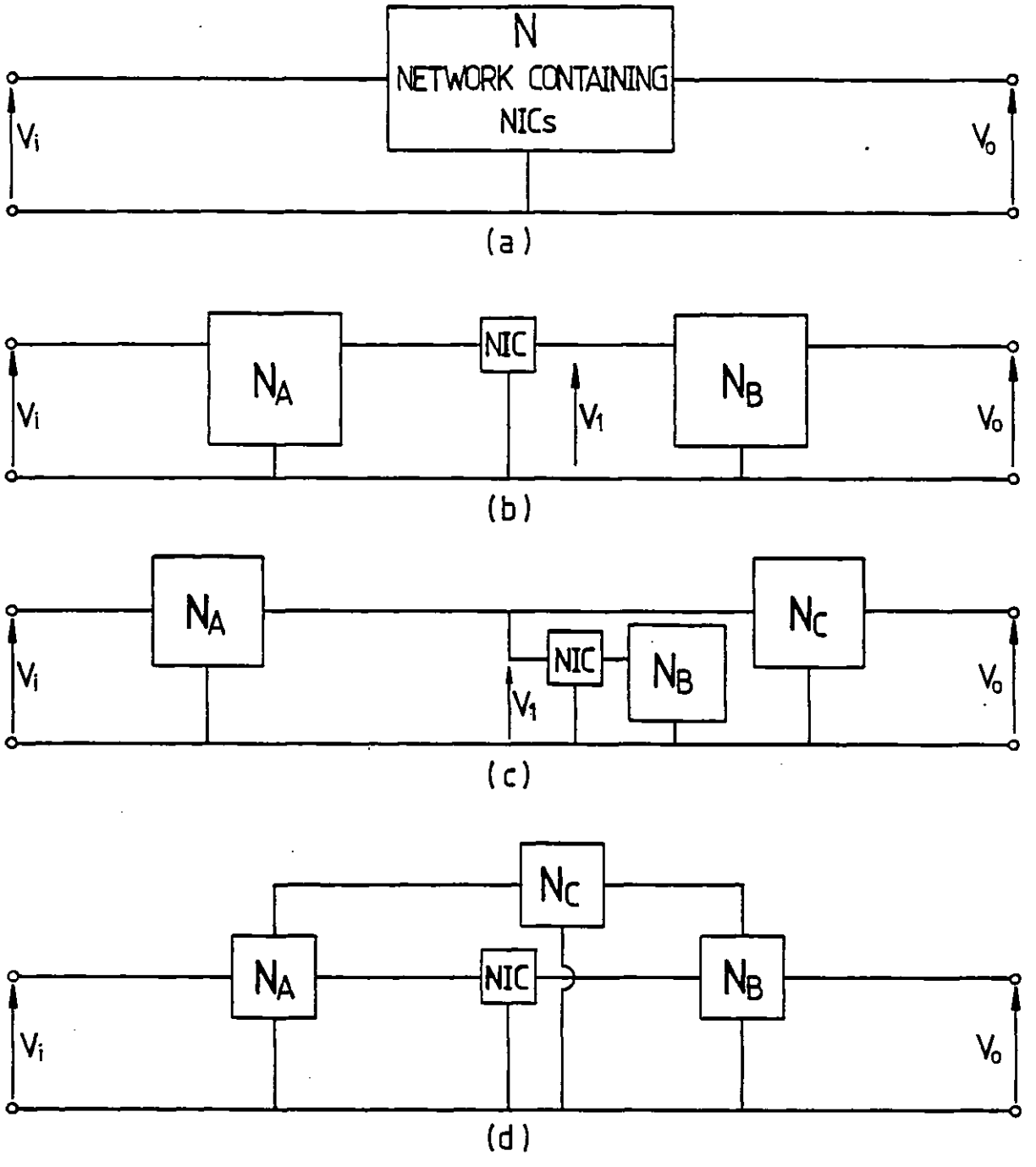

Fig 5.1 (a) A general 2-port network containing NICs. (b) Coupling NIC network. (c) Grounded NIC network. (d) Bridged NIC network.

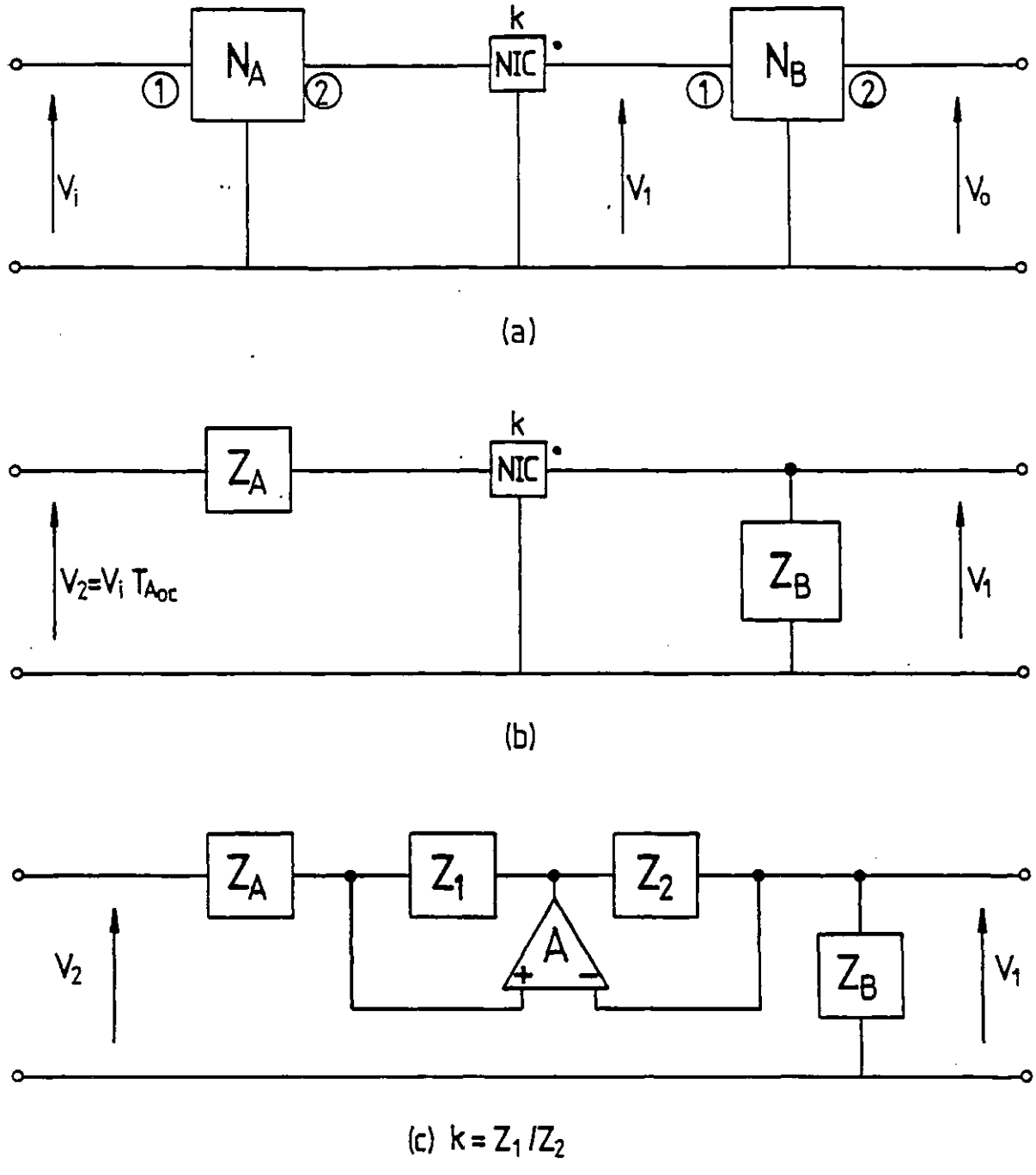

Fig 5.2 Effect of finite f_T for the case of the coupling NIC. (a) Coupling NIC network. (b) Circuit obtained by replacing the network N_B in (a) by its equivalent 1-port impedance and by replacing the network N_A by its Thevenin's equivalence. $T_{A_{oc}}$ represents the open circuit voltage transfer function of the network N_A. (c) Circuit obtained by replacing the NIC in (b) by its OP-AMP equivalent.

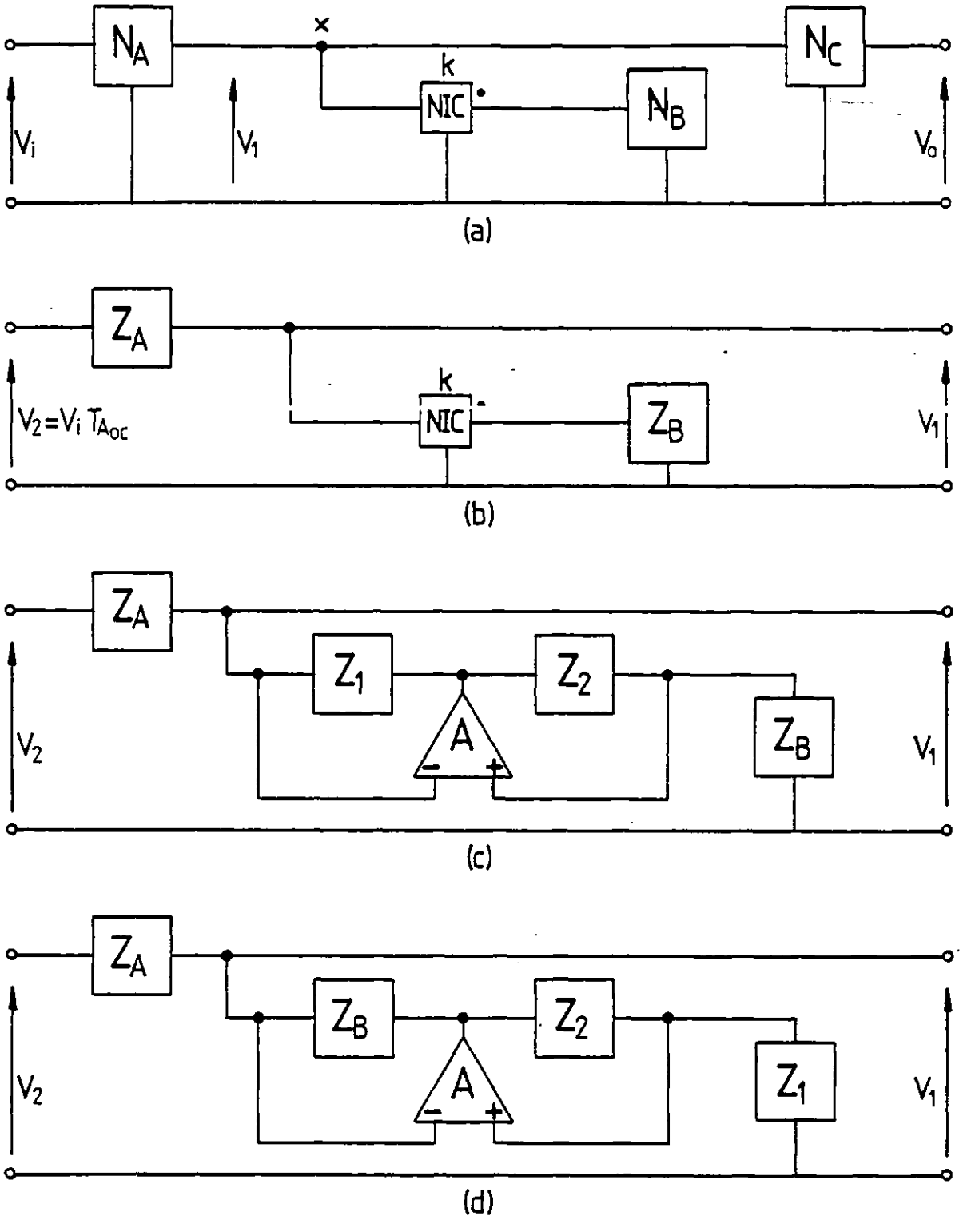

Fig 5.3 Effect of finite f_T for the case of the grounded NIC. (a) Grounded NIC network. (b) Circuit obtained by replacing the network N_B in (a) by its equivalent 1-port impedance and by replacing the network N_A by its Thevenin's equivalence. $T_{A_{oc}}$ represents the voltage transfer function at point "X" in (a) with the NIC disconnected. (c) Circuit obtained by replacing the NIC in (b) by its OP-AMP equivalent. (d) Circuit obtained by interchanging positions of impedances Z_1 and Z_B in (c).

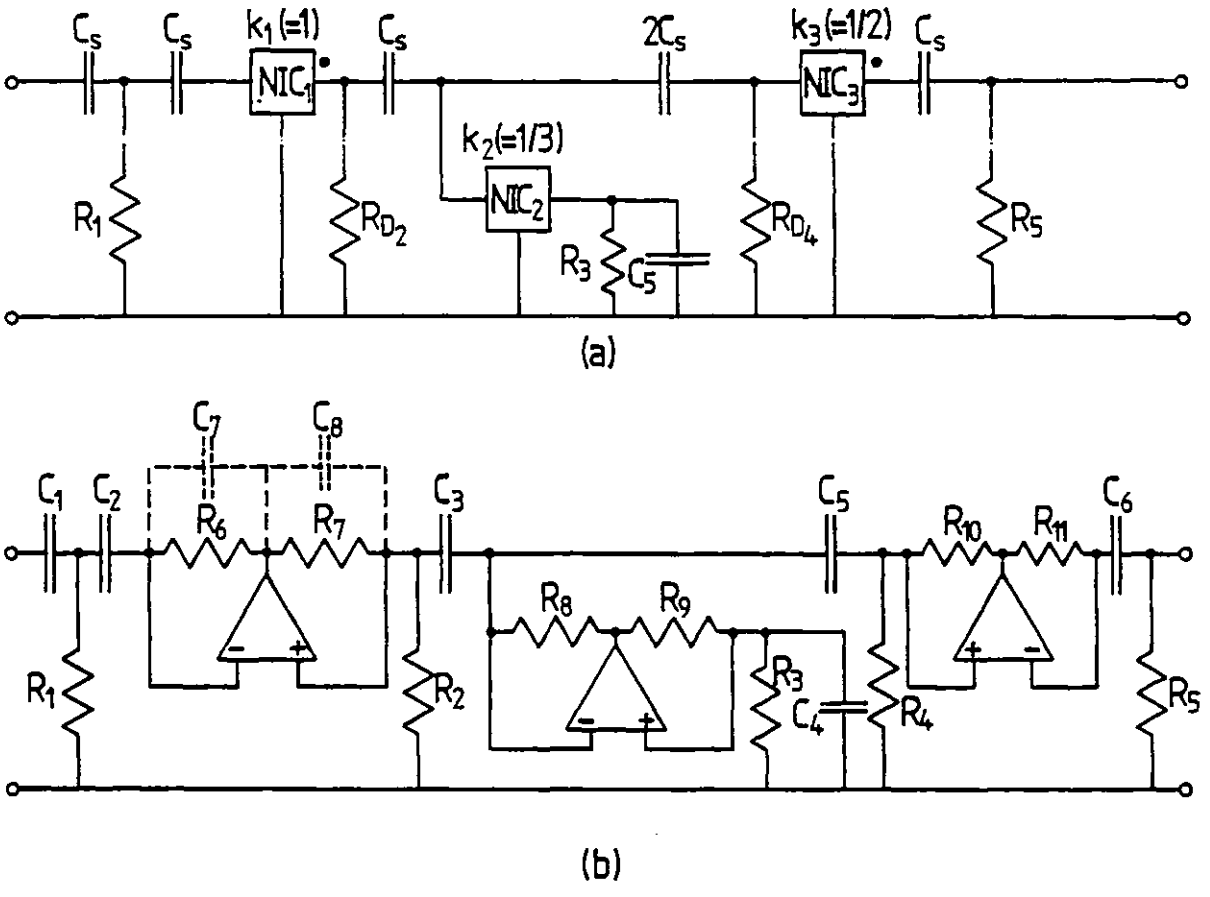

Fig 5.4 (a) Active RC realisation of a 5th order all-pole highpass filter (obtained from the circuit of Fig 4.21(c)). (b) Circuit obtained by replacing the NICs in (a) with their OP-AMP equivalents.

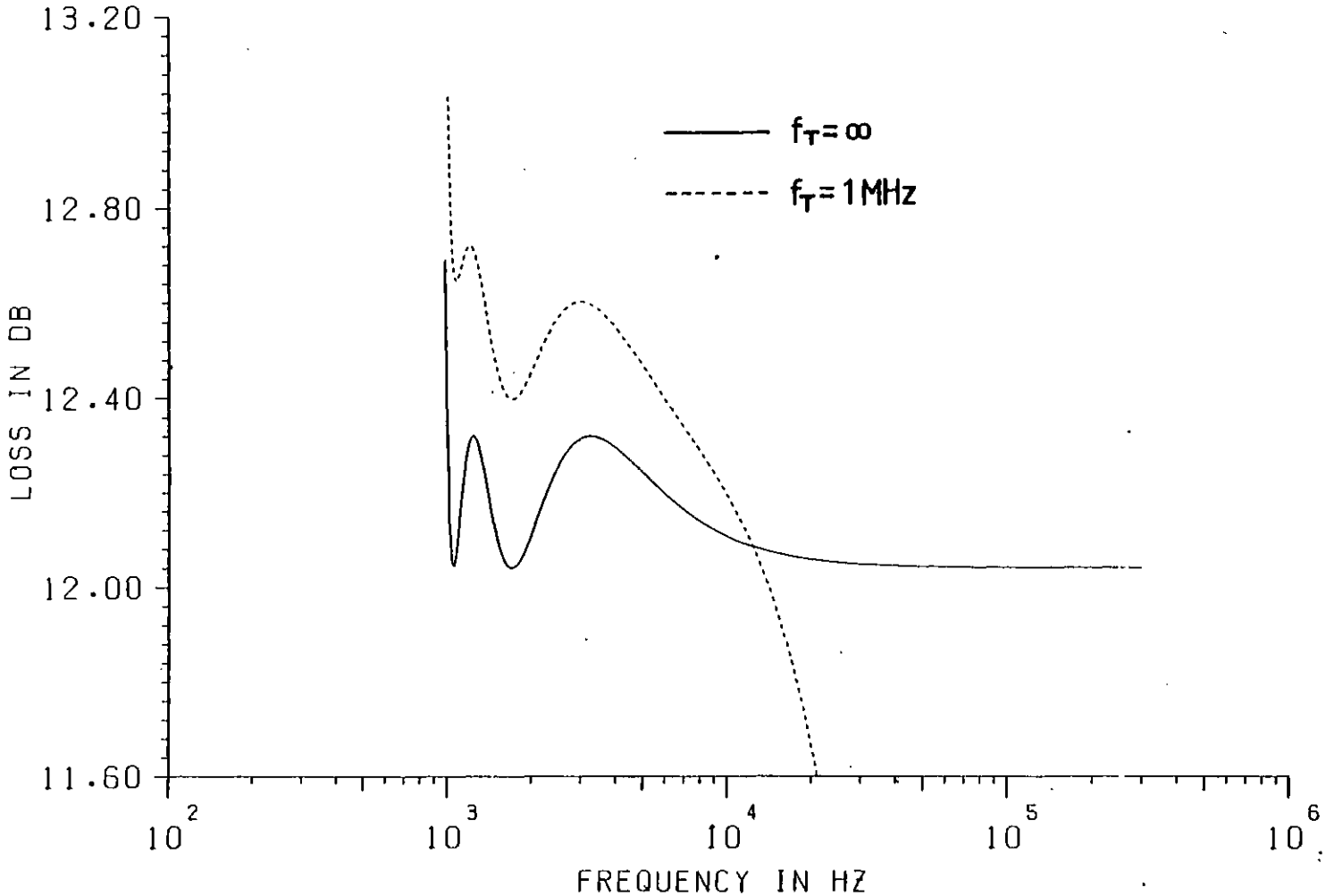

Fig 5.5 Computed frequency responses of the circuit in Fig 5.4(b) for the case of ideal and non-ideal OP-AMPs.

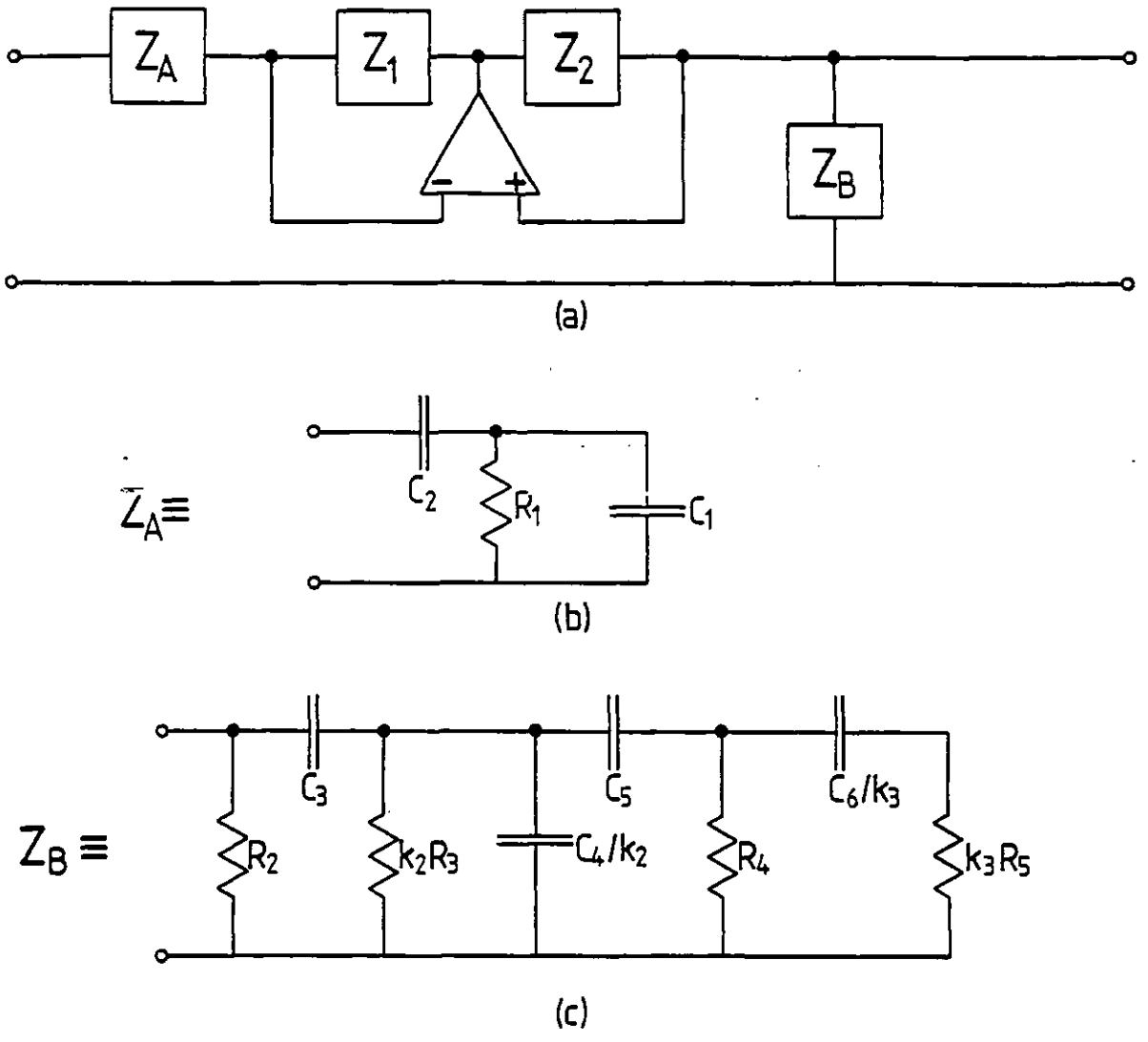

Fig 5.6 Minimising the effect of finite f_T of NIC_1 on the transfer function of the circuit in Fig 5.4(b).
(a) The equivalent circuit for minimising the effect of finite f_T. (b) Impedance equivalent to Z_A in (a). (c) Impedance equivalent to Z_B in (a).

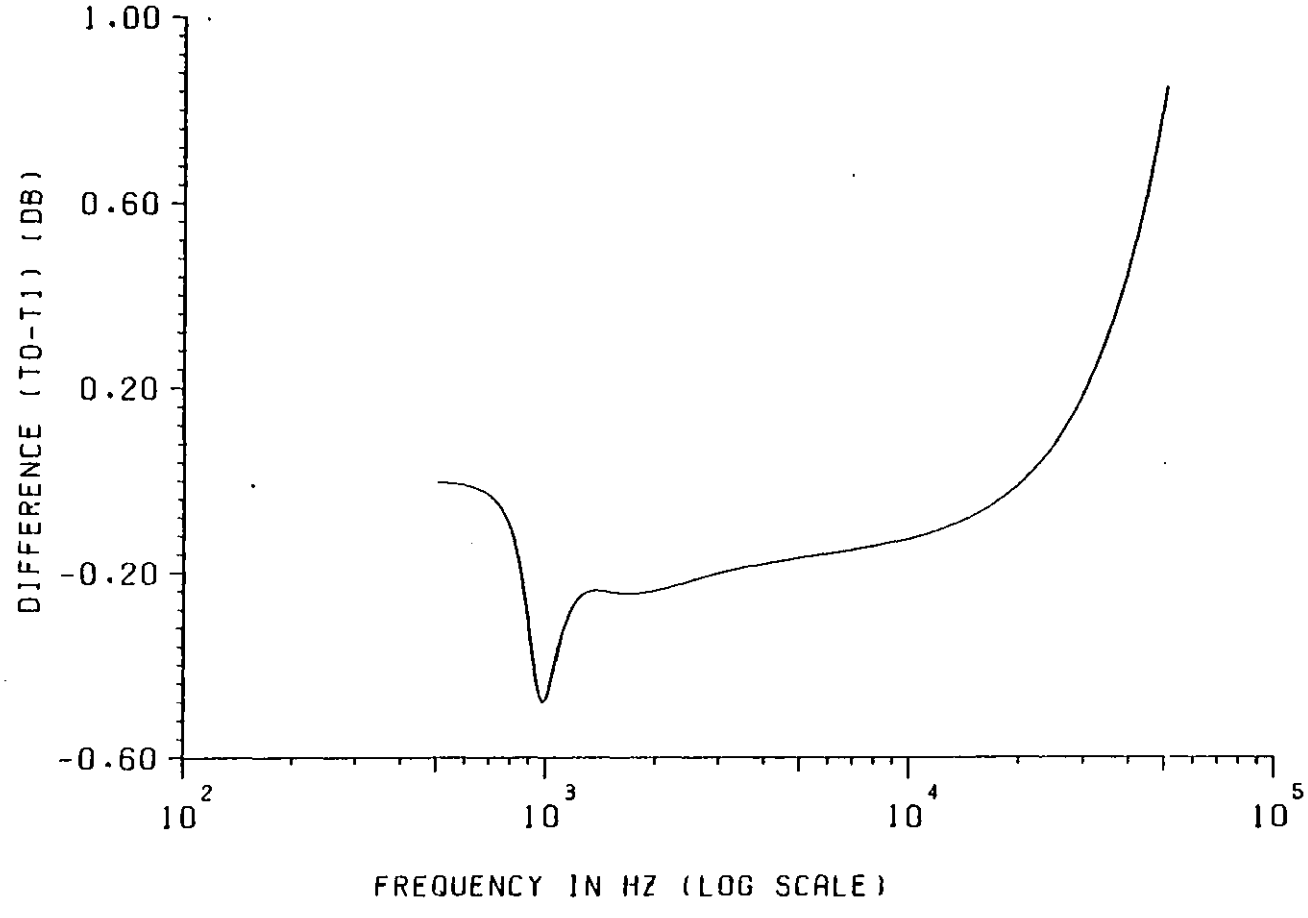

Fig 5.7 Plot of the modulus of the objective function against frequency for the case when the NIC impedances in the circuit of Fig 5.6(a) are chosen as $Z_1 = Z_2 = 1.0$ kilo-ohms.

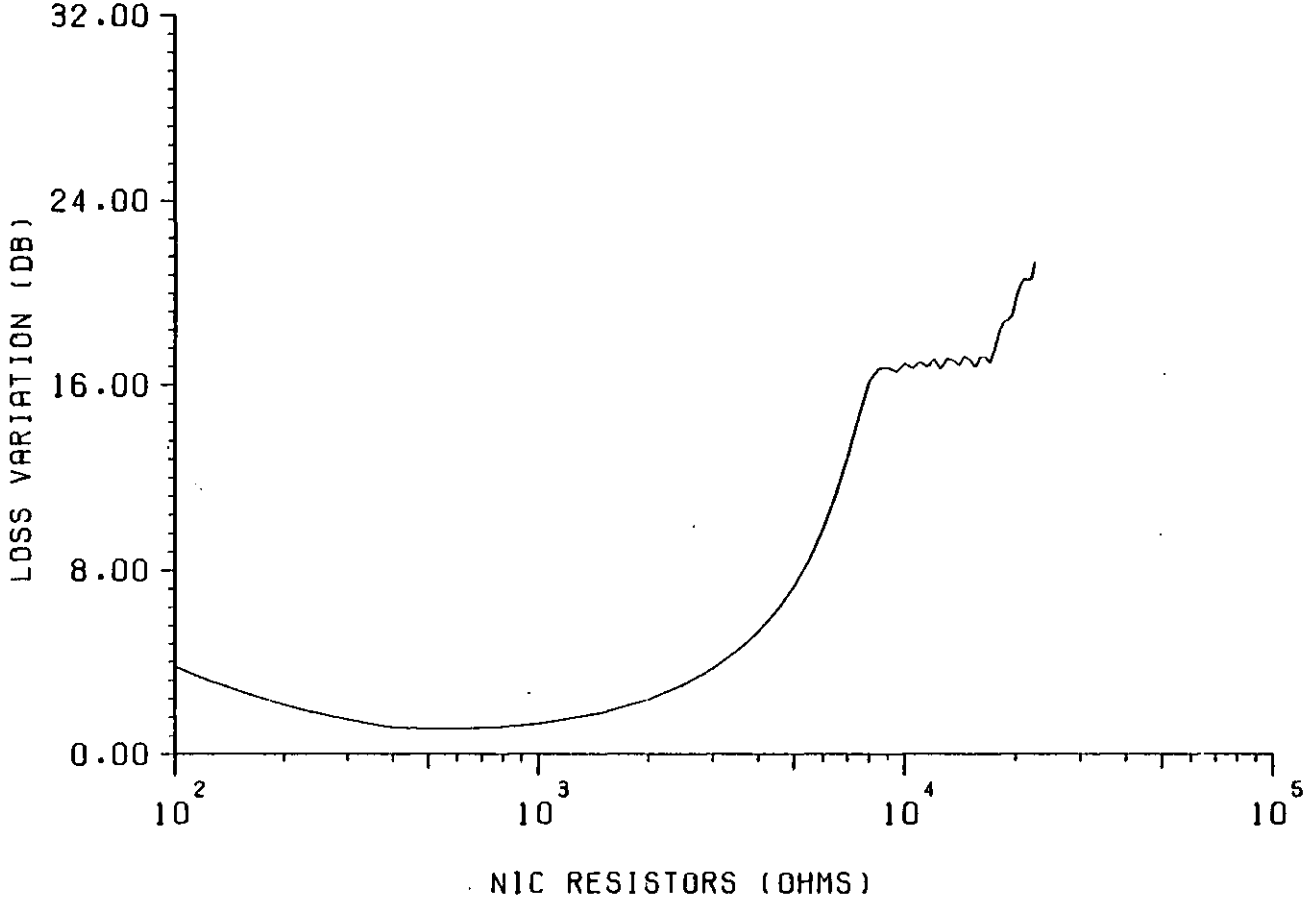

Fig 5.8 Plot of loss variation against NIC resistor value for NIC_1 of Fig 5.4(b).

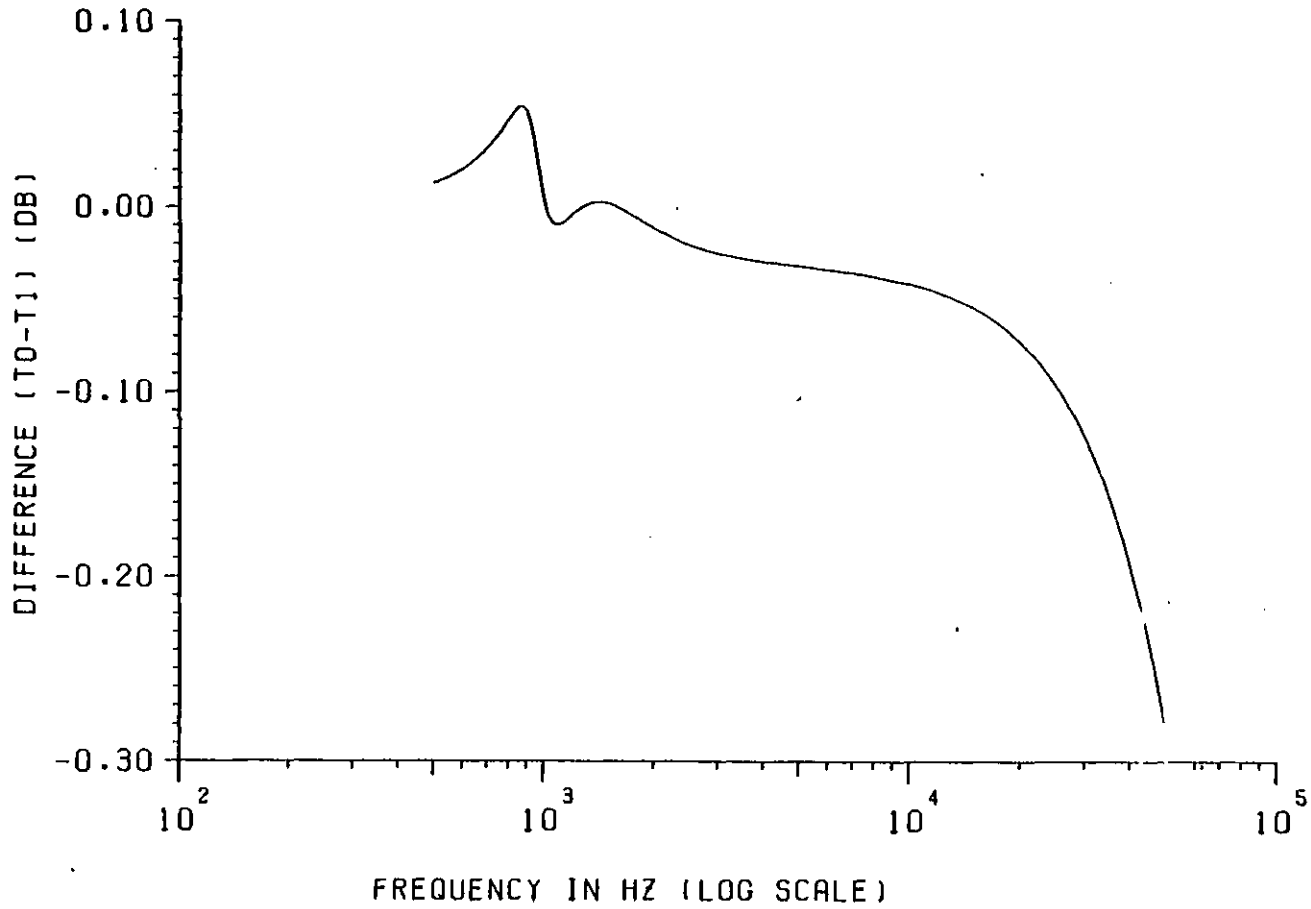

Fig 5.9 Plot of the modulus of the objective function against frequency for the case when the NIC impedances in the circuit of Fig 5.6(a) are chosen as a parallel combination of a resistor and a capacitor (R= 22.7201 kilo-ohms and C= 2.89036 nF).

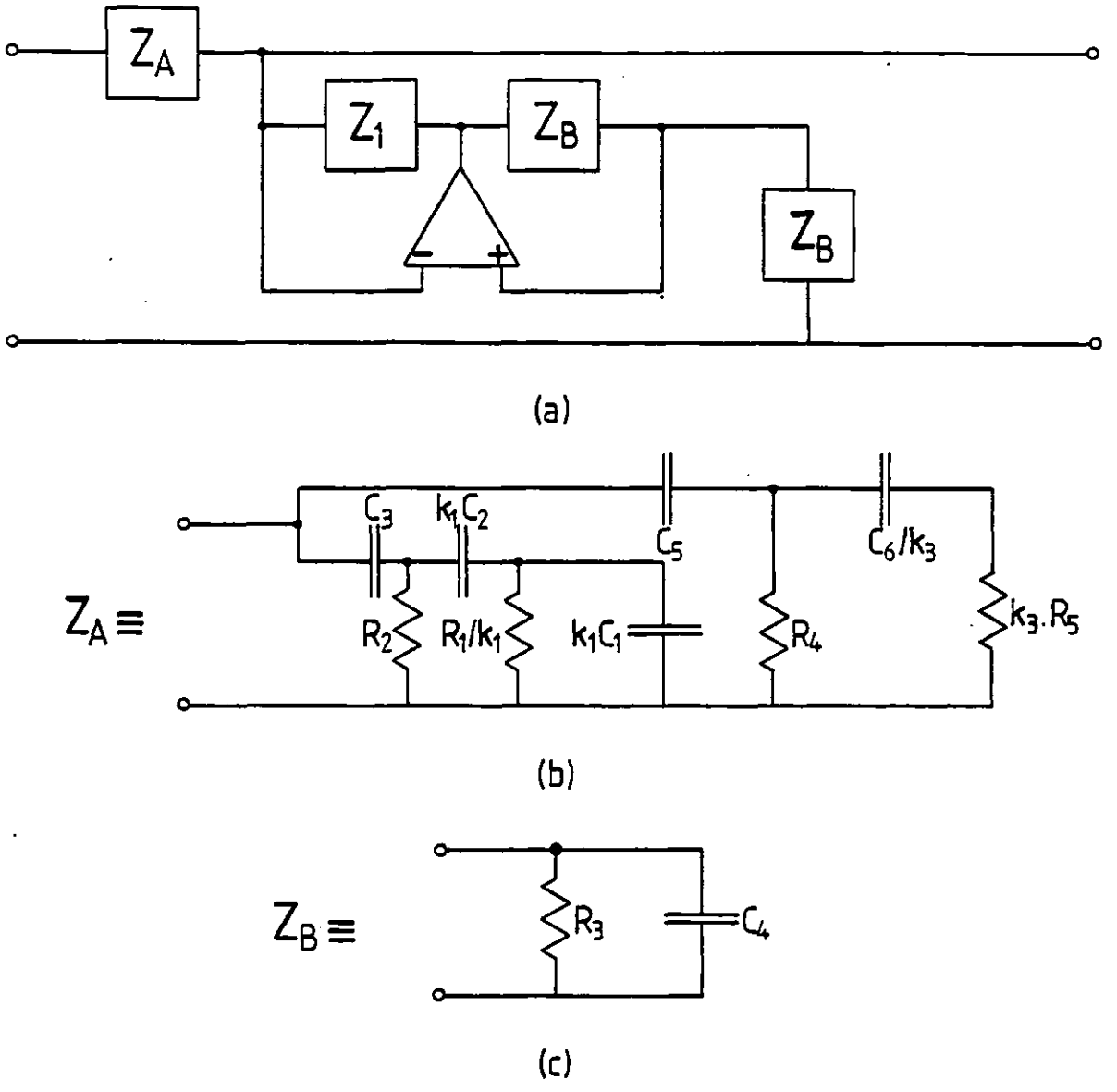

Fig 5.10 Minimising the effect of finite f_T of NIC_2 on the transfer function of the circuit in Fig 5.4(b).
(a) The equivalent circuit for minimising the effect of finite f_T. (b) Impedance equivalent to Z_A in (a). (c) Impedance equivalent to Z_B in (a).

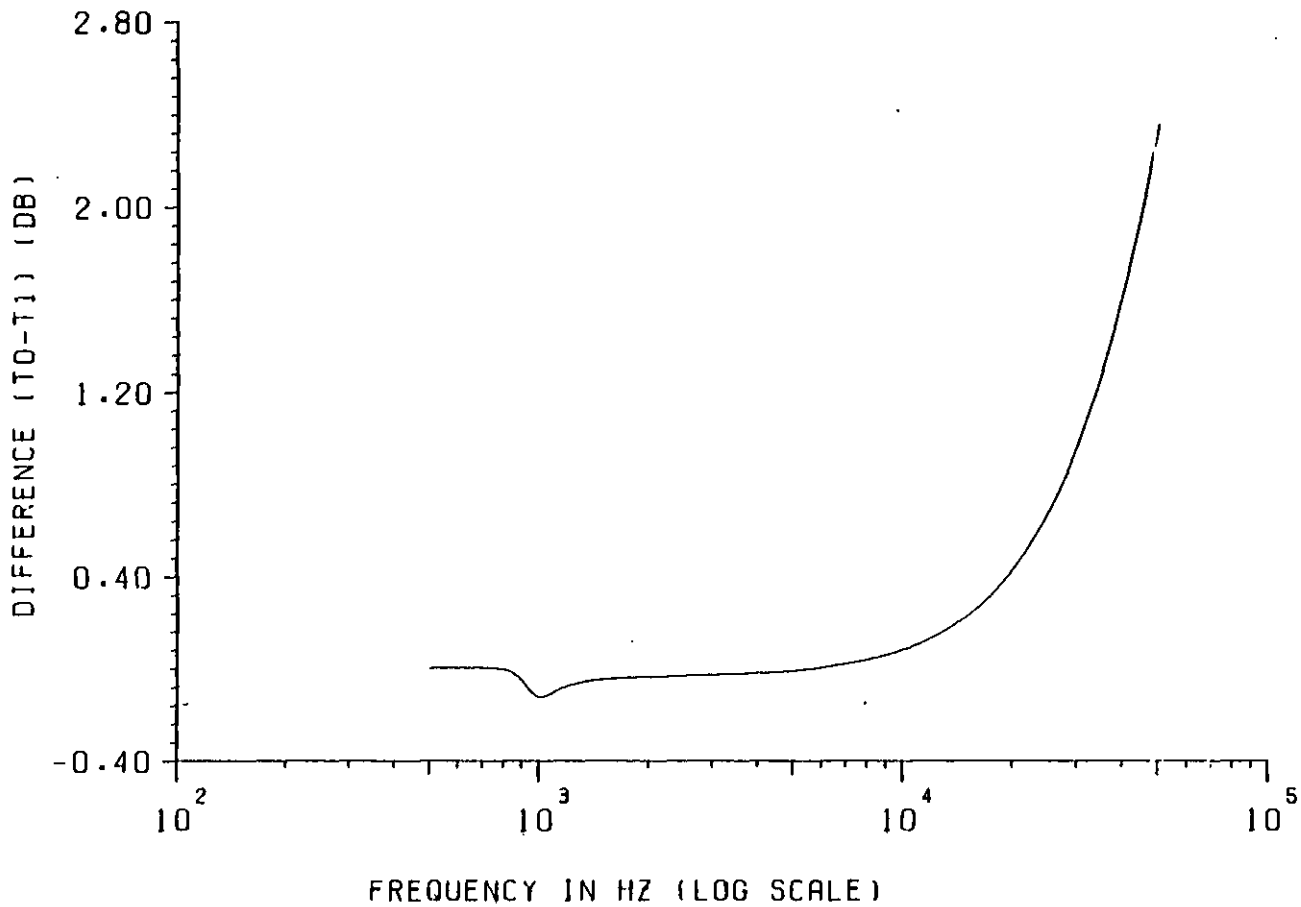

Fig 5.11 Plot of the modulus of the objective function against frequency for the case when the NIC impedances in the circuit of Fig 5.10(a) are chosen as $Z_1 = Z_2 = 1.0$ kilo-ohms.

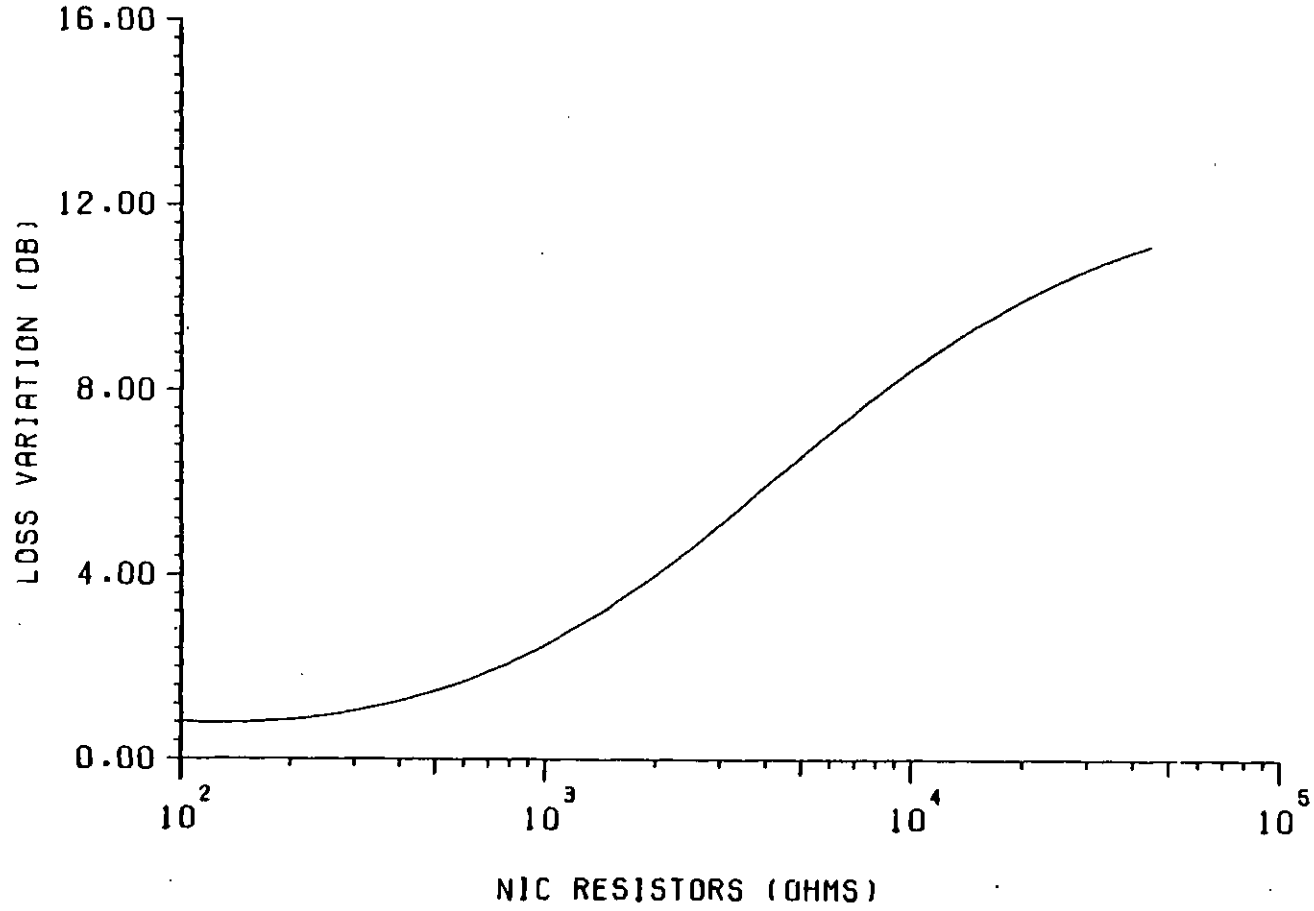

Fig 5.12 Plot of loss variation against NIC resistor value (i.e. Z_1) for NIC_2 in Fig 5.4(b) ($Z_2 = 3Z_1$).

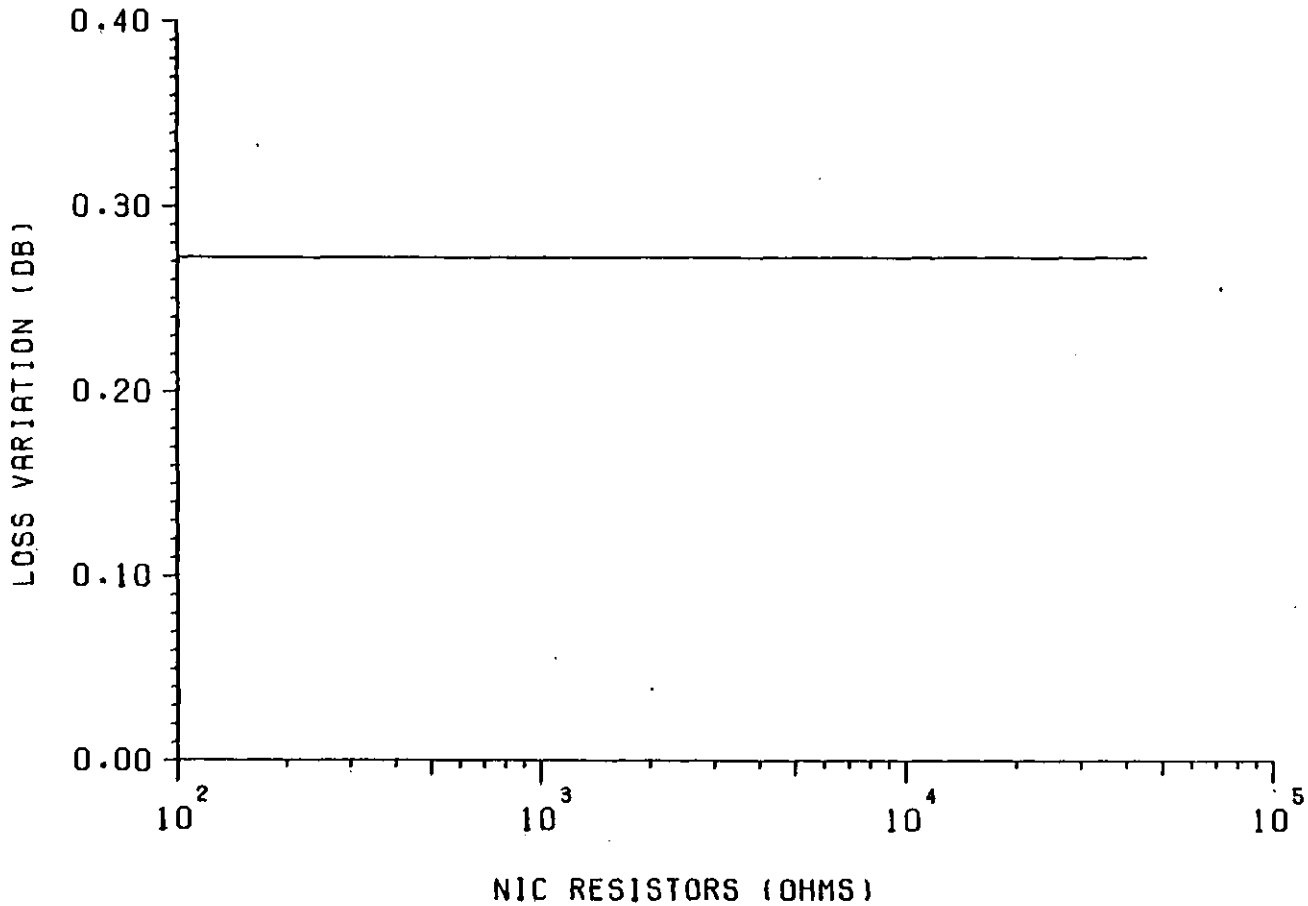

Fig 5.13 Plot of loss variation against NIC resistor value (i.e. Z_1) for NIC_2 in Fig 5.4(b) for the case when the positions of impedances Z_1 and Z_B in Fig 5.10(a) have been interchanged and $Z_2 = 3Z_1$.

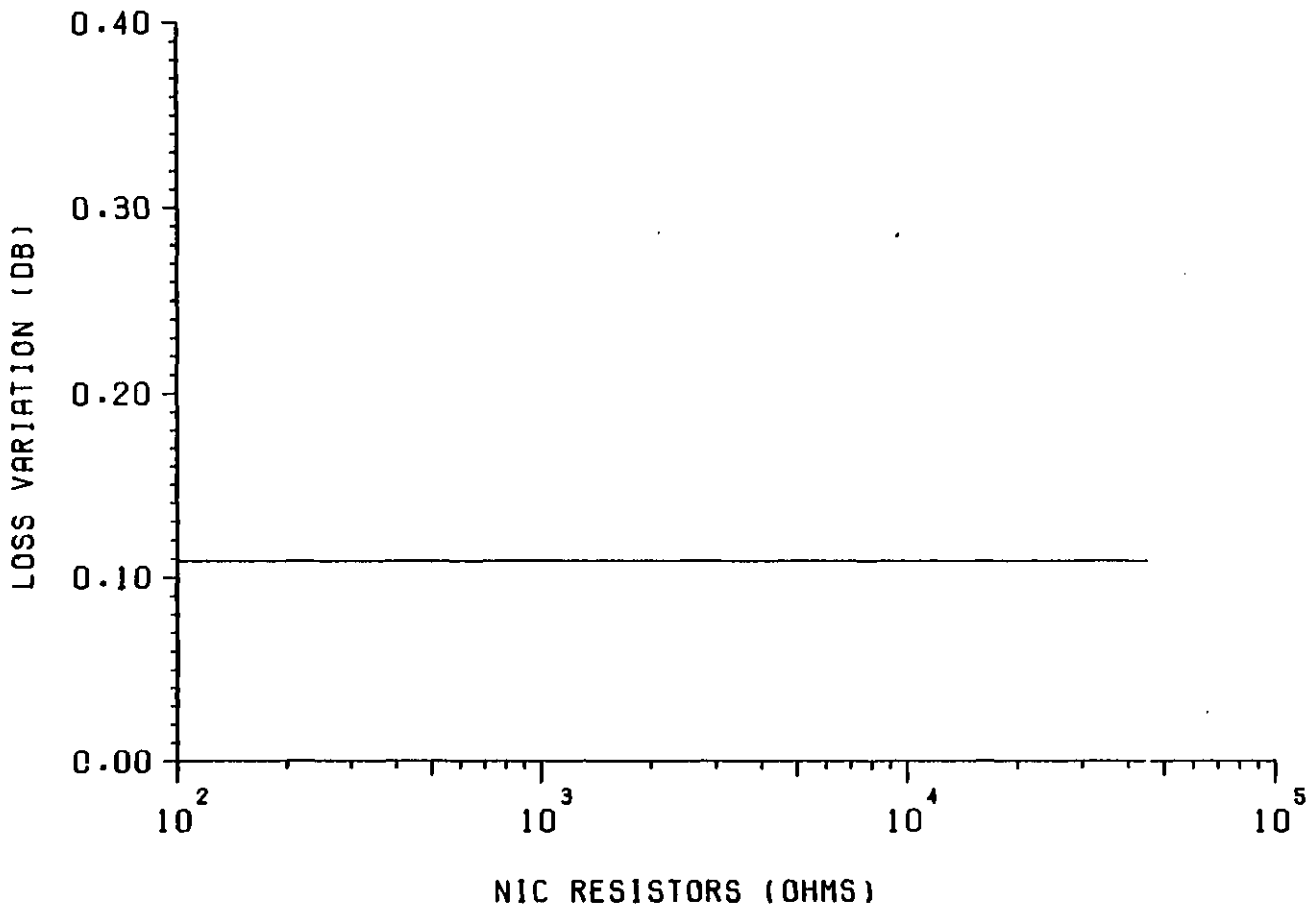

Fig 5.14 Plot of loss variation against NIC resistor value (i.e. Z_1) for NIC_2 in Fig 5.4(b) for the case when the positions of impedances Z_1 and Z_B in Fig 5.10(a) have been interchanged and $Z_2 = Z_1$.

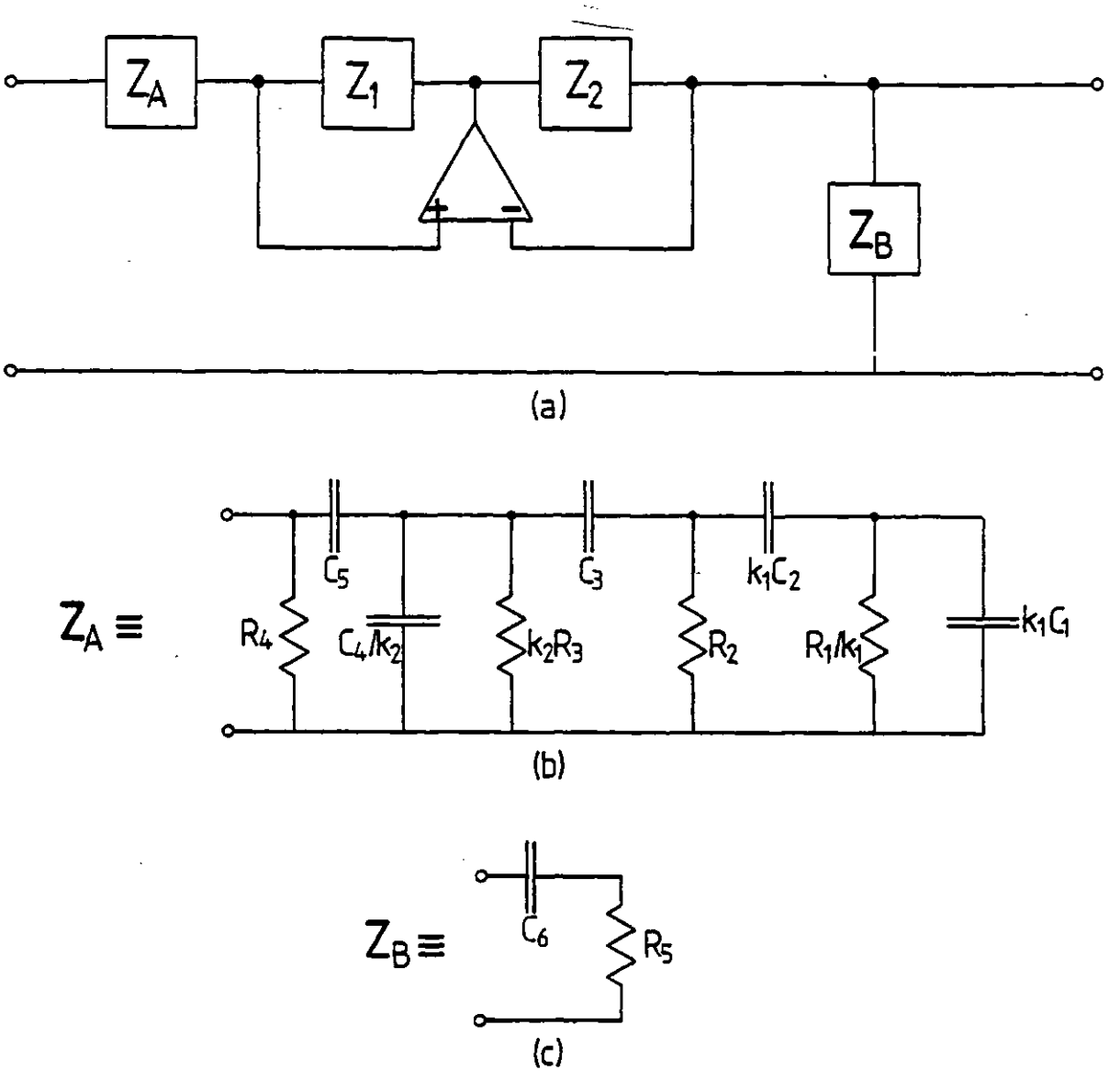

Fig 5.15 Minimising the effect of finite f_T for NIC_3 on the transfer function of the circuit in Fig 5.4(b).
(a) The equivalent circuit for minimising the effect of the finite f_T. (b) Impedance equivalent to Z_A in (a). (c) Impedance equivalent to Z_B in (a).

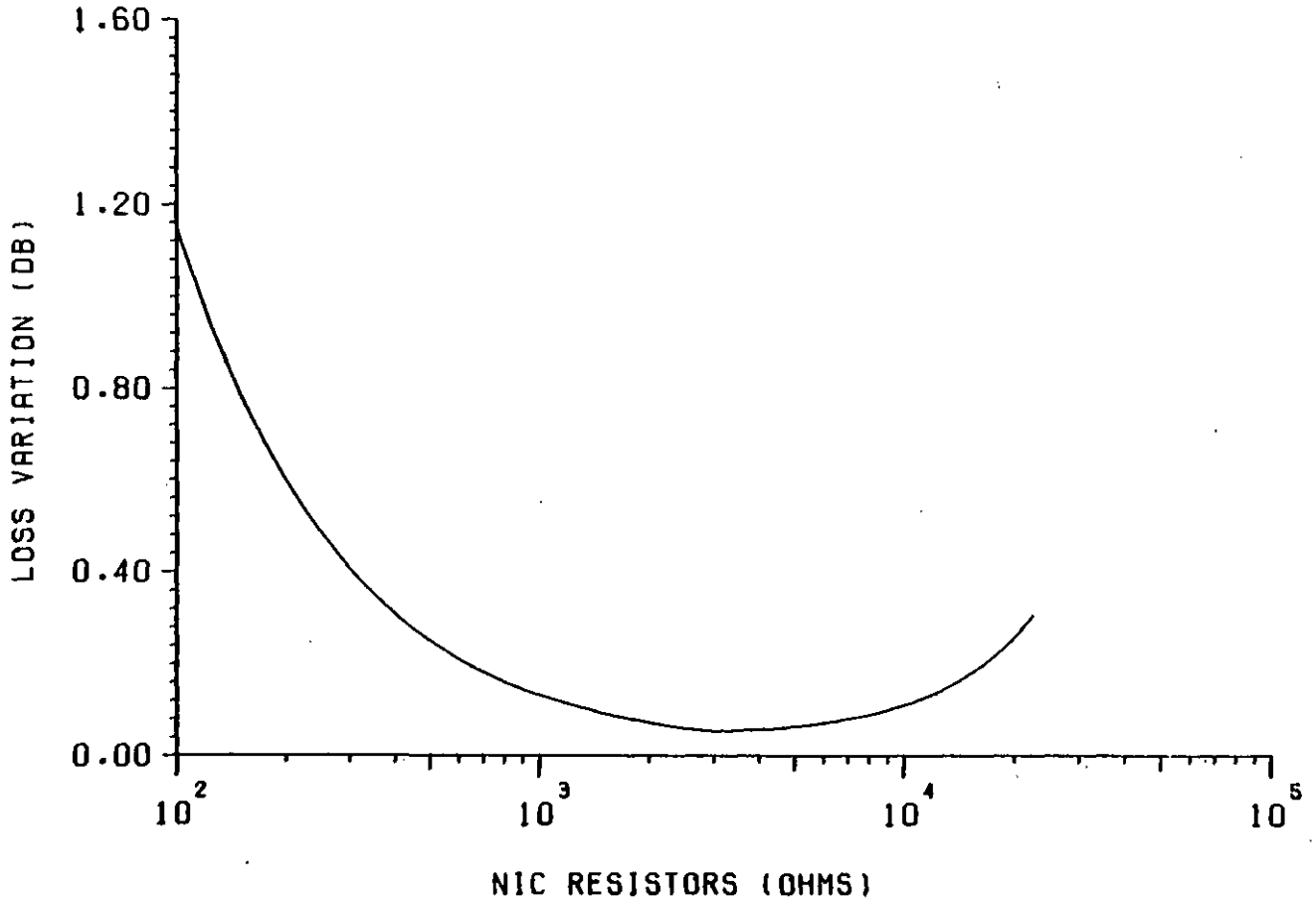

Fig 5.16 Plot of loss variation against NIC resistor value (i.e. Z_1) for NIC_3 in Fig 5.4(b) ($Z_2 = 2Z_1$).

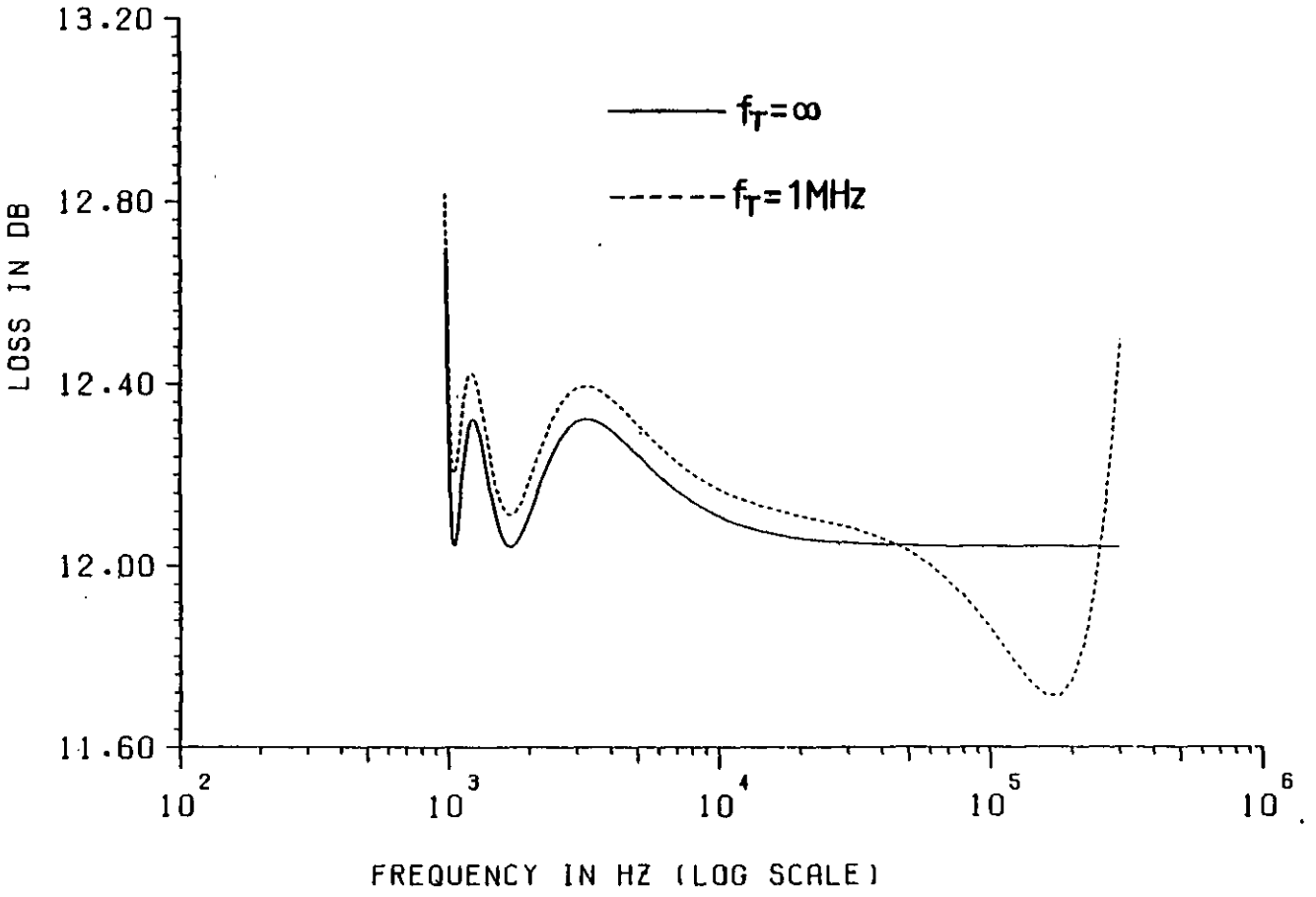

Fig 5.17 Frequency response of the circuit in Fig 5.4(b) when impedances of NIC_2 and NIC_3 are chosen optimally from the graphs of Figs 5.12 and 5.16, respectively, and the impedances of NIC_1 are chosen as a parallel combination of a resistor (= 22.7201 kilo-ohms) and a capacitor (= 2.89036 nF).

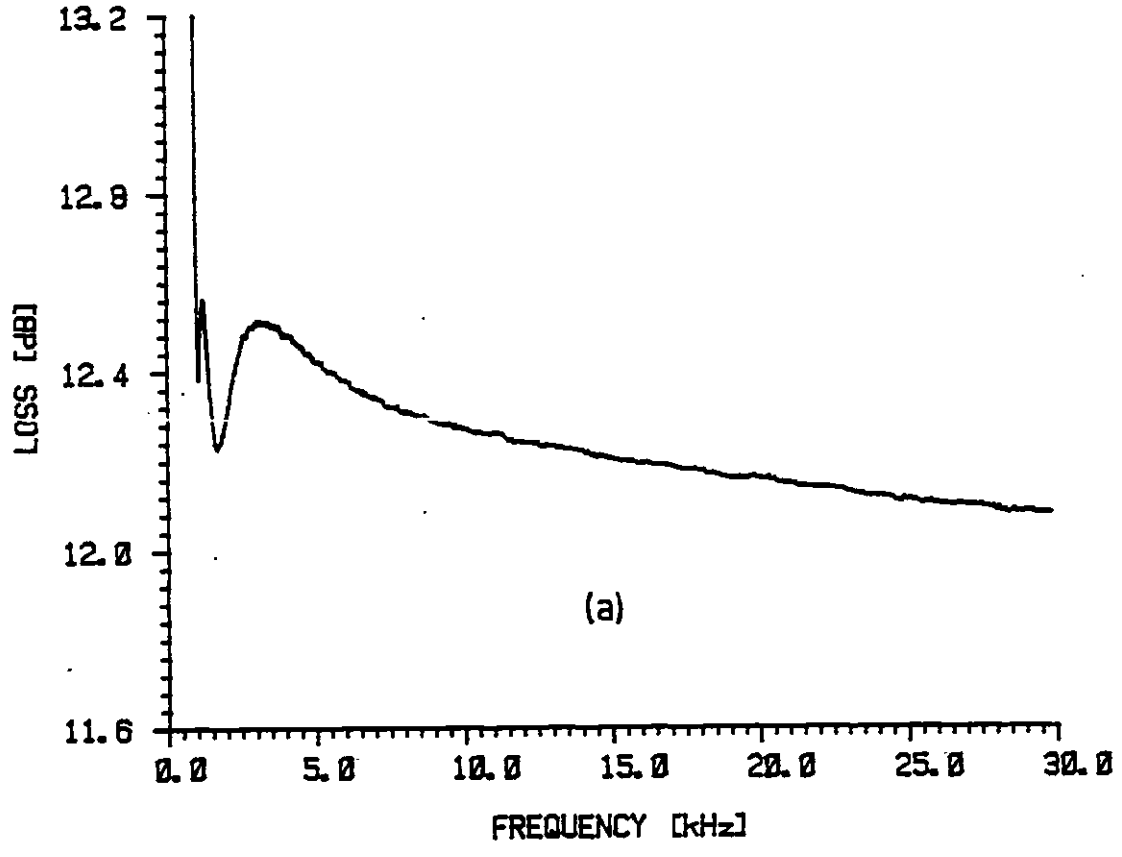

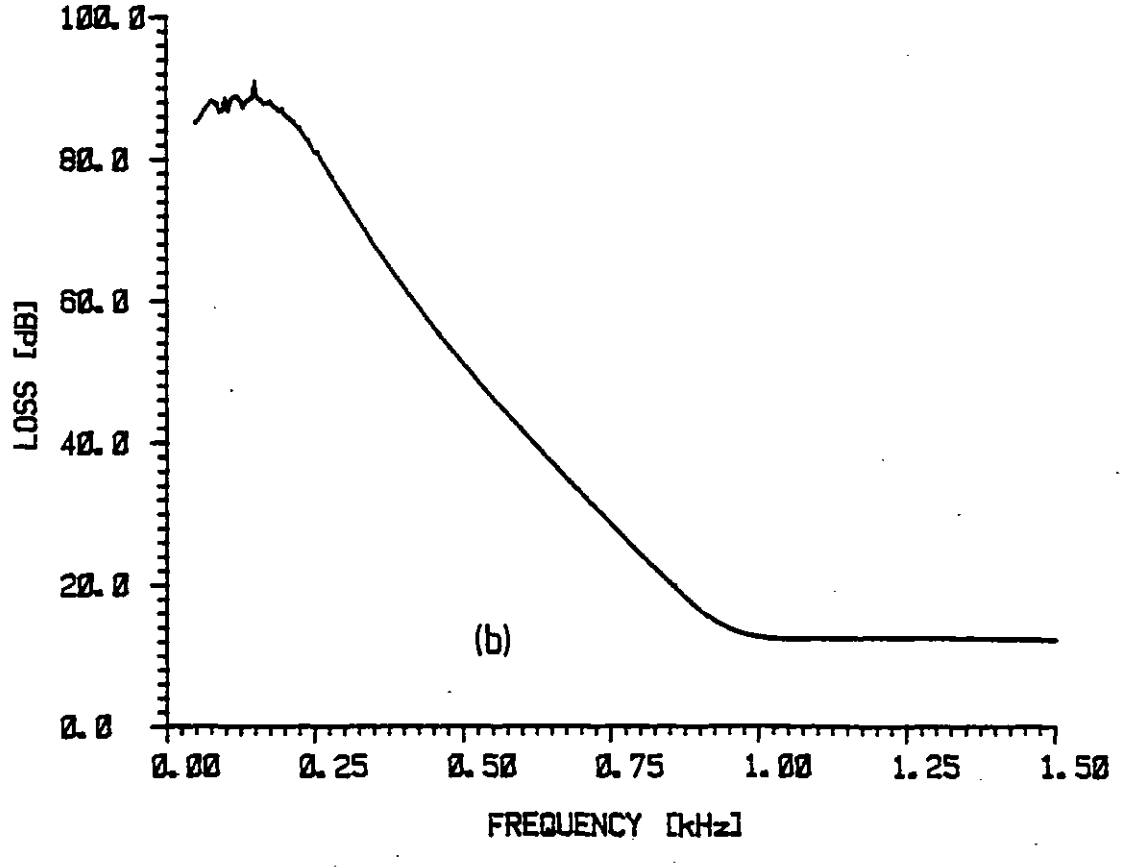

Fig 5.18 Measured frequency responses of the the discrete component model of the circuit in Fig 5.4(b).
(a) Passband response. (b) Stopband reponse.

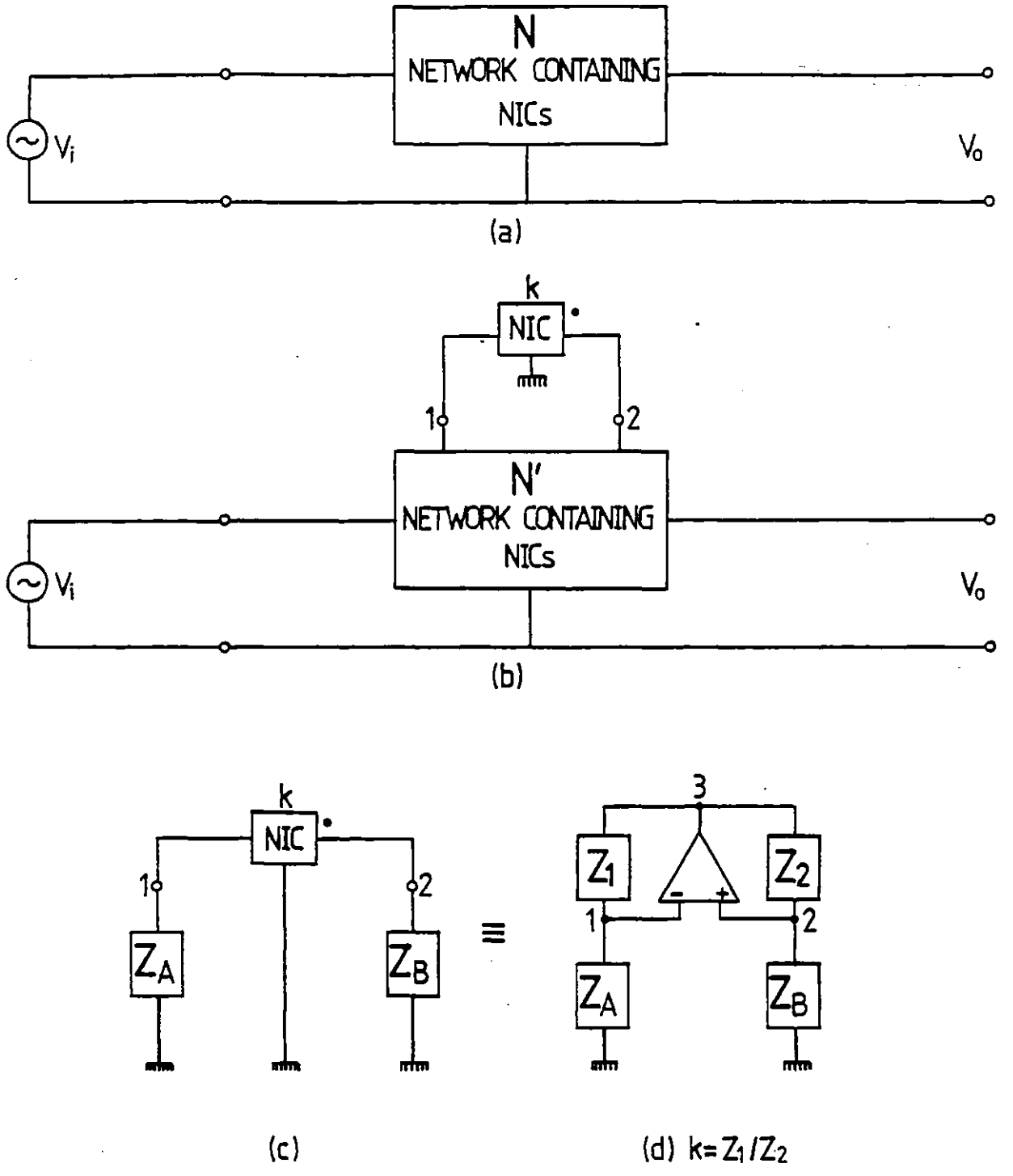

Fig 5.19 Stability consideration of NIC circuits.
(a) Network containing NICs. (b) Equivalent network of (a) with the NIC whose stability is being considered having been "pulled-out". (c) The "pulled-out" NIC in (b) terminated by its equivalent impedances Z_A and Z_B (as seen from terminals 1 and 2 in (b)). (d) NIC in (c) replaced by its OP-AMP equivalent.

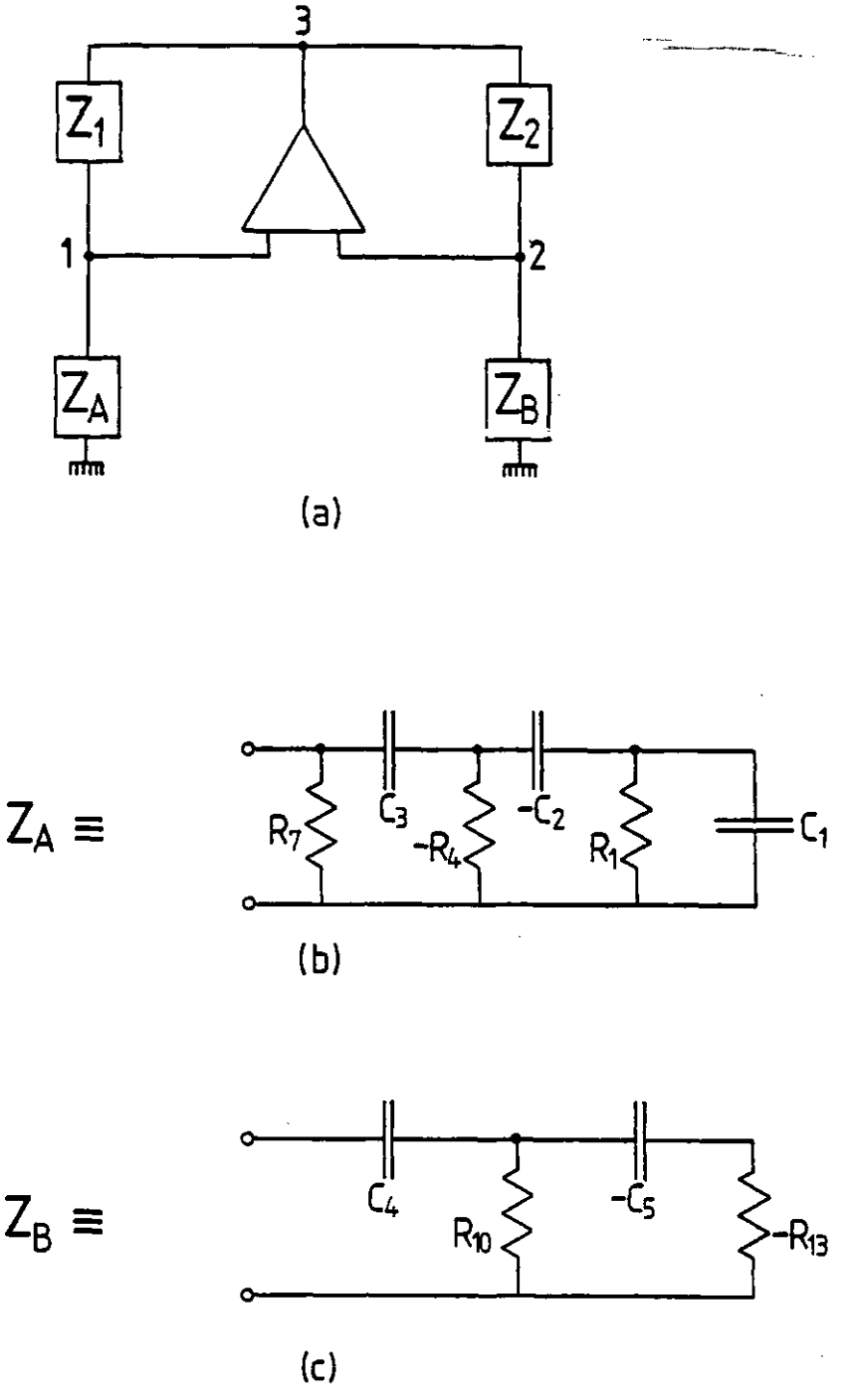

Fig 5.20 Stability consideration of NIC_3 in the circuit of Fig 4.31 (see Table 4.2 for the component values).
(a) Equivalent circuit for considering the stability of NIC_3. (b) Equivalent of impedance Z_A in (a). (c) Equivalent of impedance Z_B in (b).

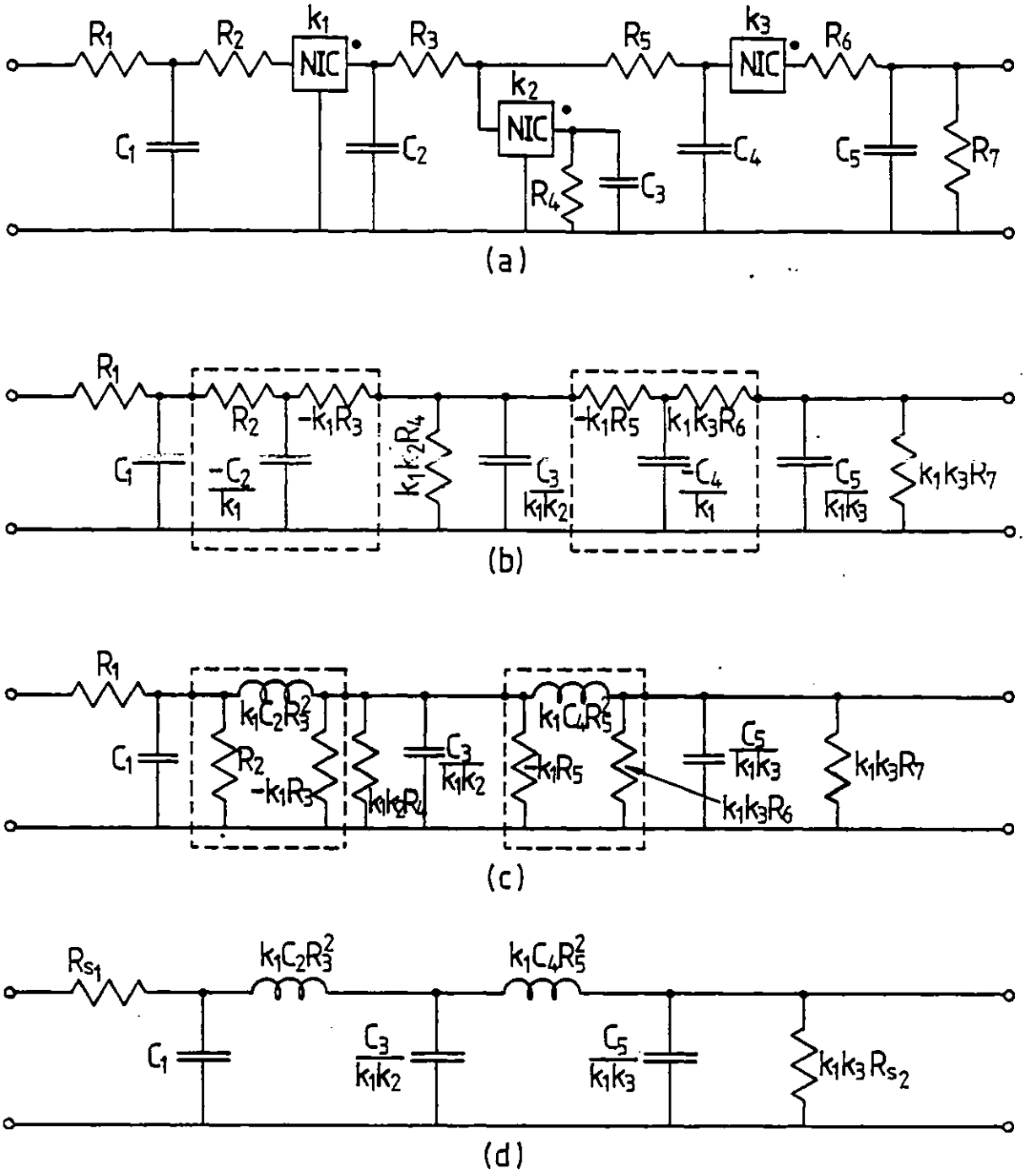

Fig A.1 A 5th order all-pole lowpass filter circuit realised using three NICs.
(a) Active RC realisation. (b) Circuit obtained by eliminating the NICs in (a). (c) Circuit obtained from from (b) by transforming the encircled T-networks into their equivalent ll-networks (assuming $R_2 = k_1 R_3$ and $R_5 = k_3 R_6$). (d) The "equivalent" prototype filter.